MYOCARDIAL AUTOPHAGIC STATUS IN DIABETIC AND NON-DIABETIC CONDITIONS

A THESIS PRESENTED

BY

RAJI. S. R

TO

SREE CHITRA TIRUNAL INSTITUTE FOR

MEDICAL SCIENCES AND TECHNOLOGY, TRIVANDRUM

Thiruvananthapuram

IN PARTIAL FULFILLMENT OF THE REQUIREMENTS

FOR THE AWARD OF

DOCTOR OF PHILOSOPHY

2021

DECLARATION BY STUDENT

I, **Ms. RAJI. S. R.**, hereby certify that I had personally carried out the work depicted in the thesis entitled **"MYOCARDIAL AUTOPHAGIC STATUS IN DIABETIC AND NON-DIABETIC CONDITIONS"** under the direct supervision of Dr. G Srinivas, Scientist F, Department of Biochemistry, SreeChitraTirunal Institute for Medical Sciences and Technology, Trivandrum, except where external help was sought and is acknowledged. No part of the thesis has been submitted for the award of any other degree or diploma prior to this date.

Date: Raji. S. R

CERTIFICATE BY THE RESEARCH GUIDE

This is to certify that **Ms. RAJI. S. R** has fulfilled the requirements prescribed for the PhD degree of the SreeChitraTirunal Institute for Medical Sciences and Technology, Trivandrum. The thesis entitled **"MYOCARDIAL AUTOPHAGIC STATUS IN DIABETIC AND NON-DIABETIC CONDITIONS"** was carried out under my direct supervision. No part of the thesis has been submitted for the award of any other degree or diploma prior to this date.

Date: Dr. G. Srinivas (Guide)

The thesis entitled

MYOCARDIAL AUTOPHAGIC STATUS IN DIABETIC AND NON-DIABETIC CONDITIONS

submitted by

RAJI. S. R

for the Degree of

Doctor of Philosophy

of

SREE CHITRA TIRUNAL INSTITUTE FOR MEDICAL SCIENCES AND TECHNOLOGY, TRIVANDRUM

Thiruvananthapuram

is evaluated and approved by

Dr. Srinivas G

(Guide) (Examiner)

Acknowledgements

Firstly I would like to express my sincere gratitude to my supervisor, Dr. G. Srinivas, Scientist F, for his guidance, advice, supervision and encouragement. I couldn't have imagined having a better advisor and mentor for my PhD study and I thank him for supporting me throughout my PhD work.

Besides my advisor I would also like to acknowledge Prof. Asha Kishore, Director, SCTIMST; Prof. K. Radhakrishnan, former Director, SCTIMST, Prof. JaganmohanTharakan, former Acting Director, SCTIMST and Dr. S, Jayasingh, former Deputy Registrar, SCTIMST for their insightful comments and encouragement with all the facilities which helped me to complete my work.

I wish to express my sincere gratitude to Prof. N. Jayakumari, HOD, Department of Biochemistry, SCTIMST, Prof. P. S. Appukuttan, Former HOD, Department of Biochemistry, SCTIMST, Dr, Shivkumar.K, Scientist G, Department of Cellular and Molecular Cardiology, SCTIMST, Dr.Renuka Nair, Former HOD, Department of Cellular and Molecular Cardiology, SCTIMST, Prof. Jayakumar. K, HOD, Department of CardioVascular and Thoracic Surgery, SCTIMST, Dr.Vivek. V. Pillai, Associate Professor, Department of CardioVascular and Thoracic Surgery, SCTIMST, Dr.HariKrisnan.V.S, Scientist D, Division of Laboratory Animal Sciences, SCTIMST.

Words are short to express deep sense of gratitude towards my friend and colleague Ms.Nandini.R.J., whose help, support suggestions and encouragement helped me in all the time of research. I acknowledge her help in conducting a part of my animal model studies. And I deeply respect her companionship for the last 14 years which still continues.

I wish to express my sincere gratitude to Dr.PriyaSrinivas, Scientist F, RGCB, for guidance and encouragement in carrying out this work and also I acknowledge the help offered by her team.

I am indebted to Ms.Surabhi.S, Mr.Anoop, Ms.Subha, Mr.Sumesh S for their help in lab works, especially immunohistochemistry experiments.

Also I acknowledge other lab members, Mr.Ashok.S for helping me in animal model studies, Ms.Sulfath.T.P and Mr.Anand. C.R for helping me in standardising oxygraph experiments and Ms.Dhanya Krishnan, Ms.BhavyaBharathan, Ms.Sreelekshmi, and Ms.MahalaxmiGanjoo for their helping hands. My sincere thanks to Dr.Deepa.D, Technical Assistant, Department of Biochemistry for her help in clinical biochemistry assays.

I would also like to extend warm thanks to my seniors, Dr.Priya P.S and Dr.SubojBabykutty for teaching me the techniques like animal cell culture and western blotting and for their love and care.

Also I thank Dr.Sourabh Nanda, Department of Cardiovascular and Thoracic Surgery, SCTIMST in patient data collection, the staff of the Department of Cardiovascular and Thoracic Surgery and the Division of Laboratory Animal Sciences, SCTIMST. Also I thank all the patients who gave their consent to be included in the study.

I greatfully acknowledge the financial support of INSPIRE for my fellowship and SERB, DST for funding the project.

Last but not least I wish to avail myself this opportunity to pay high regards to my beloved parents for their encouragement and inspiration, to my husband, for his love and support, to my in-laws for their encouragement and to my loving son, Madhav, to whom I dedicate my work, for loving me unconditionally and for his patience.

Thank God for everything.

List of Contents

List of Figures

List of Abbreviations

AD	Alzheimer's disease
ADP	Adenosine di phosphate
AGE	Advanced GlycationEndproduct
AMP	Adenosine mono phosphate
AMPK	Adenosine monophosphate- activated protein kinase
APS	Ammonium persulphate
Atg	AuTophaGy-related
ATP	Adenosine Triphosphate
Bcl-2	B cell lymphoma-2
BMI	Body mass Index
BNIP3	Bcl-2 interacting protein 3
BSA	Bovine Serum Albumin
CABG	Coronary Artery Bypass Graft
CaCl2	Calcium Chloride
CD36	Cluster of differentiation 36
CDC	Centre for Disease Control and Prevention
CMA	Chaperon-mediated autophagy
CPT-1	Carnitinepalmitoyltransferase 1
Cvt	Cytoplasm to vacuole targeting
DAB	DiaminoBenzidine
DCM	Diabetic cardiomyopathy
DNA	Deoxy ribonucleic acid
DTT	Dithiothreitol
EDTA	Ethylene DiAmineTetraAcetic Acid
EGTA	Ethylene glycol-bis(β-aminoethyl ether)-N,N,N',N'-tetraacetic acid
ER	Endoplasmic reticulum
ETC	Electron transport chain
ETF	Electron transferringflavoprotein
FABP	Fatty acid binding protein
FADH	Flavin adenine dinucleotide
FAO	Fatty Acid Oxidation
FAT	Fatty acid translocase
FATP	Fatty acid transport protein
FBS	Feotal Bovine Serum
FCCP	Carbonyl cyanide p- (trifluro-methoxy) phenyl-hydrazone
FFA	Free fatty acids
FUNDC1	FUN 14 domain-containing protein1
FW	Formula Weight
GDM	Gestational diabetes mellitus
GDP	Guanosinediphosphate
GLUT	Glucose transporter

Gpx	Glutathione peroxidise
GTP	Guanosine triphosphate
HBSP	Helix B surface peptide
HCl	Hydrochloric acid
HFpEF	Heart failure with preserved ejection fraction
HI	Hypoxic ischemic
HRP	Horse Radish Peroxidase
I/R	Ischemia reperfusion
IDF	International Diabetes Federation
IEC	Institution Ethics Committee
IGF-1	Insulin like growth factor 1
IgG	Immunoglobulin G
IGT	Impaired glucose tolerance
KCl	Potassium Chloride
LAMP2	Lysosome-associated membrane protein 2
LC3	Microtubule-associated protein1 light chain 3
LV	Left ventricle
MCF7	Michigan Cancer Foundation-7
MgCl2	Magnesium Chloride
mM	Milli Molar
Mn-SOD	Manganese superoxide dismutase
mPTP	Mitochondrial Permeability Transition Pore
mRNA	Messenger Ribonucleic acid
mTOR	Mammalian target of rapamycin
NA	Nicotinamide
NADH	Nicotinamide Adenine Dinucleotide dehydrogenase
NaHCO3	Sodium Bicarbonate
NBR1	Neighbour of BRCA1 gene1 protein
nmol	Nano Molar
NP – 40	Nonidet P - 40
NQO1	NAD(P)H Quinone Dehydrogenase 1
NYHA	New York Heart Association
OCM	Offsprings of control mother
OCR	Oxygen consumption rate
ODM	Offsprings of diabetic mother
OGTT	Oral Glucose Tolerance test
OLETF	Otsuka Long-Evans Tokushima Fatty
OPTN	Optineurin
OXPHOS	Oxidative phosphorylation
P/O	Phosphate/Oxygen
PCr	Phosphocreatine
PGC-1α	Peroxisome proliferator-activated receptor-gamma coactivator 1α
PHB2	Prohibitin 2
Pi	Inorganic phosphate
PI3P	Phosphatidyl Inositol 3-phosphate

PINK1	Phosphatase and tensin homolog- induced putative kinase1
pmol	Pico Mole
PPAR	Peroxisome proliferator-activated receptor
qRT PCR	Quantitative Real Time Polymerase Chain Reaction
RCR	Respiratory Control Ratio
RIPA	Radio immuno Precipitation Assay
ROS	Reactive Oxygen Species
rpm	Revolutions per Minute
SDS – PAGE	Sodium dodecyl sulphate Polyacrylamide gel electrophoresis
SEM	Standard error of mean
Sirt1	Sirtuin 1
SPSS	Statistical Package for the Social Sciences
STZ	Streptozotocin
SUIT	Substrate-Uncoupler-Inhibitor-Titration
T2DM	Type 2 Diabetes mellitus
TAG	Triacyl glycerol
TAX1VP1	Tax1 binding protein1
TBST	Tris Buffered Saline Tween 20
TCA	Tri carboxylic acid
TEMED	Tetramethylethylenediamine
TRIM 5	Tripartite motif-containing protein 5
tRNA	Transfer RiboNucleic acid
TSC1	Tuberous sclerosis 1
UCP	Uncoupling protein
ULK1	Unc-51 like autophagy activating kinase 1
Vps	Vacuolar protein sorting
w/v	Weight/Volume
µm	Micro Meter
µM	Micro Molar

SYNOPSIS

Background

Cardiovascular death is the leading cause of death in persons with type 2 diabetes. Itis always noted that there is a strong relation between hyperglycemia and intracellular metabolism in the myocardium which can cause changes in energetics, structure and function. Autophagy is one of the metabolic processes altered in type 2 diabetes.

Gestational diabetes during pregnancy cause serious health problems in offsprings.The excess nutrient exposure in the uterus even modifies the phenotype gene expression resulting in permanent short and long term effects in the baby.

Objectives

- Evaluation of autophagic profile in type 2 diabetic human heart
- Evaluation of autophagy in high glucose-treated H9c2 cell lines and a type 2 diabetic mice model at two time points of hyperglycemia
- Analysis of cardiac mitochondrial function regulated by autophagy at two time points in type 2 diabetic mice
- Evaluation of autophagic status in male and female offsprings of gestational diabetic rats at their weaning and adult stage
- Analysis of cardiac mitochondrial function in male and female offsprings of gestational diabetic rats at their weaning and adult stage

Hypothesis

1) Type 2 diabetes mellitus causes altered cardiac autophagy and thereby brings changes in mitochondrial respiration

2) Untreated gestational diabetes in mothers will affect cardiac autophagy and mitochondrial respiration in offsprings

Methodology

The study incudes diabetic and non diabetic human right atrial appendage tissue samples, high-glucose treated H9c2 cells, streptozotocin/nicotinamide-induced T2DM C57BL/6 mice model and STZ-induced gestational diabetic wistar rats

- High resolution respirometry was used for studying oxygen consumption rate in isolated mitochondria in the presence of fatty acid and carbohydrate substrates.

- Western blotting was used for analyzing expression levels of proteins
- Kit based assays were used for analyzing biochemical tests

Principal findings:

Human study

In diabetic human heart, reduced expression of LC3 II and LC3 II/I ratio was observed which denoted the reduced formation of autophagosomes or reduced autophagy. Increased expression of p62 indicated that the p62 was not degraded properly and the fusion between autophagosome and lysosome were defective/ altered. No significant change was found in Beclin 1 expression between the diabetic and non-diabetic groups. In short, myocardial autophagy was found to be reduced in diabetic than the non-diabetic human subjects.

High glucose-treated H9c2 cells

In H9C2 cells, no change was observed in the autophagic proteins, mitophagic proteins lysosomal proteins and regulators of autophagy at 4 h of hyperglycemia. No change was observed in the steady state level of LC3 II and its LC3 II/I ratio at 4 h .A reduced expression of phosphorylated ULK1 was noted at 48 h of hyperglycemia. A significant reduced expression is noted in Atg 5, at 48 h.The increased expression of p62 at the 48 h of hyperglycemia shows that the degradation of autophagosomes is blocked/ reduced. The reduced steady state level of LC3 II and LC3 II/I ratio at 48 h indicates reduced formation of autophagosomes or reduced autophagy. The mitophagy proteins, Parkin and PINK 1 showed reduced expression at 48 h

Type 2 diabetic mice model

- **Autophagic study**

No change was observed in the cardiac autophagic proteins, mitophagic proteins, lysosomal proteins and regulators of autophagy in 2 weeks of diabetic mice. The steady state level of LC3 II was found unchanged, but the LC3II/I ratio was found to be increased at 2 week. A reduced expression of ULK1 and pULK1 was noted in 10 week diabetic mice. The increased expression of p62 in 2 week and 10 week diabetic mice shows that the degradation of autophagosomes is blocked/reduced. No change was observed in the steady state level of

LC3 II and its LC3 II/I ratio in 10 week diabetic mice indicated autophagosome formation was similar like the control. The mitophagy proteins, Parkin showed reduced expression; while no change was observed in PINK 1 indicates the improper clearance of damaged mitochondria in the 10 week diabetic mice.

- **Role of autophagy in cardiac mitochondrial respiration**

Resveratrol (activator of autophagic process) enhanced the fatty acid-mediated state 2 and glutamate, pyruvate-mediated state 3 complex I respiration in 2 week diabetic mice mitochondria. The state 2 and state 3 complex I respiration in 10 week time point was significantly increased by the resveratrol treatment. The succinate-mediated complex I + II and complex II by the 2 week untreated diabetic mice mitochondria was significantly enhanced by the resveratrol treatment. The unchanged succinate-mediated complex I + II and complex II respiration shown by the untreated diabetic mice mitochondria in 10 week time point was significantly increased by the resveratrol treatment. Resveratrol treatment in the diabetic mice increased the state 4 respiration and maximal respiratory capacity in 2 weeks and the unchanged OCR in 10 weeks untreated diabetic mice was also significantly enhanced in both protocols

Chloroquine (inhibitor of autophagy) decreased the fatty acid-mediated state 2 and glutamate, pyruvate-mediated state 3 complex I respiration in 2 week diabetic mice mitochondria. The state 2 and state 3 complex I respiration in 10 week time point was drastically decreased by the chloroquine treatment. The succinate-mediated complex I + II and complex II by the 2 week untreated diabetic mice mitochondria was again significantly reduced by the chloroquine treatment. The succinate-mediated complex I + II and complex II respiration in 10 week time point was significantly decreased by the chloroquine treatment. Chloroquine treatment didn't alter the state 4 respiration, but the maximal respiratory capacity was significantly reduced in 2 weeks diabetic mice.

Gestational diabetic rat model

- **Cardiac autophagic profile in offsprings of gestational diabetic mother**

No change was observed in the cardiac autophagic proteins, mitophagic proteins, lysosomal proteins and regulators of autophagy of weaning and adult group of male and female ODM. A reduced expression of pULK1 was noted in adult female ODM while reduced expression of Atg 14 was noted in adult male ODM .Atg 16 was found unchanged in weaning and adult male ODM, while a significant increase was noted in weaning female ODM and a reduction was noted in adult female ODM. Atg 3 was significantly reduced in adult male and weaning and adult female ODM, while no change was observed in weaning male ODM. The increased expression of p62 in adult male and female ODM shows that the degradation of autophagosomes is blocked/reduced, while no change was observed in weaning male and female ODM. No change was observed in the steady state level of LC3 II and its LC3 II/I ratio in weaning female ODM, while a significant increase was noted in weaning male ODM indicated autophagosome formation was increased. But in adult male and female ODM, there showed a significant reduction in LC3 II and LC3 II/I ratio indicated reduced formation of autophagosome or reduced autophagy. The lysosomal proteins LAMP-2 was seen unchanged in weaning male and female ODM, while it is significantly reduced in adult male and female ODM, The regulators of autophagy, AMPKα were found unchanged in adult male and weaning female ODM. The antioxidant enzymes, MnSOD and GPx were found unchanged in weaning and adult male and female ODM indicated that the gestational diabetes didn't influence the antioxidant mechanism in offsprings

- **Cardiac mitochondrial function in offsprings**

The fatty acid-mediated state 2 complex I respiration was unchanged in weaning male ODM while it is reduced in adult male ODM. The palmitoyl L- carnitine, pyruvate and glutamate-mediated state 3 complex I respiration was reduced in weaning and adult male ODM. Succinate-mediated complex I + II and complex II respiration was not altered in weaning male ODM while a significant reduction was observed in adult male ODM. Complex II dependent state 4 respiration and maximal respiratory capacity was observed to be

unchanged in weaning male ODM while a significant reduction was noticed in adult male ODM. The glutamate/malate-mediated state 2 complex I respiration and the glutamate/malate and pyruvate-mediated state 3 complex I respiration was unchanged in weaning male ODM. The fatty acid-mediated state 2 complex I and palmitoyl L-carnitine/malate, pyruvate and glutamate-mediated and state 3 complex I respiration was unchanged in weaning female ODM corresponding to their female OCM. Succinate-mediated complex I + II, complex II, complex II-dependent state 4 respiration and maximal respiratory capacity showed an increasing tendency, but it was not significant in weaning female ODM. No change was observed in fatty acid-mediated state 2 complex I, palmitoyl L- carnitine/malate, pyruvate and glutamate-mediated state 3 complex I and state 4 respiration was observed in adult female ODM .Succinate-mediated state 3 complex I + II respiration, complex II respiration, and maximal respiratory capacity were significantly reduced in adult female ODM.

Conclusion and significance of the study

Type 2 diabetic models

Human study

In contrast to the available single work published by Munasinghe et al., on human cardiac autophagy in type 2 diabetes in New Zealand population, our results indicates decreased autophagy in diabetic than non-diabetic subjects. This is the first report regarding cardiac autophagy in type 2 diabetic subjects of Asian Indian population.

Cell line study

The main objective of the study in H9c2 cells was to analyze autophagic status in high glucose condition at two time points, 4 h and 48 h. All the autophagic proteins, mitophagic proteins, lysosomal proteins and the regulators of autophagy analyzed in the study were found unchanged at 4 h time period of hyperglycemia. It was found that when the duration of hyperglycemia was increased for 48 h for H9c2 cells caused significant reduction in autophagic and mitophagic proteins indicates that the recycling mechanism was impaired in the cardiomyoblast cells.

Mice study

The main objective of the study in untreated type 2 diabetic mice was to analyze cardiac autophagic status at two time points of diabetes, 2 weeks and 10 weeks of hyperglycemia. Mitophagic proteins, lysosomal proteins and the regulators of autophagy were found unchanged in 2 weeks of diabetic mice heart when compared with their corresponding controls. LC3 II/I ratio and p62 levels was increased in 2 week diabetic mice indicated an impaired autophagy with accumulation of autophagosomes. In 10 week diabetic mice, even though LC3 II was unchanged, a significant reduction was noted in ULK1, pULK1 and parkin and increase in p62 was observed. Both 2 week and 10 week diabetic mice showed altered cardiac autophagy indicates the accumulation of damaged or dysfunctional proteins, organelles like mitochondria inside the cardiomyocytes that in turn will worsen the oxidative stress and defective metabolism in diabetic heart.

Analysis of cardiac mitochondrial respiration in type 2 diabetes by regulating autophagy showed that administration of an autophagic activator (Resveratrol) at 2 week and 10 week of diabetic mice activated mitochondrial respiration in the heart tissue. When the diabetic mice were treated with an autophagic inhibitor (Chloroquine) at 2 week and 10 weeks, the cardiac mitochondrial respiration was significantly reduced. This study implies the importance of autophagic regulation in heart tissue during type 2 diabetes and the role of autophagy in maintaining the cardiac mitochondrial respiration.

Gestational diabetic rat model

Our results showed that cardiac autophagy is reduced or altered in the adult group of male and female ODM. But cardiac autophagy was less affected in the weaning group of male and female ODM. Most of the mitophagic and autophagic proteins were unchanged in male and female weaning group ODM. This is the first report on cardiac autophagy in male and female offsprings of gestational diabetic mothers. The study implies the impact of diabetic pregnancy or the hyperglycemic condition in the uterine environment in regulating a metabolic process, autophagy in the offsprings during their life time. It shows that the impairment or defects is more evident in their adult life.

The another objective of this study was to evaluate the mitochondrial function of offsprings (male and female) of untreated gestational diabetic mothers at two different time points of their life, weaning and adult time period. The mitochondrial respiration of the weaning (male and female) ODM irrespective of substrate combination was found to be less affected or unchanged compared to their respective OCM. But in the adult group of male ODM, a significant reduction in mitochondrial oxygen consumption was observed. The mitochondrial respiration in female adult ODM are found unchanged or less affected by diabetic pregnancy, even though they exhibited significant reduction in succinate-mediated complex I and II respiration in one of the protocol. As a result of impairment in these cellular processes, the total generation of ATP may be reduced, affecting the normal function of heart in the offsprings of diabetic mothers.

Key words: type 2 diabetes mellitus, gestational diabetes mellitus, autophagy, mitochondria, heart

I. INTRODUCTION

I.1. Diabetes mellitus

Diabetes is a group of chronic metabolic disorders in which the person has highglucose in the blood. It happens when the pancreas loses its ability to produce adequate insulin or when the body cannot properly make use of the insulin produced. International Diabetes Federation's (IDF) report in 2017 estimated that 425 million adults between the age group 20 to 79 years were affected with diabetes and projected that the numberwill increase to 629 million by 2045. The burden is suchthat 12% of world health expenditure is spent for this chronic disease management and treatment modalities. In 2045, India will overpower China and occupy the first position with the highest number of people with diabetes in the world (IDF, 2017).

Figure 1: Top ten countries with number of people with diabetes, 2017 and 2045

2017			2045		
Rank	Country/territory	Number of people with diabetes	Rank	Country/ territory	Number of people with diabetes
1	China	114.4 million (104.1-146.3)	1	India	134.3 million (103.4-165.2)
2	India	72.9 million (55.5-90.2)	2	China	119.8 million (86.3-149.7)
3	United States	30.2 million (28.8-31.8)	3	United States	35.6million (33.9-37.9)
4	Brazil	12.5 million (11.4-13.5)	4	Mexico	21.8 million (11.0-26.2)
5	Mexico	12.0 million (6.0-14.3)	5	Brazil	20.3 million (18.6-22.1)
6	Indonesia	10.3 million (8.9-11.1)	6	Egypt	16.7million (9.0-19.1)
7	Russian Federation	8.5 million (6.7-11.0)	7	Indonesia	16.7million (14.6-18.2)
8	Egypt	8.2million (4.4-9.4)	8	Pakistan	16.1 million (11.5-23.2)
9	Germany	7.5 million (6.1-8.3)	9	Bangladesh	13.7 million (11.3-18.6)
10	Pakistan	7.5 million (5.3-10.9)	10	Turkey	11.2 million (10.1-13.3)

Adapted from International Diabetes Federation report, 2017

Insulin, a peptide hormone, released by the beta cells of the pancreas plays a significant role in the regulation of blood glucose levels. If enough insulin is not produced or the produced insulin cannot exert its function properly, result in the raising of glucose levels in the blood, condition known as hyperglycemia (Wilcox, 2005).Over a long period of time, the excess glucose levels along with the hormonal imbalance can cause various undesirable effects in the body and can cause harm to the cells, resulting in progressive failure of various tissues and organs (Fowler, 2008).There are three main classification of diabetes: Type 1 diabetes mellitus, Type 2 diabetes mellitus and Gestational diabetes mellitus.

I.1.1. Type 1 diabetes mellitus

Type 1 diabetes mellitus (T1DM) or insulin dependent diabetes mellitus is an autoimmune response of the body that arises when the body's immune system destroys the insulin producing β cells in the Islets of Langerhans of pancreas. As a result, β cells cannot produce sufficient insulin or even stop producing insulin. This disease is most often identified in children and in adults, younger than 30years. So it is named as Juvenile - onset diabetes (Atkinson, 2012). As stated by IDF, more than 1,106,500 children in the world are suffering from this disease. India ranks second position in number of about 11,300 new cases of T1DM (children and adolescents <15 years) per year (IDF, 2017). The predisposing factors for type1 diabetes are not fully understood. It is usually related to genetic susceptibility (Todd, 2010) and the available information shows the impact of early childhood diet, viral and bacterial infections and family background (Heinonen M. T., Moulder R. and Lahesmaa R., 2015). At present there is no proven prevention technique for T1D. But the platform of hyperglycemia immediately requires exogenously given insulin to the patients throughout their life and a healthy control of glucose in blood can dramatically improve the quality of life.

I.1.2. Type 2 diabetes mellitus

Type 2 diabetes mellitus (T2DM) or non insulin dependent diabetes mellitus is the most widespread form and this metabolic disorder accounts for about 90% of all diabetes in the world (Mungrue, Roper and Chung, 2011). IDF's report in 2017, states that 79% of adults having diabetes are from low and middle-income countries. People between the age group 40 and 59 years are mostly affected with T2DM and it caused about 4 million deaths (IDF, 2017). The prevalence of T2DM is increasing throughout the world due to urbanization, westernization, low socioeconomic standards and their related life style changes. Some of therisk factors are overweight, unhealthy diet, physical inactivity, lack of exercise, increasing age, high blood pressure, ethnicity, family history of diabetes, impaired glucose tolerance (IGT), history of gestational diabetes etc. At initial stages of diabetes, there will be peripheral insulin resistance accompanied by a hypersecretion of insulin resulting in hypoglycemia. But as the disease progress, hyperglycemic condition avails as a result of decline of insulin secretion from the pancreatic β cells. Skeletal muscle, liver and adipose tissue are mainly affected because the demand for glucose uptake and utilization are very high in these tissues. The symptoms of T2DM are excessive thirst, hunger, dry mouth, frequent and abundant urination, lack of energy, extreme tiredness, numbness in hands and feet, blurred vision, slow healing wounds, recurrent fungal infections in the skin etc.People with diabetes have an increased probability of developing microvascular, macrovascular and miscellaneous complications in the body(Papatheodorou et al., 2016). High blood glucose levels for a long period can certainly affect the function of heart, blood vessels, sexual organs, eyes, kidneys, nerves, teeth etc.

Cardiovascular death is the leading cause of death in persons with diabetes. It can affect the functioning of blood vessels in heart and brain, leading to diabetic cardiomyopathy, heart attack and stroke. Diabetic nephropathy includes damage of small blood vessels in the kidney, characterized by the occurrence of proteinuria with a reduction in filtration rate of glomerulus. Diabetic retinopathy involves the formation of lesions in the retinal region of eye, causing blindness in the diabetic patients. Diabetic neuropathy implicate the

development of vascular deformities like thickening of capillary basement membrane, endothelial hyperplasia and hypoxia, deterioration of nerve fibers in the legs resulting in lower extremity amputations (Forbes and Cooper, 2013). People can control T2DM through their diet, exercise and life style along with recommended drugs and insulin. Research people all over the world are struggling to perceive the numerous causes of diabetes and to develop various therapeutic methods for its treatment.

Figure 2: Complications of Diabetes

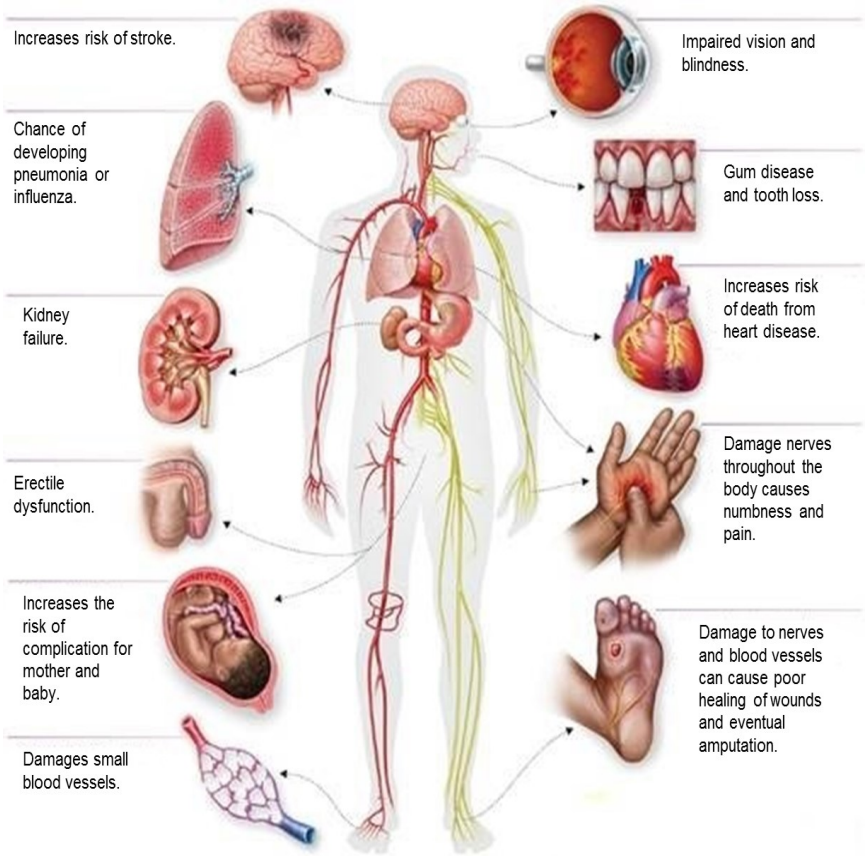

Adapted from www.macmillanlearning.com. Complications of diabetes in various organs

I.1.3. Gestational diabetes mellitus

Gestational diabetes mellitus (GDM) is defined as impaired glucose tolerance with onset or first recognition during pregnancy (ADA, 2013). One of the most prevalent metabolic disorders that cause complications in pregnancy is diabetes mellitus and can cause harm to both mother and baby. Based on a survey in 2014 by Centers for Disease Control and Prevention (CDC), the rate of GDM is very high as 9.2% and is increasing every year in theworld (DeSisto, 2014). The forecasted approximate rate for GDM in India is 79.4 million in 2030, a 151% rise from 31.7 million in 2000 (Wild et al., 2004). GDM usually disappears after pregnancy but the mother and their children are at a greater risk of developing T2DM in their future life.About 50% of the women will become T2DM within five to ten years after their delivery.Since the life style has changed a lot today, increased dependence on fast foods, unbalanced diet, overweight and obesity in child bearing age, IGT, lack of exercise, increased working stress, history of smoking, family history of diabetes, certain ethnic groups, late pregnancy, number of previous pregnancies etc can be considered as a risk factor for GDM(Mpondo, Ernest and Dee, 2015). The exact process behind GDM remains unknown. Insulin sensitivity reduces with advancing period of gestation in normal pregnancy. These changes are due to hormones produced from placenta, that will help the baby to grow and develop inside the uterus of the mother(Baz, Riveline and Gautier, 2016). As pregnancy progress, placental hormones like progesterone, estrogen, prolactin, cortisol, etc, will block the action of mother's insulin, leading to increased insulin resistance, high hepatic glucose output and decreased hepatic glycogen storage(Barbour et al., 2007). So in a physiologic condition, a compensatory increase in insulin production maintains a normal level of glucose in the mother's blood. GDM develops in certain women with defective pancreatic capacity(Kühl and Hornnes, 1986) and they are not able to make increased insulin and make use of it needed for pregnancy resulting in the accumulation of blood glucose leading to hyperglycemia.

The extra blood glucose from the mother will pass through the placenta to the baby's body resulting in high glucose level. As a result pancreas of the baby will start to produce extra

insulin to metabolize this glucose. As the baby is getting more energy, it is converted and stored as fat leading to macrosomia or fat baby(Ragnarsdottir and Conroy, 2010). The excess nutrient exposure even modifies the phenotype gene expression i.e., epigenetic modification resulting in permanent short and long term effects in the baby(Catalano et al., 2003). Some of them are abortions, placental insufficiency(Desoye and Mouzon, 2007), cardiomyopathy(Reller and aplan, 1988), hypoglycemia, hypocalcaemia, hyperbilirubinemia etc.So GDM requires adequate consideration and treatment in health related matters of pregnant women in the form of balanced diet, exercise, reducing stress, regular blood glucose monitoring, oral drugs and insulin therapy (Kampmann et al., 2015).

Figure 3: Metabolic disorders of offsprings of gestational diabetic mothers

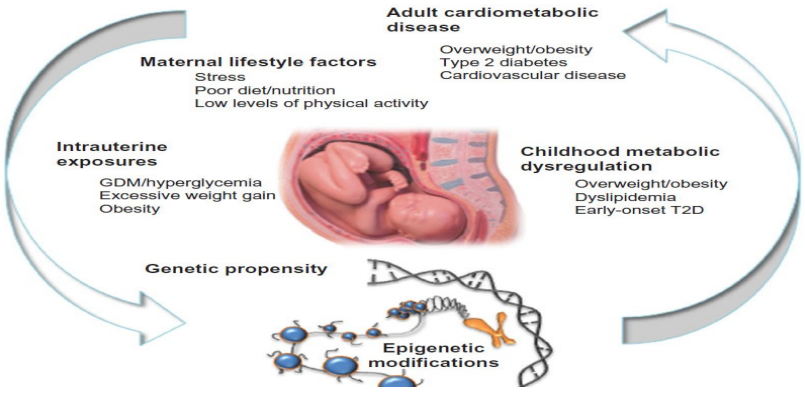

Adapted from (Estampador and Franks, 2014). Factors like poor maternal life style and the resultant exposure of feotus to hyperglycemia are responsible for metabolic disorders like obesity, type 2 diabetes mellitus, dyslipidemia etcin offsprings.

I. 2. Diabetes and heart

Diabetes mellitus is a predisposing factor for heart failure, cardiovascular morbidity and premature mortality. The mechanisms behind the accelerated heart disease in connection with T2D are not completely understood. It is always noted that there is a strong relation between hyperglycemia and intracellular metabolism in the myocardium which can cause changes in energetics, structure and function(Matheus et al., 2013). In certain patients with

diabetes, Rubler et al., found that myocardial dysfunction is characterized without any coronary artery disease, valvular disease, hypertrophy, etc and coined the condition as diabetic cardiomyopathy (DCM) even as early as in 1972 (Rubler et al., 1972). Along with cardiovascular risk factors (Wu, 1999) like obesity, hypertension, dyslipidemia, smoking, excessive stress etc, currently epigenetic factors (Keating, Plutzky and El-Osta, 2016) are also reported showing interaction between genes and environment, add the association between diabetes and cardiovascular disease. Increased left ventricular (LV) mass, LV concentric remodeling and subclinical contractile dysfunction illustrates the main structural changes happening in diabetic patients (Levelt et al., 2016). Interstitial fibrosis and hypertrophy will be present in the later stages of DCM. The increased free fatty acid (FFA) availability in diabetic patients will increase triacylglycerol levels 1.5 to 2.3 fold higher when compared to non diabetic controls (McGavock et al., 2007). Studies have shown that myocardial steatosis may be an independent factor between T2DM and LV concentric remodeling(Rijzewijk et al., 2008). The primary insult for cardiomyocytes during hyperglycemia is the altered substrate supply and utilization(Rodrigues, Cam and McNeill, 1998). The rate of transport of glucose across sarcolemmal membrane to the cardiomyocyte is very slow because of the exhaustion of transporters like GLUT 1 and 4(Russell et al., 1998). Since the circulating FFA is very high, there will be an inhibitory impact of fatty acid oxidation on pyruvate dehydrogenase complex and finally result in reduced glucose oxidation and ATP production(Liedtke et al., 1988). There will be abnormality in calcium homeostasis(Trost et al., 2002), accumulation of advanced glycation end products(Berg et al., 1999), ketosis(Kruljac et al., 2017), increased activation of protein kinase C by diacylglycerol, abnormalities of small capillaries, venules, arterioles and arteriosclerosis, myocyte cell death due to necrosis or apoptosis(Goyal and Mehta, 2013)etc in diabetic myocardium.

In the fetal heart, structure and function are greatly influenced by GDM. Congenital heart problems happen in up to 8.5 per 100 live births of offsprings of diabetic mothers (ODM)(Becerra et al., 1990). Studies have shown that women who were on insulin

treatment at the time of conception had the highest number of offsprings with congenital heart malformations(Day and Insley, 1976). However the real mechanism that modifies the fetal heart during hyperglycemia is not completely understood. Different mechanisms and metabolic pathways are altered in fetal heart during the hyperglycemic uterine environment. Some of the congenital heart defects in ODM are ventricular septal defect, double outlet right ventricle, aortic stenosis, truncus arteriosus(Ferencz et al., 1990), transposition of great arteries, hypoplastic left heart syndrome, cardiomyopathy etc. Hypertrophic cardiomyopathy is the most important among these defects in ODM(Reller and Kaplan, 1988). Some of the metabolic disorders in ODM are altered lipid metabolism, poor antioxidant systems, increased ROS production (Damasceno et al., 2002), modulation of insulin resistance and inflammation, changes in immune system, and activation of metabolic memory (Yessoufou and Moutairou, 2011).

I. 3. Autophagy

Autophagy is a vital physiologic process in eukaryotes which is highly conserved during evolution, involves the degradation of intracellular components including soluble and aggregated proteins, long lived proteins, lipids, turnover of organelles, foreign bodies (Yu, Chen and Tooze, 2017) etc. The term ‘Autophagy’ (from Greek, “auto” oneself, “phagy” to eat) was coined by Christian De Duve, a Belgian cytologist and biochemist in 1963. Autophagy plays an essential role in stress response (ROS, hypoxia), nutrient starvation, infections, energy sensing, cell death, ageing, immunity, lipid metabolism, erythropoiesis, and various pathologies (Glick, Barth and Macleod, 2010). There are mainly three types of autophagy: Microautophagy and Chaperone - mediated autophagy and macroautophagy. Microautophagy, mostly seen in yeasts and plants involves the direct uptake of cytoplasmic contents by vacuoles via direct membrane invagination (Li, Li and Bao, 2012). Chaperon mediated autophagy (CMA) is a form of autophagy in which the lysosomes will degrade the targeted molecules. It only selects those cargo having a target motif like KFERQ that upon

recognition by Chaperon proteins like HSP70, decides the delivery to the lysosomal surface where it interacts with membrane receptor Lysosomal- associated membrane protein 2A (LAMP-2A) (Kaushik et al., 2011).

Figure 4: Types of autophagy

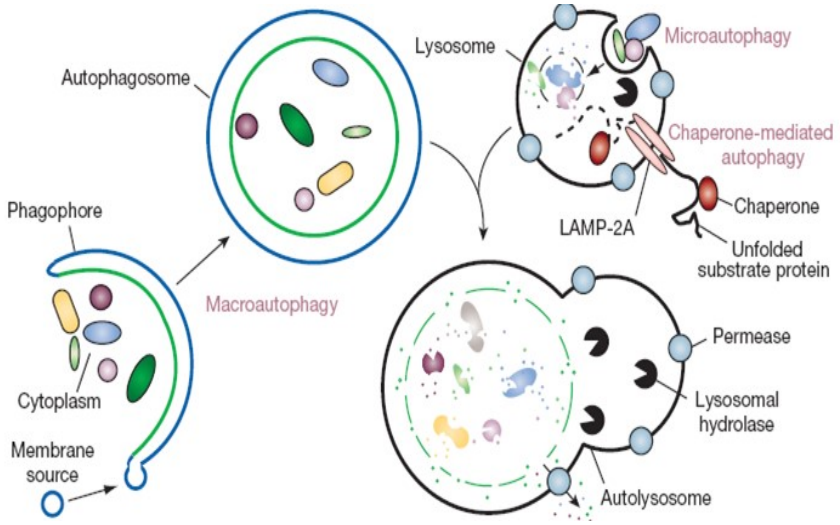

Adapted from(Mizushima et al., 2008) Different types of autophagy

Macroautophagy is the major type which includes the formation and expansion of an isolation membrane called phagophore (Yang and Klionsky, 2010). Along with the cargo, phagophore membrane fuses and finally forms the double membrane structure, autophagosome. The autophagosome then fuses with the lysosome to form autophagolysosomes or autolysosomes (Feng et al., 2014) . Inside the autolysosomes, with the help of various lysosomal enzymes, the cargo will be degraded and the remaining molecules like amino acids, fatty acids and nucleotides will be transported back to the cytosol for the synthesis of various macromolecules and for maintaining different cellular functions. So autophagy is commonly known as cellular 'recycling factory' (Galluzzi et al., 2017) that help in energy sensing and efficient generation of ATP. There are certain selective types of autophagy which involves selective or specific removal of damaged or

excess single substrate by micro or macroautophagy. Mitophagy (removal of mitochondria by autophagy) (Kubli and Gustafsson, 2012) is the best characterized selective autophagy.

Figure 5: Functions of autophagy

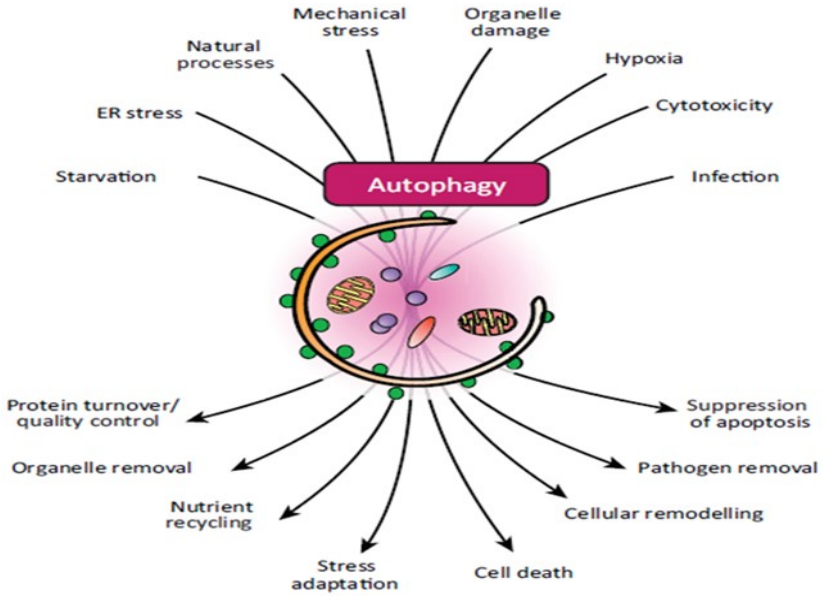

Adapted from(King, 2012). Regulations and functions of autophagic pathway

The key regulators of autophagy involves mTOR, TOR kinase, AMPK, ER stress, nutritional status, hormonal factors, temperature, time, oxygen concentration, cell density (Levine and Kroemer, 2008) etc. The outstanding work for the identification and characterization of the autophagy machinery in yeast (Tsukada and Ohsumi, 1993) brought Nobel Prize in physiology or medicine, 2016 to a cell biologist named Yoshinori Ohsumi. Since 1993, a lot of work had been started in the field of autophagy resulting in so many relevant research publications and data explaining the role of autophagy in various physiologic and pathologic processes. It is very important to master the function of each molecule of autophagic pathway that will help for the discovery of therapeutics targeting autophagy in many diseases.

I. 3. 1. Autophagy in diabetic heart

In healthy heart, autophagy is maintained at basal levels for its normal functioning(Sciarretta et al., 2014). But it is activated or inhibited in certain pathological conditions like heart failure, acute myocardial infarction, post infarction remodeling, cardiac hypertrophy, pressure overload, cardiomyopathy etc. During stress and ageing, autophagy is inhibited and associated with the development of cardiac problems(Ikeda et al., 2014). During T2DM and obesity, there is an inevitable chance of developing myocardial ischemia thereby proposing a problem in the myocardium in relation to energy crisis. Several studies have shown that the metabolic disturbances in diabetic heart are due to altered autophagy (Sciarretta et al., 2012).New studies have shown that autophagic activity was increased in T1DM while in T2DM, increased formation of autophagosome was observed, but the fusion with lysosomes, autophagic flux didn't occur resulting in autophagosome accumulation, without the degradation of misfolded proteins and organelles (Kanamori et al., 2015). Autophagic mechanisms during diabetes include the participation of many molecules like mTOR, AMPK, SIRT1, interaction between Bcl-2 and Beclin-1 etc. The change in autophagic status during diabetes depends on the animal model, experimental conditions, medications of the patients, type and duration of diabetes etc. It remains unclear whether the activation or inhibition of autophagy at different stagesof T2DM may be a reason for the defects in metabolism of myocardium.Thus the crucial role of autophagy in T2DM remains debatable.

During pregnancy, the role of autophagy starts from embryogenesis, survival of blastocysts, formation of extravillous trophoblast, placental development, implantation of embryo into uterus etc.,(Nakashima, Aoki and Saito, 2016). A recent study had shown that autophagic activity was increased in placenta and extravillous trophoblastin GDM patients (Ji et al., 2017). Since heart is a key organ which is affected in ODM, autophagy - an important physiologic process required for energy transaction is also supposed to play a significant role in controlling the myocardial metabolism. Till now, there are no studies reported about

the cardiac autophagic status of ODM and it shows the importance of studying such process in ODM.

I. 4. Cardiac mitochondria: platform for interplay of diabetes and autophagy

Mitochondria are the key components of beating heart by providing ATP through oxidative phosphorylation ie.,oxidation of fatty acids (60 – 70 % of ATP) and other substrates like glucose,lactate (30 – 40 %) etc.,(Gustafsson and Gottlieb, 2008). They are highly organized and efficient, their specific arrangement and abundance in each myocyte make them a well planned system of ATP production and transport to perform its contraction, relaxation, maintaining ion balance and metabolism(Andrienko et al., 2003). It also plays a critical role during oxidative stress, hypoxia, DNA damage and eventually leads to a cascade of events with the release of proapoptotic proteins to activate apoptosis(Gustafsson and Gottlieb, 2003) or necrotic cardiomyocyte cell death.

Some studies have shown that defects in mitochondrial energetics may be a contributing factor for the phenomenon of cardiac dysfunction in T2DM patients(Anderson et al., 2009). During diabetes, often a rise in fatty acid utilization is followed by depletion in glucose and lactate utilization. A study in type 2 diabetic patients showed impairment in cardiac mitochondrial bioenergetics where a decreased cardiac phosphocreatine/ATP ratio(Scheuermann-Freestone et al., 2003) was reported. There were changes in mitochondrial high energy phosphate metabolism, calcium handling, insulin signaling, increased ATP utilization with decreased production, decreased cardiac efficiency, marked structural changes, increased mitochondrial uncoupling with impaired mitochondrial respiratory capacity, remodeling and post transcriptional modification of mitochondrial proteome, etc(Bugger and Abel, 2010).Only a single work so far had been published on mitochondrial energetics in the myocardium of ODM. In that study, reported cardiac

mitochondrial dysfunction in newborn offsprings of diabetic pregnancy when the mothers are fed on high fat diet(Mdaki et al., 2016).

Hyperglycemia can lead to imbalances in the antioxidant capacity within the cardiomyocyte resulting in oxidative damage to a variety of biomolecules including proteins, lipids and the nucleic acids. As a result, accumulation of dysfunctional proteins and organelles such as mitochondria occursand damaged mitochondria can even increase generation of ROS through ROS induced ROS release. Before the dysfunctional mitochondria activate the cell death program, cells adopt a selective sequestration and subsequent degradation of damaged mitochondria by a process called mitophagy or mitochondrial autophagy. So the process of selective autophagy, mitophagy is required for the proper removal of dysfunctional or depolarized mitochondriain a terminally differentiated cell like cardiomyocytes during diabetic conditions. (Kobayashi and Liang, 2015).

Figure 6: Mitochondria in the diabetic heart

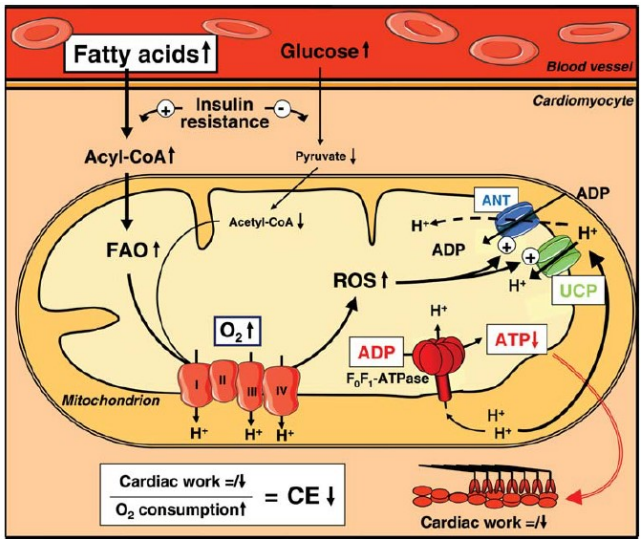

Adapted from (Bugger and Abel, 2010). Mitochondrial uncoupling andimpaired cardiac efficiency in diabetes.

So in the scenario of diabetes, controlled regulation of mitophagy is very important in a terminally differentiated cell like cardiomyocyte.A study in an *Atg 7* knockout mouse model exhibited a significant defect in mitochondrial respiration in skeletal muscle and pancreatic β

cells (Wu et al., 2009). It denotes the effective roles of autophagy in mitochondrial respiration.There are no reports about autophagy-regulatedcardiac mitochondrial respiration in T2DM and requires an immediate attention.

II. REVIEW OF LITERATURE

II. 1. Heart metabolism

The mammalian heart must contract continuously without any break for the uninterrupted flow of blood to all parts of the body. For the contraction/relaxation, continuous production and supply of ATP is needed. So a constant supply of substrates from the metabolic pool is needed for the mitochondria to generate the required ATP. 90 % of ATP generated by the cardiac mitochondria is used for its contraction. Heart depends on various substrates like fatty acids, glucose, lactate, ketone bodies, amino acids etc., for ATP production. 60-70% of ATP is produced from fatty acid oxidation, 20% from glucose oxidation and 10% from lactate (Bertrand et al., 2008). So fatty acids are the main source of energy substrate for the heart and the heart depends on Randle cycle where fatty acid and glucose metabolism inter regulate each other for the substrate utilization (Fillmore, Mori and Lopaschuk, 2014). With the help of various fatty acid transporters like CD36/FAT (fatty acid translocase) and FABP (fatty acid binding protein), fatty acid enters the cell. Fatty acyl CoA synthetase will add a CoA group to the long chain fatty acids and the CPT-1 (carnitine palmitoyl transferase 1) will convert the long chain fatty acyl-CoA to acylcarnitine for entering the mitochondria. Inside the mitochondria the acylcarnitine will be converted back to fatty acyl CoA and is used in β-oxidation. For medium chain fatty acid, these transport proteins are not required. For the production of ATP during electron transport chain mechanism, the NADH and $FADH_2$produced by fatty acid oxidation is utilized. Malonyl CoA regulates fatty acid utilization by inhibiting CPT-1 and uptake of fatty acid is blocked (Paulson, Ward and Shug, 1984). Glucose will become the most preferred substrate for the heart when the glucose and insulin concentration increases. With the help of transporters like GLUT 1 (insulin independent) and GLUT 4 (insulin dependent), glucose is up taken in to cardiomyocytes. Glucose will be converted to pyruvate during glycolysis and get converted to acetyl-CoA and taken by the mitochondria and enters Kreb cycle. The produced NADH and FADH2 are used by the electron transport system for the generation of ATP. Increased fatty acid oxidation will inhibit glucose oxidation and increased glucose oxidation block fatty acid metabolism (Randle, England and Denton, 1970). Increased citrate formed during Kreb

cycle will inhibit glycolytic enzymes like phosphofructo kinase 1 and indirectly block hexokinase (Lopaschuk et al., 2010). Acetyl CoA produced with the help of pyruvate dehydrogenase can inhibit fatty acid oxidation enzyme, 3-ketoacyl CoA thiolase. Another fatty acid oxidation enzyme, 3-hydroxy acyl CoA dehydrogenase will be inhibited by NADH produced during glucose oxidation (Olowe and Schulz, 1980).Thus it can be understood that there exists several regulatory pathways in heart that help in the optimal use of the substrates available.

Figure 7: Cardiac metabolism

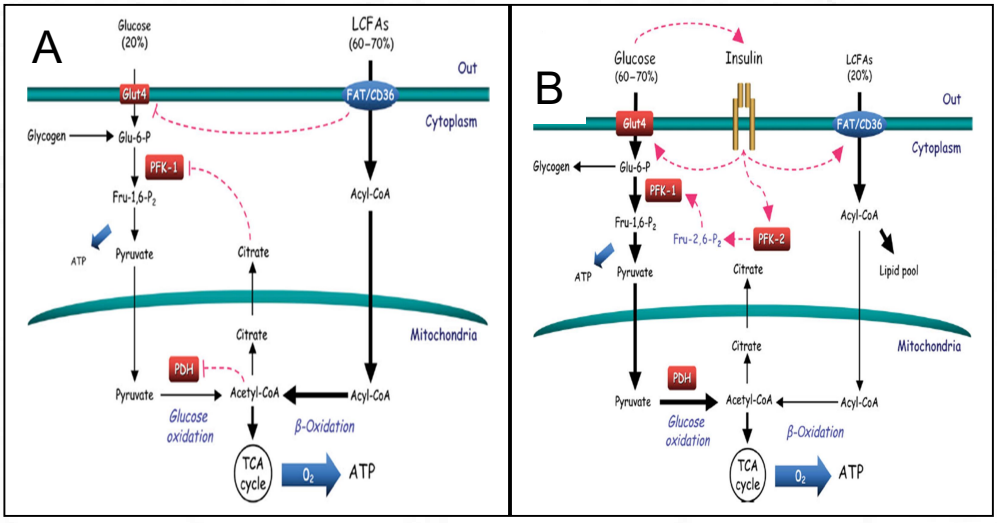

Adapted from (Bertrand et al., 2008) *Cardiac metabolism under normal (A) and insulin (B) conditions*

II. 2. Metabolic makeover in diabetic heart

In a healthy person, pancreatic β cells will uptake the increased glucose during the postprandial conditions and result in the increased production of ATP leading to the closure of ATP dependent K_{ATP} channels. This will result in accumulation of K^+ ions that depolarizes the plasma membrane thereby activating the calcium channels. It will cause an influx of calcium ions and result in insulin release (Kaufman, Li and Soleimanpour, 2015). In T2DM, this process is altered and the gradual decrease in insulin results in increased extracellular

glucose accumulation (Doliba et al., 2012). In the early stages of diabetes, the inadequate response of insulin is compensated by over production of insulin, resulting inhyperinsulinaemia. Hyperinsulinaemic condition may withstand for prolonged time period and in the later stages of diabetes due to loss of pancreatic β cell function, result in hypoinsulinaemia and hyperglycemia (Heather and Clarke, 2011). During diabetes, as insulin cannot regulate the action of hormone sensitive lipase in adipose tissue and secretion of low density lipoproteins by liver cause increase in the level of free fatty acids in the blood. As a result the peroxisome proliferator activated receptor-α (PPAR-α) will be activated in the heart and increased fatty acid uptake and decreased GLUT 4 translocation occurs in myocardium (Gulick et al., 1994). PPARα will activate the enzymes for β-oxidation resulting in enhanced β-oxidation in diabetic cardiac tissue. Due to the availability of free fatty acids, an increased level of triacylglycerol (TAG) accumulation occurs in diabetic myocardium. Since they are not able to store lipids, the long chain fatty acyl-CoA will be converted to diacylglycerol and ceramide, which are highly toxic to the cardiomyocytes. Since fatty acids are less efficient as a fuel for ATP generation than glucose, the diabetic heart with elevated fatty acid oxidation showed a 30% decrease in cardiac efficiency (Lopaschuk et al., 2010). Diabetes causes liver to produce ketone bodies, acetoacetate, β-hydroxy butyrate (Sato et al., 1995) from non-esterified fatty acids. These elevated ketone bodies will be used by the diabetic myocardium for the production of acetyl CoA can cause defects in energy metabolism (Chong, Clarke and Levelt, 2017). Various studies showed that in diabetes, increased uncoupling proteins can cause inefficiency in mitochondrial metabolism. Increased ROS can also trigger uncoupling and thereby reduced ATP production. This will ultimately affect the contractile function in the diabetic heart (Brand et al., 2004).

II. 3. Mitochondrial respiration in type 2 diabetic heart

Increased level of circulating free fatty acids and triglycerides will cause accumulation of triglycerides in diabetic cardiac tissue. As a result of accumulation of triglycerides, a

condition called cardiac steatosis arises, which finally result in cardiac dysfunction. A measure of mitochondrial efficiency, ratio of ATP produced per oxygen consumed was decreased in the diabetic heart. Increased ROS produced by the mitochondria during diabetes also lead to cardiac mitochondrial dysfunction (Anderson et al., 2009). A study in *db/db* mice showed that the cardiac pyruvate- and succinate-mediated complex I and II respiration were decreased. The long chain fatty acid utilization was decreased and resulted in accumulation of long chain β-hydroxy fatty acid in heart (Kuo et al., 1983). In another study done in *db/db* mice, cardiac mitochondria showed reduced state 3 respiration and defect in metabolizing complex I substrates, pyruvate and fatty acids. Even though the enzymes involved in β oxidation was active in diabetic heart, defect was observed in the electron transport chain complexes (Kuo, Giacomelli and Wiener, 1985). The oxygen consumption in glucose and palmitate perfused heart in ob/ob mice was increased. But the glutamate- and palmitate- mediated state 3 respiration was decreased (Boudina et al., 2005). Reduced palmitate and glutamate oxidation and ATP synthase activity was observed in subsarcolemmal mitochondrial in *db/db* mice (Dabkowski et al., 2009). A decreased cardiac fatty acid- and glutamate-mediated state 3 respiration was observed in a high fat fed streptozotocin-induced diabetic mice (Marciniak et al., 2014). Cardiac interfibrillar mitochondrial subpopulation of male FVB streptozotocin-induced diabetic mice showed reduced ATP synthase activity. Their electron transfer flavoprotein, ubiquinone oxidoreductase mRNA was significantly reduced, reflecting the altered fatty acid substrate utilization (Croston et al., 2013). A work in *db/db* mice showed decreased oxygen consumption and ATP levels in cardiomyocytes (Veeranki et al., 2016). Recent study in a streptozotocin-induced diabetic mice exhibited decreased activity of electron transport chain complex and ATP levels (Wu et al., 2017). There are many published reports on cardiac mitochondrial respiration in different models of type 2 diabetes but less reports are published on autophagy regulated mitochondrial respiration in type 2 diabetes. Impaired or deficient autophagy in cardiomyocytes leads to the accumulation of damaged or dysfunctional mitochondria. In an autophagy deficient mice model (Atg $7^{-/-}$ conditional

knockout) in pancreatic β cell and skeletal muscle, damaged and dysfunctional mitochondria were accumulated and intracellular production of ROS was very high. An altered basal mitochondrial oxygen consumption and a pronounced reduction was observed in FCCP mediated maximal oxidative capacity (Wu et al., 2009). This study showed the role of autophagy in maintaining the mitochondrial function in normal conditions. Resveratrol treatment activated autophagy and improved theATP linked mitochondrial respiration and the FCCP mediated maximal respiration in human cardiac microvascular enthothelial cells exposed to hyperglycemia (Joshi et al., 2015). Inhibitors of autophagy, chloroquine and bafilomycin treatment in the primary rat cortical neurons significantly reduced the mitochondrial oxygen consumption rate of basal, ATP linked, maximal oxidative capacity and reserve capacity (Redmann et al., 2016). There are no studies reported so far regarding the regulation of mitochondrial respiration in T2DM by controlling autophagy in heart tissue.

II. 4. Mitochondrial respiration in offsprings of diabetic and obese mothers

Gestational diabetes causes mitochondrial dysfunction in various tissues of offsprings. A study of maternal obesity where the skeletal muscle mitochondria of 3-month-old male offspring showed decreased complex II and III activity, while no change was observed in female offsprings (Shelley et al., 2009). A reduced ETC enzyme complex activity in the liver tissue in offsprings was observed in a high fat diet pregnancy of rat model (Bruce et al., 2009). In another study of high fat fed model of pregnancy, rat aortas showed reduced expression of mitochondrial complexes I, II and III in 6-month-old offsprings (Taylor et al., 2005). A work done in high fat fed pregnancy in rat showed reduced expression of complex I in soleus muscle of male offspring. Also the nuclear genes coding mitochondrial electron transport system complexes were found down regulated in the skeletal muscle (Pileggi et al., 2016). Dams fed with high fat during the pregnancy, one year old rat offspring showed reduced oxidative phosphorylation and expression of complexes I, II and V in skeletal muscle. Even though mitochondrial dysfunction were observed, the mitochondrial DNA copy

number was unchanged (Latouche et al., 2014). The expression of complex II, III and V were found reduced in liver of a 21 day-old male rat offspring of obese mothers (Borengasser et al., 2011). Reduced oxidative capacity was observed in fetal skeletal muscle of Japanese macaques mothers which are on high fat diet (McCurdy et al., 2016). In another study of maternal high fat during pregnancy, mitochondrial dysfunction was observed in skeletal muscle of offspring across three generations. F1 offsprings exhibited larger mitochondria with a lower state 3 respiration in soleus muscle. Also reduced mitochondrial complexes II, III and V, elongated mitochondria with disorganized cristae, and lipid droplet accumulation was noted in gastrocnemius muscle of F1 offsprings. F2 offspring's gastrocnemius muscle also exhibited the reduction of these mitochondrial complexes. The gastrocnemius muscle of F3 offspring had enlarged mitochondria with abnormal cristae, but no difference was observed in their electron transport chain complexes (Saben et al., 2016).

Only a single work has been published so far showing impaired cardiac function due to mitochondrial dysfunction and metabolic stress in offsprings of high fat diet fed-STZ model of pregnancy. They had analyzed the cardiac and mitochondrial function in newborn pups and they showed altered contractile and diastolic function in them. Reduced basal and maximal mitochondrial respiration, reduced ATP levels, altered spare respiratory capacity and proton leak were observed in mitochondria of neonatal isolated cardiomyocytes of ODM (Mdaki et al., 2016). Till now no reports are published regarding the cardiac mitochondrial respiration at different stages of offsprings (weaning, adult period) of diabetic mothers and also the separate analysis of cardiac mitochondrial respiration in male and female offsprings of diabetic mothers.

II. 5. Molecular mechanisms of autophagy

Autophagy is a prominent cellular pathway which involves the segregation of cytoplasmic cargo and organelles to lysosomes for their degradation. *ATG* genes, a set of specific genes

are controlling the process of autophagy. More than 30 *ATG* genes are discovered in yeast and several homologues of *ATGs* in yeast are found out in mammals which are highly preserved during evolution (Eskelinen and Saftig, 2009). The initiation process of autophagy in yeast and mammals are less understood. In yeast, a novel structure called preautophagosomal structure (PAS) is formed during the initiation process of autophagy (Noda, Suzuki and Ohsumi, 2002). Cytoplasm to vacuole targeting pathway (Cvt) is present only in yeast, involves the transport of inactive enzymes (α-mannosidase and aminopeptidase I) from cytoplasm to vacuoles (Shintani et al., 2002). In mammals it is noted that ER-mitochondrial junctions or contact sites will function as phagophore, considered as a precursor for autophagosome formation. Phagophore may contain portions of plasma membrane, golgi bodies, mitochondria and endoplasmic reticulum (Bernard and Klionsky, 2013).

Class III PI3-kinase, an enzyme plays a crucial role in initiation of autophagy which help in synthesizing phosphatidylinositol 3-phosphate (PI3P) from phosphatidylinositol. Since the PI3P is a docking lipid, it can enhance the closing of autophagosome membrane and entrapment of cytoplasmic cargoes into autpophagosomes. Beclin 1, a mammalian homolog of Atg 6 plays an important role in modulating PI3-K inase activity (Tassa et al., 2003). The second important kinase system, mammalian target of rapamycin (mTOR) can regulate autophagy by its interaction with Atg 1. For beclin 1 to get activated, it should be dissociated from its binding partner Bcl-2. The released beclin 1 will form a transient complex with Atg 14, vacuolar protein sorting (vps) 15 and lipid kinase vps 34 that forms the functional PI3K complex. The lipid kinase activity of this complexes helps in PI3P formation that contribute the targeting of various atgs to the nucleation complex. There are mainly two important proteins, Atg 14L and rubicon that form complex with Beclin 1, which regulates the autophagosome formation. If Atg 14L binds wih beclin 1 positively regulate the formation of autophagososme. But the complex formation of beclin 1 with Rubicon retards or inhibits the formation of autophagosome.

Figure 8: Beclin 1 complex in autophagy

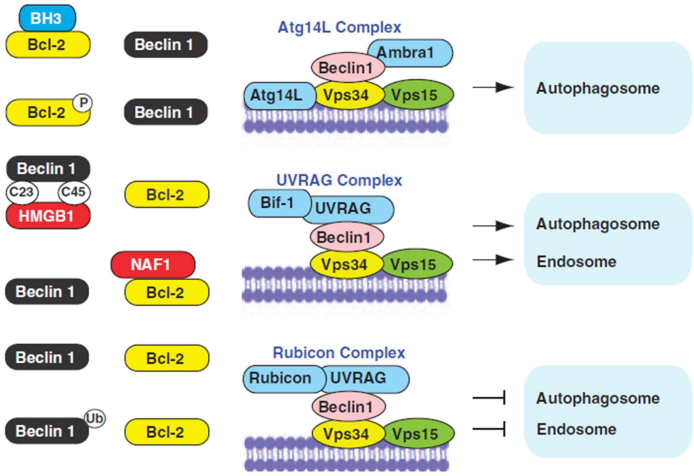

Adapted from (Kang et al., 2011). Model of Beclin 1-Bcl-2 dissociation and the complex formation with Atg 14L and Rubicon

The Atg proteins can be divided into different functional complexes. ULK1, mammalian homolog of Atg 1can be proposed as the first complex in autophagosome formation (Mariño and López-Otín, 2004). In the absence of adequate nutrients or ATP or presence of mTOR inhibitors, ULK1 can recruit Atg 11, Atg 13 and Atg 17 to form a complex which helps in the initiation of autophagy. After the assembly of Atg 1 to the membrane, the second important complex is Atg 9 and its related proteins like Atg 2 and Atg 18 that delivers membrane to the developing phagophore (Fujitani, Ueno and Watada, 2010). The Atg 1 complex can recruit Atg 5 and Atg 12 resulting in a complex formation of Atg5-Atg12.Atg 12 proteins are activated by Atg 7 and Atg 10 by formation of thioester linkage. This complex will conjugate with Atg 16L to form a multimeric complex. These Atg 5-Atg12-Atg16 complex oligomerise and are targeted to the phagophore, helps in the assembly of autophagosomes (Mizushima et al., 2003). This Atg 5-Atg 12 complex functions like a E3-like activity, helps in the attachment of LC3 (microtubule associated proteinlight chain 3), a mammalian homolog of Atg 8 in to the membrane. Newly synthesized LC3 is cleaved by a cysteine protease Atg 4, expose a glycine residue, (Gly 120) at the carboxyl terminus region termed LC3-I. This LC3-

I undergo a series of ubiquitin like reactions activated by enzymes Atg 7, Atg 3 and Atg5-Atg12-Atg16 complex (Mariño and López-Otín, 2004). This activated LC3-I will conjugate with PE to form LC3-II, which is the lipidated form of LC3 (Kabeya et al., 2000) . LC3 is the only protein, which is present in preautophagosomes and autophagosomes. So it is considered as an important marker for evaluation of autophagy since it is present in autophagosomes from initiation to degradation. An adaptor molecule p62/ SQSTM1has an unique ability of self oligomerization and a C-terminal ubiquitin associated domain for attaching with ubiquinated proteins. So it can ubiquitinate cytosolic cargoes and can attach with LC3 Inside the autophagosome membrane. Along with LC3, p62 also get degraded inside the autophagosomes. So the intracellular level of p62 also denotes the autophagic status along with LC3 and is widely used as a marker of autophagy (Komatsu and Ichimura, 2010). After maturation and closing of autophagosomes, it fuses with the lysosomes to form autophagolysosomes. Inside the autophagosomes, the cytoplasmic cargoes will be degraded with help of lysosomal enzymes (Eskelinen and Saftig, 2009).

Cathepsin D, a soluble lysosomal aspartic endopeptidase help in the degradation of cargoes inside the autophagosomes (Hasui et al., 2011). LAMP-2, lysosome associated membrane protein 2 play an important role in maintenance and adhesion of lysosomes with autophagosomes (Eskelinen et al., 2002). After the degradation of cargo, the remaining molecules like amino acids, fatty acids and nucleotides will be transported back to the cytosol for the synthesis of various macromolecules and for maintaining different cellular functions(Galluzzi et al., 2017). If adequate nutrients or ATP is present, growth factors like insulin can activate class I PI3-kinase which will activate Akt pathway and in this way mTOR will be activated and the process of autophagy will be inhibited or reduced (Fujitani, Ueno and Watada, 2010).

Figure 9: Molecular pathways regulating macroautophagy

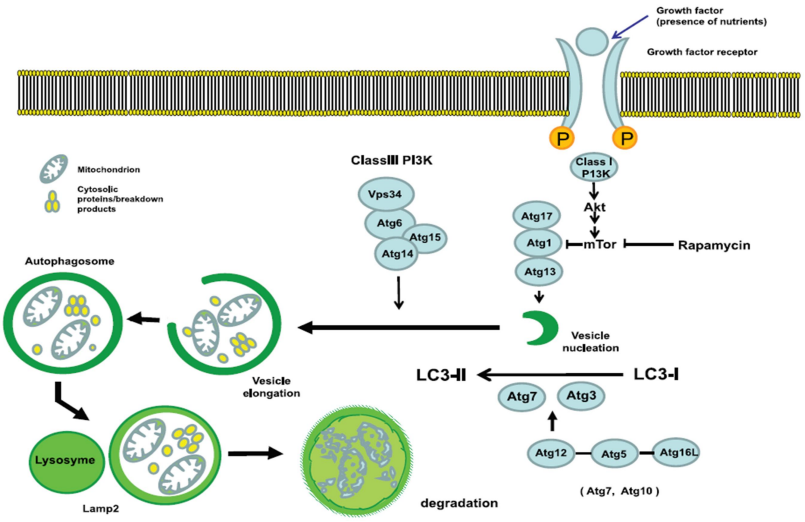

Adapted from (Fujitani, Ueno and Watada, 2010). Pathway showing the molecular mechanisms of autophagy

II.5.1. Selective autophagy

In selective autophagy, a specific organelle or molecule is targeted for the degradation. Usually it targets damaged or dysfunctional organelles like mitochondria, ER, peroxisomes and even microorganisms. Non-selective autophagy involves the bulk degradation of cytoplasmic contents during starvation etc. Based on the substrates of selective autophagy, they are given specific names such as mitophagy for mitochondria, pexophagy for peroxisomes, lysophagy for lysosomes, reticulophagy for ER, xenophagy for microbes etc (Feng et al., 2014). For each of the selective autophagy, the autophagic receptors, the proteins that bind with the substrates and targets to autophagosomes will change. Some of them are p62, NBR1, OPTN, NDP52, BNIP3, BNIP3L, ATG34, FUNDC1, PHB2, TRIM5, TAX1BP1, Atg19, and Atg32 etc (Chourasia et al., 2015)(Wei et al., 2017) and these molecules usually have a LIR (LC3 interacting region) which helps them to bind with LC3 inside the autophagosome membrane (Galluzzi et al., 2017). Among these, mitophagy is the most characterized selective autophagy (Kubli and Gustafsson, 2012).

Figure 10: Substrates of macroautophagy

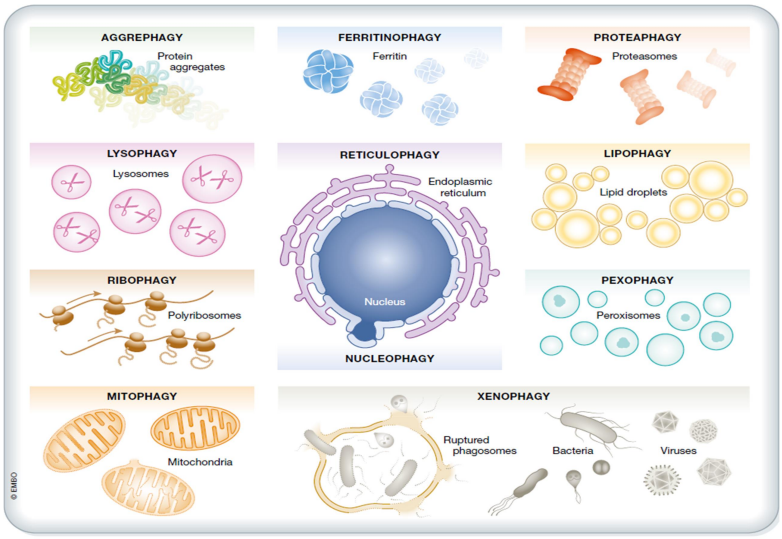

Adapted from (Galluzzi et al., 2017) Heterogeneous set of cytoplasmic entities for selective autophagy

II.5.2. Mitophagy

A well planned system of selective autophagy is needed for the elimination of damaged and dysfunctional mitochondria in the cells. Mitochondrial autophagy is so important to maintain the quality and quantity of mitochondria. There are three important pathways for mitophagy. They are Parkin/PINK 1 mediated mitophagy, BNIP3 and NIX/BNIP3L mitophagy and FUNDC1-mediated mitophagy (Ashrafi and Schwarz, 2013). The reduced mitochondrial membrane potential of the damaged mitochondria recruits PINK 1 (phosphatase and tensin homolog-induced putative kinase 1), which is nuclear-coded mitochondrial serine/threonine kinase act as a mitochondrial stress sensor (Greene et al., 2012). In healthy mitochondria, PINK 1 is imported to the inner mitochondrial membrane and gets degraded. But in the case of dysfunctional mitochondria, PINK 1 will be attached to the outer mitochondrial membrane and recruits Parkin. The activated parkin (E3 ubiquitin ligase) ubiquitinates several proteins on the outer mitochondrial membrane, that will bind to adaptor proteins like p62 and helps in

the sequestration of damaged mitochondria towards autophagosome (Koyano et al., 2014). BNIP3 (BCl-2/adenovirus E1B 19-KDa- interacting protein 3) and BNIP3-like (BNIP3L, also called NIX) are proteins which are mitochondria-localized, having LIR motifs to interact with LC3 proteins mainly involved in removal of mitochondria in reticulocyte maturation (Kundu et al., 2008: 1). FUNDC1 (FUN14 domain-containing protein 1) is an outer mitochondrial membrane protein which is mailnly invoved in hypoxia-mediated mitophagy(Liu et al., 2012). Among these pathways, Parkin-PINK 1 plays an important role in heart(Kubli et al., 2015).

Figure 11: Different pathway of mitophagy

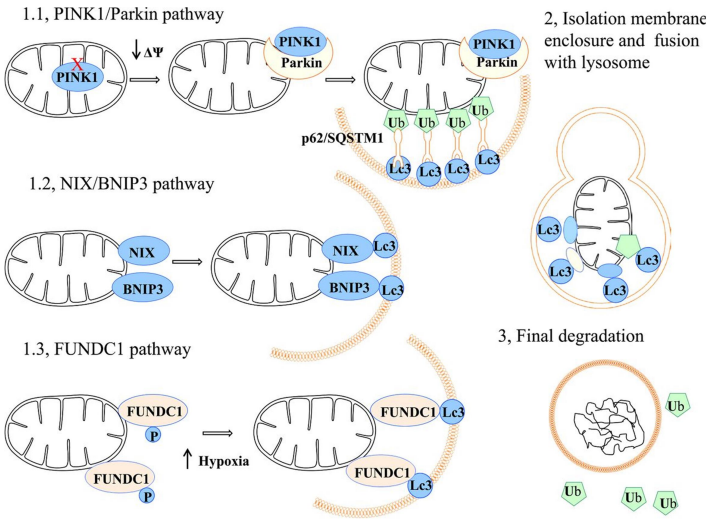

Adapted from (Bai et al., 2016) Different mitophagy mediators

II.5.3. Regulators of autophagy: mTOR and AMPK

Balanced or basal autophagy is required for maintaining the proper function of the cell. If it is lowered or excessive it may lead to cellular toxicity and result in development of pathologic conditions. So the regulation of autophagy either positively or negatively gains much importance (Chen and Klionsky, 2011). Autophagy is activated during nutrient starvation in which the autophagy induction is controlled by a molecule called mTOR (mammalian target of rapamycin), which detects signals from the cell like growth factors, amino acids, glucose,

hypoxia, energy levels etc. It has two complexes, mTOR complex I and complex II. mTORC1 is important in detection of nutrient status of cell. If there is adequate nutrient, mTOR will binds with ULK1 and autophagy induction will be inhibited. For the activation, mTOR is dissociated from the ULK1-Atg13-Atg17 complexes. Rheb, a GTP switch protein, upstream of mTORC1 can phosphorylate and activate mTORC1. Rheb is active in its GTP bound condition. A GTPase activating protein, TSC1 will replace the GTP in the Rheb with GDP and finally inactivating it. For activation of mTOR, PI3K-Akt pathway will inhibit the TSC1-TSC2 complex. Akt phosphorylates the TSC1 protein and as a result it cause the accumulation of GTP bound Rheb and that active Rheb can activate mTOR (Jung et al., 2010).

During starvation, hypoxia or increase in anabolic process, reduction of ATP in the cell occurs. The increased AMP can activate a protein known as AMPK (AMP dependent protein kinase) which will activate autophagy by its ability to inhibit mTOR complex-I (Hardie, 2011). AMPK can activate TSC1 complex thereby inhibiting Rheb and blocking mTORC1. Raptor, a subunit of mTORC1 can be phosphorylated by AMPK and leading to mTOR inhibition. Also AMPK can directly activate ULK1, the first Atg protein needed for the induction of autophagy (Roach, 2011).

Figure 12: Regulation of autophagy

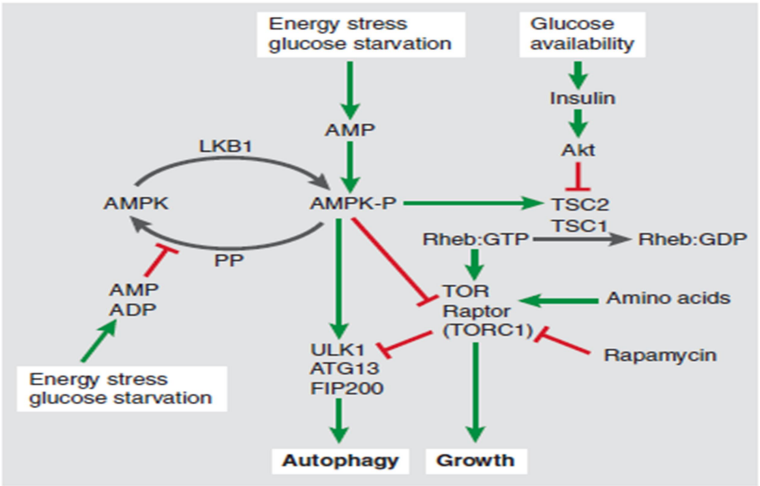

Adapted from (Hardie, 2011), Regulation of autophagy by AMPK and mTOR

II.5.4. Pharmacologic modulation of autophagy: Resveratrol and chloroquine

The process of autophagy is just like a double edged sword. It can act in a protective or destructive role according to the cellular environment. So it is very important to know the autophagic status and the crucial targets in this pathway in each of the pathologic conditions. Then only it is able to develop new pharmacological compounds that can activate or inhibit autophagy (Cheng et al., 2013).

II.5.4.1. Resveratrol as autophagic activator

Resveratrol is a stilbenoid, a natural polyphenol derivative and phytoalexin, produced by certain plants such as grapes, mulberries, blueberries etc. Although resveratrol has various targets in the body, it induces autophagy in different pathologic conditions. It activates autophagy by activating AMPK, in turn activates sirtuin 1 (SIRT1) and PGC-1α which will be a signal for the induction of autophagy (Um et al., 2010). Resveratrol can activate mitochondrial function, can elevate NAD^+/NADH ratio and also induce autophagy for clearing mutant and aggregate proteins associated with neurodegenerative diseases (Gros and Muller, 2014). Through induction of autophagic mechanisms, resveratrol was used as an anti-aging agent to increase the life span (Morselli et al., 2010). It has a protective effect in Alzheimer ’s disease (AD) by the activation of AMPK (Vingtdeux et al., 2010). Resveratrol can directly induce autophagy by blocking the mTOR-ULK1 pathway. In MCF-7 cells, cancer cell suppression was induced by resveratrol by activating autophagy in a mTOR-ULK1 dependent pathway (Park et al., 2016). Resveratrol can inhibit mTOR by attaching to its ATP binding site, thereby activating autophagy. In a type 2 diabetic model of *db/db* mice, cardiac autophagy is found to be suppressed at the final degradation step. Resveratrol treatment enhanced autophagy, suppressed hypertrophy and fibrosis and improved the cardiac function in those *db/db* type 2 diabetic mice (Kanamori et al., 2015). In a study done

in human cardiac microvascular endoothelial cells exposed to hyperglycemia, ATP linked mitochondrial respiration and the FCCP mediated maximal respiration were significantly lower and resveratrol treatment improved the mitochondrial function (Joshi et al., 2015). In a STZ diabetic model of C57BL/6 mice, resveratrol treatment reduced cardiac dysfunction and remodeling and it reduced the apoptosis and oxidative stress through enhancing the pathway of autophagy (Wang et al., 2014). Till now there are no studies reported on the regulation of cardiac mitochondrial function in T2DM by activating autophagy using resveratrol.

II.5.4.2. Chloroquine as autophagic inhibitor

Chloroquine is a drug (class 4 – aminoquinoline), lysosomotropic agent that blocks endosomal acidification. It usually accumulates in the acidic parts of the cells such as lysosomes. It leads to the inhibition of enzymes in lysosomes that need an acidic pH. So the fusion between lysosomes and autophagosomes are inhibited (Cheng et al., 2013). A study done in clear cell carcinoma, CPI-613 along with chloroquine inhibited the fusion of autophagosomes with lysosomes, induced necrosis in those cancer cells (Egawa et al., 2018). Apatinib, a tyrosine kinase inhibitor along with chloroquine induced ER stress-related apoptosis in human colorectal cancer by targeting autophagy (Egawa et al., 2018). Blockage of autophagy with chloroquine in breast cancer cells showed recurrence of early tumor (Aqbi et al., 2018). Autophagic inhibition using chloroquine and 3-methyladenine reduced rapamycin-induced protection against renal ischemia reperfusion (Li, Zhu, et al., 2018). Autophagy inhibition by a lactone component from a Chinese plant *Ligusticum chuanxiong* along with chloroquine reduced myocardial ischemia injury (Wang, Dai, et al., 2018). Chloroquine induced a progressive reduction in autophagy after myocardial infarction in rabbits(Chi et al., 2017). Hypoxic-ischemic (HI) treatment in a neonatal rat model of encephalopathy showed presence of apoptosis and autophagy proteins and is inhibited during chloroquine treatment. This inhibition of autophagy in the neurons worsened the mitochondrial dysfunction characterized by high levels of ROS, less mitochondrial

superoxide and less membrane potential (Li, Hao, et al., 2018). There was a similar report in primary rat cortical neurons, where autophagy inhibition by bafilomycin and chloroquine reduced mitochondrial quality and significantly reduced the mitochondrial OCR of basal, ATP linked, maximal oxidative capacity and reserve capacity (Redmann et al., 2016). There are no studies reported so far on the regulation of cardiac mitochondrial function in T2DM by inhibiting autophagy using chloroquine.

II.5.5. Autophagy in heart

In a terminally differentiated cell like cardiomyocytes, autophagy plays a very important role in the recycling of long lived proteins and organelles (Nishida et al., 2009). Since cardiomyocytes are rich in mitochondria, mitophagy gains much importance. As the damaged mitochondria release pro-apoptotic factors resulting in apoptosis of cardiomyocytes (Gustafsson and Gottlieb, 2003), the clearing/degradation mechanism should be properly maintained and be functional (Kim, Rodriguez-Enriquez and Lemasters, 2007). Autophagy plays a protective role in heart by maintaining in its basal level (Sciarretta et al., 2012). In cardiac HL-1 cells, activating autophagy by beclin 1 over expression reduced Bax activation and protection against ischemia-reperfusion injury (Hamacher-Brady, Brady and Gottlieb, 2006). An Atg 5 deficient heart, in their ultra structural analysis showed a aberrant, disorganized sarcomere and mitochondria were found. It resulted in increase of damaged proteins and organelles, increase in ER stress and activation of apoptosis (Sohal et al., 2001). A LAMP-2 deficient mice showed impaired degradation of proteins with accumulation of autophagososmes and showed features of cardiomyopathy (Nishino et al., 2000). These studies show the importance of basal autophagy and mitophagy in the heart.

II.5.6. Autophagy in diabetic heart

Autophagy is activated or inhibited during stress conditions. During stress and ageing, autophagy is inhibited and associated with the development of cardiac problems (Ikeda et al., 2014). There is an inevitable chance of developing myocardial ischemia and other related problems during T2DM. Several studies have shown that the metabolic disturbances in diabetic heart are due to altered autophagy (Sciarretta et al., 2012). The epicardial adipose tissue of diabetic patients showed increased autophagy and ER stress compared to subcutaneous adipose tissue from the same patients (Burgeiro et al., 2018). In a study done in STZ-induced diabetic mice showed suppressed autophagy and augmented inflammation in the heart tissue and over expression of Tax 1 binding protein had increased the autophagy, leading to decreased inflammation, reduced cardiac hypertrophy, apoptosis, fibrosis and oxidative stress (Xiao et al., 2018). In another study done in OVE26 mice, angiotensin II inhibited autophagic process and accelerated cardiac hypertrophy in the early stage of diabetes (Qian et al., 2017). Autophagy was found suppressed in a study done in STZ-induced diabetic mice. Inhibition of advanced glycation end product (AGE) prevents the cardiac remodeling and contractile dysfunction through increasing the autophagic process (Pei et al., 2018). High glucose condition in H9c2 cells had suppressed autophagy. In this study ULK 1 plays a crucial role in mitochondrial aldehyde dehydrogenase 2-offered protective effect against high glucose-induced cardiomyocyte injury by increasing autophagy (Liu et al., 2018). In obese diabetic (*ob/ob*) mice, cardiac autophagic flux was suppressed due to impaired formation of autophagosome and the suppression of autophagy is due to mTOR activation. IGF-1 (Insulin-like growth factor 1) receptor-mediated Akt activation resulted in development of hypertrophy, but it was not involved in mTOR activation and autophagy suppression (Pires et al., 2017). In an STZ-induced diabetic model, polydatin, a polyphenolic pytoalexin increased the autophagic flux and mitochondrial function by activation of sirtuin 3. Also polydatin increased the autophagic flux of cardiomyocytes in high glucose condition for 48 h (Zhang, Wang, et al., 2017). In a high fat-fed mice, blockage of RAGE (Receptor for advanced glycation end product) receptors reduced mitochondrial

damage and mitochondrial dysfunction by reducing the oxidative stress, and increasing the autophagic pathway and mitochondrial dynamics (Yu, Wang, et al., 2017). High glucose treated H9c2 cells, caused increased apoptosis with decreased autophagy and connexin43 expression. When the hyperglycemic H9c2 cells are co-treated with metformin, resulted in reduced apoptosis, increased connexin43 expression mediated through the activation of autophagic pathway(Wang, Bi, Liu, Zhao, et al., 2017). Dihydromyricetin administration to STZ-induced diabetic C57B/6J mice improved the reduced autophagy during diabetes along with reduction in oxidative stress, inflammation and improved the mitochondrial and cardiac function (Wu et al., 2017). High glucose treated H9c2 cells caused reduction in autophagy, which was enhanced by the treatment of HBSP (helix B surface peptide), a small peptide derived from helix-B domain of erythropoietin (Lin et al., 2017). In STZ-induced diabetic sirtuin3 knockout mice, increased cardiac apoptosis, mitochondrial injury and interstitial fibrosis, along with suppressed autophagy and mitophagy were observed. Over expression of sirtuin3 in diabetic mice enhanced autophagy and mitophagy, along with decreased apoptosis and inhibited the mitochondrial injury that adds a protective effect for diabetic cardiomyopathy (Yu, Gao, et al., 2017: 3). Apelin, an adipokine gene therapy in a STZ-induced diabetic mice exhibited upregulation of cardiac autophagy by activating sirtuin3 and suppression of ROS-NF-Kb pathway (Hou et al., 2015). In a rat model of T2DM, inhibition of dipeptidyl peptidase-4 improves the survival rate and reduces the acute mortality after myocardial ischemia through restoring autophagy by reducing the interaction of beclin-1 with Bcl-2 (Murase et al., 2015). A study in db/db type 2 diabetic mice, increased formation of autophagosome was observed, but the autophagic process is suppressed at final step, i.e., fusion of autophagososmes with lysosomes were defective (Kanamori et al., 2015).Otsuka Long-Evans Tokushima fatty (OLETF) diabetic rats on calorie restriction (30% energy reduction) improved diastolic function and increased cardiac telomerase activity and autophagy(Makino et al., 2015). Enhanced autophagic flux by the treatment with resveratrol in a STZ-induced diabetic mice reduced myocardial oxidative stress injury (Wang et al., n.d.). In type 2 diabetic rat model, O-GlcNAcylation of beciln-1 caused recuced autophagy in

diabetic heart (Marsh et al., 2013). In diabetic OVE26 mice, chronic administration of metformin improved the cardiac function by enhancement of autophagy through AMPK activation (Xie et al., 2011).

In contrast to the above reports, STZ-induced diabetic mice, the upregulated autophagy during diabetes was reduced by the action of catalase, which inhibited the translocation of p65 to nucleus and prevented beclin 1 mediated upregulation of autophagy (Wang, Tao, Huang, Zhan, et al., 2017). In *db/db* mice heart, down regulation of a transcription factor, SP1 (Specificity protein 1) exhibited loss of Mir30c and subsequent activation of autophagy by activation of beclin1 and it lead to diabetic cardiomyopathy (Chen et al., 2017). Liraglutide, a glucose lowering agent given to Zucker diabetic fatty rats restored the autophagy and reduction of myocardial damage by enhancement of autophagy through the activation of AMPK and inhibition of mTOR (Zhang, Ling, et al., 2017). In STZ-induced diabetes in Sprague-Dawley rats, increased autophagy was reported in myocardial ischemia-reperfusion injury. The diabetic rats when treated with N-acetylcysteine, reduced the ischemia-reperfusion injury by inhibiting the pathway of autophagy (Wang, Wang, Yan, Wang, et al., 2017). H9c2 cells cultured in a low-after-high glucose caused reduced expression of connexin43 by enhancement of autophagy involving PI3K/Akt/mTOR and MEK/$ERK_{1/2}$ signaling pathways(Bi et al., 2017). STZ-induced diabetic HFpEF (heart failure with preserved ejection fraction) mice showed excessive autophagy with decreased cardiac function and chloroquine (inhibitor of autophagy) treatment in these animals improved the cardiac diastolic function by inhibiting the process of autophagy (Yuan et al., 2016). Enhanced myocardial autophagy and fibrosis were reported in STZ-induced diabetes in rats and the treatment with sodium hydrosulfide significantly reduced fibrosis and autophagy by upregulation of PI3K/Akt1 signaling pathway (Xiao et al., 2016). Through activation of beclin-1 mediated pathway, increased autophagy was reported in right atrial appendage tissue of diabetic patients in New Zealand population (Munasinghe et al., 2016). Attenuation of cardioprotective miR-133a in left ventricular apex tissue of diabetic heart failure patients undergoing mechanical unloading resulted in upregulation of autophagy and hypertrophy

(Nandi et al., 2015). STZ-induced diabetic rat showed significant enhancement of autophagy, which played a role in juvenile diabetic cardiomyopathy and caused retardation of cardiac growth in those diabetic rats (Lee et al., 2012).

In most of the published reports, cardiac autophagy was reduced in type 2 diabetes while in some papers it was reported to be in the enhanced state. Autophagic adaptations during type 2 diabetes depend on the cellular environment, animal model, experimental conditions, medications and other co-morbidities of the patients, duration of diabetes etc. In all these studies on diabetes, autophagy was assessed at a single time point during the course of study period. Since a single time point evaluation may only be revealing the status of autophagy at that time point only and not at any other time point, it becomes difficult to ascertain the observed changes in autophagy as a stable outcome due to the disease condition. It is also not evident whether the activation or inhibition of autophagy at different stages of T2DM may be a reason for the defects in metabolism of myocardium. Hyperinsulinemic condition at the initial period and hypoinsulenimic condition at the later stage of type 2 diabetes can cause fluctuations in cardiac autophagic status. Thus the crucial role of autophagy in T2DM at different time points remains unclear and becomes an important step in understanding its critical role.

II.5.7. Autophagy in gestational diabetes

In pregnancy, the role of autophagy starts from embryogenesis, survival of blastocysts, formation of extravillous trophoblast, placental development, implantation of embryo into uterus etc.,(Nakashima, Aoki and Saito, 2016). A single nucleotide polymorphism in ATG16L in pregnant women influenced the time to delivery during labor induction with an unfavourable cervix (Doulaveris et al., 2013). The placental nutrient supply from the mother to the baby suddenly stops at birth and the neonates undergo severe starvation until it is lactated by mother. At that starvation period, autophagy is upregulated in high levels for 3-12 h in various tissues of the neonates to overcome the starvation (Kuma et al., 2004). A recent study had shown that autophagic activity was increased in placenta and extravillous

trophoblast in GDM patients (Ji et al., 2017). Autophagy plays a crucial role in high glucose-induced malformation in heart tube in chick embryos (Wang et al., 2015). Baicalin, a polyphenolic flavanoid can reduce the hyperglycemia-induced cardiovascular malformation in early chick embryos by suppressing the production of ROS and inhibiting autophagy (Wang, Liang, et al., 2018). A study in human diabetic placenta and stillborn fetal pancreas showed altered autophagy (Avagliano et al., 2017). Since heart is an important organ which is affected in offsprings of diabetic mothers (ODM), autophagy - an important physiologic process required for energy transaction is also supposed to play a significant role in controlling the myocardial metabolism. There are no studies reported so far about the cardiac autophagic status of ODM and it shows the importance of studying such process in ODM.

II. 6. Rationale of the study

It is clear from the previously published reports that type 2 diabetes leads to inhibited autophagy in animal models and cell lines under hyperglycemic conditions and also the modulators of autophagy were found to be favouring inhibition of autophagy in T2DM heart. But studies that focus on autophagic status at different time points of type 2 diabetes are very few in numbers and there is only one study that reported autophagy in type 2 diabetic human heart. But no studies have been reported in Asian Indian population. Also there are no studies that evaluate the role of autophagy in diabetic cardiac mitochondrial respiration. No studies have so far been published with regard to cardiac autophagy in offsprings of gestational diabetic mothers, even though a single paper was published on cardiac mitochondrial respiration in offsprings of gestational diabetic rat. Based on this, we proposed to evaluate cardiac autophagy in Asian Indian population. We also proposed to analyze autophagy in cardiomyoblast (H9c2) at different time points of hyperglycemia. Another study was initiated to evaluate cardiac autophagy and its role in regulating mitochondrial respiration at two time points of T2DM in mice models. Due to the paucity in data regarding effect of untreated gestational diabetes on cardiac autophagy and

mitochondrial respiration in offsprings of GDM mothers, we developed a GDM rat model and evaluated cardiac autophagy and mitochondrial respiration in their offsprings at weaning and adult stages.

II.7. Hypothesis

1) Type 2 diabetes mellitus causes altered cardiac autophagy and thereby brings changes in mitochondrial respiration

2) Untreated gestational diabetes in mothers will affect cardiac autophagy and mitochondrial respiration in offsprings

III.MATERIALS AND METHODS

III. 1. Reagents, kits, drugs and antibodies

Dulbecco's modified Eagle's medium (DMEM), Fetal Bovine Serum (FBS), Antibiotic antimycotic solution for cell culture, reagents needed for the isolation of mitochondria, various substrates, uncouplers and inhibitors for the cardiac oxygen consumption studies were purchased from Sigma Aldrich, St. Louis, MO, USA. For analyzingmitochondrial DNA copy number, qRT PCR master mix (Origin Diagnostic and Research, India), and primers (BR Biochem Life Sciences Pvt. Ltd, India) were purchased. All other reagents for the study were purchased from Sigma Aldrich, St. Louis, MO, USA.

Drugs like Streptozotocin, Nicotinamide and chloroquine were purchased from Sigma Aldrich, St. Louis, MO, USA. Resveratrol was purchased from MP Biomedicals, California, USA.

Immunohistochemistry kit (Abcam, Cambridge, UK), Insulin assay kit (RayBiotech, Norcross, GA), Glucometer and strips for random glucose analysis in mice and rat study (Accu-Chek, Roche, Germany), HbA1c kit (Nyco card Kit, Alere Technologies AS, Oslo, Norway), and plasma triglyceride assay kit (Accurex Biomedical, Mumbai, India).

Antibodies used in the study were purchased from:, LC3 B, Atg 14, Rubicon, PINK 1, LAMP2, p62/SQSTM1, OXPHOS, ANT1, UCP3, MnSOD, Glutathione peroxidase, O-GlcNAc (Abcam, Cambridge, UK), β-actin (Sigma- Aldrich, St Louis, MO, USA), Cathepsin D (Santa Cruz Biotechnology Inc., Santa Cruz, CA, USA), Beclin 1, Atgs (3,5,7,12,16L1), ULK1, pULK1 (Ser 555), mTOR, pmTOR (Ser 2448), Parkin, AMPKα, pAMPKα, sirtuins (SirT 3 and 5), vinculin, β- Tubulin, Horse Radish Peroxidase (HRP) conjugated anti rabbit and anti mouse IgG secondary antibodies (Cell Signaling Technology, Massachusetts, USA).

III. 2. Collection of human right atrial appendage

Right atrial appendage biopsy samples were obtained from type 2 diabetic and non-diabetic patients with ischemic heart disease, who underwent coronary artery bypass grafting at Sree Chitra Tirunal Institute for Medical Sciences and Technology (SCTIMST). The tissue

samples were taken from the site of right atrial cannulation during the surgery. The study was carried out with the approval of the institutional ethics committee (IEC), and informed consent was obtained from patients whose tissues were collected for the study. A portion of tissue sample was immediately dipped in buffered formalin for immunohistochemistry. A part of the cardiac tissue was flash frozen in liquid nitrogen for protein assays and stored at -80^{0}C until assayed.

Figure 13: Study design for atrial tissue experiments

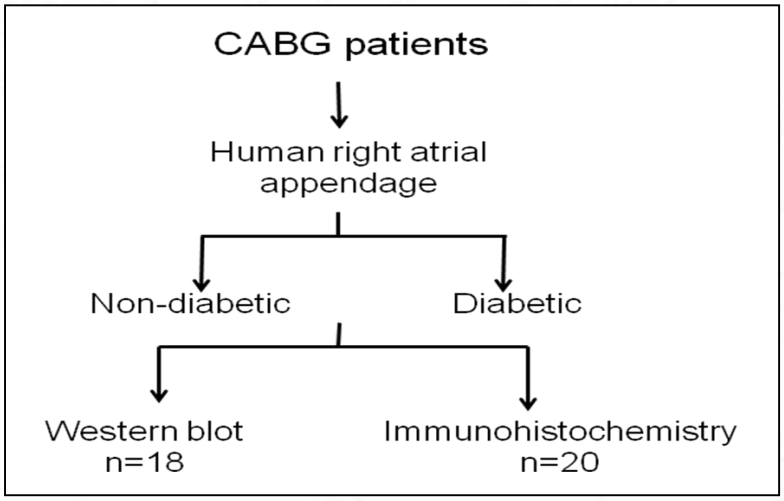

Flow chart representing the number of samples taken for each experiment.

III. 3. Cell culture and maintenance

H9c2, rat embryonic cardiac myoblast (adherent) cells were obtained from National Centre for Cell Science (NCCS), Pune. In a humidified atmosphere of 5% CO_2 at 37^{o}C, the cells were grown in 25 mm cell culture flask as monolayer culture in DMEM (5.5mM glucose) containing 10% FBS and antibiotic antimycotic solution (penicillin, streptomycin and amphotericin B). Based on the growth rate, the medium was changed every 2 days for maintaining the culture. For detaching the adherent cells from the plate/flask Trypsin-Phosphate-Versene-Glucose (TPVG) was used. The cells were centrifuged and the supernatant was removed. Then the cells were resuspended in 1.0 ml of freezing medium (75% medium, 5% FBS, 20% DMSO) and stored at -80^{0}C freezer.

Upon reaching a confluence of 60-70%, the cells were incubated with control (5.5 mmol/L) or high glucose (30 mmol/L) medium for two time points, 4h and 48 h respectively. To account for medium hyperosmolarity, the cells were incubated with mannitol (24.5 mmol/L) in normal medium containing glucose (5.5mmol/L). For all experiments DMEM containing 1% FBS was added.

Figure 14: Study design for cell culture experiments

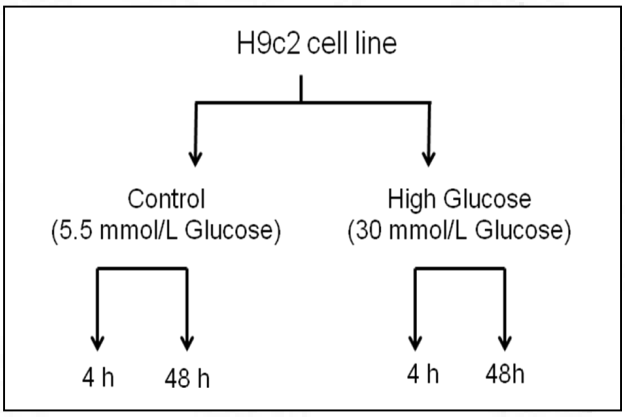

Flow chart representing the study design taken for cell culture experiments.

III. 3. 1. Reagents used

III. 3. 1. 1. DMEM preparation (1 litre) (pH 7.4)

5.5 mM DMEM (16 g), 30mM DMEM (5.5mM DMEM + 4.5 g dextrose), Sodium bicarbonate (2.2 g), Sodium pyruvate (0.11 g), 100 U/ml Penicillin/ Streptomycin, Amphoterixcin B in sterile distilled water, filtered and stored in autoclaved bottles.

III. 3. 1. 2. Phosphate-buffered saline (PBS) (pH 7.4)

Sodium chloride 137 mM, potassium chloride 2.7 mM, disodium hydrogen phosphate 10.14 mM, potassium dihydrogen phosphate 1.76 mM in sterile deionised water.

III. 3. 1. 3. TPVG solution (pH 7.4)

0.1% trypsin, 0.2% EDTA and 0.05% glucose in PBS.

III. 4. Animal models

Animals were treated according to the guidelines approved by the SCTIMST institutional animal ethics committee (IAEC) for animal care and use. Animals were bred at division of laboratory animal science, Biomedical Technology Wing, SCTIMST. For type 2 diabetes, mice model was taken and for gestational diabetes, rat model was used. All animals were housed in individually ventilated cages with proper bedding, humidity and light. They had free access to standard chow and water.A drop of blood ~ 5 µL was taken from the tail tip of animals and glucose levels were measured using glucometer. Blood glucose levels and body weight were noted on a weekly basis. Their HbA1c levels were checked just before euthanasia. After completing their corresponding time period of experiment, both mice and rat groups were sacrificed by cervical dislocation and whole heart was collected and immediately dipped in liquid nitrogen and stored at -80^0C for protein assays. Blood was collected just before sacrifice from orbital sinus and plasma was collected for insulin assay and triglyceride assay. For mitochondrial oxygen consumption studies, the sample was immersed in ice cold BIOPS solution and immediately taken for mitochondrial isolation.

III. 4.1. Type 2 diabetic mice model

For the study, C57BL/6 male mice of 8 weeks (25 – 40 mg) were used. The mice were divided into two groups: Control and diabetic. The control mice were injected with vehicle, citrate buffer. T2DM was induced in mice by intraperitoneal injection of two doses of nicotinamide (NA) (100 mg/kg) and streptozotocin (STZ) (120 mg/kg) each at alternate days after fasting for 16 h. After 15 min of injection of NA, STZ will be injected to the mice. Development of T2DM was confirmed by checking the blood glucose levels of the animals. Both the control and the diabetic group were again divided to two groups based on the time period of hyperglycemia. One group of mice were maintained hyperglycemic for 2 weeks and and the other maintained hyperglycemic for 10 weeks. After the respective time point, mice groups were sacrificed and heart and blood tissue were obtained.

Figure 15: Study design for mice experiments

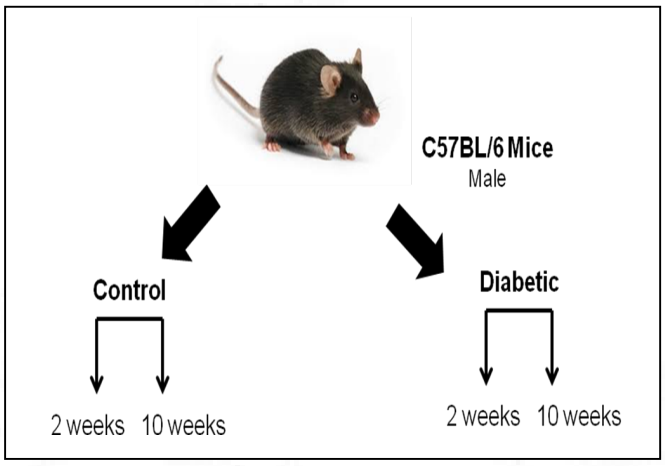

Flow chart representing the study design adapted for type 2 diabetic mice experiments.

III. 4.1.1. Oral Glucose Tolerance Test (OGTT) for mice

Both control and diabetic mice were subjected to 12h fasting and then orally given with glucose solution (2mg/total body weight) in 200µl water. Glucose values were obtained from tail tip blood before and after (at 10, 20, 30, 60 and 120 min) ingestion of glucose.

III. 4.1.2. Drug treatment for mice

For studying the mitochondrial respiration in mice by modulating autophagy, an autophagic activator, Resveratrol (5 mg/kg) and an autophagy inhibitor, Chloroquine (10 mg/kg) were injected intraperitoneal on consecutive days for 2 weeks after maintaining hyperglycemia for 2 weeks and 10 weeks.

Figure 16: Study plan for drug treatment in mice

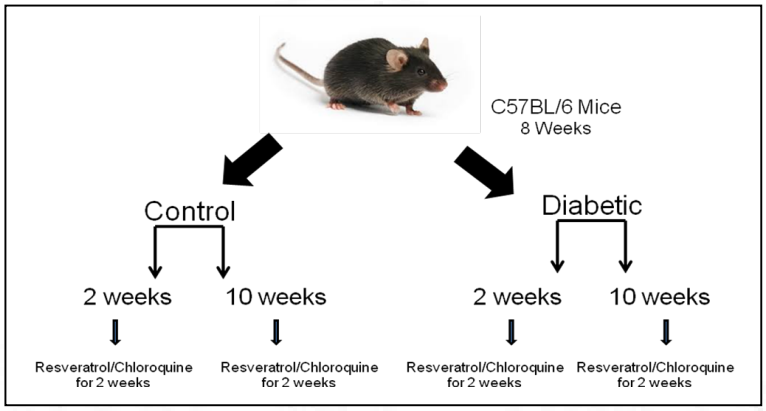

Flow chart representing the study plan adapted for drug treatment in type 2 diabetic mice

III. 4. 2. Gestational diabetic rat model

Pregnant 15-week-old Wistar rats (1st day of gestation, 250 to 350g) were taken for the study. Pregnant rats were divided into two groups: control mothers and diabetic mothers. Citrate buffer was given to the control mothers as vehicle. Diabetes was induced by intraperitoneal injection of a single dose of streptozotocin (20 mg/kg) on the 5th day of gestation. Hyperglycaemic status was analyzed by periodical checking of blood glucose levels of pregnant rats. After delivery, the suckling offsprings were allowed to stay with the mother till the weaning period. After weaning, the offsprings had free access to standard chow and water. The offsprings of control and diabetic mothers were divided into two groups both containing male and the female progenies, i.e., offspring of control mother (OCM) and offspring of diabetic mother (ODM). Each group of offsprings were taken for the study at two different time points, one at weaning age (21 days) and other at the adult age (120 days). So totally there were 8 groups. The heart tissue and the blood were exercised from those animals for further experiments.

Figure 17: Study design for rat experiments

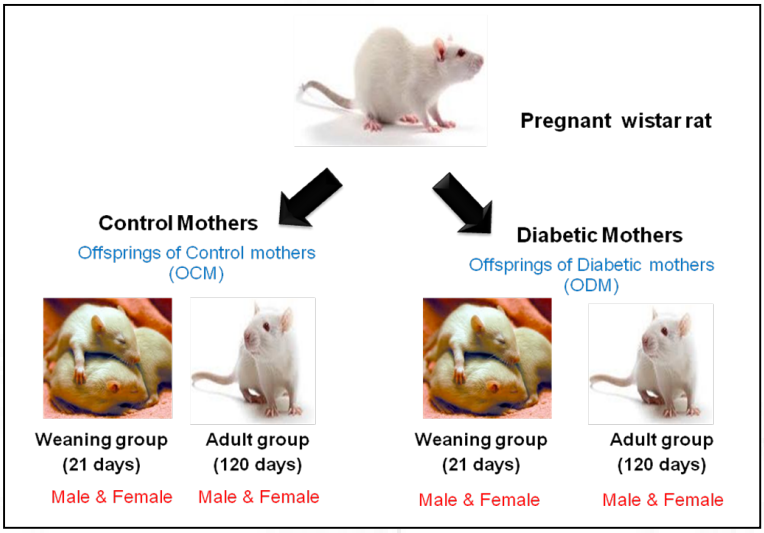

Flow chart representing the study design adapted for gestational diabetic rat experiments.

III. 4. 3. Reagents used

III. 4. 3.1. Saline preparation (1 litre)

Sodium chloride (0.9 %) in sterile autoclaved distilled water.

III. 4. 3. 2. Sodium citrate buffer (1 litre) (pH 4.5)

Tri sodium citrate (2.94 g) in saline solution.

III. 4. 3. 3. Nicotinamide solution

(100 mg/kg) NA in saline solution.

III. 4. 3. 4. Streptozotocin solution

STZ (120 mg/kg) for mice model and (20 mg/kg) for rat model in 0.05M citrate buffer.

III. 4. 3. 5. Resveratrol solution

Resveratrol (5 mg/kg) in 100 % ethanol.

III. 4. 3. 6. Chloroquine solution

Choloroquine (10 mg/kg) in saline solution.

III. 5. Western blot technique

III. 5. 1. Whole cell and tissue lysate preparation

H9c2 cells were seeded on to 100 mm culture plates and treated with or without 5.5 mmol/L DMEM, 30 mmol/L DMEM, 20 μM Chloroquine at respective time course described. At the end of treatment, cells were harvested by scraping in ice-cold PBS. Cells were washed twice with PBS and pelleted by centrifugation. The cell pellets were lysed in ice-cold Radio Immuno Precipitation Assay (RIPA) buffer containing proteinase inhibitor and phosphatase inhibitor cocktail for 1 h with intermittent vortexing (every 5 min). Lysed cells were centrifuged at 13,000 rpm for 20 min and the supernatants were aliquoted in to equal volumes and stored at -80^{0}C.

The frozen cardiac tissue samples were first weighed cut in to very small pieces using scissors inside a microfuge tube to which ice-cold RIPA buffer containing proteinase inhibitor and phosphatase inhibitor cocktail is added. Then the tissue lysate was transferred to an ice-cold homogenizer and homogenized the tissue for 5 min. The homogenized tissue lysate was then transferred to a microfuge tube for 1 hr with intermittent vortexing (every 5 min) and centrifuged for collecting the supernatant at 13,000 rpm for 20 min. The supernatant was then aliquoted in to equal volumes and stored at -80^{0}C.

III. 5. 2. Protein quantification

Using Pierce 660 nm method (Pierce Biotechnology, Massachusetts, USA), isolated proteins from cells and tissue were quantified. Cell and tissue lysate were diluted and BSA protein standards containing a range of 0.75 to 7.5 μg protein was prepared. Then a standard curve of absorbance versus standard micrograms protein was plotted and the concentration of proteins in the cell and tissue lysate was determined.

III. 5. 3. Gel electrophoresis

Isolated proteins from the cell and tissue lysate (30 – 80 µg protein) were heat denatured for 5 min and resolved on Sodium Dodecyl Sulphate- Poly Acrylamide Gel Electrophoresis (SDS-PAGE) at 100V. Resolved proteins were transferred on to nitrocellulose membrane/PVDF membrane at 10V for 40 minutes in a semi dry transfer apparatus.The membrane was blocked for 1 h at room temperature with blocking buffer (1 % BSA in TBST). The membrane was then probed with antibodies to LC3 B, Rubicon, PINK 1, LAMP2, p62/SQSTM1, ANT1, UCP3, MnSOD, Glutathione peroxidase, O-GlcNAc, Cathepsin D, Beclin 1, Atgs (3,5,7,12,14,16L1), ULK1, pULK1 (Ser 555), mTOR, pmTOR (Ser 2448), Parkin, AMPKα, pAMPKα, sirtuins (SirT 3 and 5), (1:1000), OXPHOS (1;2500) vinculin, β- Tubulin (1:5000) at 4^{o}C overnight. HRP conjugated anti rabbit (1:5000), (1:10,000) and anti mouse IgG (1:50,000) secondary antibodies were used for the study.

III. 5. 4. Chemiluminescent detection

West Pico/ West Femto Chemiluminescence Detection Kit (Pierce Biotechnology, Massachusetts, USA) or OptiBlot (Abcam, Cambridge, UK) was used for visualizing protein bands. Equal volumes of luminol and peroxide solutions were mixed and added on to the membranes. An X-ray film was used to capture light emitting bands. The film was then developed and documented in Gel Doc™ XR Imaging System (Bio-Rad Laboratories, Hercules, CA, USA) and quantified using Quantity One 1 D Analysis Software.

III. 5. 5. Reagents used

III. 5. 5. 1. Acrylamide 30%

Acrylamide- 29 % (w/v) and N, N'-methylene bisacrylamide- 1% (w/v) in 100 mL in deionized water.

III. 5. 5. 2. Blocking solution

BSA- 1 % (w/v) in 1X TBST.

III. 5. 5. 3. 10 X Electrode buffer (Running Buffer)(pH 8.3)

Trizma base – 25 mM, Glycine –192 mM, SDS –1% in deionised water.

III. 5. 5. 4. Ponceau S stain

1% Ponceau in 5% glacial acetic acid.

III. 5. 5. 5. 8 X Resolving gel buffer (pH 8.8)

SDS - 0.2%, Tris – 3 M in deionized water.

III. 5. 5 .6. RIPA (Radio Immuno Precipitation Assay) Buffer (pH 8.0)

Sodium chloride – 150 mM, NP-40 – 1.0%, Sodium deoxycholate – 0.5%, SDS – 0.1% in deionized water.

III. 5. 5. 7. SDS gel loading buffer (2X)(pH 6.8)

SDS – 4%, 2- mercaptoethanol – 10%, Glycerol – 20%, Bromophenol blue – 0.004%, Tris-, HCl - 0.125 M in deionized water.

III. 5. 5. 8. 4 X Stacking gel buffer (pH 6.8)

SDS – 0.1%, Trizma base 0.5 M in deionised water.

III. 8. 5. 9. 10 X Towbin's buffer (Transfer buffer, pH 8.3)

Trizma base – 25 mM, Glycine –192 mM, 20% methanol in deionised water.

III. 5. 5. 10. Tris-buffered saline (10 X, pH 7.6)

Tris base- 24.2 g, sodium chloride- 80 g in 1L deionized water.

III. 5. 5. 11. Tris-buffered saline with Tween-20 (TBST) [1 X]

1X TBS containing 0.5% Tween-20.

III. 5. 5. 12. To prepare 12% resolving gel (10 mL)

30% acrylamide: bis-acrylamide (29:1)	- 3 mL
8X resolving gel buffer	- 1.25 mL
TEMED	- 10 μL
20% APS	- 20 μL
Deionised water	- 5.5 mL

III. 5. 5. 13. To prepare 5% stacking gel (5 mL)

Acrylamide- bis acrylamide gel (29:1)	- 0.625 mL
Stacking gel buffer	- 1.25 mL
TEMED	- 10 μL
20% APS	- 13.5 μL
Deionised water	- 3.125 mL

III. 6. Immunohistochemistry

For demonstrating the presence and location of proteins (LC3 B, p62 and Beclin 1) in atrial sections, immunohistochemistry technique (biotin- free immunoenzymatic antigen detection system, Abcam, Cambridge, UK) was adapted. 5 μm-thick tissue sections were cut from buffered formalin-fixed, paraffin-embedded atrial biopsies. Sections were deparaffinised and rehydrated with different grades of alcohol and optimal antigen retrieval method (heat mediated) is established for each of the target protein. After blocking of endogenous peroxidases, blocking buffer is added to the sections. Antibodies to LC3 B, p62 and beclin 1 were used at a dilution of 1:100 and incubated overnight at 4^{o}C. Immunohistochemical staining was done by peroxide diamnobenzidine (DAB) method and then counterstained with hematoxylin. The sections are then dehydrated and stabilized with mounting medium. Images of tissue sections were taken in a microscope at 40X and quantified using Image J software.

III. 6. 1. Reagents used

III. 6. 1. 1. Reagents for deparaffinization

Xylene, 100 % ethanol, 95 % ethanol, 70 % ethanol, running tap water

III. 6. 1. 2. Antigen retrieval buffer

Solution A: (1 litre) (pH – 6) : Monohydrous citric acid (210.14 g) in deionised water

Solution B: (1 litre) (pH 9): Tri sodium citrate dehydrate (294.1g) in deionised water,1 mM EDTA, in deionised water

Mix 11.5 mL of solution A + 88.5 mL of solution B

III. 6. 1. 3. Tris buffered Saline (TBS) 10X (1 litre)

Trisma HCl (24.23 g) and NaCl (80.06 g) in 800 mL deionised water. Adjust pH to 7.6 and make up to 1000mL

III. 6. 1. 4. Tris-buffered saline with Tween-20 (TBST) [1 X]

1X TBS containing 0.5% Tween-20.

III. 6. 1. 5. Peroxide solution

Stock - 30 % H_2O_2. From stock, 3 % H_2O_2 was prepared.

III. 6. 1. 6. Blocking solution

BSA- 1 % (w/v) in 1X TBST.

III. 7. Mitochondrial isolation

After sacrificing mice/rat, the whole heart was immediately immersed in ice-cold BIOPS buffer for mitochondrial isolation. As described by Fontana *et al* published in Mitochondrial Physiology Network Oroboros O2k protocols (2015), mitochondria were isolated from the heart tissue by differential centrifugation. The isolated mitochondria were immediately used for oxygen consumption studies.

The protocol is as follows:

- The animals were sacrificed and dissected the heart without blood vessels and fat.
- Immediately transferred the tissue into ice cold BIOPS and washed.
- The weight of heart tissue was recorded.
- Transfered heart to a cooling petridish containing BIOPS, excised ventricle (rat experiments) or taken whole heart (mice experiments) and carefully eliminated blood clots.
- Transferred heart into 1.5 mL microfuge tube on ice with 0.5 mL of ice cold BIOPS and cut the heart tissue into small pieces with cooled scissors.
- Transferred the tissue paste into 5 mL motor glass and added 4 mL isolation buffer and dounced slowly 6-8 times (maximum 1 min at 150 rpm).

- Transferred tissue homogenate to 50 mL falcon tube and added 2 mL isolation buffer.
- Centrifuged homogenate at 800 x g for 6 minutes at 4°C.
- Transferred supernatant to new 50 mL falcon tube.
- Centrifuged the supernatant at 10,000 x g for 10 min at 4°C.
- Removed the supernatant and carefully re-suspend the mitochondrial pellet in 500 µL isolation buffer and then made the volume up to 2 mL of isolation buffer. (Pipette was not used to re-suspend, but by gentle tapping)
- Centrifuged at 10,000 x g for 10 min at 4°C.
- Removed the supernatant and carefully re-suspended the mitochondrial pellet in suspension buffer and the mitochondria was ready for using in oxygen consumption measurements.
- The protein content of mitochondria was analyzed using pierce 660 nm method.

III. 7. 1. Buffers for mitochondrial isolation

III. 7. 1. 1. BIOPS

	Final Conc.	FW	Stock Solution	Addition to 1 litre final Vol:
CaK_2EGTA	2.77 mM		100 mM	27.7 mL
K_2EGTA	7.23 mM		100 mM	72.3 mL
Na_2ATP	5.77 mM	551.1		3.180 g
$MgCl_2.6H_2O$	6.56 mM	203.3		1.334 g
Taurine	20 mM	125.1		2.502 g
Na_2Phosphocreatine	15 mM	255.1		3.827 g
Imidazole	20 mM	68.1		1.362 g
Dithiothreitol (DTT)	0.5 mM	154.2		0.077 g
MES hydrate	50 mM	195.2		9.76 g

BIOPS contain the following ion concentrations:

Ca^{2+} free	0.1µM
Mg^{2+} free	1mM
MgATP	5mM
Ionic strength	160mM

- Adjusted the pH to 7.1 (with 5 M KOH) at 0º C. Store BIOPS and K_2EGTA/CaK_2EGTA solutions at -20º C in plastic vials.

III. 7. 1. 2.Mitochondrial respiration medium (MiR05)

	FW	Final Conc (mM)	Addition to 1 litre final Vol:
EGTA	380.4	0.5	0.190 g
$MgCl_2.6H_2O$	203.3	3	0.610 g
K-lactobionate	358.3	60	120 mL of 0.5 M stock
Taurine	125.1	20	2.502 g
KH_2PO_4	136.1	10	1.361 g
HEPES	238.3	20	4.77 g
Sucrose	342.3	110	37.65 g
BSA (FA free)		1 g/L	1 g

Preparation of MiR05 stock solution

- Weighed given amounts of the listed chemicals (expect BSA and lactobionic acid) and transferred to a 1000 mL glass beaker.
- The big lumps were mechanically disrupted. (It was recommended to do this before adding water, because during dissolution these lumps do not disintegrate easily).
- Added ~ 800 mL H_2O and dissolved using a magnetic stirrer at ~30ºC.
- Added 120 mL of K-lactobionate stock solution.
- Adjusted the pH to 7.1 with 5 N KOH at 30ºC.
- Dissolved the BSA in a subsample of the MiR05 stock solution and added to the final MiR05 (Separate preparation of the BSA solution is recommended, since BSA produces foams that do not dissolve easily).
- Added H_2O to a final volume of 1000 mL and checked the pH and finally MiR05 was prepared.
- Divided into 40 mL portions in plastic vials and stored at -20ºC.
- Each vial was warmed to 37^0C before use and foam formation was avoided by gentle shaking. (It was recommended to use the stock solution on a single day only, to avoid microbial contamination of the respiration medium).

Preparation of K-lactobionate stock solution

Dissolved 35.83 g lactobionic acid in 100 mL H_2O, adjust pH to 7.0 with KOH, and adjusted volume to 200 mL with H_2O. pH - 7.1 (5 N KOH), divided and frozen at -20º C in falcon tube.

III. 7. 1. 3.Isolation buffer

Stock solution	Final Conc.	Addition to 200 ml final volume
D-Mannitol	225 mM	90 mL
Sucrose	75 mM	30 mL
EGTA	1 mM	2 mL
BSA	1 g/L	0.2 g

III. 7. 1. 4. Suspension buffer

Stock Solution	Conc.	FW	Addition to 1 litre final volume
D-Mannitol	0.5 M	182.17	91.085 g
Sucrose	0.5 M	342.3	171.15 g
EGTA	0.1 M	380.35	38.35 g

III. 8. Mitochondrial function studies

Mitochondrial oxidative phosphorylation and oxygen consumption as an element of mitochondrial function was done using Oxygraph O2K. Isolated cardiac mitochondrial suspension (10 µL) was added to each 2-mL chamber containing mitochondrial respiration buffer (MiR05). Data acquisition and analysis of oxygen consumption rate (OCR) were done with Datlab 5 software (Oroboros, Innsbruck, Austria). Using micro syringes, the various substrates or inhibitors or uncouplers for respiratory experiments were carefully added to the respiration medium in the chambers in a step-by-step manner.

For the oxygen consumption study of cardiac mitochondria, two mitochondrial substrate/inhibitor protocols were adapted:

Fatty acid + Carbohydrate protocol (Chamber A)

State 1, the first respiratory state in an oxygraphic protocol is achieved when isolated mitochondria are added to mitochondrial respiration medium containing oxygen and inorganic phosphate, but no ADP and no reduced respiratory substrates. State 2, substrate limited state of residual oxygen consumption was measured with palmitoyl- L-carnitine (Pal) (25 µmol/L) and malate (M) (2 mmol/L) ($PalM_0$), give oxygen consumption rate through β oxidation. After addition of ADP (5 mmol/L) to the medium, state 3 respiration ($PalM_{ADP}$) is achieved which will provide electrons to electron transferring flavoprotein (ETF) and complex I. The outer mitochondrial membrane integrity was evaluated by stimulation of respiration by exogenously added cytochrome *c* (2 µmol/L). The normalized *c* effect was expressed as flux control factor. Then the carbohydrate substrates like pyruvate ($PalMP_{ADP}$) (5 mmol/L), glutamate ($PalMPG_{ADP}$) (10 mmol/L) and succinate ($PalMPGS_{ADP}$) (10 mmol/L) are sequentially added. Adding pyruvate or glutamate as substrates, display capacity of complex I and succinate give that of complex II by being donors of electrons to specific molecules in electron transport system.

Figure 18: Fatty acid + Carbohydrate protocol

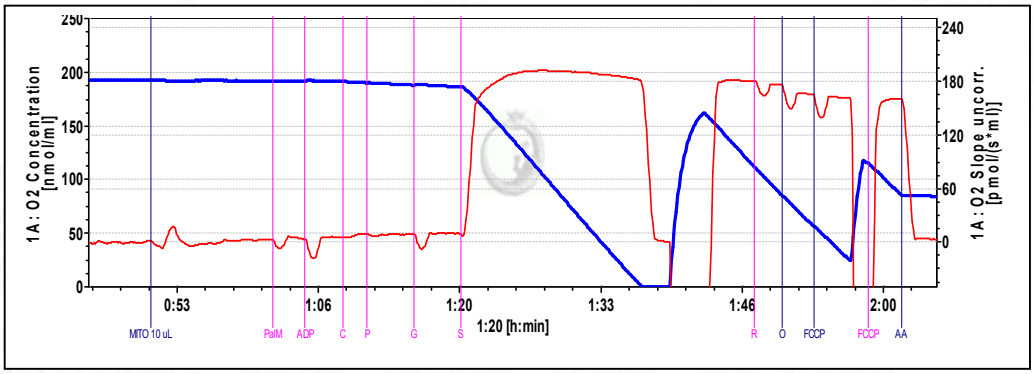

Datfile representing the fatty acid + carbohydrate protocol of isolated cardiac mitochondria.

Carbohydrate protocol (Chamber B)

In this protocol, carbohydrate substrate combinations were only used to detect electron flow through complexes I and II. Complex I–dependent state 2 respiration was determined in the

presence of 10 mmol/L glutamate (G) and 2 mmol/L malate (GM_0). In the presence of 5 mmol/L ADP, Complex I–dependent state 3 respiration (GM_{ADP}) was measured. The integrity of the outer mitochondrial membrane was confirmed by the absence of a significant increase in respiration after the addition of cytochrome *c* (2 µmol/L). Followed, pyruvate (P) (5 mmol/L) stimulated complex I dependent state 3 respiration (GMP_{ADP}) and succinate (S)(10 mmol/L) stimulated complex II respiration ($GMPS_{ADP}$) was measured.

Figure 19: Carbohydrate protocol

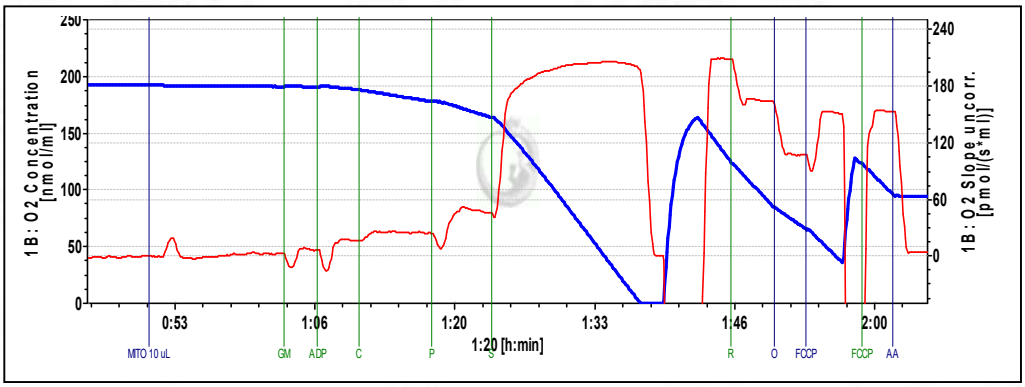

Datfile representing the carbohydrate protocol of isolated cardiac mitochondria.

In both protocols, after succinate addition, complex I was inhibited by rotenone (0.05 µmol/L), and complex II-dependent state 3 respiration (S_{Rot}) was obtained. State 4 respiration or LEAK respiration (S_{Omy}) obtained after state 3, was determined by addition of an inhibitor of ATP synthase, oligomycin (2.5 µmol/L). In the presence of an uncoupler FCCP (1 µmol/L), complex II- dependent maximal respiratory capacity (S_{FCCP}) was measured. Finally the concentration of oxygen is depleted in the closed oxygraph chamber and zero oxygen was brought down by the addition of antimycin-A (AA) (2.5 µmol/L) to inhibit complex III- mediated respiration.

Table 1: Two protocols for mitochondrial oxygen consumption study

Fatty Acid + Carbohydrate Protocol (Chamber A)				**Carbohydrate protocol** (Chamber B)			
S/ U/ I	**Event**	**Volume (µL)**	**State**	**S/ U/ I**	**Event**	**Volume (µL)**	**State**
Mitochondria	MITO	10	State 1	Mitochondria	MITO	10	State 1
Palmitoyl-Carnitine Malate	PCM	5 5	State 2	Glutamate Malate	GM	10 5	State 2
Adenosine 5' diphosphate	ADP	20	State 3 ETF	Adenosine 5' diphosphate	ADP	20	State 3 CI
Cytochrome *c*	C	1		Cytochrome *c*	C	1	
Pyruvate	P	5	State 3 ETF + CI	Pyruvate	G	5	State 3 CI
Glutamate	G	10	State 3 ETF + CI	Succinate	S	20	State 3 CI + CII
Succinate	S	20	State 3 ETF + CI + CII	Rotenone	Rot	1	State 3 CII
Rotenone	Rot	1	State 3 CII	Oligomycin	O	1	State 4
Oligomycin	O	1	State 4	Carbonyl cyanide p-trifluoro-methoxy phenyl-hydrazone	FCCP	1+1	ETS
Carbonyl cyanide p-trifluoro-methoxy phenyl-hydrazone	FCCP	1+1	ETS	Antimycin A	AA	1	ROX
Antimycin A	AA	1	ROX	-	-	-	-

III. 8. 1. Chemicals for mitochondrial substrate-uncoupler-inhibitor titration (SUIT) protocols

III. 8. 1. 1 Substrates

Substrate	FW	Stock solution Conc. (mM)	Stock solution Amount	Final Conc. In 2ml	
				Chamber A	Chamber B
G: L- Glutamic acid	169.1	2000	3.382 g/ 10 mL H_2O	10 mM	10 mM
M: L-Malic acid	134.1	400	536 mg/10 mL H_2O	2 mM	2 mM
P: Pyruvic acid sodium salt	110	2000	44 mg/ 0.2 mL H_2O	5 mM	5 mM
S: Succinate disodium salt, hexahydrate	270.1	1000	2.701 g/ 10 mL H_2O	10 mM	10 mM
Pal: Palmitoyl-DL-carnitine-HCl	436.1	10	8.72 mg/ 2 mL H_2O	25 µM	-
***c*:** Cytochrome *c*	12500	4	50 mg/ mL H_2O	2 µM	2 µM
D: ADP (Adenosine 5' diphosphate, potassium salt)	501.3	500	0.501 g/ 2 mL H_2O	5 mM	5 mM

III. 8. 1. 2. Uncouplers

Uncouplers	FW	Stock solution Conc (mM)	Stock solution Amount	Final concentration in 2ml	
				Chamber A	Chamber B
F(FCCP): Carbonyl cyanide p-(trifluoro-methoxy) phenyl-hydrazone	254.2	1	2.54 mg/ 10mL ethanol	0.5+0.5 µM	0.5+0.5 µM

III. 8. 1. 3.Inhibitors

Inhibitors	FW	Stock solution Conc. (mM)	Stock solution Amount	Final concentration in 2ml	
				Chamber A	Chamber B
AA: Antimycin A	540	5	11 mg/ 4mL ethanol	2.5 µM	2.5 µM
Omy: Oligomycin	800	5	4 mg/ 1mL ethanol	2.5 µM	2.5 µM
Rot: Rotenone	394.4	1	3.94 mg/10mL ethanol	0.05 µM	0.05 µM

III. 9. Statistical analysis

All statistical calculations were carried out with the SPSS tool and graphs were prepared using Graph Pad Prism software program. Values are expressed as the mean ± standard deviation (SD). The significance of the difference from the respective control for each experimental test conditions was assayed by Student's *t*-test wherever the respective distribution is normal otherwise Mann Whitney U test was followed. For all statistical analysis, differences between means were considered statistically significant at a *p*- value of less than 0.05.

IV.A. RESULTS

(T2DM)

Human study

IV.A.1.Patient Characteristics

Right atrial appendage was obtained from 40 human patients who underwent coronary artery bypass surgery, during a period of 24 months and those tissue samples were used for western blot analysis and immunohistochemistry. The characteristics of the patients taken for the study are presented in Table 2.

Table 2: Patient characteristics

Characteristics	**Non diabetic (n=20)**	**Diabetic (n=20)**	***p* value**
Age (years)	56.9± 1.4	59.38± 1.1	0.18
BMI (kg/m^2)	23.42± 0.75	25.27± 0.49	0.036*
HbA1c (mg/dL)	6.21± 0.12	7.87± 0.19	<0.001***
Random blood glucose (mg/dL)	104.15± 5.01	169.67± 7.86	<0.001***
LVEF (%)	62.12± 1.41	62.03± 1.2	0.963
Total cholesterol (mg/dL)	161.4± 7.7	142.04± 6.06	0.051
HDL cholesterol (mg/dL)	36.96± 2	36.74± 1.16	0.215
Triglycerides (mg/dL)	41.44± 6.7	30.66± 4.4	0.184
NYHA class	Class II	Class II	

*The total number of non-diabetic patients selected for various experiments in the study is 20 and that of diabetic patients is 20. The HbA1c and random blood glucose levels vary significantly between the 2 groups, while all other parameters are matched, except BMI, which was also varied significantly in diabetic patients when compared with non-diabetic patients. (p-value *<0.05, ***<0.001)*

The patient subjects selected for the study were grouped to non-diabetic and diabetic based on their HbA1c and random blood glucose levels. The diabetic group was having a mean HbA1c level of 7.87% and mean random blood glucose level of 169.67mg/dL that were significantly higher than non-diabetic group. All other parameters were not significantly different including BMI, triglyceride level, cholesterol level, left ventricular ejection fraction and NYHA class. Patients with type 1 diabetes, atrial fibrillation, or left ventricular ejection

fractions less than 30 % were excluded from this study.

IV.A.1.1. Decreased autophagy in human diabetic heart

In order to study the process of autophagy in diabetic human heart, we evaluated the expression of some of the important markers of autophagic machinery by western blot technique and immunohistochemistry.

Beclin 1 (mammalian homolog of Atg 6), interacts with other proteins (Atg 14, rubicon etc) and help in the formation of Beclin 1-Vps34-Vps15 core complexes, thereby promotes the autophagic process. Western blot analysis revealed no significant difference in expression of Beclin 1 in diabetic heart tissue when compared with the non- diabetic (Figure 20)

Figure 20: Expression of Beclin 1

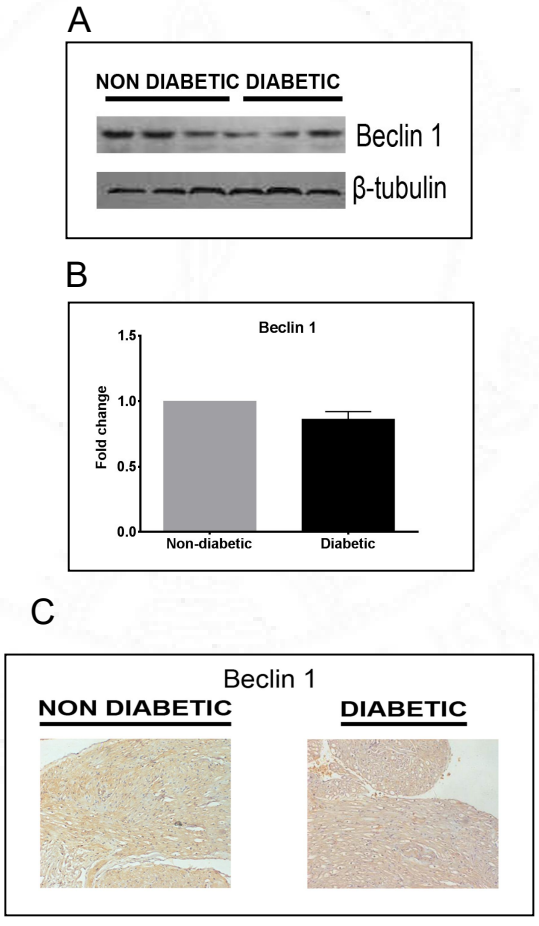

Expression of Beclin 1 was showed by western blotting (A) and IHC (C) in diabetic human heart tissue. (B)The bar graphs represent the fold change in expression of the respective protein. Error bars represent ±SD (n = 8 in each group)

p62 is widely used as an autophagic marker. It isan adaptor molecule that targets the cytoplasmic cargoes for autophagy, which directly binds with LC3 in the autophagosome membrane and is selectively degraded during autophagy. Thus degradation of p62 and theresultant decreased levels of p62 indicates the occurrence of autophagy, while increased levels of p62 indicates inhibited autophagy. In the present study, significant increase in p62 expression levels in the diabetic than the non diabetic heart tissue was observed (Figure 21)

Figure 21: Expression of p62

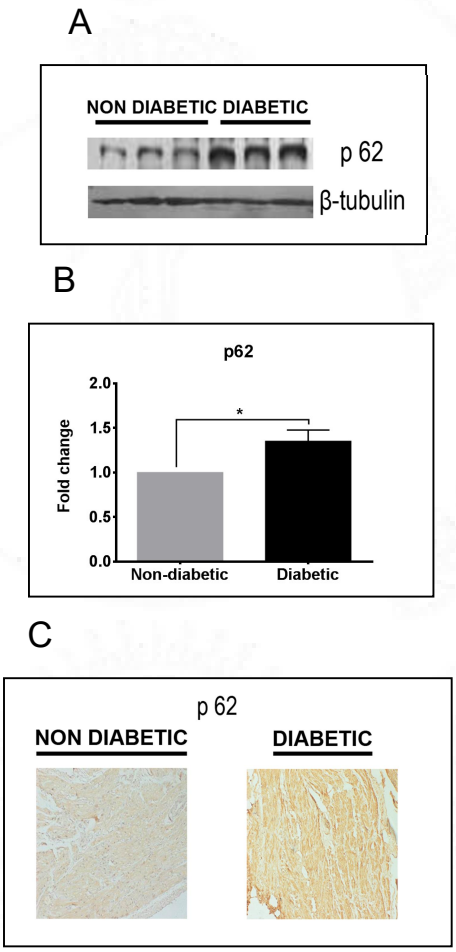

Expression of p62 was showed by western blotting(A) and IHC (C) in diabetic human heart tissue. (B)The bar graphs represent the fold change in expression of p62. Error bars represent ±SD (p-value<0.05) (n = 8 in each group)*

The most widely used autophagic marker is LC3 (mammalian homologue of Atg 8) because the level of LC3-II indicates the number of autophagosomes in the cells. Expression of LC3-II level at a given time point (steady state level) was analyzed using western blot technique and was found to be decreased in the diabetic than the non diabetic heart tissue (Figure 22)

Figure 22: Expression of LC3 II

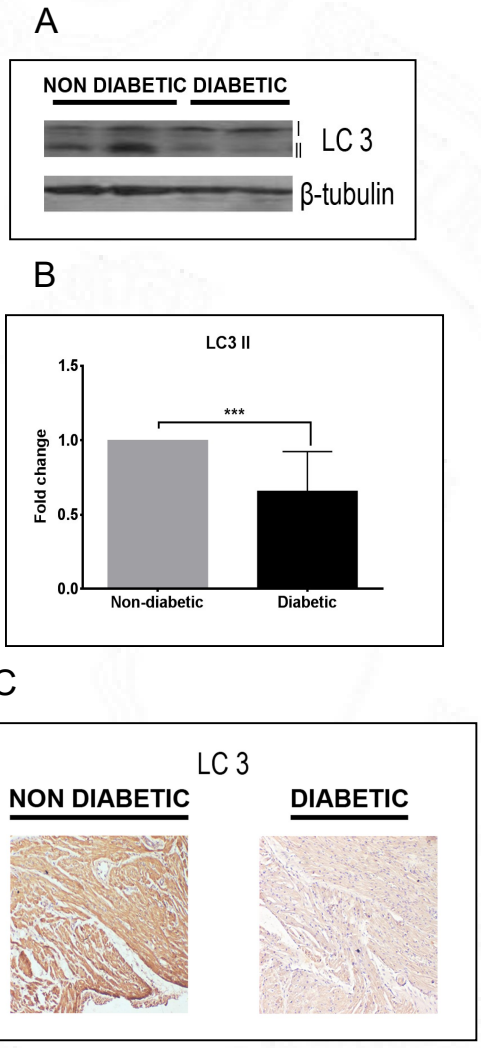

*Expression of LC3 II was showed by western blotting(A) and IHC (C) in diabetic human heart tissue.(B) The bar graphs represent the fold change in expression of LC3II. Error bars represent ±SD (p-value***<0.001) (n = 18 in each group)*

Since LC3 II was formed from LC3 I, a ratio of LC3 II/I was also analyzed. LC3 II/I ratio was also significantly reduced in the diabetic than the non diabetic heart tissue (Figure 23)

Figure 23: Expression of LC3 II/I

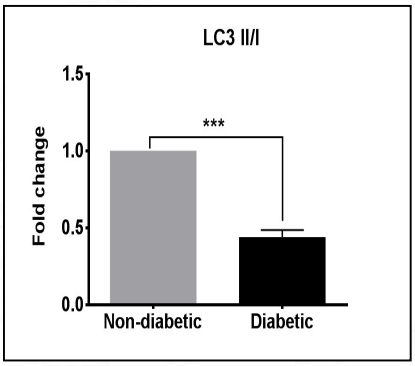

*LC3 II/I ratio was calculated from the western blot data and the bar graphs represent the fold change of the LC3II/I ratio in diabetic cardiac tissue. Error bars represent ±SD (p-value ***<0.001)(n =18 in each group)*

Findings:

- **In diabetic human heart,reduced expression of LC3 II and LC3 II/I ratio was observed which denoted the reduced formation of autophagosomes or reduced autophagy**
- **Increased expression of p62 indicated that the p62 was not degraded properly and the fusion between autophagosome and lysosome were defective/ altered.**
- **No significant change was found in Beclin 1 expression between the diabetic and non-diabetic groups.**
- **In short, myocardial autophagy was found to be reduced in diabetic than the non-diabetic human subjects.**

Cell Line study

To study the process of cardiomyocyte autophagy in hyperglycemic conditions, H9c2 cells were incubated with control (5.5 mmol/L) or high glucose (30 mmol/L) medium for two time points, 4 h and 48 h respectively.

IV.A.2. Autophagic profile in hyperglycemic H9c2 cells

In order to study the process of autophagy in two different time points of hyperglycemia (4 h and 48 h), we evaluated the expression of some of the important autophagic proteins, mitophagic proteins, lysososmal proteins and regulators of autophagic machinery.If there is lack of adequate nutrients, ULK1 (mammalian homolog of Atg 1) can recruit ATG11, ATG13, and ATG17 to form a complex that signals induction of autophagy. The expression of ULK1 was found unchangedat the 4 h and 48 h of hyperglycemic condition in H9c2 cells (Figure 24)

Figure 24: Expression of ULK1

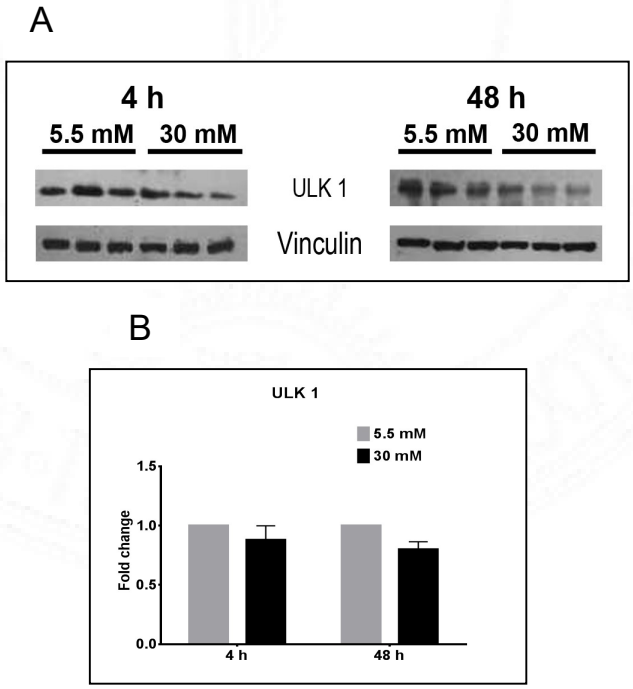

(A) Expression of ULK1 was showed by western blotting in H9c2 cells at specific time points (4 h and 48 h of hyperglycemia). (B) The bar graphs represent the fold change in expression of ULK1 in H9c2 cells at specific time points. Error bars represent ±SD of determinations from three independent experiments.

Its phosphorylated form pULK1 was found to be unchanged at the 4 h and significantly reduced at 48 h of hyperglycemic condition in H9c2 cells (Figure 25)

Figure 25: Expression of pULK1

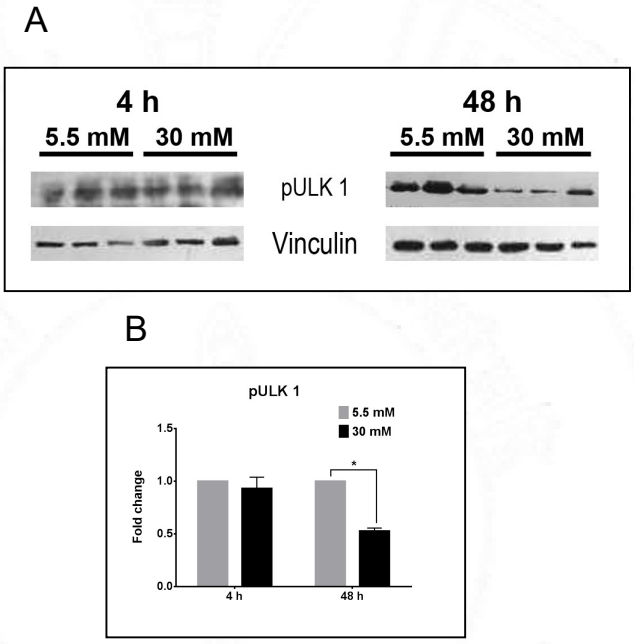

(A) Expression of pULK1 was showed by western blotting in H9c2 cells at specific time points (4 h and 48 h of hyperglycemia). (B) The bar graphs represent the fold change in expression of pULK1 in H9c2 cells at specific time points. Error bars represent ±SD of determinations from three independent experiments.

Activated ULK1 phosphorylates another molecule, Beclin 1(mammalian homolog of Atg 6), thereby increasing the activity of Atg 14 containing complexes, which promotes the autophagic process. Western blot analysisrevealed no significant difference in expression of Beclin 1 at the 4 h and 48 h of hyperglycemic condition in H9c2 cells (Figure 26)

Figure 26: Expression of Beclin 1

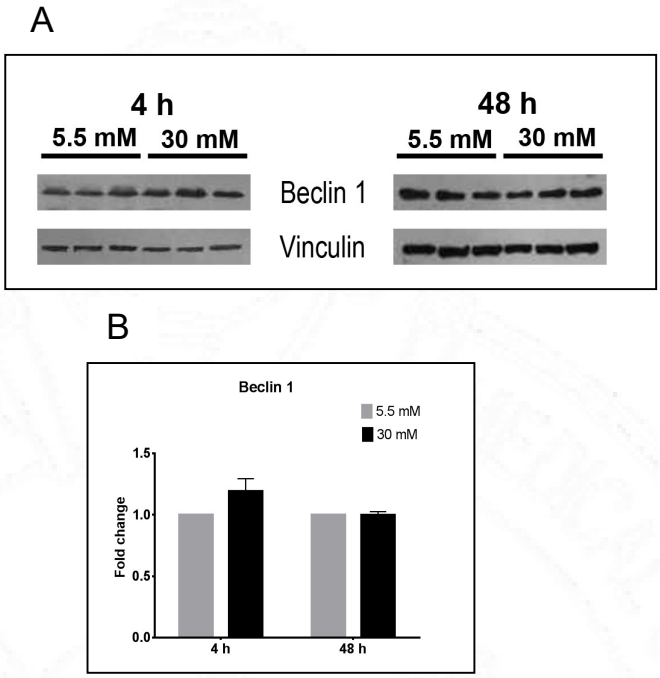

(A) Expression of Beclin 1 was showed by western blotting in H9c2 cells at specific time points (4 h and 48 h of hyperglycemia). (B) The bar graphs represent the fold change in expression of beclin1 in H9c2 cells at specific time points. Error bars represent ±SD of determinations from three independent experiments.

The expression of Atg 14 was found unchanged at the 4 h and 48 h of hyperglycemic condition in H9c2 cells (Figure 27)

Figure 27: Expression of Atg 14

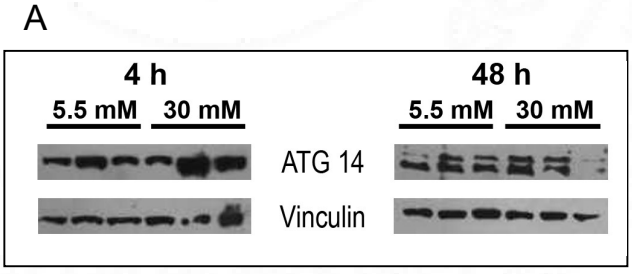

B

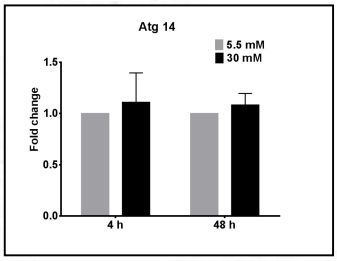

(A) Expression of Atg 14 was showed by western blotting in H9c2 cells at specific time points (4 h and 48 h of hyperglycemia). (B) The bar graphs represent the fold change in expression of Atg14 in H9c2 cells at specific time points. Error bars represent ±SD of determinations from three independent experiments.

Beclin 1 binds with another molecule, Rubicon if there is inhibition in the initiation step of autophagy. We didn't observe any change in the expression of rubicon at the 4 h and 48 h of hyperglycemic condition in H9c2 cells (Figure 28).

Figure 28: Expression of Rubicon

A

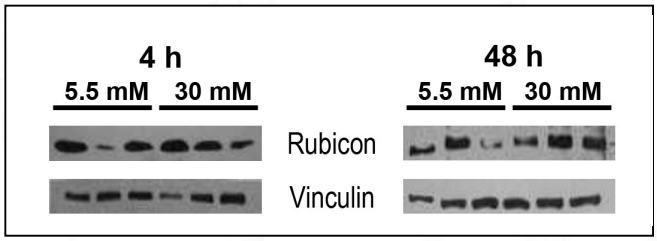

B

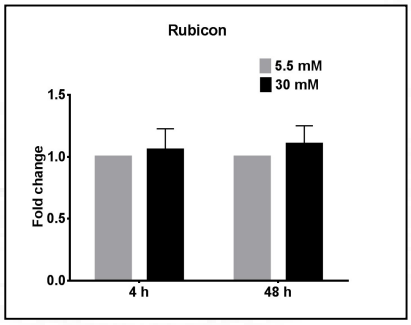

(A) Expression of Rubicon was showed by western blotting in H9c2 cells at specific time points (4 h and 48 h of hyperglycemia). (B) The bar graphs represent the fold change in expression of rubicon in H9c2 cells at specific time points. Error bars represent ±SD of

determinations from three independent experiments.

Once the maturation of autophagosome started, Atg 7 is recruited and it helps in the conjugation of Atg 5 to Atg 12 through a glycyl lysine isopeptide bond and Atg 5-Atg12 conjugate form a multimeric complex with Atg 16L. The expression of Atg 5 was significantly reduced at 48 h, while no change was observed at 4 h hyperglycemic condition of H9c2 cells (Figure 29).

Figure 29: Expression of Atg 5

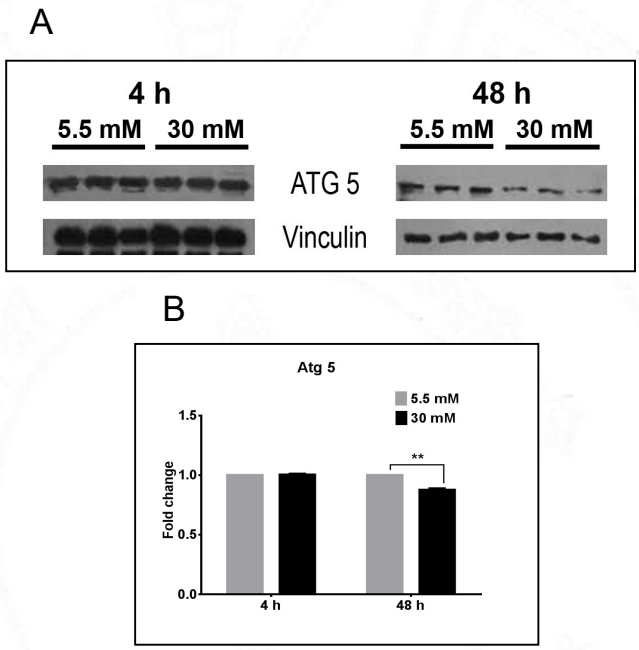

*(A) Expression of Atg 5 was showed by western blotting in H9c2 cells at specific time points (4 h and 48 h of hyperglycemia). (B) The bar graphs represent the fold change in expression of Atg5 in H9c2 cells at specific time points. Error bars represent ±SD of determinations from three independent experiments. (p-value**<0.01)*

The expression of Atg 7 (Figure 30), Atg 12 (Figure 31) and Atg 16 (Figure 32) was found unchanged at 4 h and 48 h of hyperglycemic condition in H9c2 cells

Figure 30: Expression of Atg 7

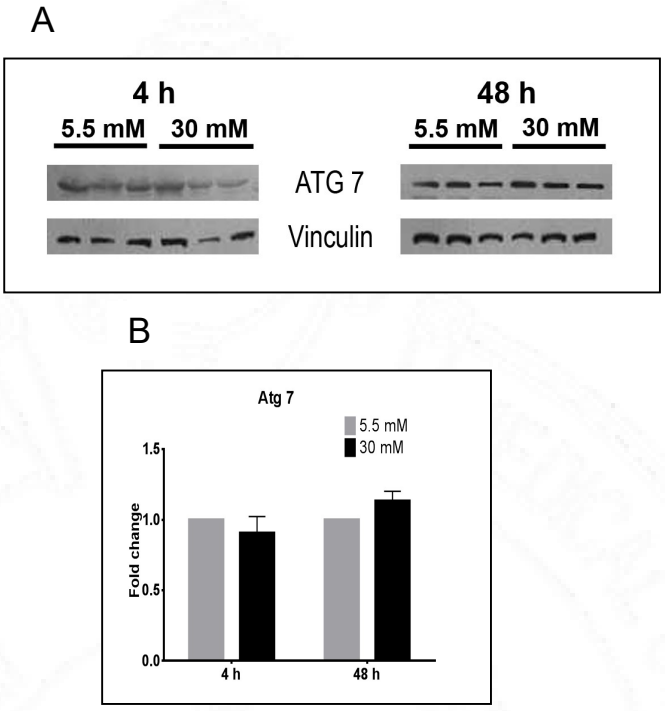

(A) Expression of Atg 7 was showed by western blotting in H9c2 cells at specific time points (4 h and 48 h of hyperglycemia). (B) The bar graphs represent the fold change in expression of Atg7 in H9c2 cells at specific time points. Error bars represent ±SD of determinations from three independent experiments.

Figure 31: Expression of Atg 12

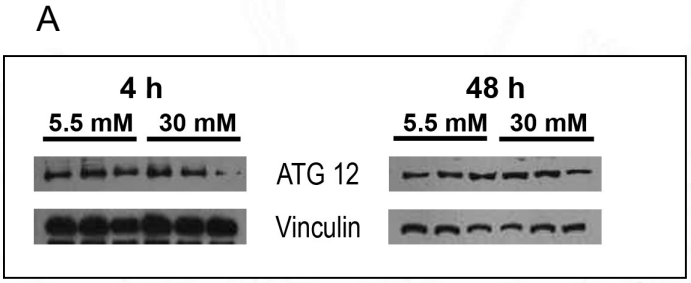

B

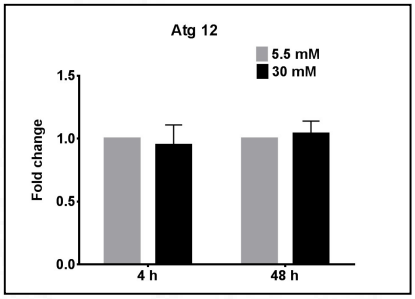

(A) Expression of Atg 12 was showed by western blotting in H9c2 cells at specific time points (4 h and 48 h of hyperglycemia). (B) The bar graphs represent the fold change in expression of Atg12 in H9c2 cells at specific time points. Error bars represent ±SD of determinations from three independent experiments.

Figure 32: Expression of Atg 16

A

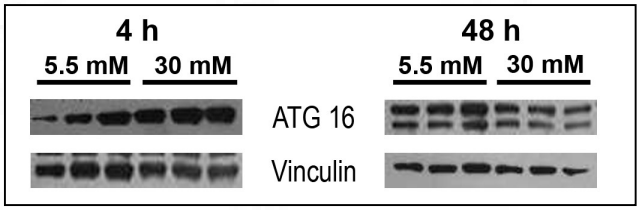

B

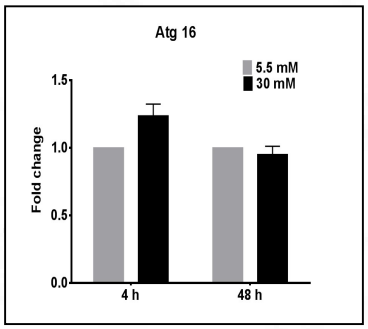

(A) Expression of Atg 16 was showed by western blotting in H9c2 cells at specific time points (4 h and 48 h of hyperglycemia). (B) The bar graphs represent the fold change in expression of Atg16 in H9c2 cells at specific time points. Error bars represent ±SD of determinations from three independent experiments.

The Atg5-Atg12 complex functions like an E3-like enzyme to start the next step of

autophagososme formation where LC3 is attached to the phosphatidylethanolamine (PE) in the membrane. Enzymes like Atg 3 and Atg 7 are mediating the conjugation of LC3 to PE in which the (non lipidated form) LC3 I is converted to (lipidated) LC3 II, which binds to PE, help in the elongation of the autophagosome membrane. We analyzed the expression of Atg 3 and found to be unaltered at 4 h and 48 h of hyperglycemic condition in H9c2 cells (Figure 33)

Figure 33: Expression of Atg 3

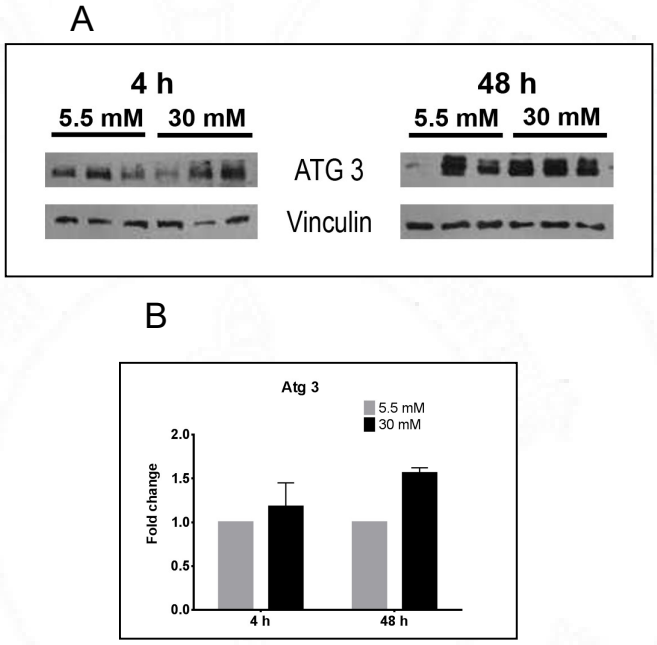

(A) Expression of Atg 3 was showed by western blotting in H9c2 cells at specific time points (4 h and 48 h of hyperglycemia). (B) The bar graphs represent the fold change in expression of Atg3 in H9c2 cells at specific time points. Error bars represent ±SD of determinations from three independent experiments.

Degradation of p62, an adaptor molecule that target the cytoplasmic cargoes for autophagy, which directly binds with LC3 in the membrane and is selectively degraded during autophagy. So p62 is also widely used as a autophagic marker along with LC3. The p62 expression levels showed a significant increase at 48 h and unchanged at 4 h hyperglycaemic condition of H9c2 cells (Figure 34)

Figure 34: Expression of p62

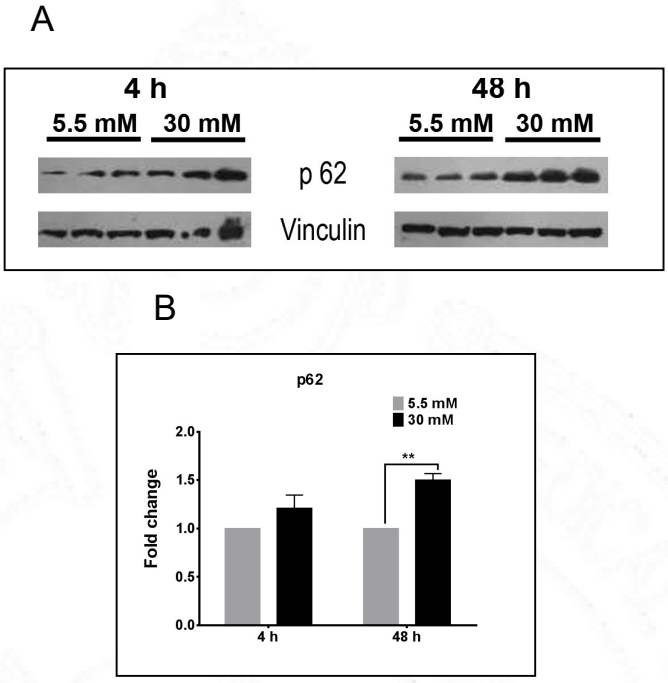

*(A) Expression of p62 was showed by western blotting in H9c2 cells at specific time points (4 h and 48 h of hyperglycemia). (B) The bar graphs represent the fold change in expression of the respective protein in H9c2 cells at specific time points. Error bars represent ±SD of determinations from three independent experiments. (p-value **<0.01)*

The most widely used autophagic marker is LC3 (mammalian homologue of Atg 8) because the level of LC3-II indicates the number of autophagosomes in the cells. Expression of LC3-II level at a given time point (steady state level) was analyzed using western blot technique and was found to be unchanged at 4 h and a significant reduction is observed at 48 h of hyperglycemia of H9c2 cells (Figure 35).

Figure 35: Expression of LC3 II

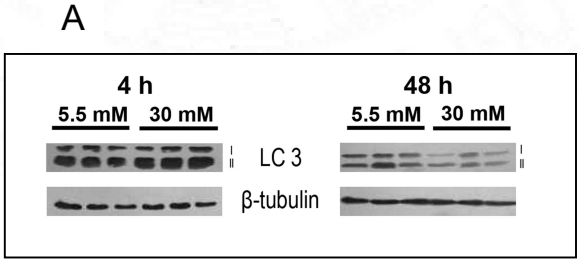

B

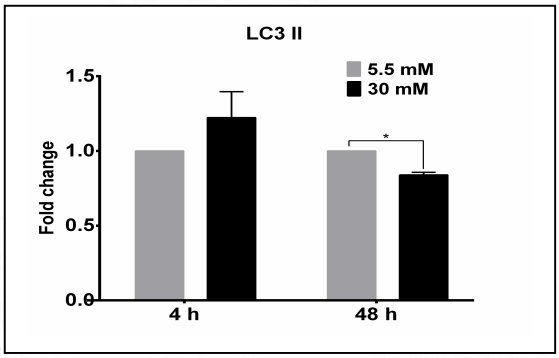

(A) Expression of LC3 II was showed by western blotting in H9c2 cells at specific time points (4 h and 48 h of hyperglycemia). (B) The bar graphs represent the fold change in expression of the respective protein in H9c2 cells at specific time points. Error bars represent ±SD of determinations from three independent experiments.

Since LC3 II was formed from LC3 I, a ratio of LC3 II/I was also analyzed. LC3 II/I ratio was also significantly unchanged at 4 h and a significant reduction is observed at 48 h of hyperglycemia of H9c2 cells (Figure 36).

Figure 36: Expression of LC3 II/I

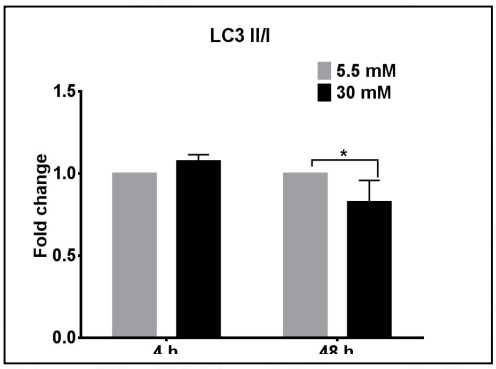

*LC3 II/I ratio was calculated from the western blot data of H9c2 cells at specific time points (4 h and 48 h of hyperglycemia). The bar graphs represent the fold change of the LC3II/I ratio in H9c2 cells at specific time points. Error bars represent ±SD SD of determinations from three independent experiments. (p-value *<0.05)*

We have also analyzed the expression of two important molecules, Parkin and PINK 1

involved in mitophagy. Upon mitochondrial depolarization, PINK 1 will be activated on the outer membrane and it recruits parkin to the mitochondria. Parkin will ubiquitinates different proteins on the mitochondrial membrane. The adaptor molecule, p62 will binds to the ubiquinated proteins and attach with LC3 that target the clearance of dysfunctional mitochondria by autophagososmes. The expression of PINK 1 was observed to be unchanged at 4 h and a significant lower expression noted at 48 h of hyperglycemic condition in H9c2 cells (Figure 37).

Figure 37: Expression of PINK 1

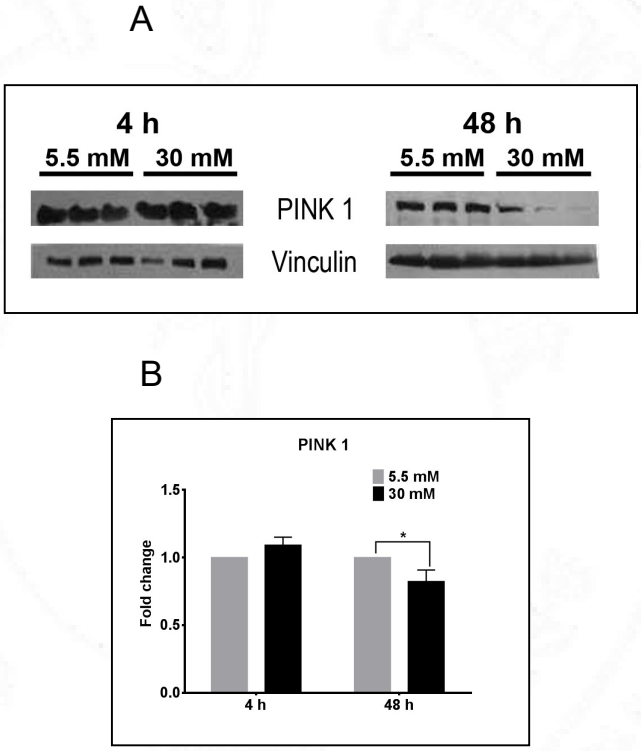

*(A) Expression of PINK 1 was showed by western blotting in H9c2 cells at specific time points (4 h and 48 h of hyperglycemia). (B) The bar graphs represent the fold change in expression of the respective protein in H9c2 cells at specific time points. Error bars represent ±SD of determinations from three independent experiments. (p-value *<0.05)*

The expression of Parkin also was found to be unaltered at 4 h and a significant lower expression observed at 48 h of hyperglycemic condition in H9c2 cells (Figure 38).

Figure 38: Expression of Parkin

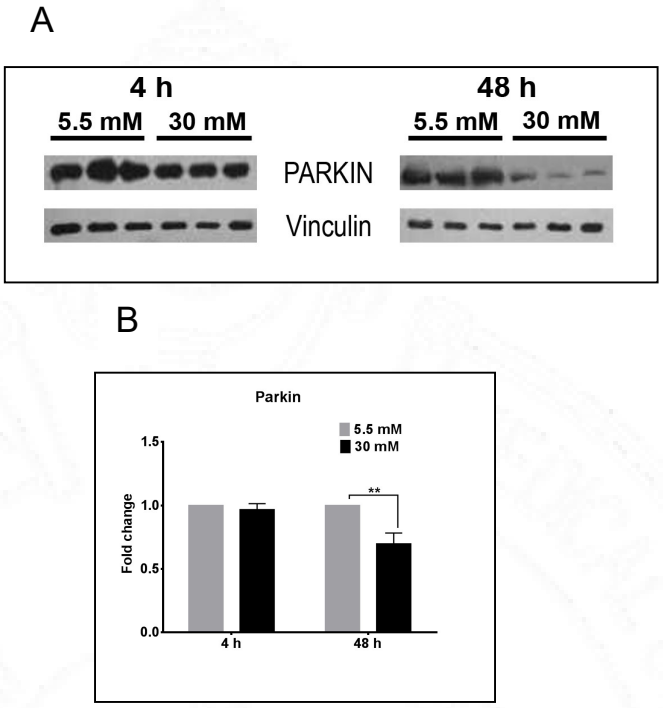

*(A) Expression of Parkin was showed by western blotting in H9c2 cells at specific time points (4 h and 48 h of hyperglycemia). (B) The bar graphs represent the fold change in expression of the respective protein in H9c2 cells at specific time points. Error bars represent ±SD of determinations from three independent experiments. (p-value **<0.01)*

Since lysosomes play an important role in autophagy, we have analyzed two molecules, cathepsin D and LAMP-2 associated with lysosomes. Cathepsin D, a lysososmal aspartyl protease was found to be unchanged at 4 h and 48 h of hyperglycemic condition in H9c2 cells (Figure 39).

Figure 39: Expression of Cathepsin D

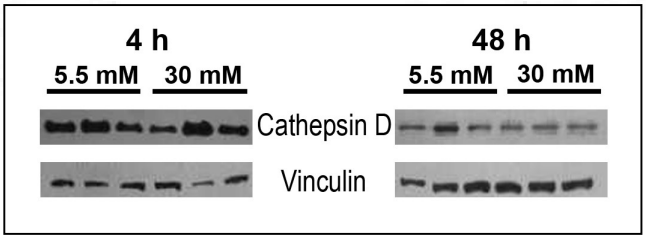

B

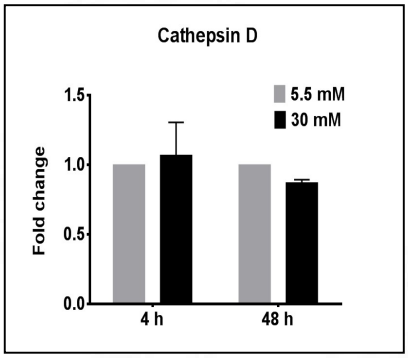

(A) Expression of Cathepsin D was showed by western blotting in H9c2 cells at specific time points (4 h and 48 h of hyperglycemia). (B) The bar graphs represent the fold change in expression of the respective protein in H9c2 cells at specific time points. Error bars represent ±SD of determinations from three independent experiments.

LAMP-2, lysosome associated membrane protein-2, a receptor seen in lysosomes for the selective degradation of cytosolic proteins was found to be unchanged at 4 h and 48 h of hyperglycemic condition in H9c2 cells (Figure 40).

Figure 40: Expression of LAMP-2

A

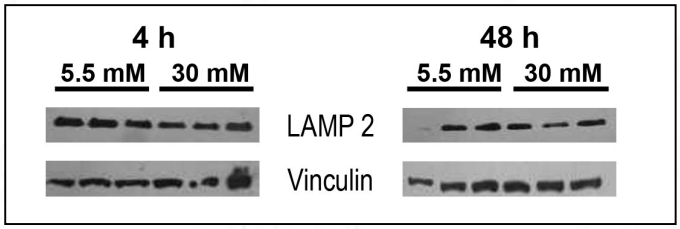

B

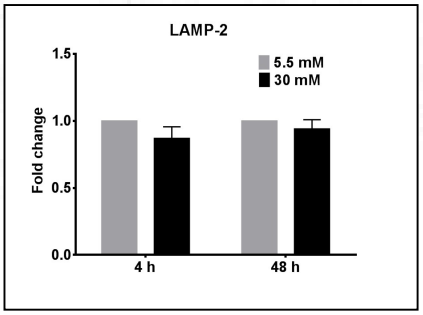

(A) Expression of LAMP-2 was showed by western blotting in H9c2 cells at specific time points (4 h and 48 h of hyperglycemia). (B) The bar graphs represent the fold change in expression of the respective protein in H9c2 cells at specific time points. Error bars represent ±SD of determinations from three independent experiments.

We have analyzed some of the important regulators of autophagy, AMPK and mTOR. During starvation or ATP depletion, autophagy is activated by the energy sensor molecule, AMPK through its capacity to inhibit mTOR complex I. AMPKα expression was found to be unchanged at 4 h and 48 h of hyperglycemic condition in H9c2 cells (Figure 41).

Figure 41: Expression of AMPKα

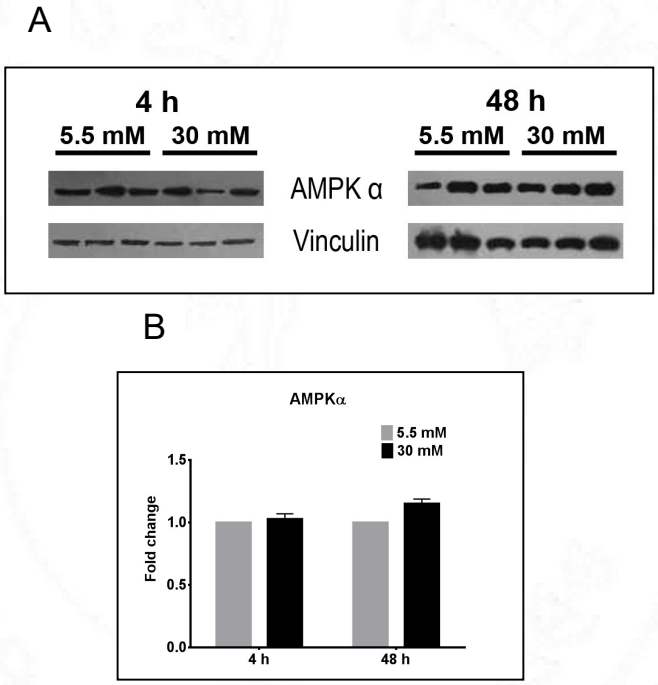

(A) Expression of AMPKα was showed by western blotting in H9c2 cells at specific time points (4 h and 48 h of hyperglycemia). (B) The bar graphs represent the fold change in expression of the respective protein in H9c2 cells at specific time points. Error bars represent ±SD of determinations from three independent experiments.

Phosphorylated form of AMPKα was also found to be unchanged inat 4 h and 48 h of hyperglycemic condition in H9c2 cells (Figure 42).

Figure 42: Expression of pAMPKα

A

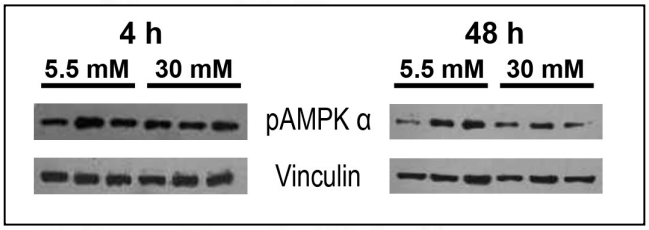

B

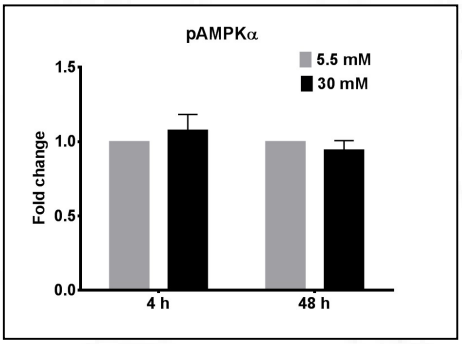

(A) Expression of pAMPkα was showed by western blotting in H9c2 cells at specific time points (4 h and 48 h of hyperglycemia). (B) The bar graphs represent the fold change in expression of the respective protein in H9c2 cells at specific time points. Error bars represent ±SD of determinations from three independent experiments.

mTOR, an inhibitor of autophagy, was also found to be unchanged at 4 h and 48 h of hyperglycemic condition in H9c2 cells (Figure 43).

Figure 43: Expression of mTOR

A

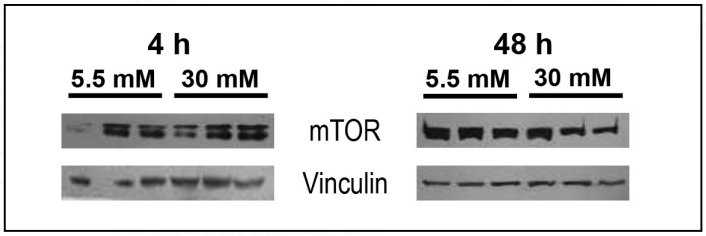

B

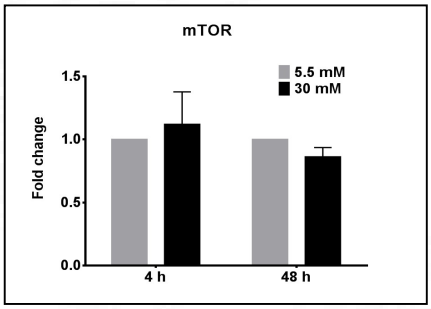

(A) Expression of mTOR was showed by western blotting in H9c2 cells at specific time points (4 h and 48 h of hyperglycemia). (B) The bar graphs represent the fold change in expression of the respective protein in H9c2 cells at specific time points. Error bars represent ±SD of determinations from three independent experiments.

The phosphorylated mTOR was also found to be be unchanged at 4 h and 48 h of hyperglycemic condition in H9c2 cells (Figure 44).

Figure 44: Expression of pmTOR

A

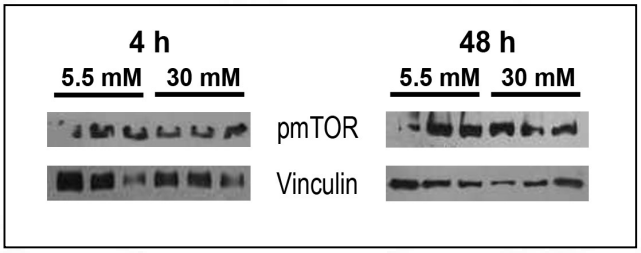

B

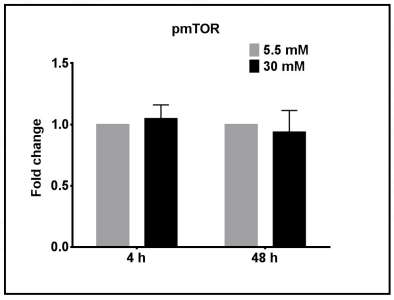

(A) Expression of pmTOR was showed by western blotting in H9c2 cells at specific time points (4 h and 48 h of hyperglycemia). (B) The bar graphs represent the fold change in expression of the respective protein in H9c2 cells at specific time points. Error bars represent ±SD of determinations from three independent experiments.

Findings:

- **In H9C2 cells, no change was observed in the autophagic proteins (ULK1, pULK1, Beclin 1, Rubicon, Atgs -3,5,7,12,14 &16, p62), mitophagic proteins (PINK 1, Parkin), lysosomal proteins(Cathepsin D, LAMP-2) and regulators of autophagy (AMPKα, pAMPKα, mTOR, pmTOR) at 4 h of hyperglycemia.**
- **No change was observed in the steady state level of LC3 II and its LC3 II/I ratio at 4 h indicated autophagosome formation was similar like its corresponding control**
- **A reduced expression of phosphorylated ULK1 was noted at 48 h of hyperglycemia indicates the initial complex formation with Atg 11, 13 and 17 may get altered or reduced**
- **A significant reduced expression is noted in Atg 5, at 48 h indicates a reduced formation of Atg5-Atg12 complex.**
- **ULK 1, Beclin 1, Rubicon and other Atgs (3, 7, 12, 14 and 16) didn't show any change with corresponding controls at 48 h.**
- **The increased expression of p62 at the 48 h of hyperglycemia shows that the degradation of autophagosomes is blocked/reduced.**
- **The reduced steady state level of LC3 II and LC3 II/I ratio at 48 h indicates reduced formation of autophagosomes or reduced autophagy.**
- **The mitophagy proteins, Parkin and PINK 1 showed reduced expression at 48 h indicates the improper clearance of damaged mitochondria.**

- **The lysosomal proteins (cathepsin D and LAMP-2) and the regulators of autophagy (AMPKα, pAMPKα, mTOR, pmTOR) were found unchanged at 48 h of hyperglycemia.**

Mice study

IV.A.3. Establishment of T2DM mice model

For the study, C57BL/6 mice were used for creating STZ/NA-induced type 2 diabetes mellitus. Weekly analysis of blood glucose and body weight of the animal indicated that STZ/NA-injected mice had significantly high glucose levels (Figure 45), while maintaining same body weight as the controls throughout the 10 weeks of the study (Figure 46).

Figure 45: Random blood glucose measurements over time

A B

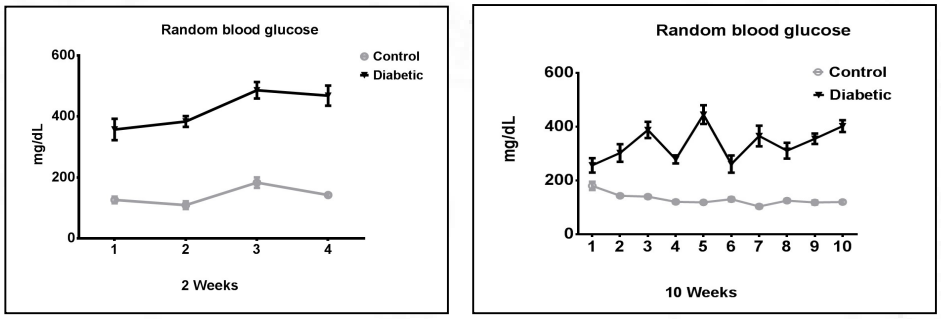

The random blood glucose measurements over time were higher for diabetic mice at 2 weeks(A) and 10 weeks (B). Error bars represent ± SD. (n=6 in each group)

Figure 46: Body weight measurement over time

A B

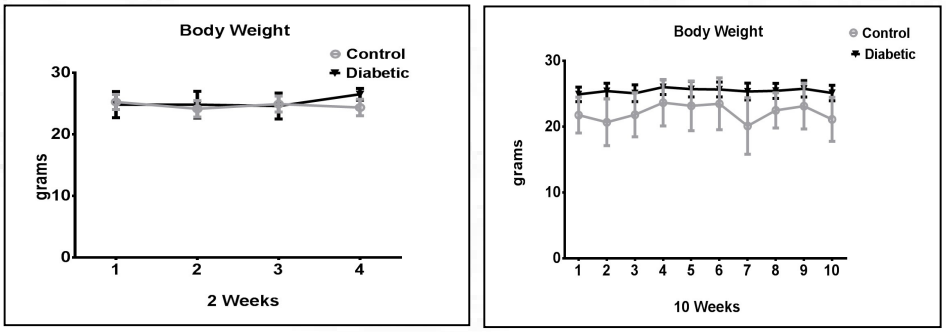

The body weight of diabetic mice wassimilar to that of the control mice at 2 weeks (A) and 10 weeks (B). Error bars represent ± SD.(n=6 in each group)

The oral glucose tolerance test showed that the blood glucose level after glucose load (a gold standard for detecting type 2 diabetes) was higher in diabetic mice than the control mice (Figure 47).

Figure 47: Oral glucose tolerance test

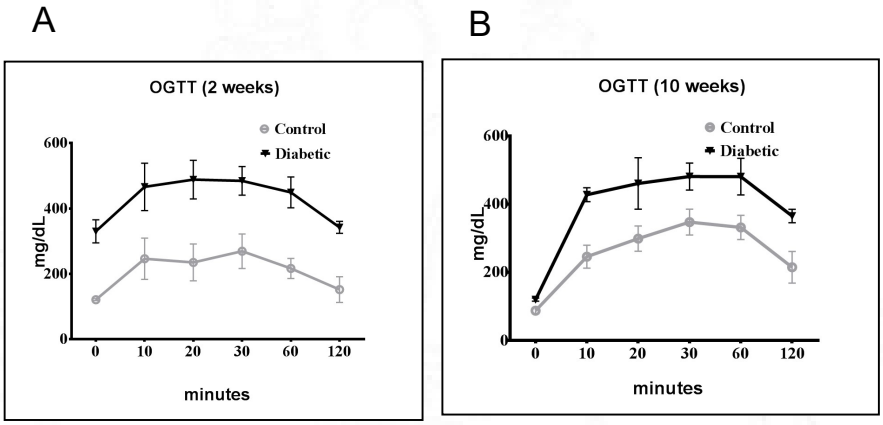

Higher level of plasma glucose was observed in diabetic mice on glucose load at both 2 weeks(A) and 10 weeks (B).Error bars represent ±SD.(n=6 in each group)

The glycosylated hemoglobin levels checked at the time of euthanasia in diabetic mice at two time points were significantly higher than their corresponding controls (Figure 48 A). The plasma insulin levels in diabetic mice were not significantly different from that of control micein 2 weeks and 10 weeks and this indicated that the STZ/NA-induced diabetes mellitus was type 2 and not type 1 (Figure 48 B). The plasma triglyceride level (Figure 48 C) was not altered in diabetic mice while there were significantly higher levels of plasma cholesterol levels in diabetic mice at 2 weeks time point but not at 10 weeks (Figure 48 D).

Figure 48: Blood plasma parameters

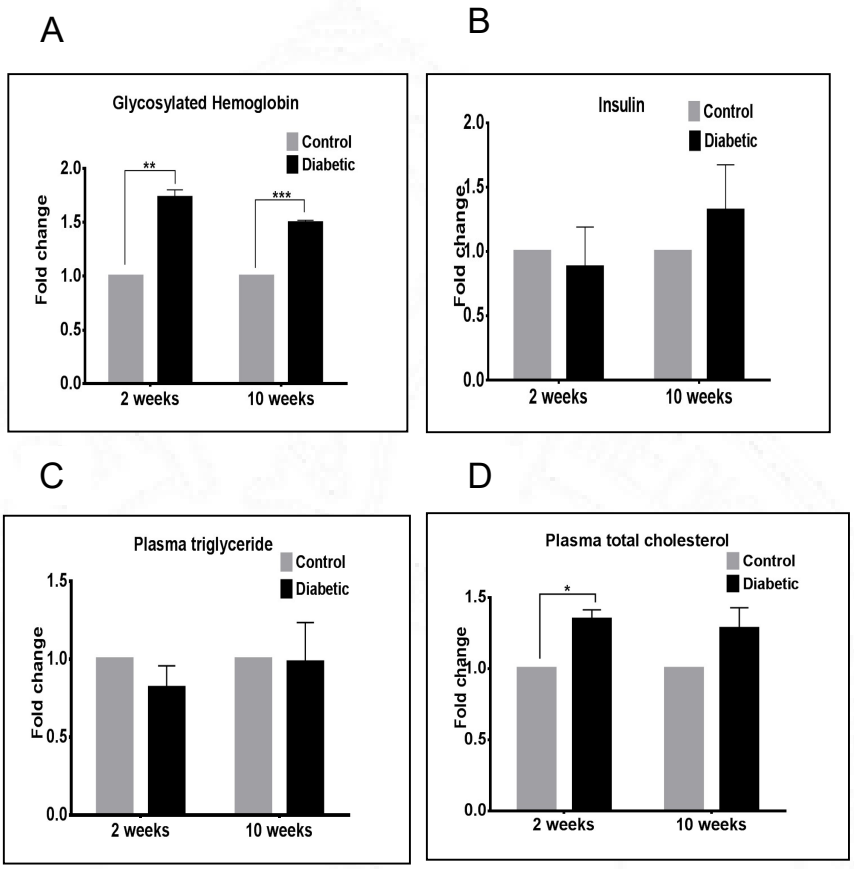

*(A)Higher HbA1c levels in 2 week and 10 week diabetic mice (B) Plasma insulin levels in STZ/NA-induced diabetic mice weresimilar to that of control mice. (C) Plasma triglyceride levels showed unaltered levels in diabetic mice (D) A significant increase in plasma cholesterol levels at 2 weeks time point. Error bars represent ± SD.(p-value *<0.05**<0.01***<0.001) (n=6 in each group)*

The heart weight: body weight ratio was calculated in diabetic mice at both time points and found that the values were similar to that of their corresponding controls (Figure 49). This indicated that till 10 weeks of untreated diabetes, no structural changes like hypertrophy/cardiomyopathy occurred in mice diabetic heart.

Figure 49: Heart weight to body weight ratio

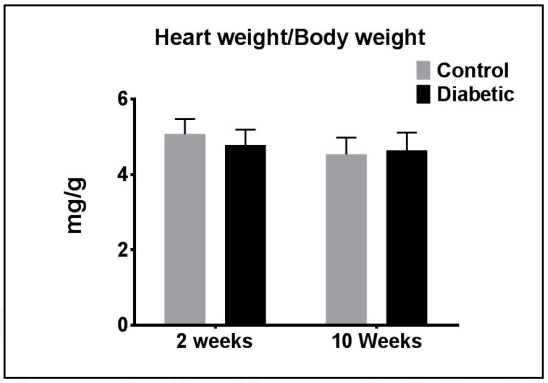

Bar graph showing the ratio of heart weight (milligrams) and body weight (grams) of mice at 2 weeks and 10 weeks of untreated diabetes. The error bars represent ± SD. (n=6 in each group)

Findings:

- **Hyperglycemia was maintained in C57BL/6 mice till 10 weeks, which was the longest duration selected for the study**
- **Unchanged body weight and insulin levels showed that the diabetes mellitus developed in mice was of type 2**
- **No change in heart weight: body weight ratio showed absence of hypertrophy or cardiomyopathy at two time points**

IV.A.3.1. Cardiac autophagic profile in type 2 diabetes

In order to study the cardiac autophagic process in 2 week and 10 week diabetic mice, we evaluated the expression of some of the important markers and regulators of autophagic machinery by western blot technique.

ULK1 (mammalian homolog of Atg 1) is found unchanged in the 2 week and reduced in 10 week diabetic mice heart (Figure 50).

Figure 50: Expression of ULK1

A

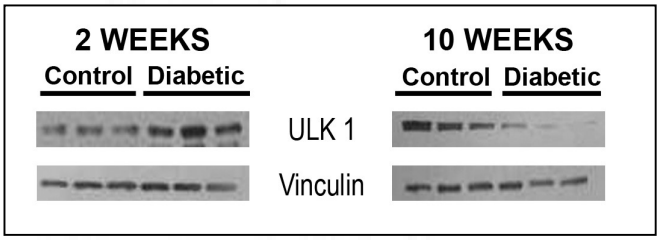

B

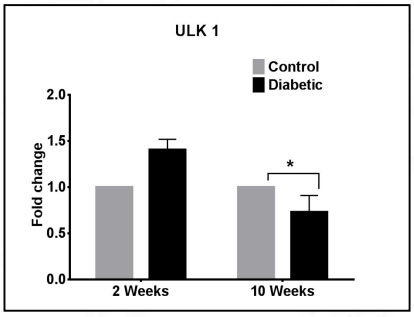

(A) Expression of ULK1 was showed by western blotting in 2 week and 10 week diabetic mice heart. (B) The bar graphs represent the fold change in expression of the respective protein in 2 week and 10 week diabetic mice heart. Error bars represent ±SD. (n=6 in each group).

Active form, pULK1 is also found to be unchanged in the 2 week and significantly reduced in

10 week diabetic mice heart (Figure 51)

Figure 51: Expression of pULK1

A

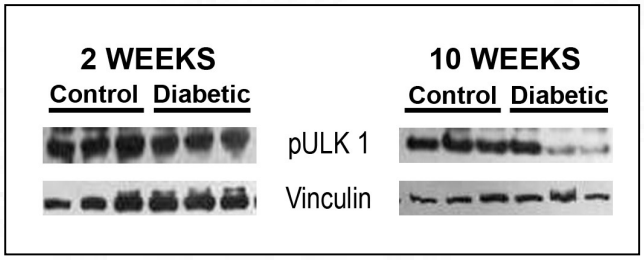

B

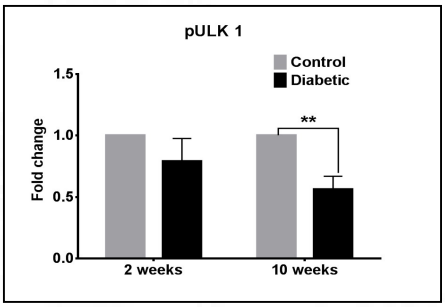

(A) Expression of pULK1 was showed by western blotting in 2 week and 10 week diabetic mice heart. (B) The bar graphs represent the fold change in expression of the respective protein in 2 week and 10 week diabetic mice heart. Error bars represent ±SD. (n=6 in each group).

Western blot analysis revealed that no significant difference in expression of Beclin 1

was noted in the 2 week and 10 week diabetic mice heart (Figure 52).

Figure 52: Expression of Beclin 1

A

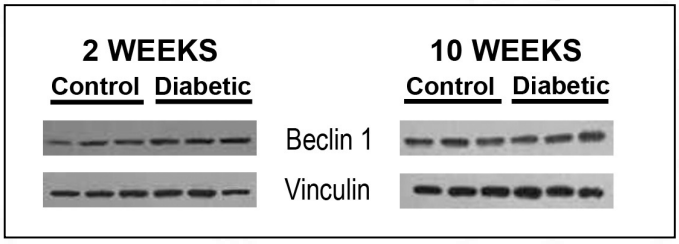

B

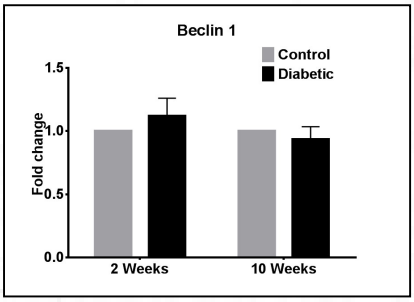

(A) Expression of Beclin 1 was showed by western blotting in 2 week and 10 week diabetic mice heart. (B) The bar graphs represent the fold change in expression of the respective protein in 2 week and 10 week diabetic mice heart. Error bars represent ±SD. (n=6 in each group).

Atg 14 expression was found unchanged in the 2 week and 10 week diabetic mice heart (Figure 53).

Figure 53: Expression of Atg 14

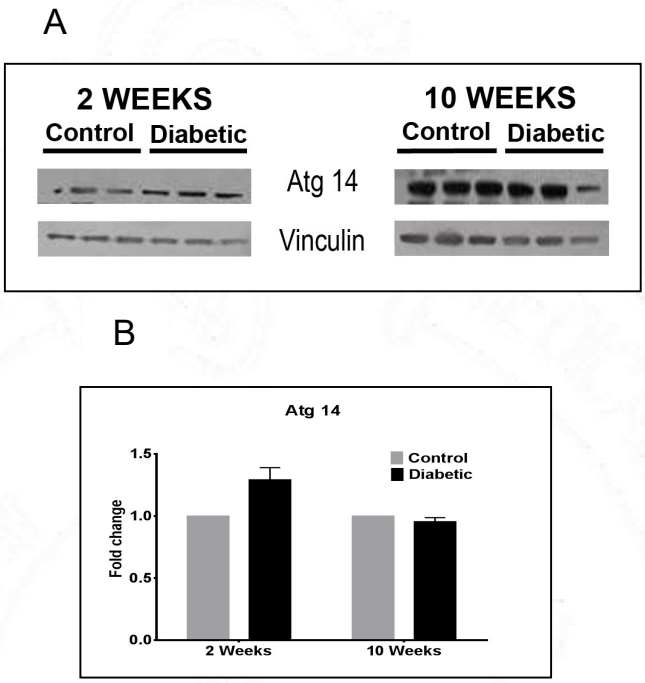

(A) Expression of Atg 14 was showed by western blotting in 2 week and 10 week diabetic mice heart. (B) The bar graphs represent the fold change in expression of the respective protein in 2 week and 10 week diabetic mice heart. Error bars represent ±SD. (n=6 in each group).

No change in the expression of rubicon was noticed in the 2 week and 10 week diabetic mice heart (Figure 54)

Figure 54: Expression of Rubicon

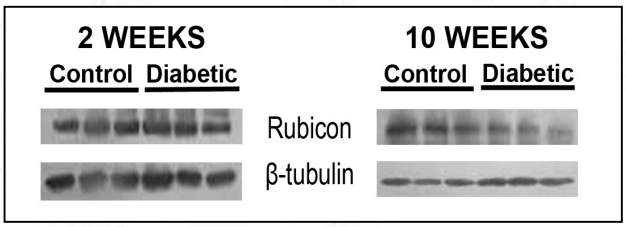

B

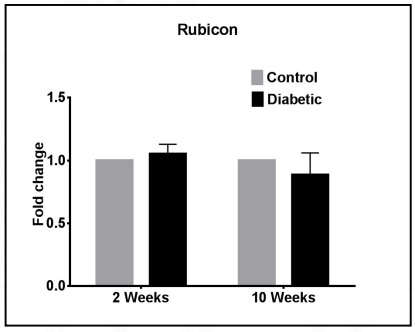

(A) Expression of Rubicon was showed by western blotting in 2 week and 10 week diabetic mice heart. (B) The bar graphs represent the fold change in expression of the respective protein in 2 week and 10 week diabetic mice heart. Error bars represent ±SD. (n=6 in each group).

The expression of Atg 5 (Figure 55), Atg 7 (Figure 56) and Atg 12 (Figure 57) were found unchanged in the 2 week and 10 week diabetic mice heart.

Figure 55: Expression of Atg 5

A

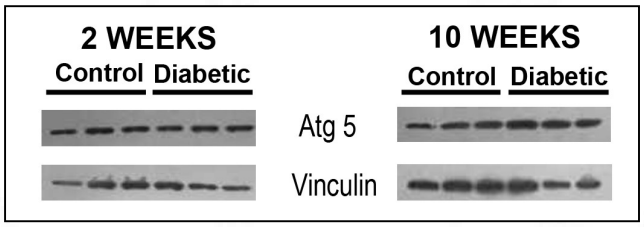

B

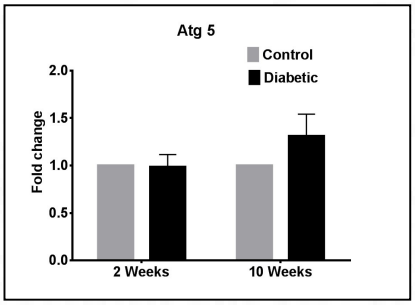

(A) Expression of Atg 5 was showed by western blotting in 2 week and 10 week diabetic mice heart. (B) The bar graphs represent the fold change in expression of the respective protein in 2 week and 10 week diabetic mice heart. Error bars represent ±SD. (n=6 in each group).

Figure 56: Expression of Atg 7

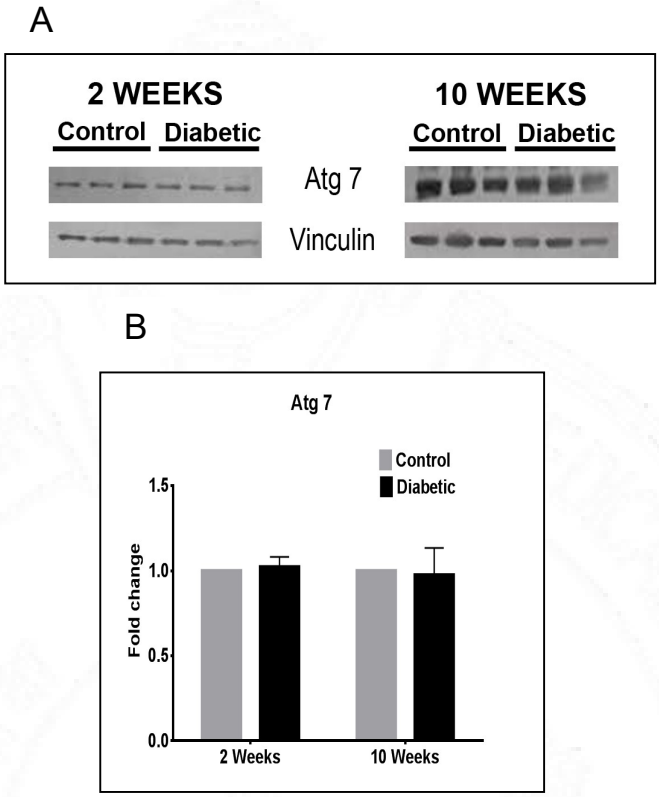

(A) Expression of Atg 7 was showed by western blotting in 2 week and 10 week diabetic mice heart. (B) The bar graphs represent the fold change in expression of the respective protein in 2 week and 10 week diabetic mice heart. Error bars represent ±SD. (n=6 in each group).

Figure 57: Expression of Atg 12

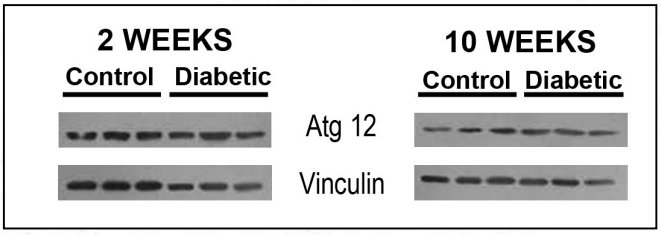

B

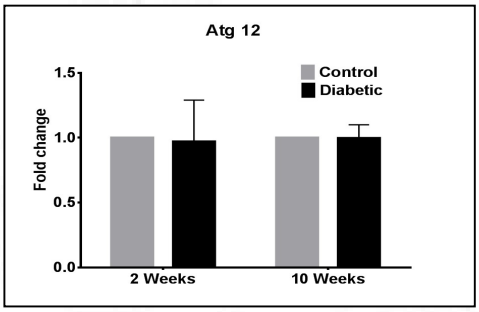

(A) Expression of Atg 12 was showed by western blotting in 2 week and 10 week diabetic mice heart. (B) The bar graphs represent the fold change in expression of the respective protein in 2 week and 10 week diabetic mice heart. Error bars represent ±SD. (n=6 in each group).

There was no change in expression of Atg 16 in 2 week diabetic heart, while a significant reduction was observed in 10 week diabetic mice heart (Figure 58).

Figure 58: Expression of Atg 16

A

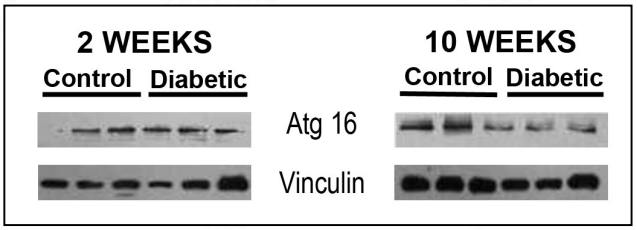

B

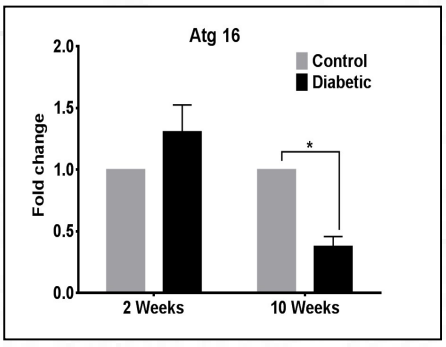

*(A) Expression of Atg 16 was showed by western blotting in 2 week and 10 week diabetic mice heart. (B) The bar graphs represent the fold change in expression of the respective protein in 2 week and 10 week diabetic mice heart. Error bars represent ±SD. (p-value *<0.05) (n=6 in each group).*

The expression of Atg 3 was found to be unaltered in 2 week and 10 week diabetic mice heart (Figure 59).

Figure 59: Expression of Atg 3

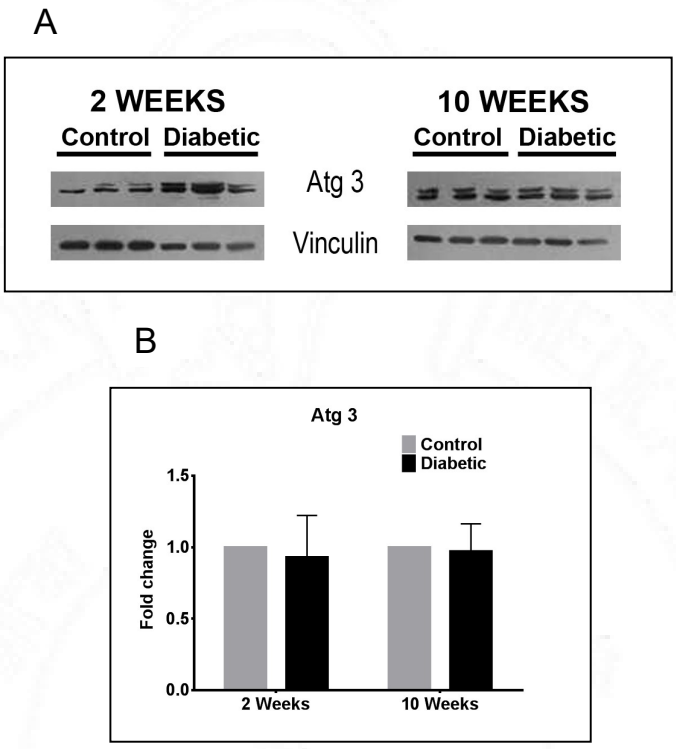

(A) Expression of Atg 3 was showed by western blotting in 2 week and 10 week diabetic mice heart. (B) The bar graphs represent the fold change in expression of the respective protein in 2 week and 10 week diabetic mice heart. Error bars represent ±SD. (n=6 in each group).

The p62 expression levels showeda significant increasein 2 week and 10 week diabetic mice heart (Figure 60).

Figure 60: Expression of p62

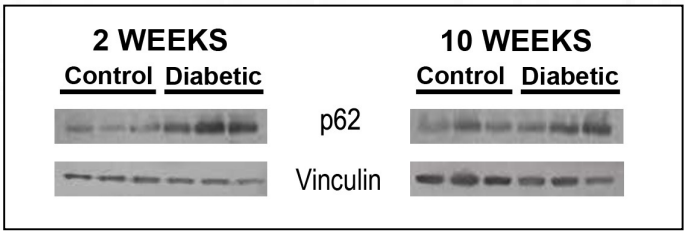

B

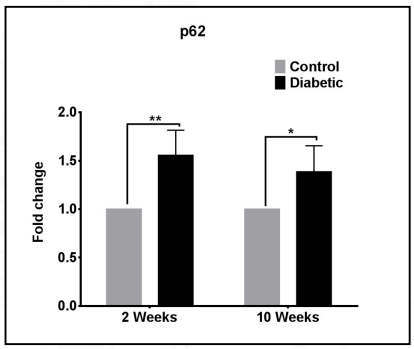

(A) Expression of p62 was showed by western blotting in 2 week and 10 week diabetic mice heart. (B) The bar graphs represent the fold change in expression of the respective protein in 2 week and 10 week diabetic mice heart. Error bars represent ±SD.
*(p-value *<0.05**<0.01) (n=6 in each group).*

Expression of LC3-II level at a given time point (steady state level) was analyzed using western blot technique and is found to be unchanged in 2 week and 10 week diabetic mice heart (Figure 61).

Figure 61: Expression of LC3 II

A

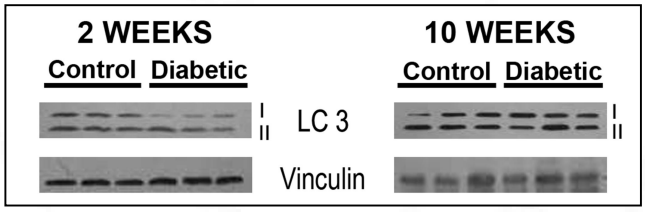

B

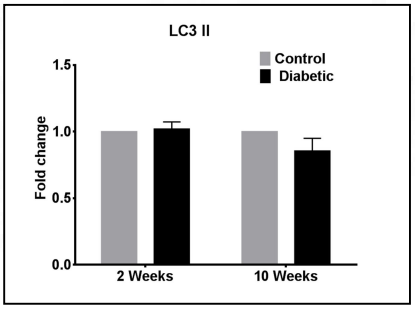

(A) Expression of LC3 II was showed by western blotting in 2 week and 10 week diabetic mice heart. (B) The bar graphs represent the fold change in expression of the respective protein in 2 week and 10 week diabetic mice heart. Error bars represent ±SD.(n=6 in each group).

LC3 II/I ratio was also significantly increased in 2 week, while no change was observed in 10 week diabetic mice (Figure 62).

Figure 62: Expression of LC3 II/I

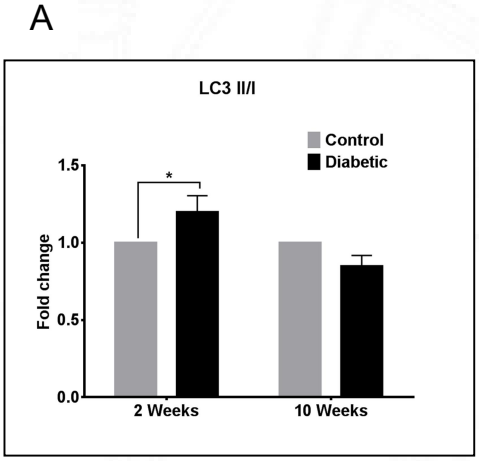

*LC3 II/I ratio calculated from the western blot data of 2 week and 10 week diabetic mice. The bar graphs represent the fold change of the LC3II/I ratio in 2 week and 10 week diabetic mice. Error bars represent ±SD.(p-value *<0.05)(n=6 in each group).*

The expression of PINK 1 was observed to be unchanged in in 2 week and 10 week diabetic mice heart (Figure 63).

Figure 63: Expression of PINK 1

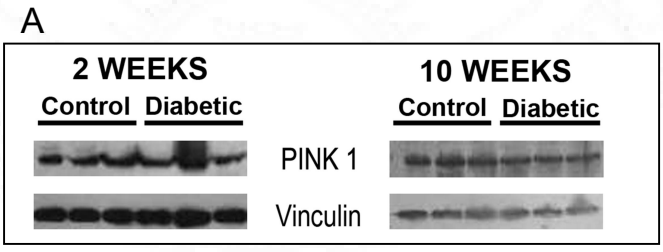

B

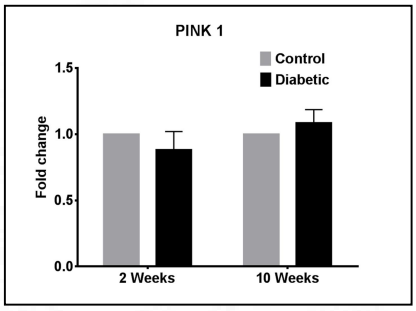

(A) Expression of PINK 1 was showed by western blotting in 2 week and 10 week diabetic mice heart. (B) The bar graphs represent the fold change in expression of the respective protein in 2 week and 10 week diabetic mice heart. Error bars represent ±SD.(n=6 in each group).

The expression of Parkin also was found to be unaltered in 2 week and a significant reduction is noted in 10 week diabetic mice heart (Figure 64).

Figure 64: Expression of Parkin

A

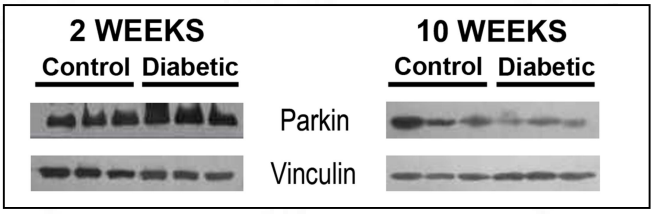

B

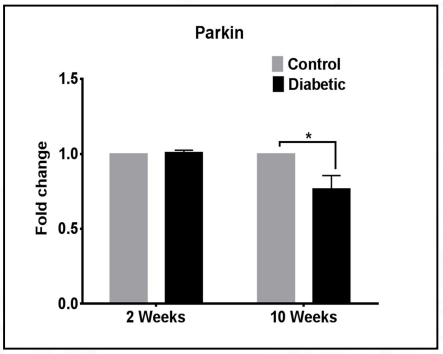

(A) Expression of Parkin was showed by western blotting in 2 week and 10 week diabetic mice heart. (B) The bar graphs represent the fold change in expression of the respective

*protein in 2 week and 10 week diabetic mice heart. Error bars represent ±SD.(p-value *<0.05)(n=6 in each group).*

Cathepsin Dwas found to be unchanged in 2 week and 10 week diabetic mice heart (Figure 65).

Figure 65: Expression of Cathepsin D

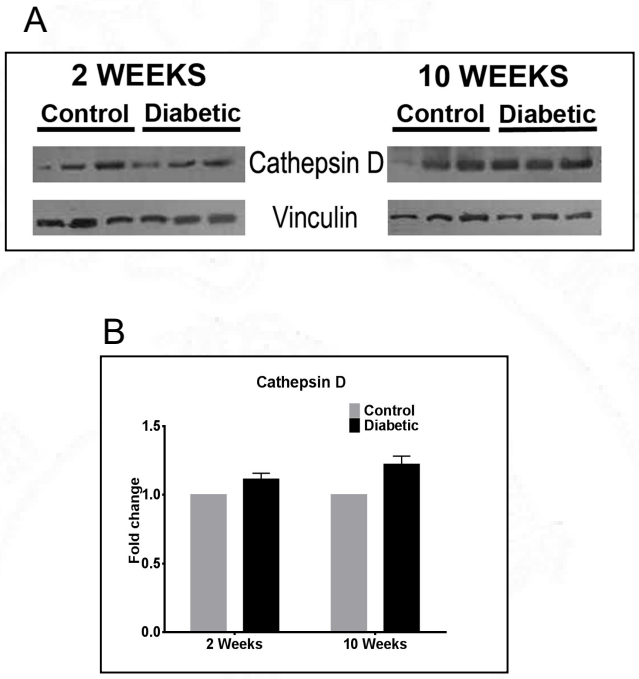

(A) Expression of Cathepsin D was showed by western blotting in 2 week and 10 week diabetic mice heart. (B) The bar graphs represent the fold change in expression of the respective protein in 2 week and 10 week diabetic mice heart. Error bars represent ±SD.(n=6 in each group).

LAMP-2 (lysosome associated membrane protein-2) was found to be unchanged in 2 week and 10 week diabetic mice heart (Figure 66).

Figure 66: Expression of LAMP-2

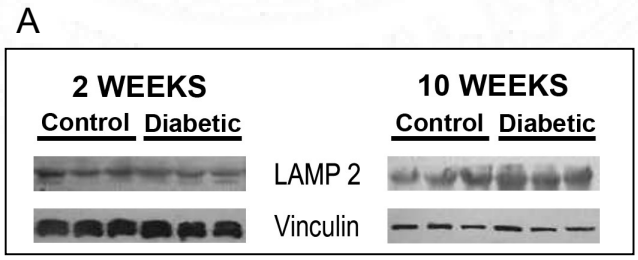

B

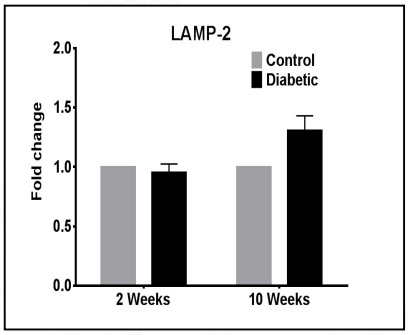

(A) Expression of LAMP-2 was showed by western blotting in 2 week and 10 week diabetic mice heart. (B) The bar graphs represent the fold change in expression of the respective protein in 2 week and 10 week diabetic mice heart. Error bars represent ±SD.(n=6 in each group).

AMPKα expression was found to be unchanged in 2 week and 10 week diabetic mice heart (Figure 67).

Figure 67: Expression of AMPKα

A

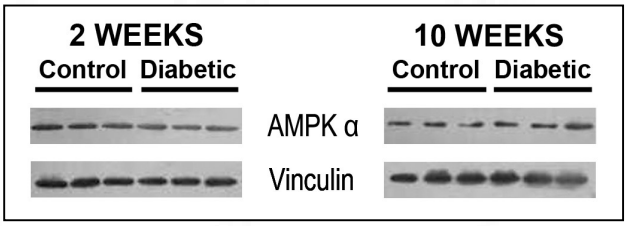

B

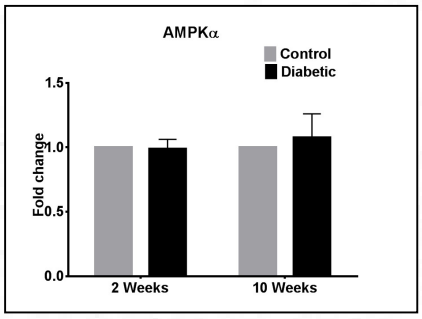

(A) Expression of AMPKα was showed by western blotting in 2 week and 10 week diabetic mice heart. (B) The bar graphs represent the fold change in expression of the respective protein in 2 week and 10 week diabetic mice heart. Error bars represent ±SD.(n=6 in each group).

Phosphorylated form of AMPKα was found to be unchanged in 2 week and 10 week diabetic mice heart (Figure 68).

Figure 68: Expression of pAMPKα

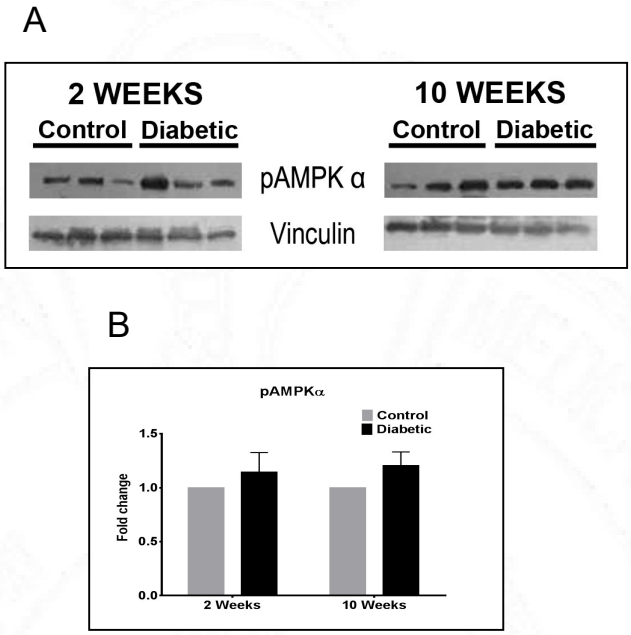

(A) Expression of pAMPKα was showed by western blotting in 2 week and 10 week diabetic mice heart. (B) The bar graphs represent the fold change in expression of the respective protein in 2 week and 10 week diabetic mice heart. Error bars represent ±SD.(n=6 in each group).

mTOR was also found to be unchanged in 2 week and 10 week diabetic mice heart (Figure 69).

Figure 69: Expression of mTOR

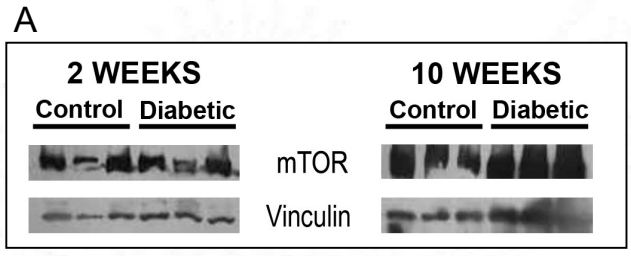

B

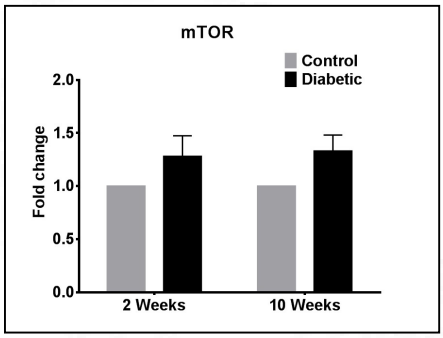

(A) Expression of mTOR was showed by western blotting in 2 week and 10 week diabetic mice heart. (B) The bar graphs represent the fold change in expression of the respective protein in 2 week and 10 week diabetic mice heart. Error bars represent ±SD.(n=6 in each group).

Phosphorylated mTOR was also found to be be unchanged in 2 week and 10 week diabetic mice heart (Figure 70)

Figure 70: Expression of pmTOR

A

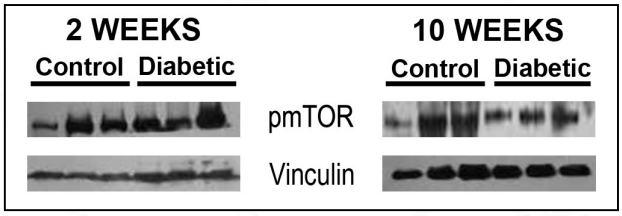

B

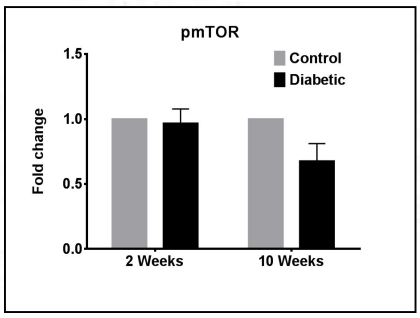

(A) Expression of pmTOR was showed by western blotting in 2 week and 10 week diabetic mice heart. (B) The bar graphs represent the fold change in expression of the respective

protein in 2 week and 10 week diabetic mice heart. Error bars represent ±SD.(n=6 in each group).

Findings:

- **No change was observed in the cardiac autophagic proteins (ULK1, pULK1, Beclin 1, Rubicon, Atgs -3,5,7,12,14 &16), mitophagic proteins (PINK 1, Parkin), lysosomal proteins (Cathepsin D, LAMP-2) and regulators of autophagy (AMPKα, pAMPKα, mTOR, pmTOR) in 2 weeks of diabetic mice**
- **The steady state level of LC3 II was found unchanged, but the LC3II/I ratio was found to be increased at 2 week indicates an increased autophagosome formation or impaired degradation/ accumulation of autophagosome.**
- **A reduced expression of ULK1 and pULK1 was noted in 10 week diabetic mice indicates the initial complex formation with Atg 11, 13 and 17 may get altered or reduced**
- **Beclin 1, Rubicon and other Atgs (3, 5, 7, 12, 14 and 16) didn't show any change with corresponding controls in 10 week diabetic mice.**
- **The increased expression of p62 in 2 week and 10 week diabetic mice shows that the degradation of autophagosomes is blocked/reduced.**
- **No change was observed in the steady state level of LC3 II and its LC3 II/I ratio in 10 week diabetic mice indicated autophagosome formation was similar like the control**
- **The mitophagy proteins, Parkin showed reduced expression; while no change was observed in PINK 1 indicates the improper clearance of damaged mitochondria in the 10 week diabetic mice.**
- **The lysosomal proteins (cathepsin D and LAMP-2) and the regulators of**

autophagy (AMPKα, pAMPKα, mTOR, pmTOR) were found unchanged in 10 week diabetic mice

IV.A.3.2. Analysis of cardiac mitochondrial respiration by modulating autophagy

In order to analyze the activity of mitochondrial electron transport chain complexes by regulating the process of autophagy in type 2 diabetic conditions, high-resolution respirometry was used. For that 10µl aliquot of the isolated mitochondrial suspension (from the treated and non-treated mice whole heart at specific time points) is added to chamber A and chamber B, then followed by the step by step addition of substrates (palmitoyl L-carnitine, malate, ADP, pyruvate, glutamate, succinate), uncoupler (FCCP) and inhibitors (rotenone, oligomycin, antimycin).The OCR was expressed in pmol/s*mg of mitochondrial protein and the values are ROX corrected. ROX represented the residual oxygen flux due to some oxidative side reactions when electron transport pathway is inhibited in the mitochondria by antimycin.

IV.A.3.2.1. Cardiac mitochondrial respiration by activating autophagy (Resveratrol)

Fatty acid + carbohydrate SUIT protocol

To determine whether an activator of autophagy (Resveratrol) can alter cardiac mitochondrial function in diabetic conditions, the animals were treated with resveratrol for 2 weeks after maintaining the hyperglycemic condition for 2 weeks and 10 weeks respectively. After the addition of palmitoyl L-carnitine and malate in chamber A, the untreated diabetic mice mitochondria showed an increase in the state 2 (leak) fatty acid-mediated respiration ($PalM_0$) at 2 weeks, while there was no change in 10 weeks when compared with their corresponding controls. Upon treatment of diabetic mice with resveratrol, the mitochondria showed a significant increase in the state 2 fatty acid-mediated respiration ($PalM_0$) at 2 weeks and 10 weeks (Figure 71).

Figure 71: Resveratrol increased fatty acid-mediated state 2 complex I respiration in 2 week and 10 week diabetic mice

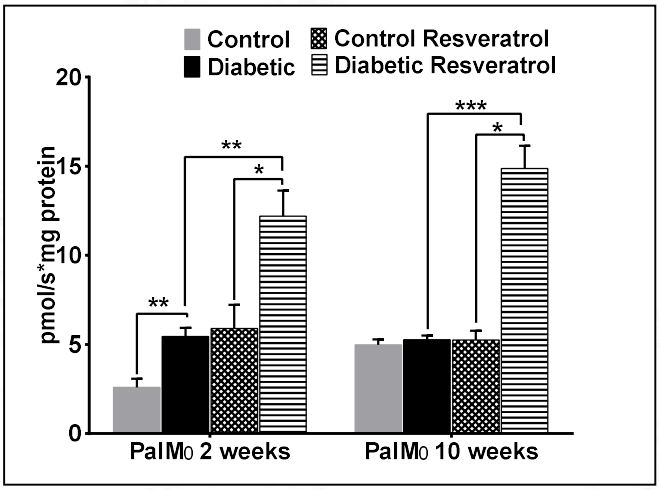

Substrates palmitoyl L-carnitine and malate ($PalM_0$) mediated state 2 complex I respiration. Values are represented as mean ± SD. (p-value<0.05, **<0.01, ***<0.001) (n=6 in each group)*

In state 3 fatty acid-mediated respiration ($PalM_{ADP}$), the untreated diabetic mice mitochondria showed an increase at 2 weeks, while there was no change noted in 10 weeks when compared with their respective controls. When treated with resveratrol, the mitochondria isolated from diabetic mice showed a significant increase in the state 3 palmitoyl L- carnitine, mediated respiration ($PalM_{ADP}$) at 2 weeks and 10 weeks (Figure 72).

Figure 72: Resveratrol increased fatty acid-mediated state 3 complex I respiration in 2 week and 10 week diabetic mice

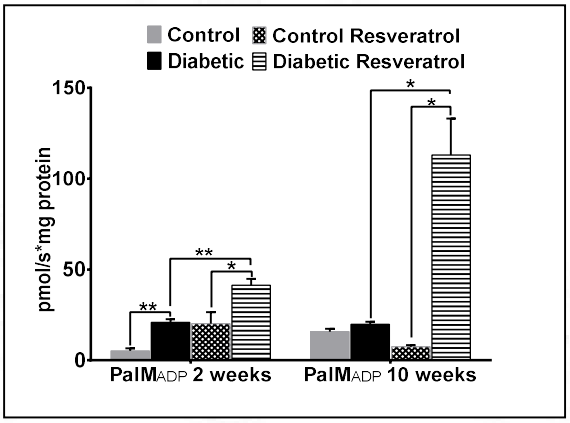

*Substrates palmitoyl L-carnitine and malate (PalM) followed by ADP-mediated state 3 complex I respiration. Values are represented as mean ± SD. (p-value *< 0.05, **<0.01) (n=6 in each group)*

The state 3 complex I respiration mediated by pyruvate ($PalMP_{ADP}$) showed an increase at 2 weeks, while there was no change noted in 10 weeks in untreated diabetic mice mitochondria. The resveratrol treatment further enhanced the pyruvate-mediated state 3 complex I respiration($PalMP_{ADP}$) in mitochondria of diabetic mice at 2 week and 10 week time points (Figure 73).

Figure 73: Resveratrol enhanced pyruvate-mediated state 3 complex I respiration in 2 week and 10 week diabetic mice

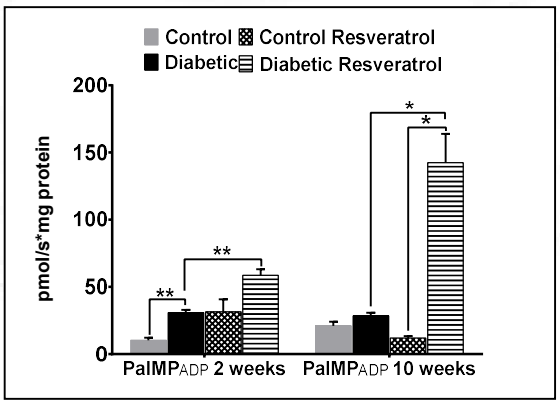

*Substrates palmitoyl L-carnitine and malate (PalM) followed by ADP and pyruvate-mediated state 3 complex I respiration. Values are represented as mean ± SD. (p value * <0.05, **<0.01) (n=6 in each group).*

Like the pyruvate-mediated state 3 complex I respiration, when the substrate glutamate was added to the mitochondria, state 3 complex I respiration ($PalMPG_{ADP}$) showed an increase at 2 weeks, while there was no change noted in 10 weeks in untreated diabetic mice mitochondria. The resveratrol treatment further enhanced the glutamate ($PalMPG_{ADP}$) mediated state 3 complex I respiration in mitochondria of diabetic mice at 2 week and 10 week time points (Figure 74).

Figure 74: Resveratrol enhanced glutamate-mediated state 3 complex I respiration in 2 week and 10 week diabetic mice

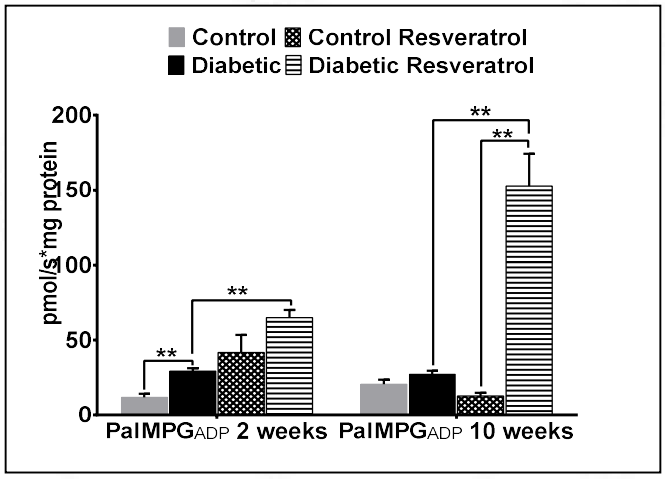

*Substrates palmitoyl L-carnitineand malate (PalM) followed by ADP, pyruvate and glutamate-mediated state 3 complex I respiration. Values are represented as mean ± SD. (p-value *<0.05, **<0.01) (n=6 in each group).*

Unlike the palmitoyl L-carnitine/malate, pyruvate and glutamate-mediated state 3 complex I respiration, when succinate was added, there showed a decreased state 3 complex I + II respiration($PalMPGS_{ADP}$) at 2 weeks untreated diabetic mice, even though no change was observed in 10 weeks untreated diabetic mice. But after the resveratrol treatment, state 3 complex I + II respiration ($PalMPGS_{ADP}$) was enhanced in mitochondria of diabetic mice at 2 week and 10 week time points (Figure 75).

Figure 75: Resveratrol treatment caused increase in complex I + II state 3 respiration in both 2 week and 10 week diabetic mice

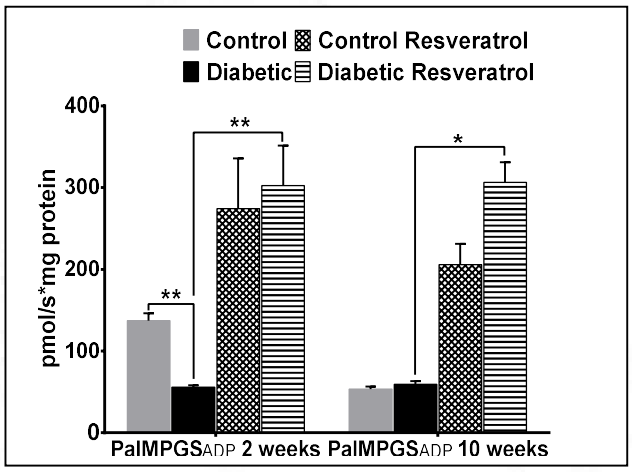

*Substrates palmitoyl L-carnitine/malate (PalM) followed by ADP, pyruvate, glutamate and succinate-mediated state 3 complex I + II respiration. Values are represented as mean ± SD. (p-value *< 0.05,**<0.01) (n=6 in each group).*

State 3 complex II respiration (obtained after addition of rotenone, inhibitor of complex I), (S_{Rot}) showed a decreased OCR at 2 weeks and unchanged respiration was observed in 10 weeks untreated diabetic mice mitochondria. The resveratrol treatment in the diabetic mice at 2 week and 10 week time points enhanced the succinate mediated complex II respiration (S_{Rot}) (Figure 76).

Figure 76: Resveratrol treatment caused increase in state 3 complex II respiration in both 2 week and 10 week diabetic mice

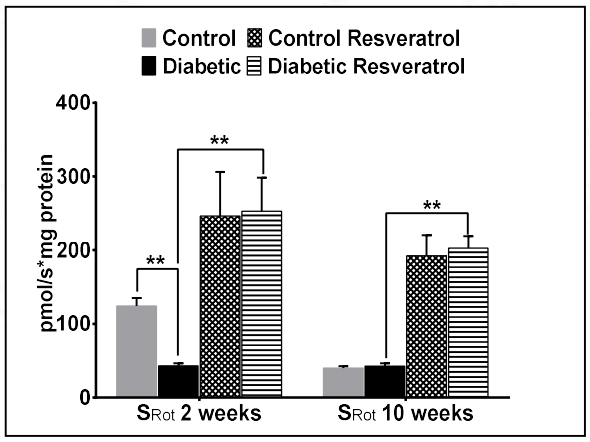

*Substrates succinate and ADP, inhibitor- rotenone mediated state 3 complex II respiration. Values are represented as mean ± SD (p-value *< 0.05**<0.01) (n=6 in each group).*

State 4 respiration obtained after the addition of oligomycin (S_{Omy}) was found to be decreasedat 2 weeks and unchanged respiration was observed in 10 weeks untreated diabetic mice mitochondria. The resveratrol treatment in the diabetic mice at 2 week and 10 week time points enhanced complex II mediated state 4 respiration (Figure 77).

Figure 77: Resveratrol treatment enhanced state 4 complex II respiration in both 2 week and 10 week diabetic mice

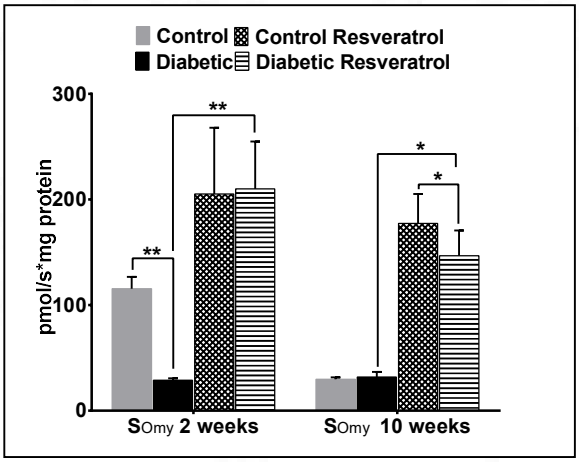

*Succinate-mediated complex II state 4 respiration in presence of oligomycin. Values are represented as mean ± SD (p-value *< 0.05**<0.01) (n=6 in each group).*

The maximal respiratory capacity obtained after the addition of uncoupler FCCP (S_{FCCP}) was found to be decreasedat 2 weeks and unchanged respiration was observed in 10 weeks untreated diabetic mice mitochondria. The resveratrol treatment in the diabetic mice at 2 week and 10 week time points significantly enhanced complex II mediated maximal respiration (Figure 78).

Figure 78: Resveratrol treatment enhanced complex IImaximal respiration in both 2 week and 10 week diabetic mice

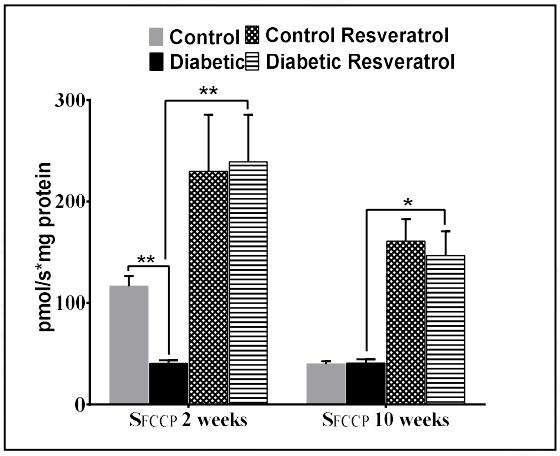

*Complex II maximal respiration in presence of FCCP. Values are represented as mean ± SD (p-value *< 0.05**<0.01) (n=6 in each group).*

Findings:

- **The fatty acid-mediated state 2 and glutamate and pyruvate-mediated state 3 complex I respiration was found to be increased in the 2 week hyperglycemic condition, while an unchanged state 2 and state 3 complex I respiration was observed in the 10 week untreated diabetic mice mitochondria**
- **Succinate-mediated complex I + II and complex II respiration werelower in the 2 week time period, even though no change was noticed in 10 week period of hyperglycemia in untreated diabetic mice mitochondria**
- **State 4 respiration and maximal respiratory capacity was observed to be decreased in 2 weeks while an unchanged respiration was observed in the 10 week untreated diabetic mice mitochondria**
- **Resveratrol (activator of autophagic process) further enhanced the fatty acid-mediated state 2 and glutamate, pyruvate-mediated state 3 complex I respiration in 2 week diabetic mice mitochondria**

- **The unchanged state 2 and state 3 complex I respiration shown by the untreated diabetic mice mitochondria in 10 week time point was significantly increased by the resveratrol treatment**
- **The decreased respiration shown by succinate-mediated complex I + II and complex II by the 2 week untreated diabetic mice mitochondria was significantly enhanced by the resveratrol treatment**
- **The unchanged succinate-mediated complex I + II and complex II respiration shown by the untreated diabetic mice mitochondria in 10 week time point was significantly increased by the resveratrol treatment**
- **Resveratrol treatment in the diabetic mice increased the state 4 respiration and maximal respiratory capacity in 2 weeks and the unchanged OCR in 10 weeks untreated diabetic mice was also significantly enhanced**

Carbohydrate SUIT protocol

After the addition of glutamate and malate in chamber B, the untreated diabetic mice mitochondria showed unchanged state 2 (leak) respiration (GM_0) at 2 weeks and 10 weeks when compared with their corresponding controls, while resveratrol treated diabetic mice mitochondria showed a significant increase in the glutamate/malate-mediated state 2 (leak) respiration at 2 weeks and 10 weeks (Figure 79).

Figure 79: Resveratrol treatment increased glutamate-mediated state 2 complex I respiration in both 2 week and 10 week diabetic mice

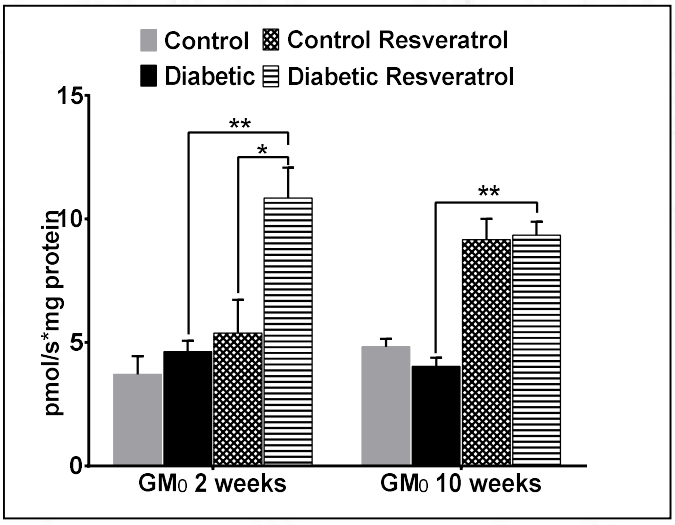

Substrates glutamate/malate-mediated state 2 complex I respiration. Values are represented as mean ± SD. (p-value< 0.05**<0.01) (n=6 in each group).*

In state 3 glutamate-mediated respiration (GM_{ADP}), the untreated diabetic mice mitochondria showed a decrease at 2 weeks, while no change was noticed in 10 weeks. Resveratrol treated diabetic mice mitochondria showed a significant increase in the state 3 glutamate-mediated respiration (GM_{ADP}) at 2 weeks and 10 weeks (Figure 80).

Figure 80: Resveratrol treatment caused increase in glutamate-mediated state 3 complex I respiration in both 2 week and 10 week diabetic mice

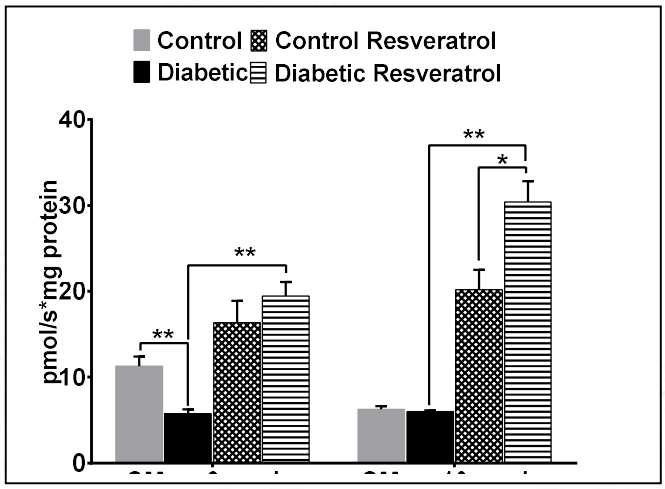

Substrates glutamate and malate followed by ADP-mediated state 3 complex I respiration. Values are represented as mean ± SD. (p-value< 0.05**<0.01) (n=6 in each group).*

The state 3 complex I respiration mediated by glutamate, malate and pyruvate (GMP_{ADP}) showed a decrease at 2 weeks, while there showed increased respiration in 10 week untreated diabetic mice mitochondria. The resveratrol treatment also enhanced the pyruvate- mediated state 3 complex I respiration (GMP_{ADP}) in mitochondria of diabetic mice at 2 week and 10 week time points (Figure 81).

Figure 81: Resveratrol treatment enhanced pyruvate-mediated state 3 complex I respiration in both 2 week and 10 week diabetic mice

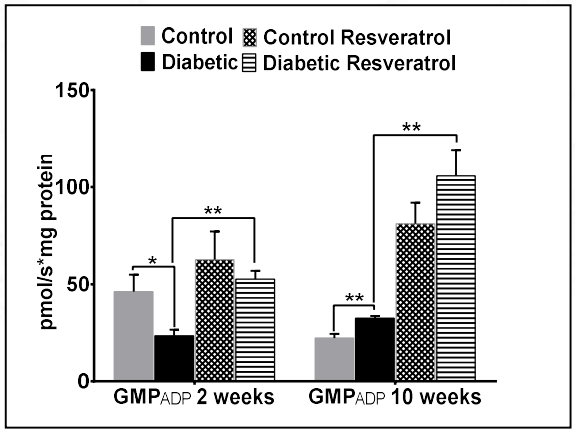

Substrates glutamate and malate followed by ADP and pyruvate-mediated state 3 complex I respiration. Values are represented as mean ± SD. (p-value< 0.05**<0.01) (n=6 in each group).*

When succinate was added, there showed a decreased state 3 complex I + II respiration($GMPS_{ADP}$) at 2 weeks untreated diabetic mice. Even though no change was observed in 10 weeks untreated diabetic mice mitochondria, the resveratrol treatment enhanced state 3 complex I + II respiration ($GMPS_{ADP}$) in mitochondria of diabetic mice at 2 week and 10 week time points (Figure 82).

Figure 82: Resveratrol treatment enhanced state 3 complex I + II respiration in both 2 week and 10 week diabetic mice

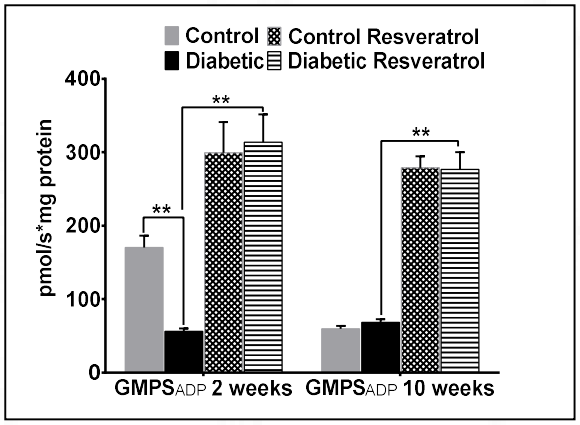

*Substrates glutamate and malate followed by ADP,pyruvate and succinate mediated state 3 complex I + II respiration. Values are represented as mean ± SD. (p-value**<0.01) (n=6 in each group).*

State 3 complex II respiration (obtained after addition of rotenone, inhibitor of complex I), (S_{Rot}) showed a decreased OCR at 2 weeks and unchanged respiration was observed in 10 weeks untreated diabetic mice mitochondria. The resveratrol treatment in the diabetic mice at 2 week and 10 week time points enhanced the succinate mediated complex II respiration (S_{Rot}) (Figure 83).

Figure 83: Resveratrol treatment enhanced state 3 complex II respiration in both 2 week and 10 week diabetic mice

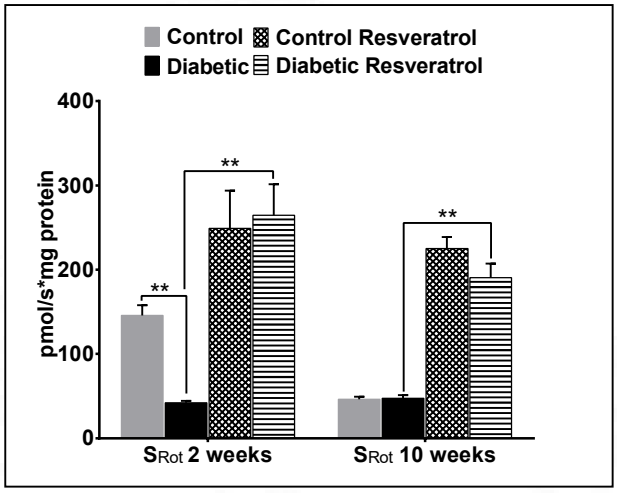

*State 3 complex II respiration of control and diabetic mitochondria with substrate succinate and inhibitor rotenone. Values are represented as mean ± SD. (p-value **<0.01) (n=6 in each group).*

State 4 respiration obtained after the addition of oligomycin (S_{Omy}) was found to be decreasedat 2 weeks and unchanged respiration was observed in 10 weeks untreated diabetic mice mitochondria. The resveratrol treatment in the diabetic mice at 2 week and 10 week time points enhanced state 4 respiration (Figure 84).

Figure 84: Resveratrol treatment enhanced complex II state 4 respiration in both 2 week and 10 week diabetic mice

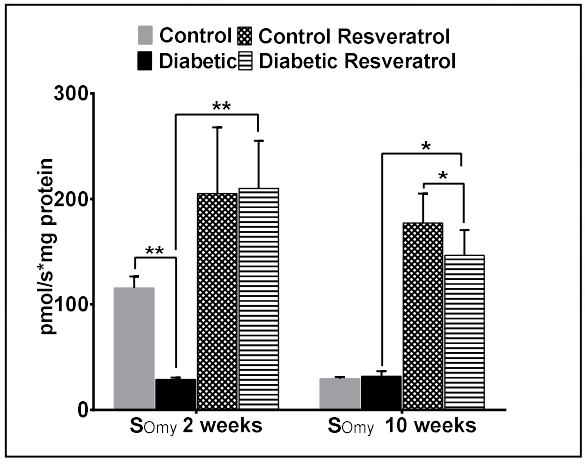

*State 4 respiration in presence of oligomycin. Values are represented as mean± SD (p-value *< 0.05**<0.01) (n=6 in each group).*

The maximal respiratory capacity obtained after the addition of uncoupler FCCP (S_{FCCP}) was found to be decreasedat 2 weeks and unchanged respiration was observed in 10 weeks untreated diabetic mice mitochondria. The resveratrol treatment in the diabetic mice at 2 week and 10 week time points significantly enhanced maximal respiration of complex II (Figure 85).

Figure 85: Resveratrol treatment enhanced maximal respiration of complex II in both 2 week and 10 week diabetic mice

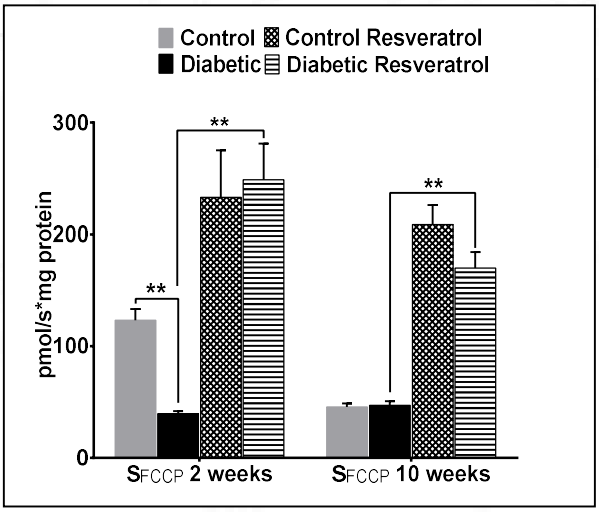

*Maximal respiration of complex II in presence of FCCP. Values are represented as mean ± SD (p-value *< 0.05**<0.01) (n=6 in each group).*

Findings:

- **The glutamate/malate-mediated state 2 complex I respiration was found to be unchanged in 2 week and 10 week untreated diabetic mice mitochondria**
- **State 3 respiration of complex I mediated by glutamate/malate in presence of ADP was found to be decreased in 2 week, even though no change was observed in 10 week untreated diabetic mice mitochondria**
- **State 3 complex I respiration mediated by pyruvate was found to be decreased in 2 week, but showed an increase in the 10 week untreated diabetic mice mitochondria**

- **Succinate-mediated complex I + II and complex II respiration was lower in the 2 week time period, even though no change was noticed in 10 week period of hyperglycemia in untreated diabetic mice mitochondria**
- **State 4 respiration and maximal respiratory capacity was observed to be decreased in 2 weeks while an unchanged respiration was observed in the 10 week untreated diabetic mice mitochondria**
- **Resveratrol (activator of autophagic process) enhanced glutamate-mediated state 2 respiration and glutamate/malate and pyruvate-mediated state 3 complex I respiration in 2 week and 10 week diabetic mice mitochondria**
- **The decreased succinate-mediated complex I + II and complex II respiration shown by the 2 week untreated diabetic mice mitochondria was significantly enhanced by the resveratrol treatment**
- **The unchanged succinate-mediated complex I + II and complex II respiration shown by the untreated diabetic mice mitochondria in 10 week time point was significantly increased by the resveratrol treatment**
- **Resveratrol treatment in the diabetic mice increased the state 4 respiration and maximal respiratory capacity in 2 weeks and the unchanged OCR in 10 weeks untreated diabetic mice was also significantly enhanced**

IV.A.3.2.2. Cardiac mitochondrial respiration by inhibiting autophagy (Chloroquine)

Fatty acid + carbohydrate SUIT protocol

To analyze whether an inhibitor of autophagy (Chloroquine) can alter cardiac mitochondrial function in diabetic conditions, the animals were treated with chloroquine for 2 weeks after maintaining the hyperglycemic condition for 2 weeks and 10 weeks respectively. After the addition of substrates, inhibitors and uncouplers in chamber A, the untreated diabetic mice mitochondria showed an increase in the state 2 (leak) fatty acid mediated respiration

($PalM_0$) at 2 weeks while there was no change in 10 weeks when compared with their corresponding controls. Upon treatment of the diabetic mice with chloroquine, the isolated cardiac mitochondria showed a further decrease in the state 2 fatty acid-mediated respiration ($PalM_0$) at 2 weeks and 10 weeks (Figure 86).

Figure 86: Chloroquine decreased fatty acid-mediated state 2 complex I respiration in 2 week and 10 week diabetic mice

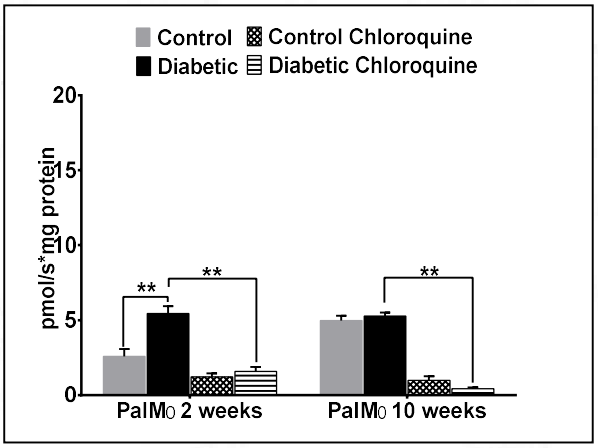

*Substrates palmitoyl L-carnitine and malate ($PalM_0$) mediated state 2 Complex I respiration. Values are represented as mean ± SD. (p-value **<0.01) (n=6 in each group)*

In state 3 fatty acid-mediated respiration ($PalM_{ADP}$), the untreated diabetic mice mitochondria showed a significant increase at 2 weeks, while there was no change noted in 10 weeks. When treated the diabetic mice with chloroquine, the mitochondria showed a significant decrease in the state 3 palmitoyl L- carnitine, mediated respiration ($PalM_{ADP}$) at 2 weeks and 10 weeks (Figure 87).

Figure 87: Chloroquine decreased fatty acid-mediated state 3 complex I respiration in 2 week and 10 week diabetic mice

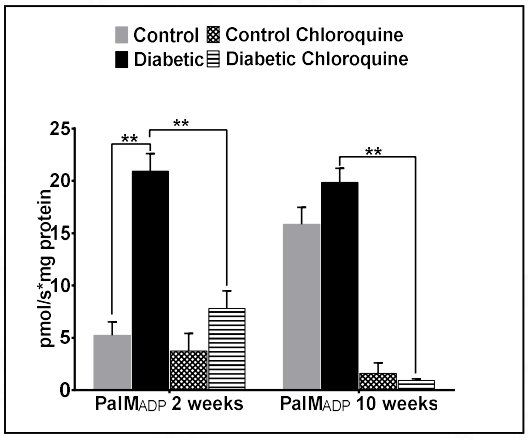

*Substrates palmitoyl L-carnitine and malate (PalM) followed by ADP-mediated state 3 complex I respiration. Values are represented as mean± SD. (p-value **<0.01) (n=6 in each group)*

The state 3 complex I respiration mediated by pyruvate ($PalMP_{ADP}$) showed an increase at 2 week, while there was no change noted in 10 weeks untreated diabetic mice mitochondria. When treated the diabetic mice with chloroquine, the mitochondria showed a significant decrease in the state 3 pyruvate mediated respiration ($PalMP_{ADP}$) at 2 weeks and 10 weeks (Figure 88).

Figure 88: Chloroquine decreased pyruvate-mediated state 3 complex I respiration in 2 week and 10 week diabetic mice

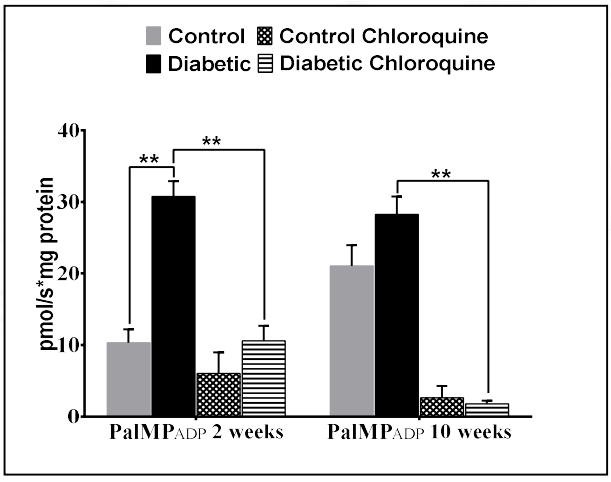

*Substrates palmitoyl L-carnitine and malate (PalM) followed by ADP and pyruvate-mediated state 3 complex I respiration. Values are represented as means ± SD. (p value, **<0.01) (n=6 in each group).*

Like the pyruvate-mediated state 3 complex I respiration, when the substrate glutamate was added to the mitochondria, state 3 complex I respiration ($PalMPG_{ADP}$) showed an increase at 2 weeks, while there was no change noted in 10 weeks in untreated diabetic mice mitochondria. The chloroquine treatment further decreased the glutamate ($PalMPG_{ADP}$) mediated state 3 complex I respiration in mitochondria of diabetic mice at 2 week and 10 week time points (Figure 89).

Figure 89: Chloroquine decreased glutamate-mediated state 3 complex I respiration in 2 week and 10 week diabetic mice

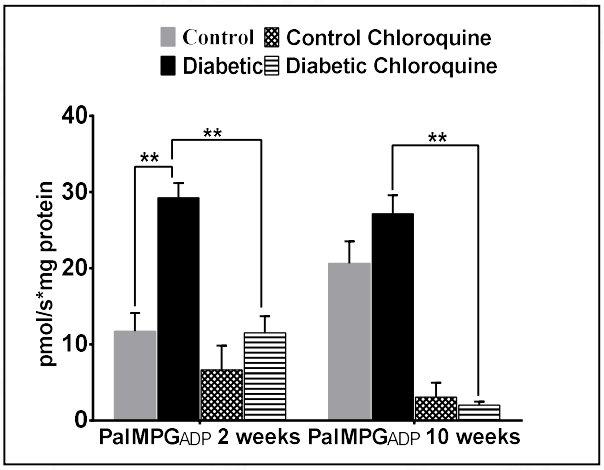

*Substrates palmitoyl L-carnitine and malate (PalM) followed by ADP, pyruvate and glutamate-mediated state 3 complex I respiration. Values are represented as mean ± SD. (p value, **<0.01) (n=6 in each group).*

Unlike the palmitoyl L-carnitine/malate, pyruvate and glutamate-mediated state 3 complex I respiration, when succinate ($PalMPGS_{ADP}$) was added, there was a decreased state 3 complex I + II respiration at 2 weeks untreated diabetic mice. Even though no change was observed in 10 weeks untreated diabetic mice,. the chloroquine treatment further decreased state 3 complex I + II respiration ($PalMPGS_{ADP}$ in mitochondria of diabetic mice at 2 week and 10 week time points (Figure 90).

Figure 90: Chloroquine treatment caused decrease in complex I + II state 3 respiration in both 2 week and 10 week diabetic mice

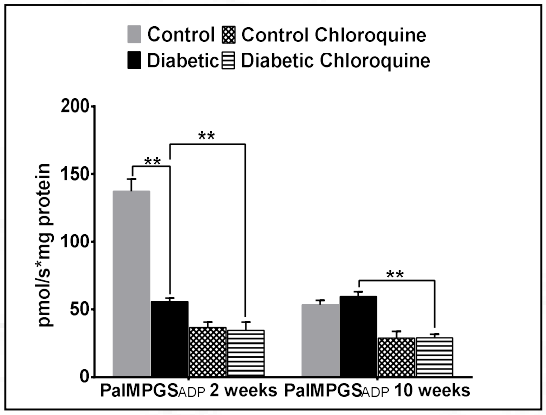

*Substrates palmitoyl L-carnitine and malate (PalM) followed by ADP, pyruvate, glutamate and succinate-mediated state 3 complex I + II respiration. Values are represented as mean ± SD. (p value, **<0.01) (n=6 in each group)*

State 3 complex II respiration (obtained after addition of rotenone, inhibitor of complex I), (S_{Rot}) showed a decreased OCR at 2 weeks and unchanged respiration was observed in 10 weeks untreated diabetic mice mitochondria. The chloroquine treatment in the diabetic mice at 2 week and 10 week time points further decreased the succinate-mediated complex II respiration (S_{Rot}) (Figure 91).

Figure 91: Chloroquine treatment caused decrease in state 3 complex II respiration in both 2 week and 10 week diabetic mice

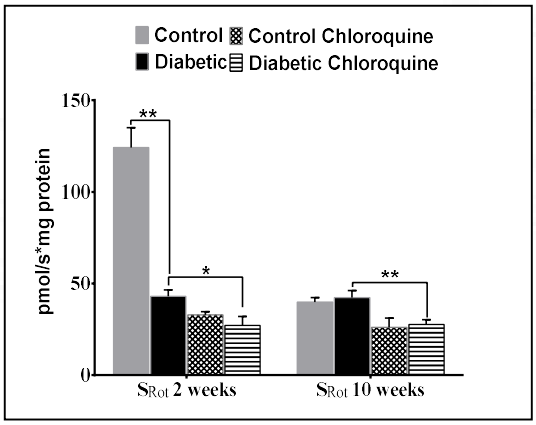

*Substrates succinate and ADP, inhibitor- rotenone mediated state 3 complex II respiration. Values are represented as mean ± SD (p-value *< 0.05**<0.01) (n=6 in each group).*

State 4 respiration obtained after the addition of oligomycin (S_{Omy}) was found to be decreasedat 2 weeks and unchanged respiration was observed in 10 weeks untreated diabetic mice mitochondria. The chloroquine treatment in the diabetic mice at 2 week and 10 week didn't change the state 4 respiration (Figure 92).

Figure 92: Chloroquine treatment did not alter state 4 respiration in both 2 week and 10 week diabetic mice

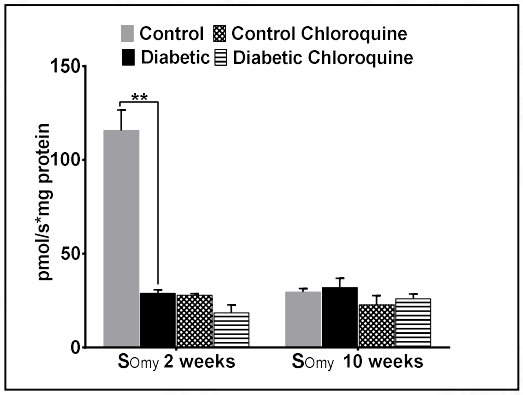

*State 4 respiration in presence of oligomycin. Values are represented as means ± SD (p-value **<0.01) (n=6 in each group).*

The maximal respiratory capacity obtained after the addition of uncoupler FCCP (S_{FCCP}) was found to be decreasedat 2 weeks and unchanged respiration was observed in 10 weeks untreated diabetic mice mitochondria. The choroquine treatment in diabetic mice at 2 week and 10 week time points significantly decreased the complex II maximal respiration (Figure 93).

Figure 93: Chloroquine treatment decreased complex II maximal respiration in both 2 week and 10 week diabetic mice

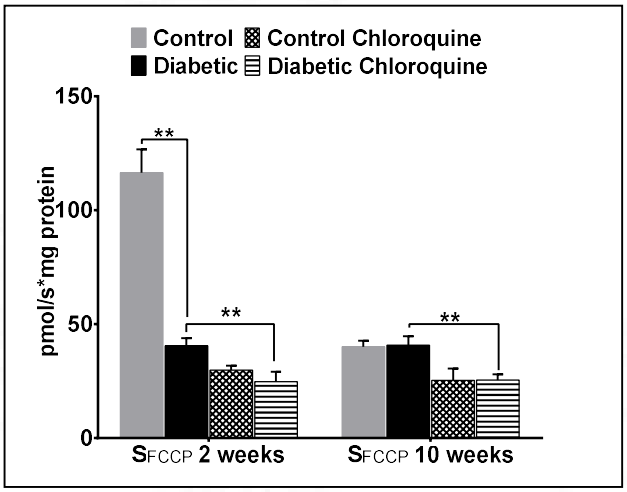

*Complex II maximal respiration in presence of FCCP. Values are represented as mean ± SD (p-value **<0.01) (n=6 in each group).*

Findings:

- **The fatty acid-mediated state 2 and glutamate, pyruvate-mediated state 3 complex I respiration was found to be increased in the 2 week hyperglycemic condition, while an unchanged state 2 and state 3 complex I respiration was observed in the 10 week untreated diabetic mice mitochondria**
- **Succinate-mediated Complex I + II and Complex II respiration was lower in the 2 week time period, even though no change was noticed in the Complex I + II and Complex II respiration in 10 week period of hyperglycemia in untreated diabetic mice mitochondria**
- **State 4 respiration and maximal respiratory capacity was observed to be decreased in 2 weeks while an unchanged respiration was observed in the 10 week untreated diabetic mice mitochondria**
- **Chloroquine (inhibitor of autophagy) decreased the fatty acid-mediated state**

2 and glutamate, pyruvate-mediated state 3 complex I respiration in 2 week diabetic mice mitochondria

- **The unchanged state 2 and state 3 complex I respiration shown by the untreated diabetic mice mitochondria in 10 week time point was drastically decreased by the chloroquine treatment**
- **The decreased respiration shown by succinate-mediated complex I + II and complex II by the 2 week untreated diabetic mice mitochondria was again significantly reduced by the chloroquine treatment**
- **The unchanged succinate-mediated complex I + II and complex II respiration shown by the untreated diabetic mice mitochondria in 10 week time point was significantly decreased by the chloroquine treatment**
- **Chloroquine treatment didn't alter the state 4 respiration, but the maximal respiratory capacity was significantly reduced in 2 weeks diabetic mice and the unchanged OCR in 10 weeks untreated diabetic mice was significantly reduced**

Carbohydrate SUIT protocol (Chloroquine)

After the addition of glutamate and malate in the chamber B, the untreated diabetic mice mitochondria showed unchanged state 2 (leak) respiration (GM_0) at 2 weeks and 10 weeks when compared with their corresponding controls. When treated the diabetic mice with chloroquine, the mitochondria showed a significant decrease in the glutamate and malate mediated state 2 (leak) respiration at 2 weeks and 10 weeks (Figure 94).

Figure 94: Chloroquine treatment show decreased glutamate-mediated state 2 complex I respiration in both 2 week and 10 week diabetic mice

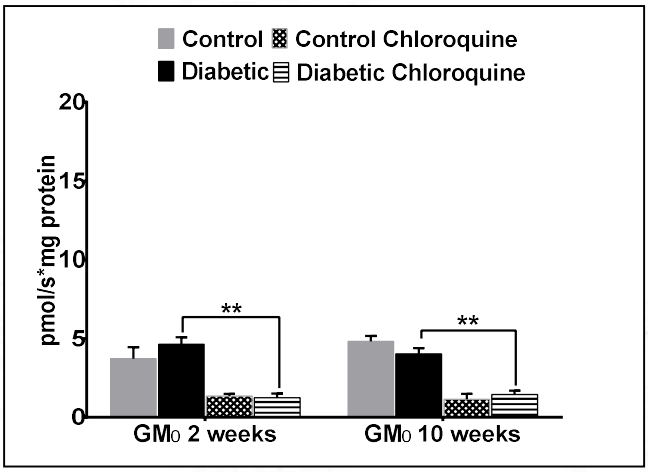

*Substrates glutamate and malate mediated state 2 complex I respiration. Values are represented as mean ± SD. (p-value**<0.01) (n=6 in each group).*

In state 3 glutamate-mediated respiration (GM_{ADP}), the untreated diabetic mice mitochondria showed a decrease at 2 weeks, while no change was noticed in 10 weeks. Chloroquine treated diabetic mice mitochondria showed a significant decrease in the state 3 glutamate/malate-mediated respiration (GM_{ADP}) at 2 weeks and 10 weeks (Figure 95).

Figure 95: Chloroquine treatment caused decrease in glutamate-mediated state 3 complex I respiration in both 2 week and 10 week diabetic mice

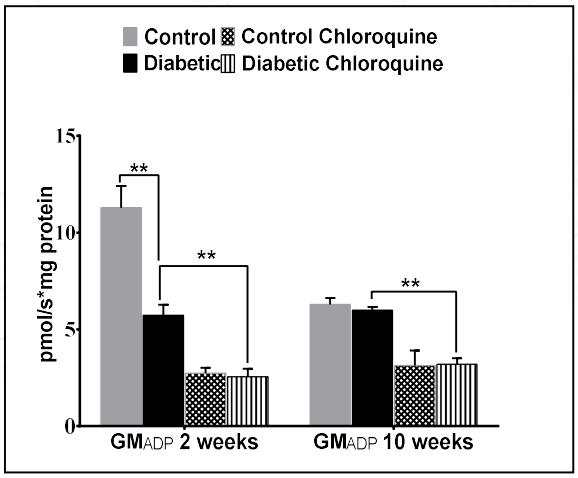

*Substrates glutamate and malate followed by ADP-mediated state 3 complex I respiration. Values are represented as mean ± SD. (p-value**<0.01) (n=6 in each group).*

The state 3 complex I respiration mediated by glutamate, malate and pyruvate (GMP_{ADP}) showed a decreased respiration at 2 weeks, while there showed a increased respiration in 10 week untreated diabetic mice mitochondria. The chloroquine treatment significantly decreased the pyruvate-mediated state 3 complex I respiration(GMP_{ADP}) in mitochondria of diabetic mice at 2 week and 10 week time points (Figure 96).

Figure 96: Chloroquine treatment decreased pyruvate-mediated state 3 complex I respiration in both 2 week and 10 week diabetic mice

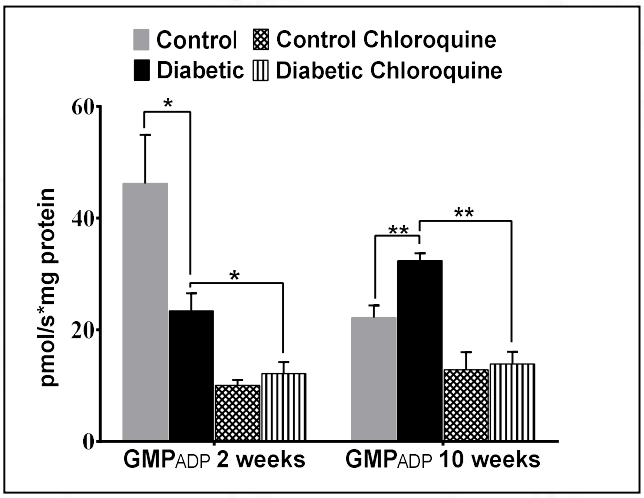

Substrates glutamate and malate followed by ADP and pyruvate-mediated state 3 complex I respiration. Values are represented as mean ± SD. (p-value< 0.05**<0.01) (n=6 in each group).*

When succinate was added, there showed a decreased state 3 complex I + II respiration ($GMPS_{ADP}$) at 2 weeks untreated diabetic mice. Even though no change was observed in 10 weeks untreated diabetic mice mitochondria, the chloroquine treatment lowered state 3 complex I + II respiration ($GMPS_{ADP}$) in mitochondria of diabetic mice at 2 week and 10 week time points (Figure 97).

Figure 97: Chloroquine treatment reduced state 3 complex I + II respiration in both 2 week and 10 week diabetic mice

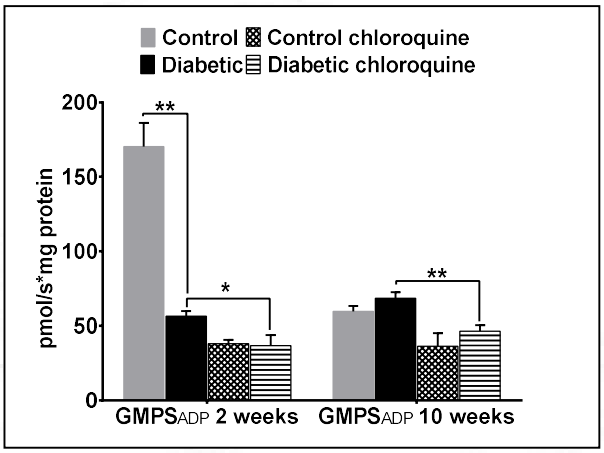

Substrates glutamate and malate followed by ADP and pyruvate and succinate-mediated state 3 complex I + II respiration. Values are represented as mean ± SD. (p-value< 0.05**<0.01) (n=6 in each group).*

State 3 complex II respiration (obtained after addition of rotenone, inhibitor of complex I), (S_{Rot}) showed a decreased OCR at 2 weeks and unchanged respiration was observed in 10 weeks untreated diabetic mice mitochondria. The chloroquine treatment in the diabetic mice at 2 week and 10 week time points reduced the succinate mediated complex II respiration (S_{Rot}) (Figure 98).

Figure 98: Chloroquine treatment reduced state 3 complex II respiration in both 2 week and 10 week diabetic mice

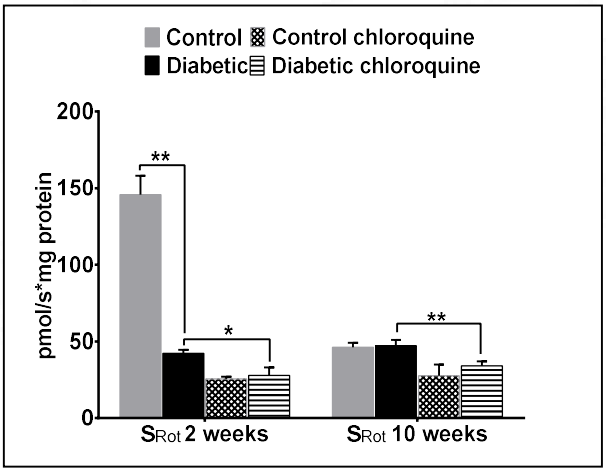

State 3 complex II respiration of control and diabetic mitochondria with substrate succinate and inhibitor rotenone. Values are represented as mean ± SD. (p-value< 0.05**<0.01) (n=6 in each group).*

State 4 respiration obtained after the addition of oligomycin (S_{Omy}) was found to be decreasedat 2 weeks and unchanged respiration was observed in 10 weeks untreated diabetic mice mitochondria. The chloroquine treatment in the diabetic mice at 2 week and 10 week didn't change the state 4 respiration (Figure 99).

Figure 99: Chloroquine treatment didn't alter state 4 respiration in both 2 week and 10 week diabetic mice

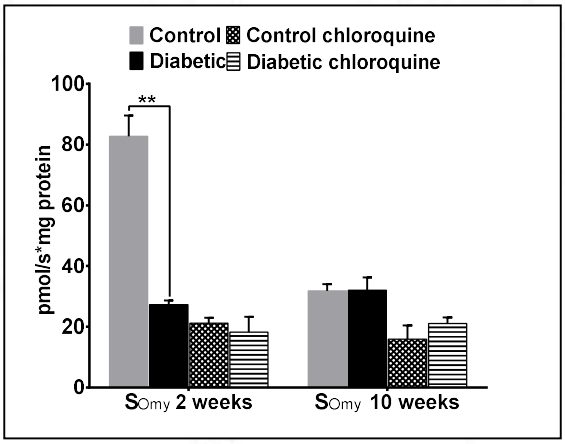

*State 4 respiration in presence of oligomycin. Values are represented as means ± SD (p-value *< 0.05**<0.01) (n=6 in each group).*

The maximal respiratory capacity obtained after the addition of uncoupler FCCP (S_{FCCP}) was found to be decreasedat 2 weeks and unchanged respiration was observed in 10 weeks untreated diabetic mice mitochondria. The chloroquine treatment in the diabetic mice at 2 week and 10 week time points significantly reduced complex II maximal respiration (Figure 100).

Figure 100: Chloroquine treatment lowered complex II maximal respiration in both 2 week and 10 week diabetic mice

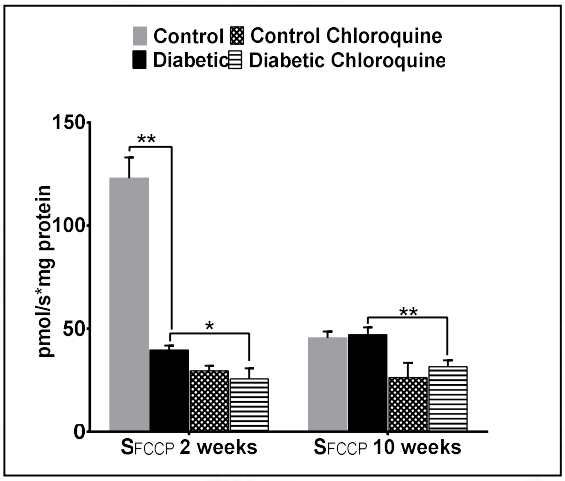

*Complex II maximal respiration in presence of FCCP. Values are represented as means ±SD (p-value *< 0.05**<0.01) (n=6 in each group).*

Findings:

- **The glutamate/malate-mediated state 2 complex I respiration was found to be unchanged in 2 week and 10 week untreated diabetic mice mitochondria**
- **State 3 complex I respiration mediated by glutamate and malate in presence of ADP was found to be decreased in 2 week, even though no change was observed in 10 week untreated diabetic mice mitochondria**
- **State 3 complex I respiration mediated by pyruvate was found to be decreased in 2 week, but showed an increase in the 10 week untreated diabetic mice mitochondria**
- **Succinate-mediated complex I + II and complex II respiration was lower in the 2 week time period, even though no change was noticed in the complex I + II and complex II respiration in 10 week period of hyperglycemia in untreated diabetic mice mitochondria**

- **State 4 respiartion and maximal respiratory capacity was observed to be decreased in 2 weeks while an unchanged respiration was observed in the 10 week untreated diabetic mice mitochondria**
- **Chloroquine (inhibitor of autophagy) decreased glutamate/malate-mdiated state 2 and state 3 complex I respiration and pyruvate-mediated state 3 complex I respiration in 2 week diabetic mice mitochondria**
- **The unchanged state 2 and state 3 complex I respiration shown by the untreated diabetic mice mitochondria in 10 week time point was drastically decreased by the chloroquine treatment**
- **The decreased respiration shown by succinate-mediated complex I + II and complex II by the 2 week untreated diabetic mice mitochondria was again significantly reduced by the chloroquine treatment**
- **The unchanged succinate-mediated complex I + II and complex II respiration in the untreated diabetic mice mitochondria at 10 week time point was significantly decreased by the chloroquine treatment**
- **Chloroquine treatment didn't alter the state 4 respiration, but the maximal respiratory capacity was significantly reduced in 2 weeks diabetic mice and the unchanged OCR in 10 weeks untreated diabetic mice was also significantly reduced**

V.A. DISCUSSION (T2DM)

V.A.1. Autophagy in diabetic human heart

The aim of the study was to evaluate the autophagic status in right atrial appendage tissue obtained from diabetic patients undergoing CABG surgery. Based on our results, myocardial autophagy is reduced in diabetic than the non-diabetic patients. This is the first report on Asian Indian cardiac autophagy in type 2 diabetes. Only a single work has been published so far regarding the autophagy in diabetic human cardiac tissue. In that study, contrast to our results, increased autophagy was reported in diabetic than the non-diabetic patients of New Zealand population (Munasinghe et al., 2016). Our results showed reduced expression of LC3 II and LC3 II/I ratio indicating the reduced formation of autophagosomes. The adaptor molecule p62 expression was increased and Beclin-1 levels were unchanged in diabetic samples. In the study conducted in New Zealand population, they found a marked increase in LC3 II and Beclin-1 and decrease in p62. Even though the number of samples taken is almost same in both studies, the contrasting result may be due to the difference in ethnicity/NYHA class of human subjects included in the study. Our study included Asian Indians belonging to NYHA class II. The duration of diabetes in each of the patients may vary in both the studies.T2DM is always associated with obesity and include risk factors like high circulating LDL, triglycerides, amino acids etc and this high intracellular nutrient energy status may lead to suppression of autophagy in T2DM. In Munasinghe's study, cardiac autophagy was compared between diabetic and non-diabetic patient groups of similar BMI values, but in our study the BMI status of diabetic patients differ significantly. The explanation to the increased autophagy may be the role of fatty acids collected in the heart during type 2 diabetes which was reported by Rovito *et al* and they have shown that fatty acids induced autophagy by activating PPARγ (Rovito et al., 2015). However, we have not provided any evidence in the current study regarding the role of fatty acids behind the altered autophagy. Another report contrasting to our results was published, in which upregulation of autophagy and hypertrophy were observed after attenuation of cardioprotective miR-133a in left ventricular apex tissue of diabetic heart failure patients undergoing mechanical unloading (Nandi et al., 2015). In a recent study done in peripheral

mononuclear cells of newly diagnosed T2DM and advanced duration of T2DM patients showed decreased expression of LC3II and mitophagic markers like parkin and PINK 1(Bhansali et al., 2017). In our study, there were some limitations regarding the unavailability of healthy human heart, a true control for the study. The tissue samples obtained from the non diabetic CABG patients cannot be a perfect control for the study. The patients, both diabetic and non-diabetic included in the study were having ischemic heart disease and were on numerous medications. However, we have selected groups similar with respect to age, sex, lipid levels, NYHA class, medications etc., while a single variable, hyperglycemic status, was different among the patient groups. In order to avoid such limitations, studying the autophagic process in high glucose-treated H9c2 cell line and C57BL/6J mice model with induced type 2 diabetes, can provide a perfect control and evaluate autophagic status at two different time points of diabetes.

V.A.2. Autophagic adaptations in hyperglycemic H9c2 cells

The main objective of the study in H9c2 cells was to analyze autophagic status in high glucose condition at two time points, considerably a shorter time period of 4 h and longer time point of 48 h. We didn't observe any change in the autophagic, mitophagic proteins, proteins associated with lysosomes and the regulators of autophagy in high glucose-treated H9c2 for 4 h time period of hyperglycemia. But the high glucose-treated H9c2 cells maintained for 48 h showed significant decrease in autophagy, exhibited by the decreased levels of LC3 II, pULK1, Atg 5, parkin and PINK 1 and increased p62 levels, even though the lysososmal proteins and regulators were found unchanged at 48 h of hyperglycemia. The results indicated the effect of duration of hyperglycemia on regulating the process of autophagy in H9c2 cells. A time period of 48 h of hyperglycemia can damage or alter the various proteins in the cells including autophagic proteins. The mitophagy proteins, parkin and PINK 1 showed reduced expression at 48 h and indicated the improper clearing mechanism of damaged mitochondria. In a recent study, it was shown that high glucose condition in H9c2 cells suppressed autophagy. In this study ULK 1 played a crucial role in

mitochondrial aldehyde dehydrogenase 2-mediated protective effect against high glucose-induced cardiomyocyte injury by increasing autophagy (Liu et al., 2018). A study done in high glucose (33.3 mM) treated H9c2 cells for 96 h showed decreased autophagy and administration of metformin protected H9c2 cells against high glucose induced apoptosis and connexin43 downregulation through the induction of autophagic pathway (Wang, Bi, Liu, Zhao, et al., 2017). Wang et al., in another study showed that treatment with resveratrol can also protect H9c2 cells against high glucose (25 mM for 24 h) induced apoptosis and connexin43 downregulation through the induction of autophagic pathway (Wang, Bi, Liu, Han, et al., 2017). High glucose-treated neonatal mouse cardiomyocytes for 48 h showed decreased autophagy and treatment withpolydatin, a phytoalexin, increased the autophagic flux (Zhang, Wang, et al., 2017).High glucose (33 mM) treated H9c2 cells for 48 h caused reduction in autophagy, which was enhanced by the treatment of HBSP (helix B surface peptide), a small peptide derived from helix-B domain of erythropoietin (Lin et al., 2017). Excessive palmitate-treated (400 μM) H9c2 for 24 h induced apoptosis through the inhibition of autophagy (Hsu et al., 2016). Through activation of autophagy, fasudil, a Rho-kinase inhibitor suppressed high glucose (25 mM for 24 h) induced apoptosis in H9c2 cells (Gao et al.,2016). Exposure of H9c2 to high glucose (30 mM) for 48 h inhibited autophagy by the reduced expression of AMPK and treatment with metformin normalized autophagy and reduced apoptosis (He et al., 2013). In our results also at 48 h, autophagy is reduced but the AMPK levels were unchanged. In contrast to our results, a study in high glucose (25 mM) - treated H9c2 for 24 h caused enhancement of autophagy mediated by FoxO1 and when they were treated with epigallocatechin-3-gallate (EGCG, a green tea-derived polyphenol) reduced FoxO1 expression and ROS resulting in reduced autophagy (Liu et al., 2014). High glucose (28mM) treated H9c2 cells for 48 h exhibited cardiomyocyte death mediated through MCP-1 (monocyte chemotactic protein-1) along with increased autophagy, ROS and ER stress (Younce et al., 2010). Autophagic status in high glucose condition in H9c2 cells are evaluated at a single time point in all these published reports. No reports are published so far regarding autophagy at different time points as autophagic

status during hyperglycemia fluctuates depending upon the concentration of metabolites at a specific time point in the cells.

V.A.3. Type 2 diabetic mice model

The present study was carried out in order to check the effect of untreated T2DM for two different time periods of hyperglycemia (2 and 10 weeks)on cardiac autophagy and to analyze the cardiacmitochondrial respiration modulated by autophagy by using an autophagic activator (resveratrol) and an inhibitor of autophagy (chloroquine). These time periods are equivalent to 1.7 years and 8.3 years of untreated T2DM in human(The Mouse in Biomedical Research, Volume 4 - 2nd Edition," n.d.). For the study,T2DM was developed by injecting streptozotocin and nicotinamide in C57BL/6 mice. As described by Nakamura *et al*., using this combination of STZ/NA, we were able to develop a non- obese type 2 diabetic mice model(Nakamura et al., 2006). Body weight, random blood glucose and oral glucose tolerance test (OGTT) data were analyzed and these revealed that the mice developed hyperglycemia and it was maintained for 10 weeks without any decrease or increase in body weight. Heart weight to body weight ratio was found to be unchanged in diabetic mice which indicates that at the time of sacrifice, the diabetic mice heart did not develop hypertrophy or other structural changes till the 10 week period of hyperglycemia. Also the HbA1c levels during sacrifice were high for the diabetic mice at 2 week and 10 week time period.Theinsulin levels of 2 week diabetic mice were maintained similar to that of the control group and an increase in its levels were observed at 10 week time point, although insignificant, indicated a trend towards development of hyperinsulinemia at an extended time period of T2DM. Plasma triglyceride levels were unchanged in 2 week and 10 week diabetic mice while total cholesterol levels were found to be increased after 2 weeks of hyperglycemia and then maintained like control group at 10 weeks. Together these data showed the development of a non-obese T2DM mice model.

V.A.3.1 Autophagic status in type 2 diabetic mice

The main objective of the study in type 2 diabetic mice was to analyze cardiac autophagic status at two time points of diabetes, 2 weeks and 10 weeks of hyperglycemia. Mitophagic proteins, lysosomal proteins and the regulators of autophagy were found unchanged in 2 weeks of diabetic mice heart when compared with their corresponding controls. The LC3 II ratio was found unchanged even though the LC3 II/I ratio and p62 levels was increased in 2 week diabetic mice indicated an impaired autophagy with accumulation of autophagosomes. In 10 week diabetic mice, a significant reduction was noted in ULK1, pULK1 and increase in p62 was noted. LC3 II and LC3 II/I ratio was unchanged at 10 week hyperglycemia when compared to specific controls. Reduction in parkin levels indicated that the mitophagy pathway is altered and accumulation of damaged or dysfunctional mitochondria may occur in heart tissue. In a study done in obese diabetic (*ob/ob*) mice, cardiac autophagic flux is suppressed due to impaired formation of autophagosome and the suppression of autophagy is due to mTOR activation. The LC3 II and Atg 3 levels were found to be decreased and the p62 and Atg 7 expression were increased in the *ob/ob* mice. The Atg 5 and Atg 12 were found unchanged in this study (Pires et al., 2017). In an STZ-induced diabetic model, polydatin, a polyphenolic pytoalexin increased the autophagic flux and mitochondrial function by activation of sirtuin 3. There observed an increased LC3 II and decreased p62 during polydatin treatment (Zhang, Wang, et al., 2017). In a high fat-fed mice, blockage of RAGE (Receptor for advanced glycation end product) receptors reduced mitochondrial damage and mitochondrial dysfunction by reducing the oxidative stress, and increasing the autophagic pathway and mitochondrial dynamics. The ratio of LC3 II/I ratio, p62 and parkin were found unchanged in high fat – fed wild type mice while a high LC3 ratio and parkin with decreased p62 was observed in normal diet $RAGE^{-/-}$ mice (Yu et al., 2017). Dihydromyricetin administration to STZ-induced diabetic C57B/6J mice improved the reduced autophagy during diabetes along with reduction in oxidative stress, inflammation and improved the mitochondrial and cardiac function. In this study western blot analysis revealed reduced LC3 II/I ratio, beclin-1 and Atg 7, while p62 expression was increased.

Dihydromyricetin administration to the diabetic animals restored autophagy by increasing LC3 II/I ratio, beclin-1 and Atg 7 and decreased p62 levels (Wu et al., 2017). Increased cardiac apoptosis, mitochondrial injury and interstitial fibrosis, along with suppressed autophagy and mitophagy were observed in STZ-induced diabetic sirtuin3 knockout mice. Transmission electron microscopy revealed less number of autophagososmes and LC3 II expression was also reduced in STZ- treated wild type mice and in Sirt3 knockout mice, further reduction of autophagosomes and LC3 II were noticed. Over expression of sirtuin3 in diabetic mice enhanced autophagy and mitophagy, along with decreased apoptosis and inhibited the mitochondrial injury that adds a protective effect for diabetic cardiomyopathy (Yu, Gao, et al., 2017: 3). Apelin, an adipokine gene therapy in a STZ-induced diabetic mice exhibited upregulation of cardiac autophagy showed by the increased expression of beclin-1 and LC3 II and activating sirtuin3 and suppression of ROS-NF-Kb pathway (Hou et al., 2015).In a rat model of T2DM,through restoring autophagy by reducing the interaction of beclin-1 with Bcl-2, inhibition of dipeptidyl peptidase-4 improves the survival rate and reduces the acute mortality after myocardial ischemia. The LC3 II levels and the LC3 positive autophagososmes were not changed in diabetic rat after myocardial infarction (MI). But the altered expression was shown by reduced AMPK/ULK1 levels, reduced Akt/mTOR/S6 and increased beclin 1 levels after MI. Vildagliptin, an anti-diabetic drug, inhibitor of DPP-4 reduced beclin 1-Bcl-2 interaction and the expression of LC3 II and number of autophagososmes are increased in diabetic mice.(Murase et al., 2015). Like this study, in our results also, the cardiac autophagic alterations at 10 week hyperglycemia was shown by reduced expression of ULK1 and pULK1, while no change was observed in LC3 II, AMPK, mTOR and beclin-1. A study in db/db type 2 diabetic mice, increased formation of autophagosome was observed, but the autophagic process is suppressed at final step, i.e., fusion of autophagososmes with lysosomes were defective. The expression of LC3 II, p62 and mTOR in type 2 diabetic mice was high, but the cathepsin level was reduced. Ultrastructural examination showed very few lysosomes, degenerated mitochondria and incomplete autolysosomes in type 2 diabetic hearts. The AMPK expression and the ATP

content were also reduced in them. Treatment with resveratrol in diabetic mice improved the cardiac diastolic function while chloroquine administration aggravated the systolic and diastolic function in type 2 diabetic mice.(Kanamori et al., 2015). Otsuka Long-Evans Tokushima fatty (OLETF) diabetic rats on calorie restriction (30% energy reduction) improved diastolic function and increased cardiac telomerase activity and autophagy. LC3 II was significantly increased in diabetic rats, while no change was observed in beclin-1 expression on calorie restriction in diabetic rats (Makino et al., 2015).

V.A.3.2. Mitochondrial respiration regulated by autophagy

The present study was carried out to assess the cardiac mitochondrial respiration in T2DM by modulating autophagic process. Autophagy is an important cellular pathway involved in the degradation and quality maintenance of proteins, lipids, organelles especially mitochondria. So in our study, we wanted to analyze the role of autophagy in controlling the mitochondrial respiration by either activating or inhibiting autophagy. For development of T2DM model, diabetes was induced by intraperitoneal injection of STZ/NA in C57BL/6 mice (Materials and Methods). After maintaining the hyperglycemic condition in mice for a period of 2 weeks and 10 weeks, the autophagic activator (Resveratrol) and inhibitor (Chloroquine) is administered for continuous 14 days and the mice were sacrificed for heart tissue.

V.A.3.2.1. Regulation of cardiac mitochondrial function by activating autophagy (Resveratrol)

Resveratrol was used as autophagic activator in the study. Resveratrol treatment didn't change the body weight or blood glucose/HbA1c level in the diabetic mice. As previously described, mitochondria were isolated from the whole heart of untreated and treated control and diabetic mice and their OCR was analyzed using high resolution respirometry. In the two different SUIT protocols, resveratrol had enhanced the complex I and complex II respiration in type 2 diabetic mice at both 2 week and 10 week time points. Resveratrol increased the activity of electron transport chain complexes in presence of fatty acid and carbohydrate substrates at the two time points in diabetic mice. The fatty acid +

carbohydrate-mediated and carbohydrate substrate-mediated state 2 complex I respiration, their state 3 complex I respiration along with pyruvate and glutamate and succinate mediated complex I + II , complex II respiration were significantly increased in the diabetic mice. Our data correlates to a study done in a rat model, in which resveratrol co-treatment enhanced the pyruvate-mediated state 3 complex I respiration in cardiac mitochondria by attenuating the effect of HIV protease inhibitors (Symington et al., 2017). The complex II-dependent leak or state 4 respiration was also increased in diabetic mice indicates a change in proton leak or mitochondrial membrane potential due to substrate oxidation(Brand and Nicholls, 2011). The FCCP-mediated maximal respirationwas found to be increased in the resveratrol treated diabetic mice at two time periods. It is to be noted thatin our study, the heart mitochondrial succinate-mediated complex I + II respiration in the untreated control and diabetic mice heart showed the maximal respiratory capacity than the FCCP-mediated respiration (eventhough FCCP-mediated respiration is named maximal respiration, the maximal respiration is obtained only when succinate was added in the case of cardiac mitochondria). Same scenario was noted in a mitochondrial respiratory study done in human heart failure patients (right atrial appendage), where the maximal ETS capacity was obtained from complexes I + II when the substrate succinate was added to the mitochondria ($PMGS_{ADP}$)(Lemieux et al., 2011). In a study done in human cardiac microvascular enthothelial cells exposed to hyperglycemia, ATP linked mitochondrial respiration and the FCCP-mediated maximal respiration were significantly lower and resveratrol treatment improved the mitochondrial function (Joshi et al., 2015). A recent study done in human nucleus pulposus cells, resveratrol reduced the mitochondrial dysfunction and apoptosis induced by the cytotoxicity of H_2O_2 by activating autophagic process (Zhang, Xu, et al., 2017) . In a primary skin fibroblast cells obtained from patients with Parkinson disease, resveratrol treatmentenhanced the mitochondrial oxidative capacity (Ferretta et al., 2014).In a STZ diabetic model of C57BL/6 mice, resveratrol treatment reduced cardiac dysfunction and remodeling and it reduced the apoptosis and oxidative stress through enhancing the pathway of autophagy (Wang et al., 2014). In an autophagy deficienct mice model (Atg $7^{-/-}$

conditional kockout) in pancreatic β cell and skeletal muscle, damaged and dysfunctional mitochondria were accumulated and intracellular ROS was very high and an altered basal mitochondrial OCR and a pronouncedreduction was observed in FCCP mediated maximal oxidative capacity (Wu et al., 2009). In a type 2 diabetic model of db/db mice, cardiacautophagy was found to be suppressed at the final degradation step. Resveratrol treatment enhanced autophagy, suppressed hypertrophy and fibrosis and improved the cardiac function in those db/db type 2 diabetic mice (Kanamori et al., 2015). In our study resveratrol treatment, (the autophagic activator) improved the cardiac mitochondrial oxygen consumption rate in 2 week and 10 week diabetic mice.

V.A.3.2.2. Modulation of cardiac mitochondrial function by inhibiting autophagy (Chloroquine)

In the current study, chloroquine, autophagy inhibitor neither changed the body weight or blood glucose level of control and diabetic mice. Chloroquine decreased the complex I and complex II respiration when two different SUIT protocols were followed to study mitochondrial respiration in type 2 diabetic mice at both 2 week and 10 week time points.The activity of electron transport chain complexes in presence of fatty acid and carbohydrate substrates was decreased by chloroquine treatment at the two time points in diabetic mice. The fatty acid + carbohydrate substrate combination- mediated and carbohydrate substrate-mediated state 2 complex I respiration, state 3 complex I respiration along with pyruvate, glutamate and succinate-mediated complex I + II, complex II respiration were significantly decreased in the diabetic mice. Chloroquine treatment didn't alter the complex II dependent leak or state 4 respiration in diabetic mice and this indicated that the proton leak or mitochondrial membrane potential was not altered. The FCCP-mediated uncoupled respiration was found to be decreased in the chloroquine treated diabetic mice at two time periods. In a study done in rat model of pressure overload hypertrophy, high dose chloroquine (50 mg/kg/day for 2 weeks) caused mitochondrial fragmentation and cristae destruction. They found large number of autophagosomes containing fragmented

mitochondria (Chaanine et al., 2015). Hypoxic-ischemic (HI) treatment in a neonatal rat model of encephalopathy showedpresence of apoptosis and autophagy proteins and is inhibited during chloroquine treatment. This inhibition of autophagy in the neurons worsened the mitochondrial dysfunction characterized by high levels of ROS, less mitochondrial superoxide and less membrane potential(Li, Hao, et al., 2018). There was a similar report in primary rat cortical neurons, where autophagy inhibition by bafilomycin and chloroquine reduced mitochondrial quality and energetic function. Another study which corroborated our result was reported, where chloroquine (40 μM) along with bafilomycin (10 nM) treatment in the primary neurons significantly reduced the basal mitochondrial respiration, ATP-linked respiration, maximal oxidative capacity and reserve capacity (Redmann et al., 2016).

VI.A. CONCLUSION (T2DM)

The current study in cardiac type 2 diabetes involves three model systems. They are human heart tissue, H9c2 cell line and an animal model of type 2 diabetes. Cardiac autophagy was analyzed in three models of diabetes. In mice model of type 2 diabetes, the cardiac mitochondrial respiration regulated by autophagy was also evaluated.

In contrast to the available single work published by Munasinghe et al., on human cardiac autophagy in type 2 diabetes in New Zealand population, our results indicates decreased autophagy in diabetic than non-diabetic subjects. This is the first report regarding cardiac autophagy in type 2 diabetic subjects of Asian Indian population.

The main objective of the study in H9c2 cells was to analyze autophagic status in high glucose condition at two time points, 4 h and 48 h. All the autophagic proteins, mitophagic proteins, lysosomal proteins and the regulators of autophagy analyzed in the study were found unchanged at 4 h time period of hyperglycemia. It was found that when the duration of hyperglycemia was increased for 48 h for H9c2 cells caused significant reduction in autophagic and mitophagic proteins indicates that the recycling mechanism was impaired in the cardiomyoblast cells.

The main objective of the study in untreated type 2 diabetic mice was to analyze cardiac autophagic status at two time points of diabetes, 2 weeks and 10 weeks of hyperglycemia. Mitophagic proteins, lysosomal proteins and the regulators of autophagy were found unchanged in 2 weeks of diabetic mice heart when compared with their corresponding controls. LC3 II/I ratio and p62 levels was increased in 2 week diabetic mice indicated an impaired autophagy with accumulation of autophagosomes. In 10 week diabetic mice, even though LC3 II was unchanged, a significant reduction was noted in ULK1, pULK1 and parkin and increase in p62 was observed. Both 2 week and 10 week diabetic mice showed altered cardiac autophagy indicates the accumulation of damaged or dysfunctional proteins, organelles like mitochondria inside the cardiomyocytes that in turn will worsen the oxidative stress and defective metabolism in diabetic heart.

Analysis of cardiac mitochondrial respiration in type 2 diabetes by regulating autophagy showed that administration of an autophagic activator (Resveratrol) at 2 week and 10 week

of diabetic mice activated mitochondrial respiration in the heart tissue. When the diabetic mice were treated with an autophagic inhibitor (Chloroquine) at 2 week and 10 weeks, the cardiac mitochondrial respiration was significantly reduced. This study implies the importance of autophagic regulation in heart tissue during type 2 diabetes and the role of autophagy in maintaining the cardiac mitochondrial respiration.

Combining the data from three models of diabetes, we can propose that myocardial autophagy is reduced in type 2 diabetic conditions, even though the duration of hyperglycemia plays an important role in regulating autophagic proteins. Our results shows that the autophagy status in diabetic conditions is fluctuating throughout the different stages of diabetes and its profile cannot be explained by evaluating the process in a single time point. In cardiac tissue, the impairment in the process of autophagy may lead to the accumulation of damaged and dysfunctional organelles and proteins (especially mitochondria). It can also slow down the rate of formation of macromolecules as autophagic degradation can result in release of amino acids, nucleotides etc. Since autophagy regulates mitochondrial respiration, defect in this process can create imbalance in energy generation within cardiomyocytes which in turn affect the normal functioning of heart.

IV.B. RESULTS
(GDM)

Rat study

IV. B.1. Development of gestational diabetes model

Pregnant wistar rats were used for the development of gestational rat model using streptozotocin as described in a paper (Nasu-Kawaharada et al., 2013). In that paper they had injected 60 mg/kg STZ on 2ndday of gestation. We had adopted that method, but the mortality rate of offsprings was so high. So we standardized the STZ amount and reduced it to20 mg/kg STZ and injection is given to rats on 5th day of gestation. Animals were hyperglycemic within 2 days after the injection and the animals with glucose level higher than 400mg/dL was taken as diabetic for the study. On every 7th day till the delivery of rat, body weight and random glucose were noted and it revealed that the animals were maintaining the hyperglycemic condition throughout the pregnancy period. The body weight of diabetic mother was slightly lower than the control mother (Figure 101).

Figure 101: Body weight measurements over time

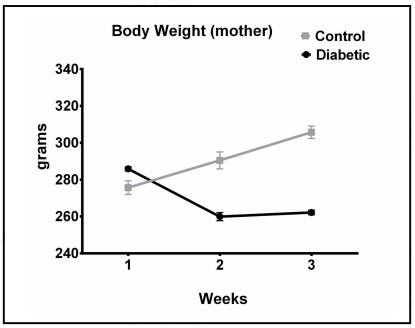

The body weight of control and diabetic mother rat till the delivery.Error bars represent +SD. (n=6 in each group)

Figure 102: Random blood glucose measurements over time

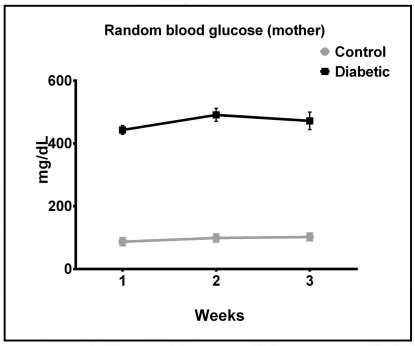

Random blood glucose measurements till delivery of control and diabetic mother rat. Error bars represent ± SEM. (n=6 in each group)

The blood glucose of the mother were checked until the pups were weaned on the 22nd day in order to know whether the GDM mother maintained the hyperglycemic condition (Figure 102), so that the pups could drink milk rich in glucose. The HbA1c level of the diabetic mother at the time of weaning of offsprings was > 7% and is significantly higher than the control mother rats (Figure 103).

Figure 103: HbA1c levels

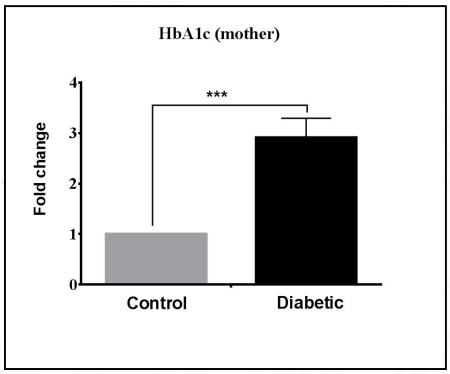

HbA1c levels of control and diabetic mother rats at the time of delivery. *Error bars represent ± SEM. (p-value ***<0.001) (n=6 in each group)*

The number of offsprings in diabetic mothers was less than control mothers. Still birth was high in GDM mothers. Also the lactation was not properly maintained and the mortality rate of offsprings (immediately after delivery) was high in diabetic mothers.

Body weight noted at the time of euthanasia of the weaning group (male and female) ODM didn't change when compared to their OCM, but the adult group (male and female) ODM showed a significant weight gain than the corresponding OCM (Figure 104).

Figure 104: Body weight of offsprings

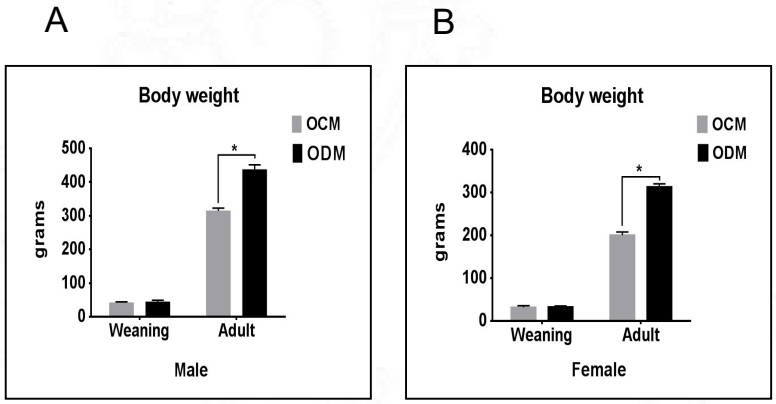

*The body weight of male(A) and female(B) offsprings at the time of euthanasia. Error bars represent ± SD. (p-value *<0.05) (n=6 in each group)*

Even though offsprings are born to a diabetic mother, both male and female offsprings were normoglycemic at weaning and adult period and their HbA1c level at the time of euthanasia was similar to that of their corresponding controls.

The heart weight: body weight ratio was calculated in offsprings of diabetic mothers at both time points and found that the values were similar to that of their corresponding controls in the weaning and adult group of male and female ODM. This indicated that no structural changes like hypertrophy/cardiomyopathy occurred in the heart tissue of male and female ODM (Figure 105).

Figure 105: Heart to body weight ratio

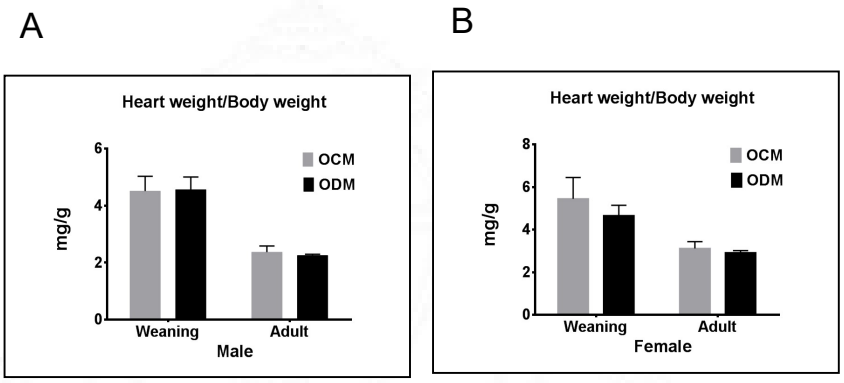

Bar graph showing the ratio of heart weight (milligrams) and body weight (grams) of rat at weaning and adult group of male(A) and female(B) ODM. The error bars represent ± SD. (n=6 in each group)

Findings:

- **Hyperglycemia was maintained in diabetic mother wistar rats throughout pregnancy**
- **Body weight of weaning male and female ODM was similar to their corresponding OCM**
- **A significant increase in body weight was shown by adult male and female ODM**
- **No change in heart weight: body weight ratio showed absence of hypertrophy or cardiomyopathy in weaning and adult group of male and female ODM**
- **Both weaning and adult group of male and female ODM were normoglycemic throughout the study**

IV. B.2. Cardiac autophagic profile in offsprings of diabetic mothers

In order to study the cardiac autophagic process in offsprings of diabetic mothers, we evaluated the expression of some of the important markers and regulators of autophagic machinery.

ULK1 (mammalian homolog of Atg 1) is found unchanged in the weaning and adult group of male (Figure 106 A & B) and female (Figure 106 A & C) ODM.

Figure 106: Expression of ULK1

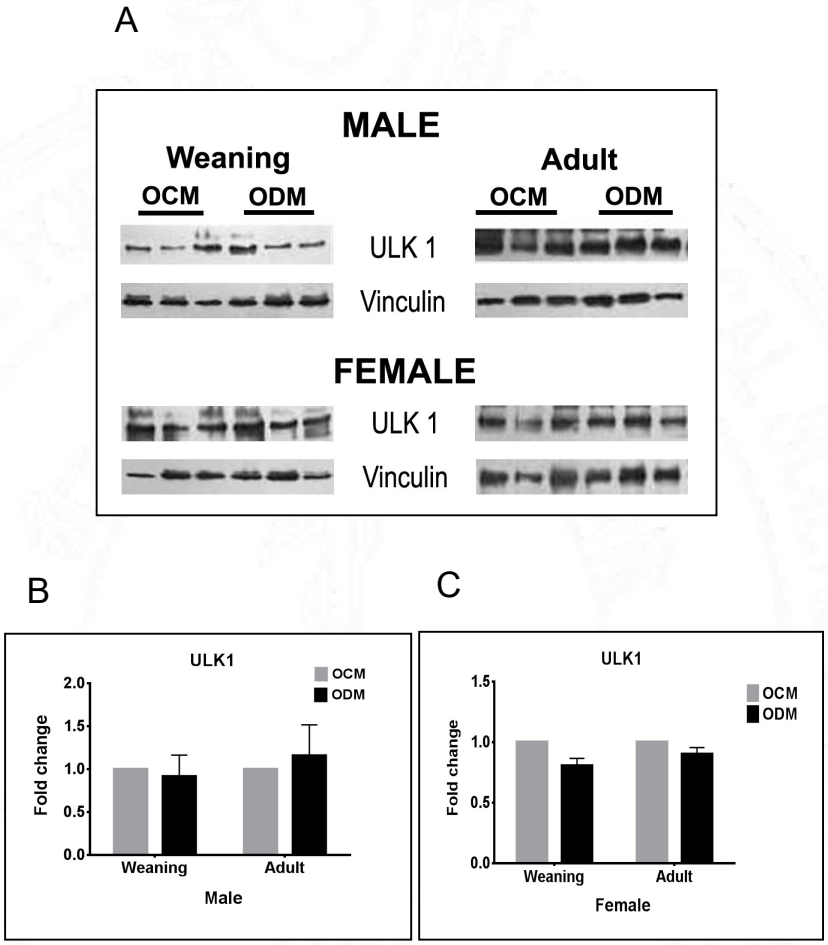

Expression of ULK1 was showed by western blotting in male and female ODM (A). The bar graphs represent the fold change in expression of the respective protein in male (B) and female(C) ODM. Error bars represent ±SD. (n= 6 in each group).

pULK1 is also found to be unchanged in the weaning and adult group of male (Figure 107 A & B) and weaning female (Figure 107 A & C) ODM. But a significant reduction was observed in adult female ODM.

Figure 107: Expression of pULK1

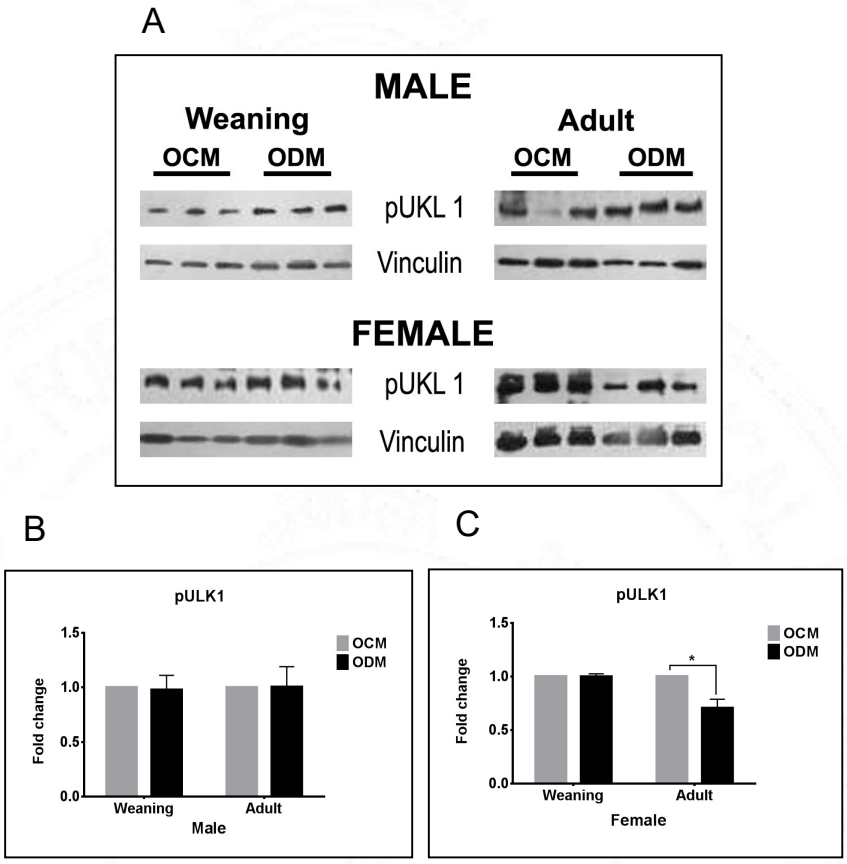

*Expression of phosphorylated form of pULK1 was showed by western blotting in male and female ODM (A). The bar graphs represent the fold change in expression of the respective protein in male (B) and female (C) ODM. Error bars represent ±SD. (p-value *<0.05) (n= 6 in each group).*

No significant difference in expression of Beclin 1 was noted in the weaning and adult group of male (Figure 108 A & B) and female (Figure108 A & C) ODM.

Figure 108: Expression of Beclin 1

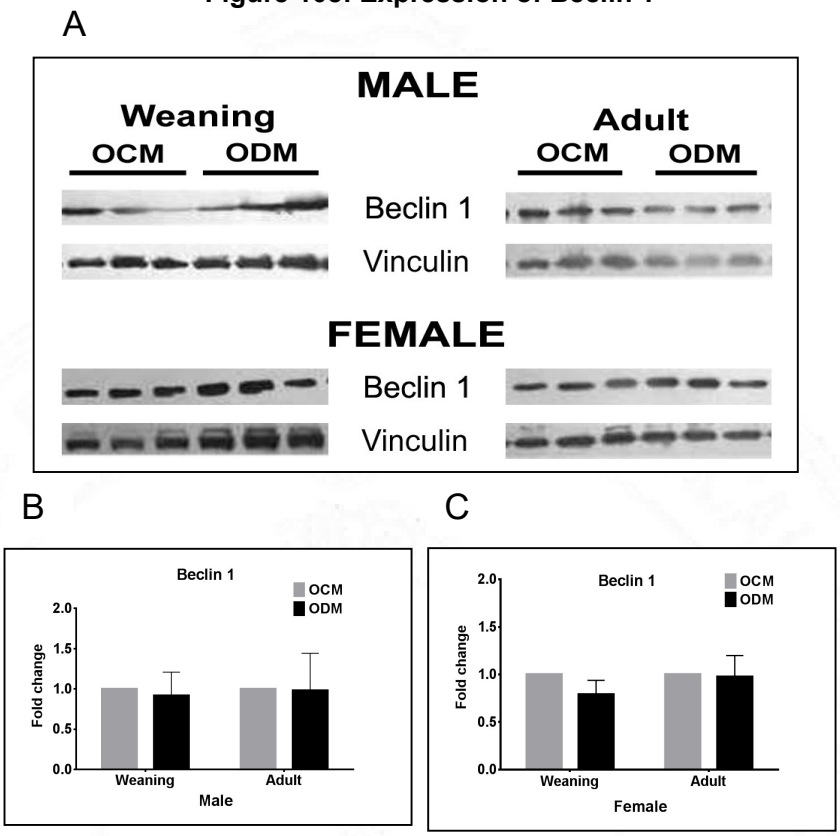

Expression of Beclin 1was showed by western blotting in male and female ODM (A). The bar graphs represent the fold change in expression of the respective protein in male (B) and female (C) ODM. Error bars represent ±SD. (n= 6 in each group).

The expression of Atg 14 was found decreased in adult male ODM, while no change was observed in weaning male (Figure 109 A & B) ODM and weaning and adult female (Figure 109 A & C) ODM.

Figure 109: Expression of Atg 14

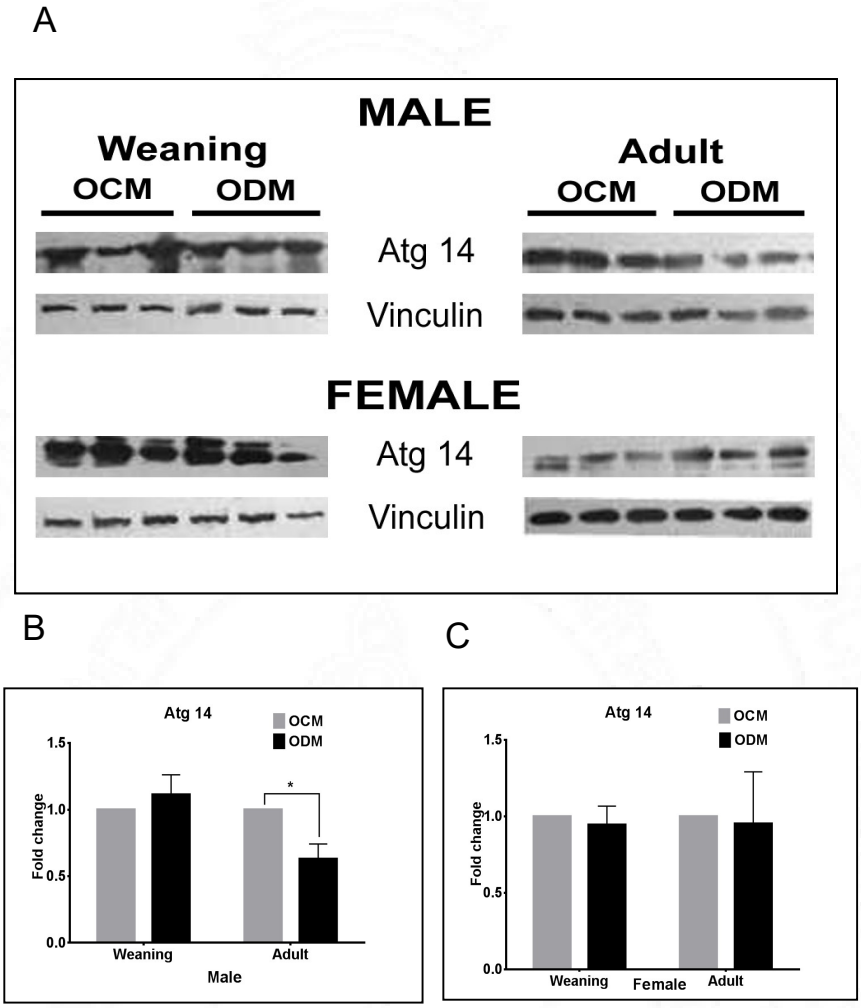

*Expression of Atg 14 was showed by western blotting in male and female ODM (A). The bar graphs represent the fold change in expression of the respective protein in male (B) and female (C) ODM. Error bars represent ±SD. (p-value *<0.05) (n= 6 in each group).*

We didn't observe any change in the expression of rubicon in weaning and adult group of male (Figure 110 A & B) and female (Figure 110 A & C) ODM.

Figure 110: Expression of Rubicon

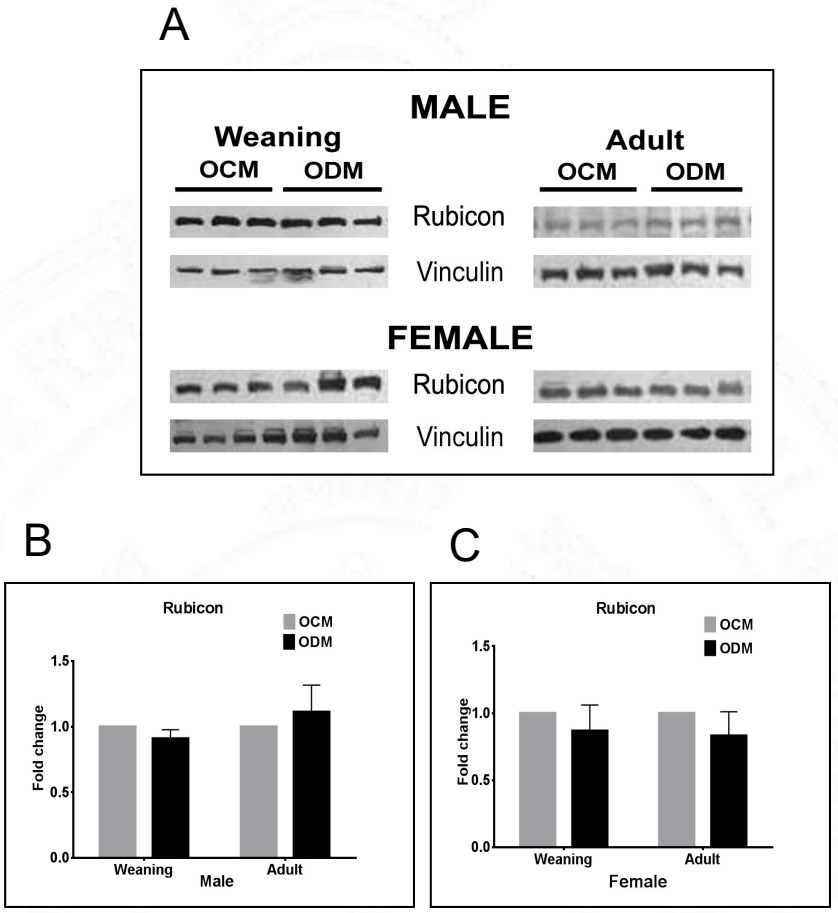

Expression of Rubicon was showed by western blotting in male and female ODM (A). The bar graphs represent the fold change in expression of the respective protein in male (B) and female (C) ODM. Error bars represent ±SD. (n= 6 in each group).

The expression of Atg 5 (Figure 111), Atg 7(Figure 112) and Atg 12 (Figure 113) were found unchanged in weaning and adult group of male and female ODM.

Figure 111: Expression of Atg 5

A

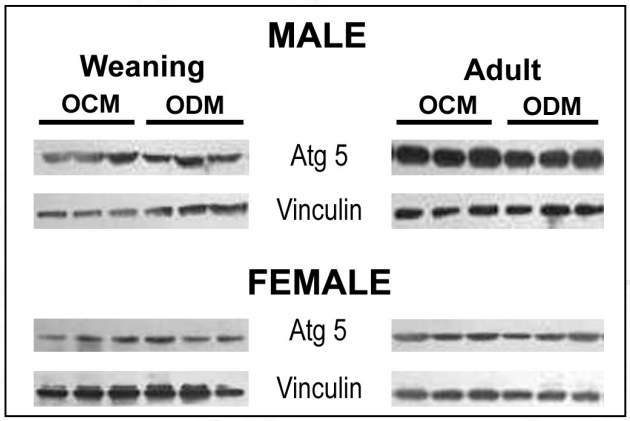

B

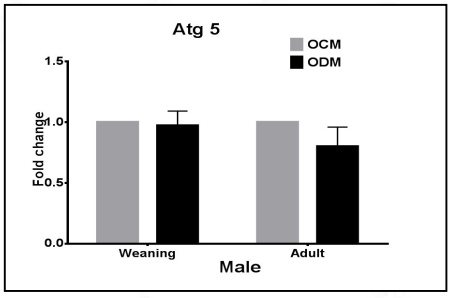

C

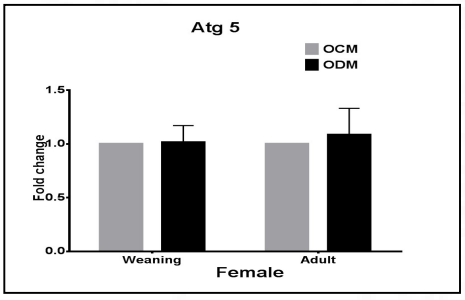

Expression of Atg 5 was showed by western blotting in male and female ODM (A). The bar graphs represent the fold change in expression of the respective protein in male (B) and female (C) ODM. Error bars represent ±SD. (n= 6 in each group).

Figure 112: Expression of Atg 7

A

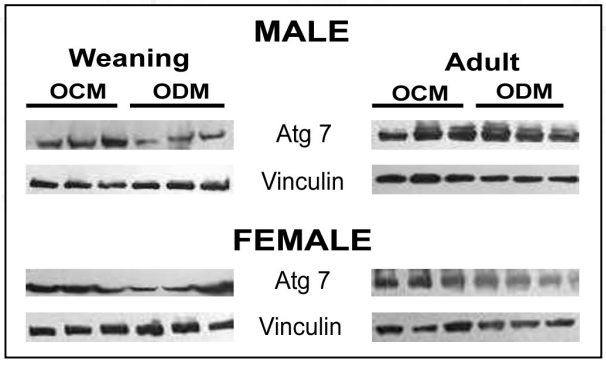

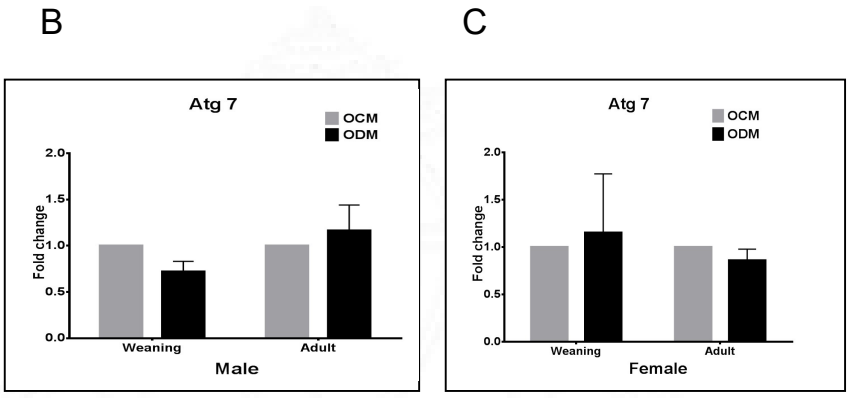

Expression of Atg 7 was showed by western blotting in male and female ODM (A). The bar graphs represent the fold change in expression of the respective protein in male (B) and female (C) ODM. Error bars represent ±SD. (n= 6 in each group).

Figure 113: Expression of Atg 12

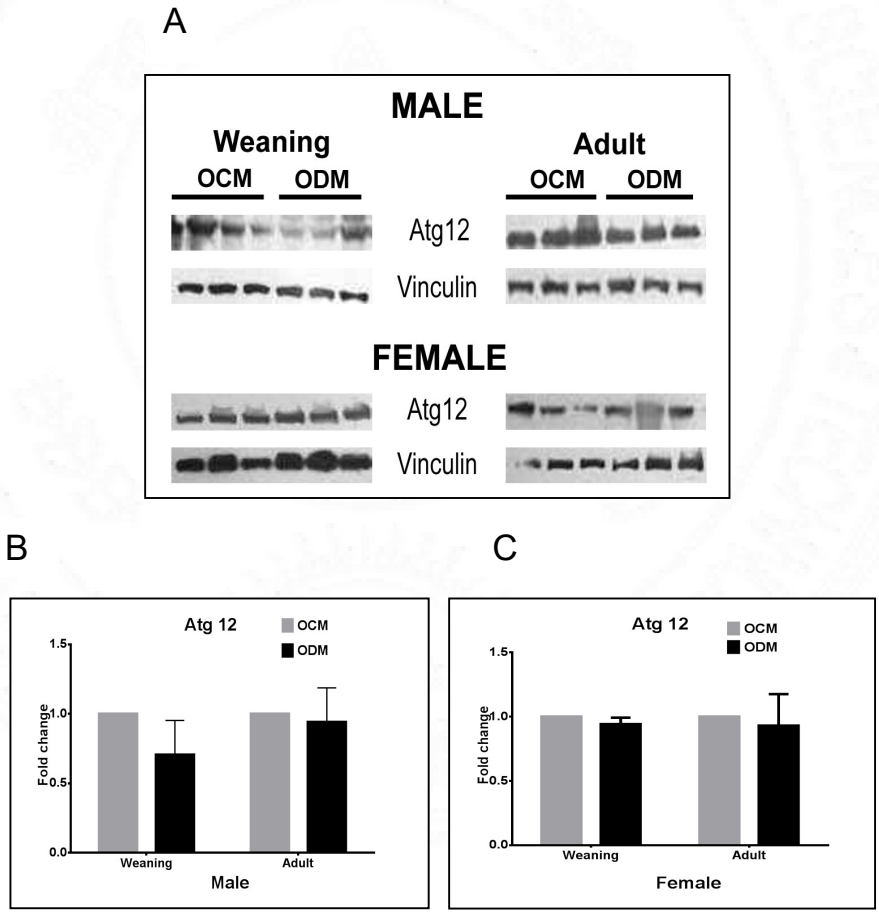

Expression of Atg 12 was showed by western blotting in male and female ODM (A). The bar graphs represent the fold change in expression of the respective protein in male (B) and female (C) ODM. Error bars represent ±SD. (n= 6 in each group).

There was no change in expression of Atg 16 in weaning and adult male ODM (Figure 114 A & B), even though a significant increase in the levels of Atg 16 was observed in weaning female ODM and a significant reduction is noted when they became adult (Figure 114 A & C).

Figure 114: Expression of Atg 16

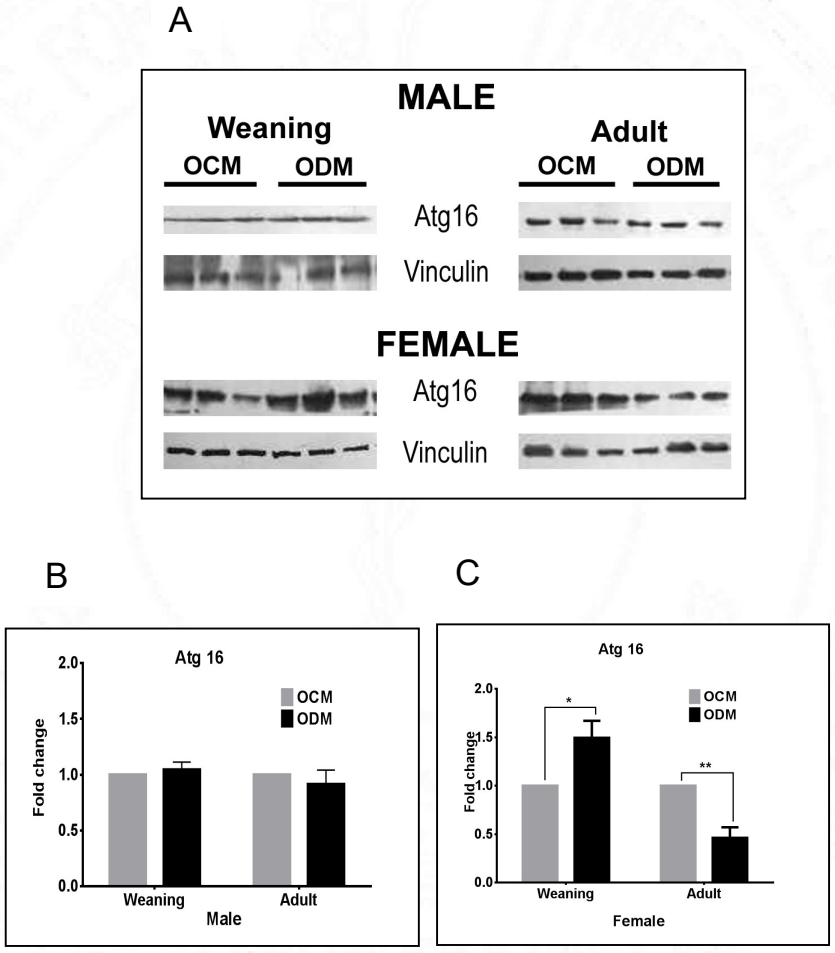

*Expression of Atg 16 was showed by western blotting in male and female ODM (A). The bar graphs represent the fold change in expression of the respective protein in male (B) and female (C) ODM. Error bars represent ±SD. (p-value *<0.05**<0.01) (n= 6 in each group).*

Atg 3 expression was significantly reduced in adult male ODM (Figure 115 A & B), weaning and adult female ODM (Figure 115 A & C). A reduction in Atg 3 is observed in weaning male ODM, but insignificant.

Figure 115: Expression of Atg 3

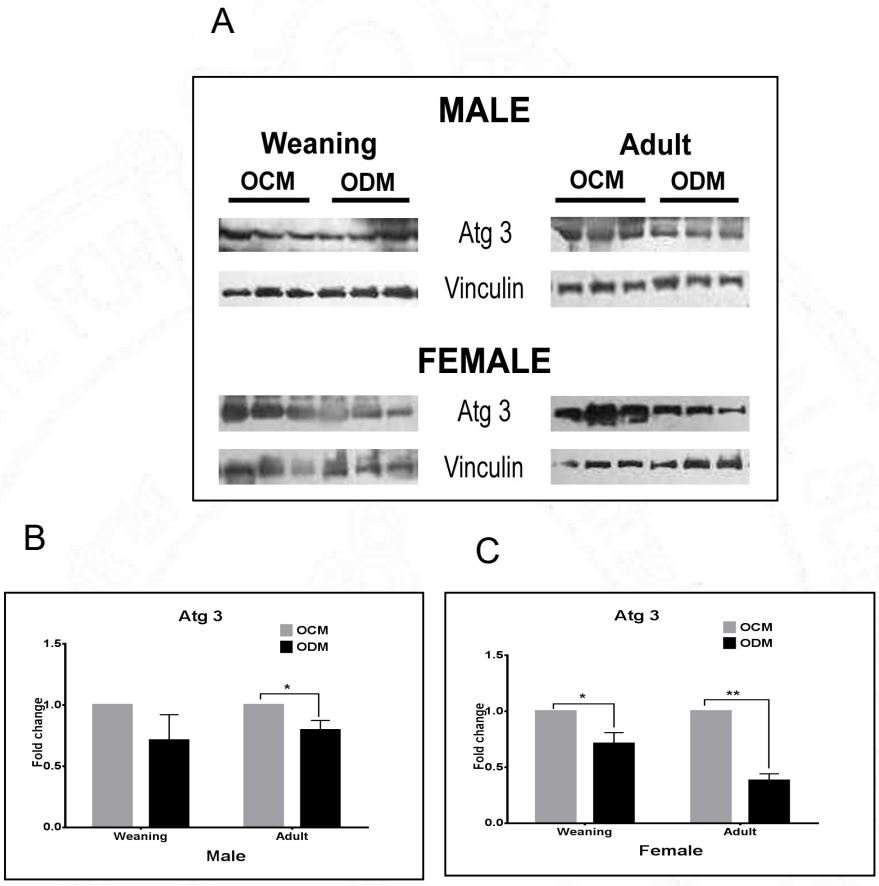

*Expression of Atg 3 was showed by western blotting in male and female ODM (A). The bar graphs represent the fold change in expression of the respective protein in male (B) and female (C) ODM. Error bars represent ±SD. (p-value *<0.05**<0.01) (n= 6 in each group).*

The p62 (adaptor molecule) expression levels were unaltered in the weaning male and female ODM, while a significant increased expression is noted in adult male (Figure 116 A & B) and female (Figure 116 A & C) ODM.

Figure 116: Expression of p62

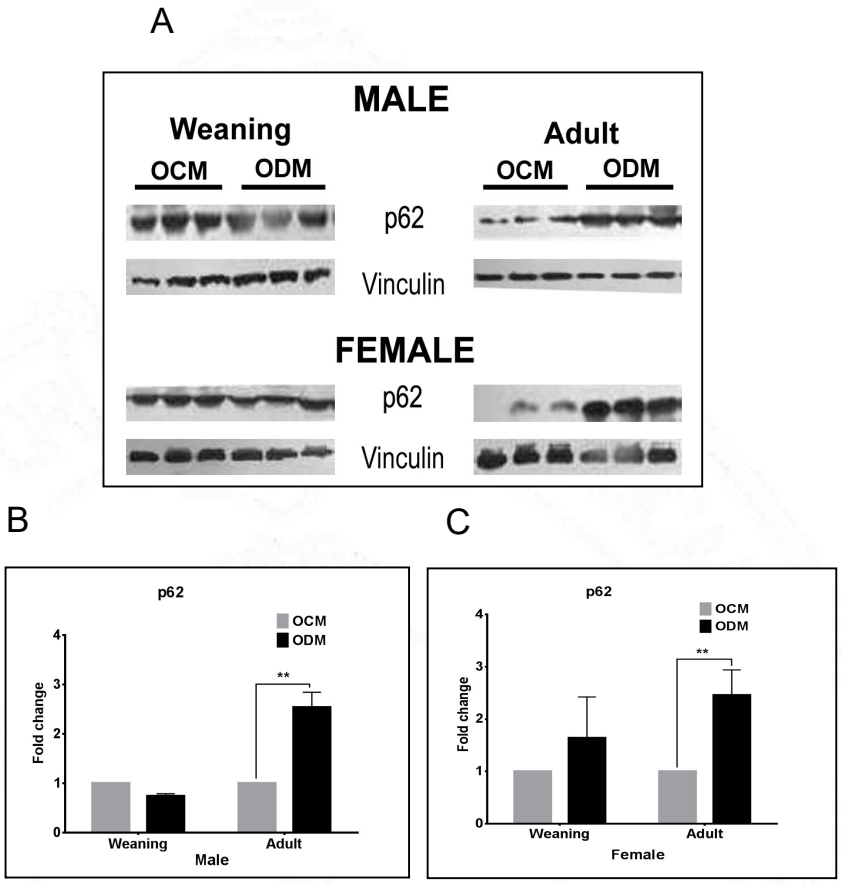

*Expression of p62 was showed by western blotting in male and female ODM (A). The bar graphs represent the fold change in expression of the respective protein in male (B) and female (C) ODM. Error bars represent ±SD. (p-value**<0.01) (n= 6 in each group).*

Expression of LC3-II level at a given time point (steady state level)was analyzed using western blot technique and is found to be significantly reduced in adult male (Figure 117 A & B) and female (Figure 117 A & C) ODM. An increased expression of LC3 II is found in the weaning group of male and female ODM, but in females it is not significant.

Figure 117: Expression of LC3 II

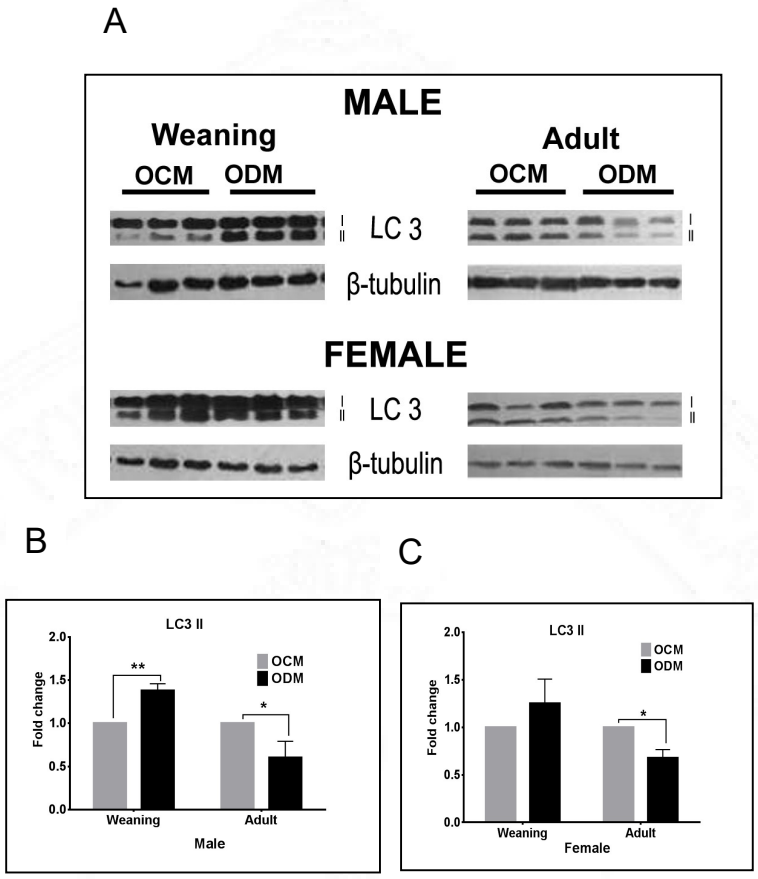

*Expression of LC3 II was showed by western blotting in male and female ODM (A). The bar graphs represent the fold change in expression of the respective protein in male (B) and female (C) ODM. Error bars represent ±SD. (p-value *<0.05**<0.01) (n= 6 in each group).*

Like the LC3 II expression, LC3 II/I ratio was also significantly reduced in adult male (Figure 118 A) and female (Figure 118 B) ODM. Unchanged LC3 II/I ratio was noted in weaning female ODM, while a significant increase was noted in weaning male ODM.

Figure 118: Expression of LC3 II/I

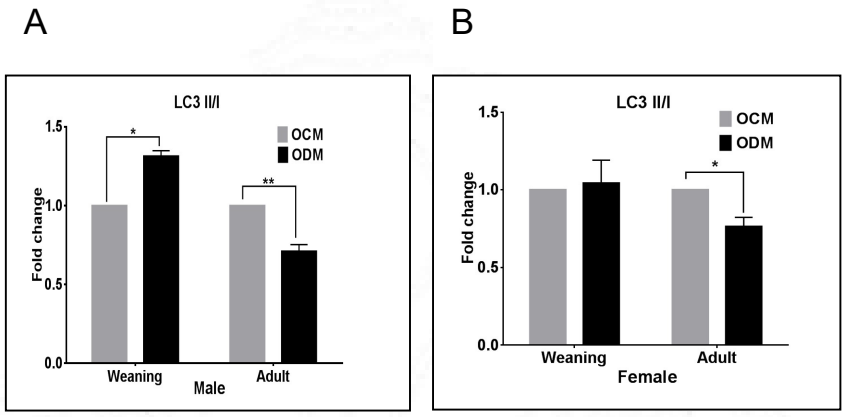

*The bar graphs represent the fold change of the LC3II/I ratio in male (A) and female (B) ODM. Error bars represent ±SD. (p-value *<0.05**<0.01) (n= 6 in each group).*

The expression of PINK 1 was observed to be unchanged in weaning and adult group of male (Figure 119 A & B) and female (Figure 119 A & C) ODM.

Figure119: Expression of PINK 1

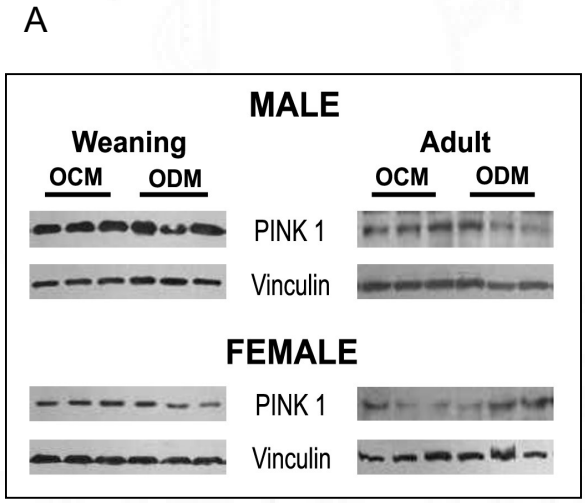

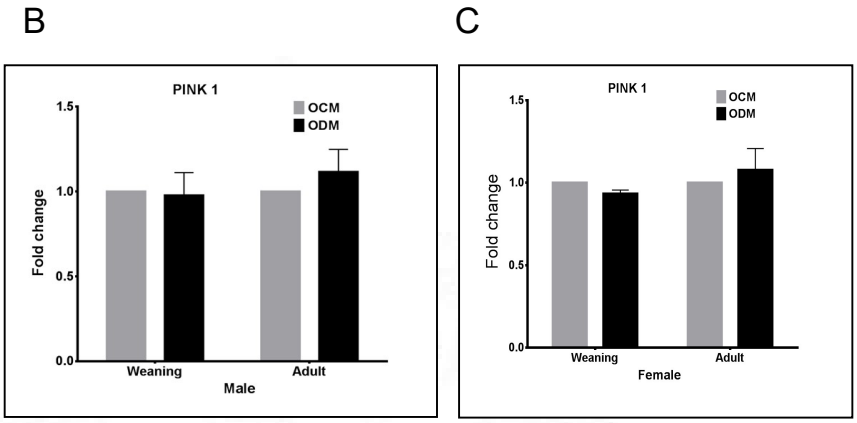

Expression of PINK 1 was showed by western blotting in male and female ODM (A). The bar graphs represent the fold change in expression of the respective protein in male (B) and female (C) ODM. Error bars represent ±SD. (n= 6 in each group).

The expression of Parkin also was found to be unaltered in weaning and adult group of male (Figure 120 A & B) and female (Figure 120 A & C) ODM.

Figure 120: Expression of Parkin

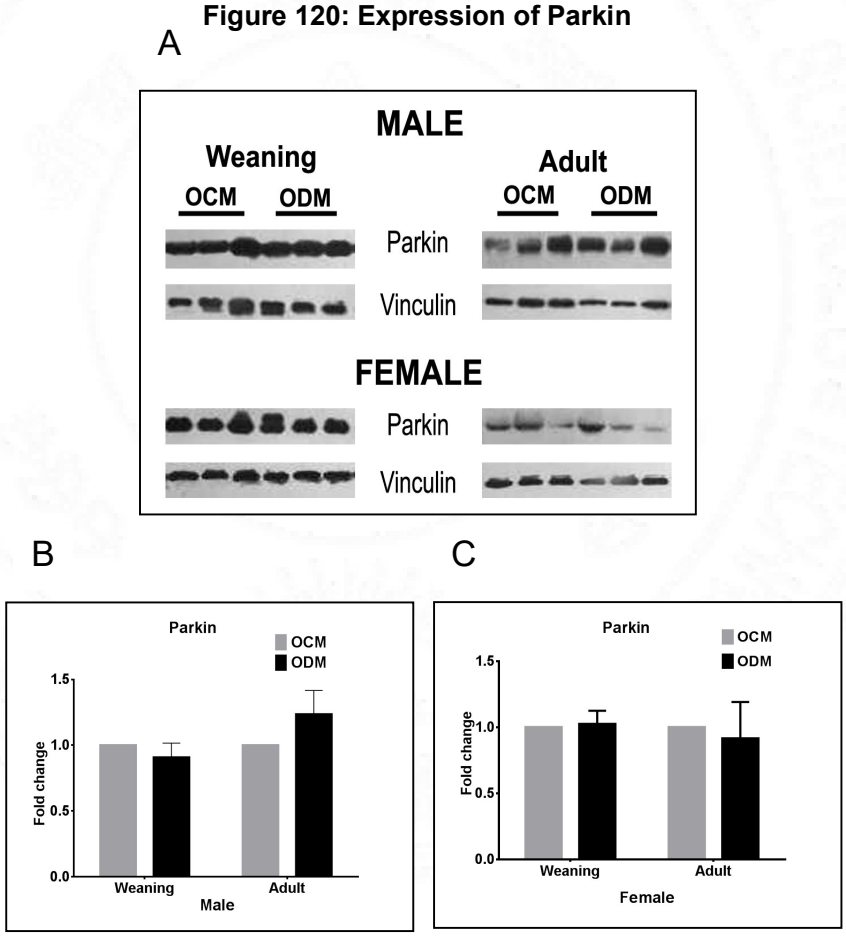

Expression of Parkin was showed by western blotting in male and female ODM (A). The bar graphs represent the fold change in expression of the respective protein in male (B) and female (C) ODM. Error bars represent ±SD. (n= 6 in each group).

Cathepsin D, a lysososmal aspartyl protease was found to be unchanged in weaning and adult group of male (Figure 121 A & B) and female (Figure 121 A & C) ODM.

Figure 121: Expression of Cathepsin D

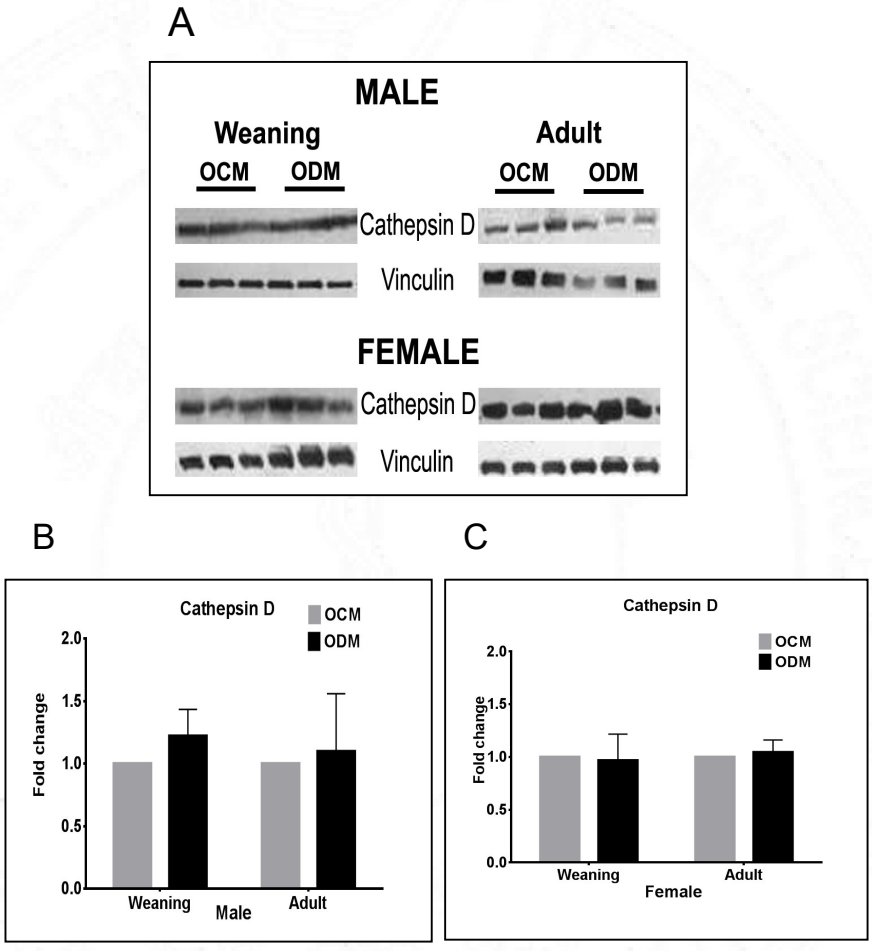

Expression of Cathepsin D was showed by western blotting in male and female ODM (A). The bar graphs represent the fold change in expression of the respective protein in male (B) and female (C) ODM. Error bars represent ±SD. (n= 6 in each group).

LAMP-2 was significantly reduced in the adult male (Figure 122 A & B) and female (Figure 122 A & C) ODM, while no change was observed in weaning male and female ODM.

Figure 122: Expression of LAMP-2

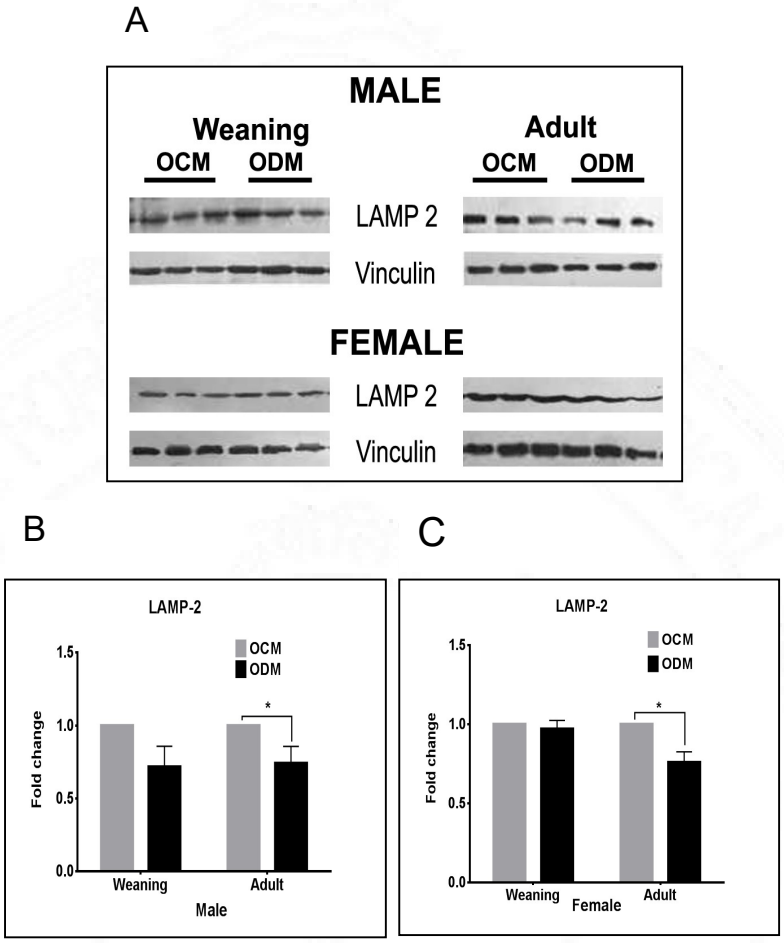

*Expression of LAMP-2 was showed by western blotting in male and female ODM (A). The bar graphs represent the fold change in expression of the respective protein in male (B) and female (C) ODM. Error bars represent ±SD. (p-value *<0.05) (n= 6 in each group).*

AMPKα expression was found to be significantly decreased in the adult group of female ODM, while no change was observed in adult male (Figure 123 A & B) ODM. It showed an increased expression in the weaning male and unchanged in weaning female (Figure 123A & C) ODM.

Figure 123: Expression of AMPKα

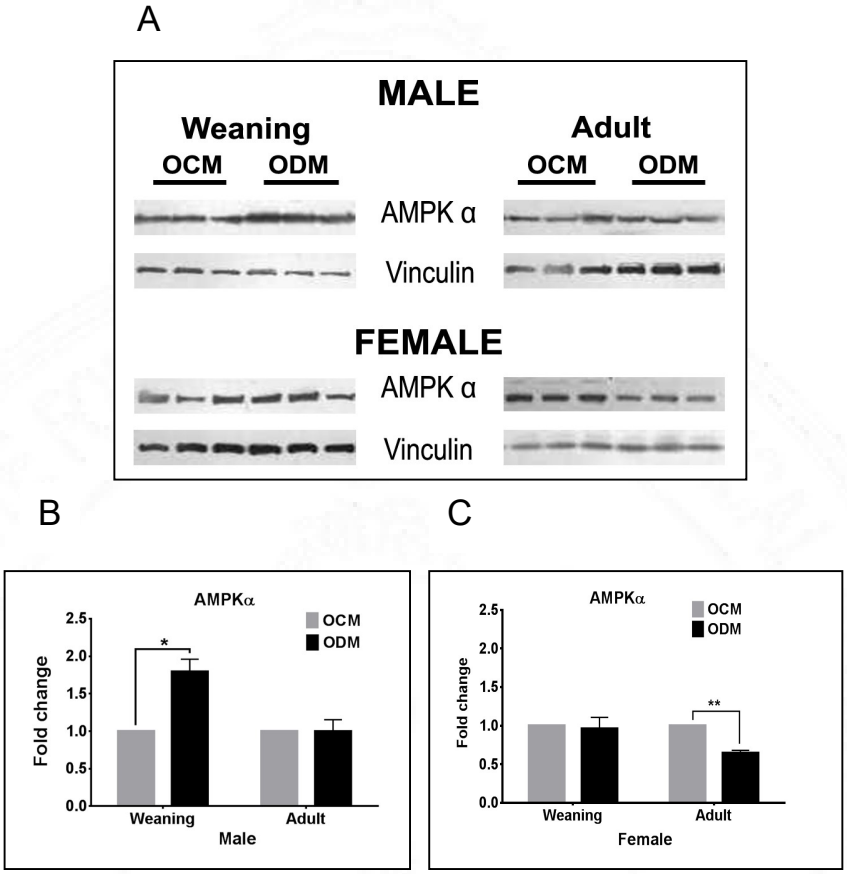

*Expression of AMPKα was showed by western blotting in male and female ODM (A). The bar graphs represent the fold change in expression of the respective protein in male (B) and female (C) ODM. Error bars represent ±SD. (p-value *<0.05**<0.01) (n= 6 in each group).*

PAMPKα was found to be unchanged in weaning and adult group of male (Figure 124 A &

B) and female (Figure 124 A & C) ODM.

Figure 124: Expression of pAMPKα

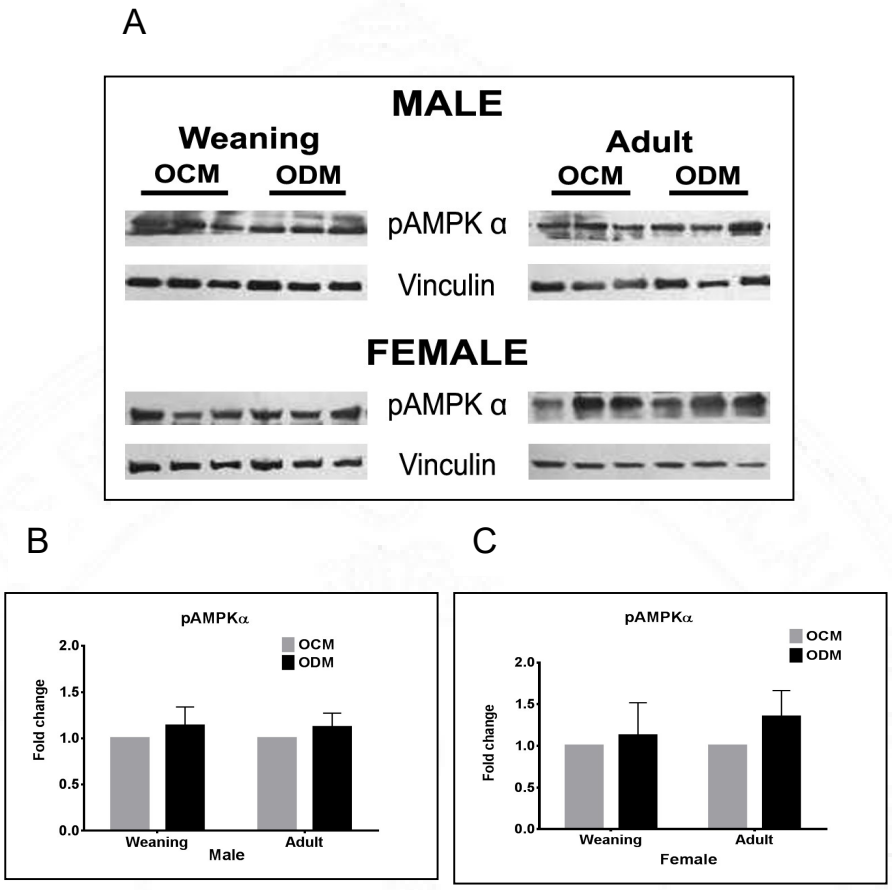

Expression of pAMPKα was showed by western blotting in male and female ODM (A). The bar graphs represent the fold change in expression of the respective protein in male (B) and female (C) ODM. Error bars represent ±SD. (n= 6 in each group).

mTOR, an inhibitor of autophagy, was also found to be unchanged in weaning and adult group of male (Figure 125 A & B) and female (Figure 125 A & C) ODM.

Figure 125: Expression of mTOR

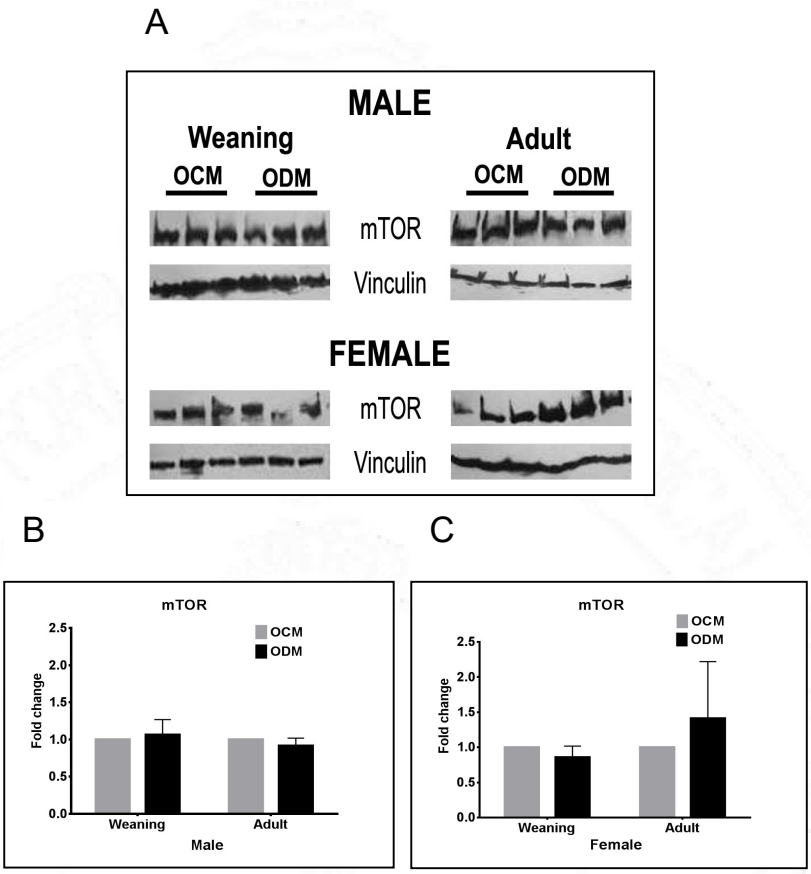

Expression of mTOR was showed by western blotting in male and female ODM (A). The bar graphs represent the fold change in expression of the respective protein in male (B) and female (C) ODM. Error bars represent ±SD. (n= 6 in each group).

The phosphorylated mTOR was also found to be be unchanged in weaning and adult group of male (Figure 126 A & B) and female (Figure 126 A & C) ODM.

Figure 126: Expression of pmTOR

A

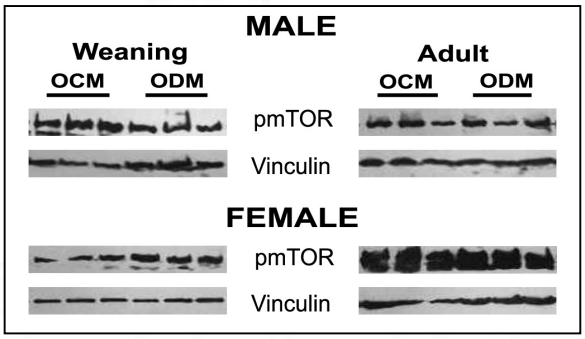

B

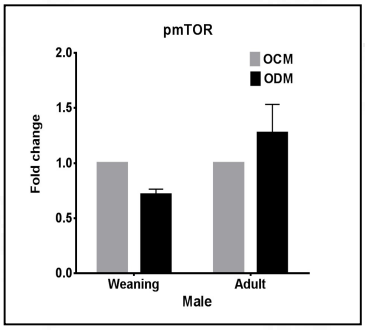

C

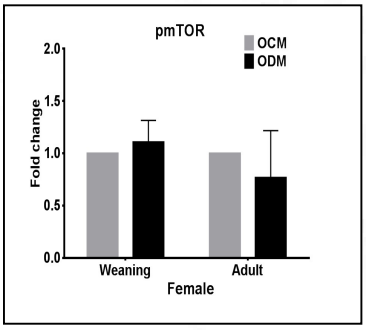

Expression of pmTOR was showed by western blotting in male and female ODM (A). The bar graphs represent the fold change in expression of the respective protein in male (B) and female (C) ODM. Error bars represent ±SD. (n= 6 in each group).

Findings:

- **No change was observed in the cardiac autophagic proteins (ULK1, Beclin 1, Rubicon, Atgs - 5, 7 & 12), mitophagic proteins (PINK 1, Parkin), lysosomal proteins (Cathepsin D) and regulators of autophagy (pAMPKα, mTOR, pmTOR) of weaning and adult group of male and female ODM**

- **A reduced expression of pULK1 was noted in adult female ODM indicates the initial complex formation with Atg 11, 13 and 17 may get altered or reduced**

- **A reduced expression of Atg 14 was noted in adult male ODM indicates the complex formation of Atg 14 with beclin 1 may get reduced, resulting in the reduced formation of autophagosome**

- **Atg 16 was found unchanged in weaning and adult male ODM, while a significant increase was noted in weaning female ODM and a reduction was noted in adult female ODM, indicates the multimeric complex formation of Atg 16 with Atg 5-Atg12 complex may get altered resulting in reduced formation of autophagosome in adult female ODM, while Atg 16 favours autophagosome formation in weaning female ODM**

- **Atg 3 which helps in the incorporation of LC3 into PE was significantly reduced in adult male and weaning and adult female ODM, while no change was observed in weaning male ODM. It indicates the reduced formation of autophagosome in adult male and weaning and adult female ODM**

- **The increased expression of p62 in adult male and female ODM shows that the degradation of autophagosomes is blocked/reduced, while no change was observed in weaning male and female ODM**

- **No change was observed in the steady state level of LC3 II and its LC3 II/I ratio in weaning female ODM, while a significant increase was noted in weaning male ODM indicated autophagosome formation was increased. But in adult male and female ODM, there showed a significant reduction in LC3 II and LC3 II/I ratio indicated reduced formation of autophagosome or reduced autophagy**

- **The lysosomal proteins LAMP-2 was seen unchanged in weaning male and female ODM, while it is significantly reduced in adult male and female ODM, shows that the number of lysososmes may be reduced in the adult group and**

as result, it will affect the fusion between autophagosomes and lysosomes and the cargoes will not get properly degraded

- **The regulators of autophagy, AMPKα were found unchanged in adult male and weaning female ODM, while a increase in weaning male ODM and decrease in adult female ODM was observed. Even though the phosphorylated form of AMPKα was found unchanged in all groups**

IV.B.3. Analysis of expression of antioxidant enzymes

Inorder to check whether the gestational diabetes had affected the antioxidant system of offspring's cardiac tissue, we analyzed the expression of two antioxidative enzymes, MnSOD and glutathione peroxidase. Mitochondrion-located superoxide dismutase (MnSOD) was observed to be unchanged inweaning and adult group of male (Figure 127 A & B) and female (Figure 127 A & C) ODM.

Figure 127: Expression of MnSOD

A

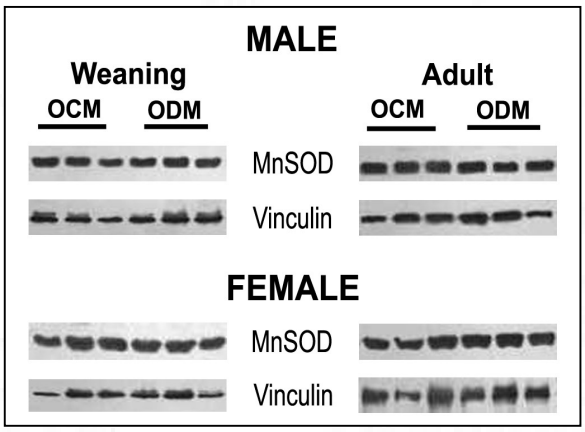

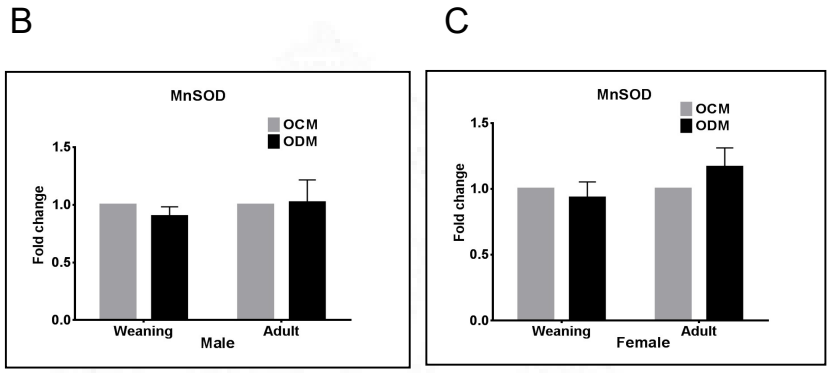

Expression of MnSOD was showed by western blotting in male and female ODM (A). The bar graphs represent the fold change in expression of the respective protein in male (B) and female (C) ODM. Error bars represent ±SD. (n= 6 in each group).

The expression of cytosolic glutathione peroxidase (GPx) was also found to be unchanged inweaning and adult group of male (Figure 128A & B) and female (Figure 128A & C) ODM.

Figure 128: Expression of GPx

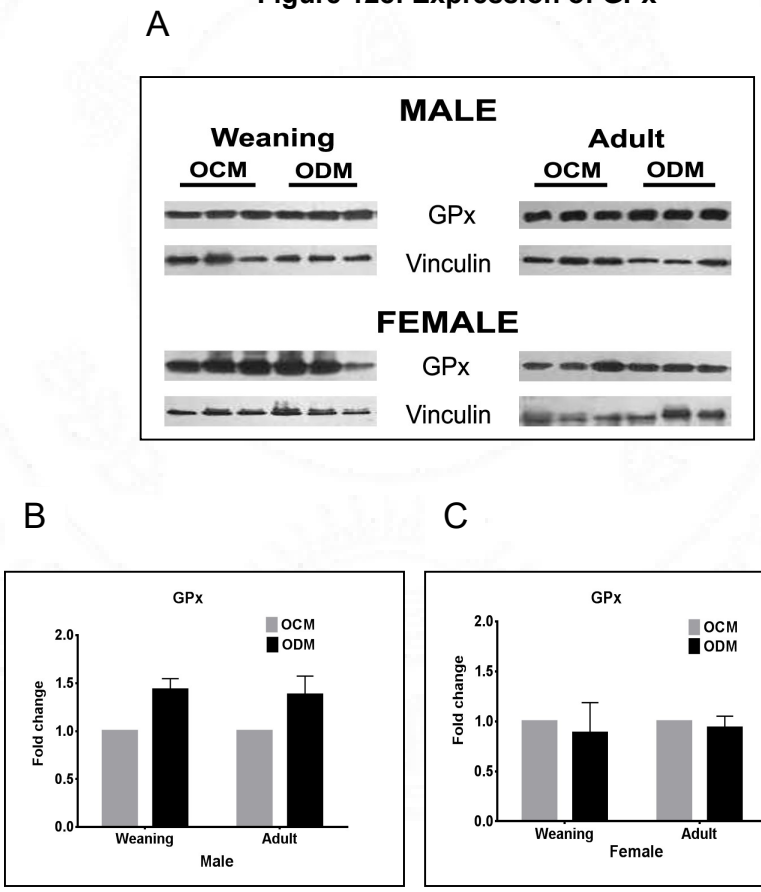

Expression of GPx was showed by western blotting in male and female ODM (A). The bar graphs represent the fold change in expression of the respective protein in male (B) and female (C) ODM. Error bars represent ±SD. (n= 6 in each group).

Findings:

- **The antioxidant enzymes, MnSOD and GPx were found unchanged in weaning and adult male and female ODM indicated that the gestational diabetes didn't influence the antioxidant mechanism in offsprings**

IV.B.4. Cardiac mitochondrial respiration in offsprings of diabetic mothers (ODM)

To analyze whether gestational diabetes mellitus alter cardiac mitochondrial function in the offsprings (male and female) of diabetic mothers (ODM), we checked the mitochondrial respiration in isolated mitochondria (from rat ventricle) by high-resolution respirometryand compared with their corresponding controls (offsprings of control mother (OCM)). After the addition of 10µl aliquot of the mitochondrial suspension to each of the chambers A and B, then followed by the step by step addition of substrates (palmitoyl L- carnitine, malate, ADP, pyruvate, glutamate, succinate), uncoupler (FCCP) and Inhibitors (rotenone, oligomycin, antimycin).

IV. B.4.1. Maternal hyperglycemia altered mitochondrial respiration in adult male ODM

Fatty acid + carbohydrate SUIT protocol

The addition of palmitoyl L- carnitine and malate showed no significant difference in the mitochondrial state 2 respiration complex I respiration in the weaning male ODM, while a significant reduction is observed in fatty acid-mediated state 2 respiration ($PalM_0$) of adult male ODM when compared with their corresponding male OCM. State 3 complex I respiration mediated by palmitoyl L- carnitine and malate ($PalM_{ADP}$) in presence of ADP in

mitochondria of weaning male ODM and adult male ODM showed significant lower OCR when related to their specific male OCM. Pyruvate- ($PalMP_{ADP}$) and glutamate- ($PalMPG_{ADP}$) mediated state 3 complex I respiration was also found to be decreased in mitochondria of weaning and adult male ODM. Succinate-mediated state 3 complex I + II ($PalMPGS_{ADP}$) mitochondrial respiration was seen to be unchanged in weaning male ODM, but a significant reduction is noted in the adult male ODM. Succinate-mediated state 3 complex II respiration (in presence of rotenone) (S_{Rot}) in weaning male ODM was similar to that of weaning male OCM. But a significant reduction is observed in adult male ODM. Complex II dependent state 4 or leak respiration (in presence of oligomycin) (S_{Omy}) is noted to be unchanged in weaning male ODM, while a significant reduction was noted in adult male ODM when compared to their respective male OCM. When the uncoupler FCCP was added to the chamber A, the complex II-dependent maximal respiration (S_{FCCP}), was seen to be unchanged in weaning male ODM,but in the adult male ODM, it was found to be significantly decreased (Figure 129 and 130).

Figure 129: Mitochondria of weaning male ODM show altered fatty acid, pyruvate & glutamate substrate utilization

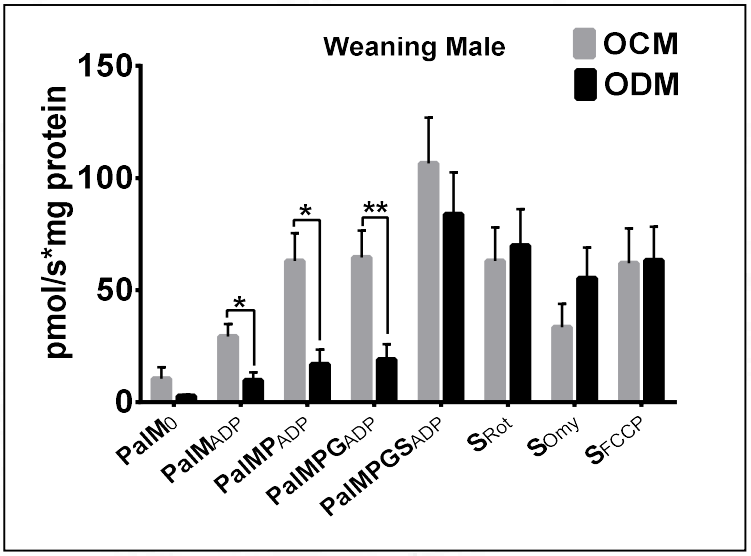

Mitochondrial states of respiration of weaning male offsprings with substrates palmitoyl L-carnitine and malate followed by pyruvate, glutamate and succinate, inhibitors rotenone and oligomycin and the uncoupler FCCP. $PalM_0$ - State 2 respiration, $PalM_{ADP}$ - State 3

*respiration of palmitoyl L- carnitine and malate, $PalMP_{ADP}$ - State 3 respiration of both palmitoyl L-carnitine, malate and pyruvate, PalMPG- State 3 respiration of palmitoyl L-carnitine, malate with pyruvate and glutamate, PalMPGS- State 3 respiration of palmitoyl L-carnitine, malate with pyruvate, glutamate and succinate, S_{Rot} - State 3 respiration of succinate after inhibition of complex I activity by rotenone, S_{Omy} - State 4 respiration by oligomycin, where complex V activity is blocked and S_{FCCP} – complex II-dependent maximal respiratory capacity by FCCP. Values are represented as mean ± SD. (p-value *<0.05**<0.01) (n=8 in each group).*

Figure 130: Mitochondria of adult male ODM show altered fatty acid + carbohydrate substrate utilization

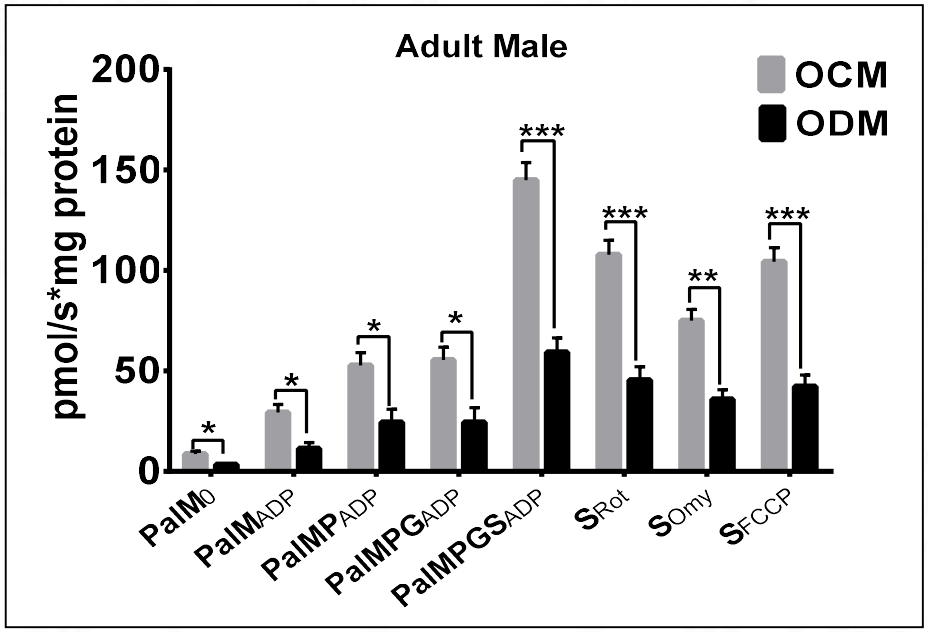

*Mitochondrial states of respiration of adult male offsprings with substrates palmitoyl L-carnitine and malate followed by pyruvate, glutamate and succinate, inhibitors rotenone and oligomycin and the uncoupler FCCP. $PalM_0$ - State 2 respiration, $PalM_{ADP}$ - State 3 respiration of palmitoyl L- carnitine and malate, $PalMP_{ADP}$ - State 3 respiration of both palmitoyl L-carnitine, malate and pyruvate, PalMPG- State 3 respiration of palmitoyl L-carnitine, malate with pyruvate and glutamate, PalMPGS- State 3 respiration of palmitoyl L-carnitine, malate with pyruvate, glutamate and succinate, S_{Rot} - State 3 respiration of succinate after inhibition of complex I activity by rotenone, S_{Omy} - State 4 respiration by oligomycin, where complex V activity is blocked and S_{FCCP} – complex II-dependent maximal respiratory capacity by FCCP. Values are represented as mean ± SD. (p-value *<0.05**<0.01***<0.001) (n=8 in each group).*

Findings:

- **The fatty acid-mediated state 2 complex I respiration was unchanged in weaning male ODM while it is reduced in adult male ODM**
- **The palmitoyl L- carnitine, pyruvate and glutamate-mediated state 3 complex I respiration was reduced in weaning and adult male ODM**
- **Succinate-mediated complex I + II and complex II respiration was not altered in weaning male ODM while a significant reduction was observed in adult male ODM**
- **Complex II dependent state 4 respiration and maximal respiratory capacity was observed to be unchanged in weaning male ODM while a significant reduction was noticed in adult male ODM**

Carbohydrate SUIT protocol

When the substrates glutamate and malate was added to chamber B, the state 2 complex I respiration in mitochondria for the weaning male ODM and OCM was found to be similar, while a significant reduction is observed in state 2 respiration (GM_0) of adult male ODM. State 3 complex I respiration mediated by glutamate and malate (GM_{ADP}) in presence of ADP in mitochondria of weaning male ODM and adult male ODM were unchanged with respect to their specific male OCM. Mitochondria of weaning male ODM showed no significant change in pyruvate-mediated state 3 complex I respiration(GMP_{ADP}). But the adult male ODM presented a significantly reduced pyruvate mediated state 3 complex I respiration. Succinate-mediated state 3 complex I + II ($GMPS_{ADP}$) mitochondrial respiration was seen to be unchanged in weaning male ODM, but a significant reduction is noted in the adult male ODM. Succinate-mediated state 3 complex II respiration (in presence of rotenone) (S_{Rot}) in weaning male ODM showed an increasing tendency in weaning male OCM. But a significant reduction is observed in adult male ODM. An increased state 4 complex II respiration or leak respiration (in presence of oligomycin) (S_{Omy}), eventhough not

significant, was observed in weaning male ODM, while a significant reduction was noted in adult male ODM when compared to their respective male OCM.The complex II-dependent maximal respiration by adding FCCP, (S_{FCCP}) also showed an increasing trend in weaning male ODM and it was significantly decreased in the adult male ODM (Figure 131 and 132).

Figure 131: Mitochondria of weaning male ODM show unaltered carbohydrate substrate utilization

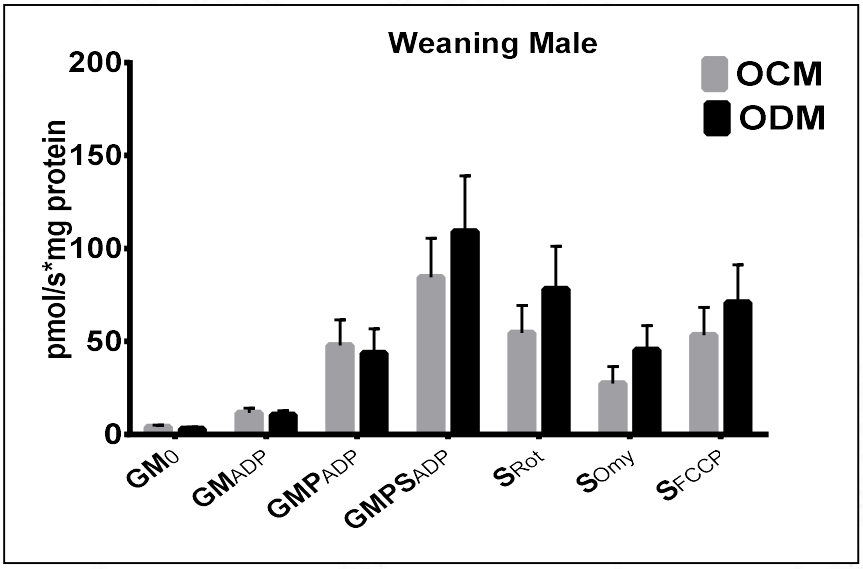

States of respiration in mitochondria of weaning male ODM with substrates glutamate, malate, pyruvate and succinate, inhibitors rotenone and oligomycin and the uncoupler FCCP.GM_0 - State 2 respiration, GM_{ADP} – glutamate/malate-mediated state 3 complex I respiration, GMP_{ADP}– glutamate/malate and pyruvate-mediated state 3 complex I respiration, $GMPS_{ADP}$– glutamate/malate, pyruvate and succinate mediated state 3 complex I + II respiration, S_{Rot} – succinate mediated state 3 complex II respiration after inhibition of complex I by rotenone, S_{Omy} - State 4 respiration by oligomycin, where complex V activity is blocked and S_{FCCP} - complex II dependent maximal respiratory capacity by FCCP. Values are represented as mean ± SD. (n=8 in each group).

Figure 132: Mitochondria of adult male ODM show altered carbohydrate substrate utilization

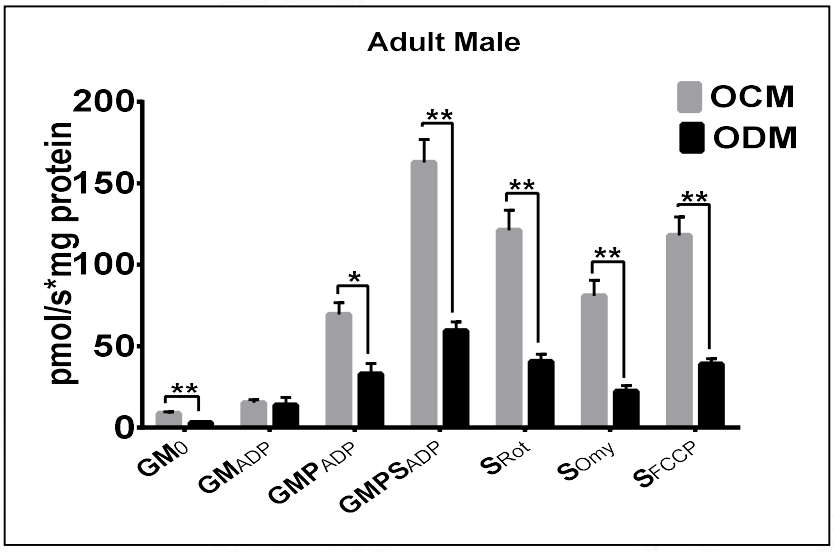

*States of respiration in mitochondria of adult male ODM with substrates glutamate, malate, pyruvate and succinate, inhibitors rotenone and oligomycin and the uncoupler FCCP.GM_0 - State 2 respiration, GM_{ADP} – glutamate/malate-mediated state 3 complex I respiration, GMP_{ADP}– glutamate/malate and pyruvate-mediated state 3 complex I respiration, $GMPS_{ADP}$– glutamate/malate, pyruvate and succinate-mediated state 3 complex I + II respiration, S_{Rot} – succinate-mediated state 3 complex II respiration after inhibition of complex I by rotenone, S_{Omy}- state 4 respiration byoligomycin, where complex V activity is blocked and S_{FCCP} - complex II dependent maximal respiratory capacity by FCCP. Values are represented as mean± SD. (p-value *<0.05**<0.01) (n=8 in each group).*

Findings:

- **The glutamate/malate-mediated state 2 complex I respiration and the glutamate/malate and pyruvate-mediated state 3 complex I respiration was unchanged in weaning male ODM**
- **Succinate-mediated complex I + II, complex II respiration, complex II-dependent state 4 respiration and maximal respiratory capacity showed an increasing tendency, but it was not significant in weaning male ODM.**
- **No change was observed in glutamate/malate-mediated state 3 complex I respiration in adult male ODM**
- **State 2 complex I respiration of glutamate/malate respiration, state 3 complex I respiration of glutamate/malate, pyruvate and succinate-mediated state 3**

complex I + II respiration, succinate-mediated complex II respiration, state 4 respiration and maximal respiratory capacity were significantly reduced in adult male ODM

IV.B.4.2. Mitochondrial OCR was less affected in female ODM

Fatty acid + carbohydrate SUIT protocol

Fatty acid-mediated (palmitoyl L- carnitine and malate) state 2 complex I respiration ($PalM_0$) showed no significant difference in the mitochondria of weaning and adult female ODM when compared with their corresponding female OCM. State 3 complex I respiration mediated by palmitoyl L- carnitine and malate ($PalM_{ADP}$) in presence of ADP in mitochondria of weaning and adult female ODM showed unchanged OCR. Pyruvate ($PalMP_{ADP}$) and glutamate ($PalMPG_{ADP}$) mediated state 3 complex I respiration of weaning and adult female ODM was similar to their respective female OCM. Succinate-mediated state 3 complex I +II ($PalMPGS_{ADP}$) mitochondrial respiration showed an increasing tendency, but not significant in weaning female ODM, but a significant reduction is noted in the adult female ODM. Succinate-mediated state 3 complex II respiration (in presence of rotenone) (S_{Rot}) in weaning female ODM presented an increased respiration (not significant). But a significant reduction was observed in adult female ODM. Complex II-dependent state 4 or leak respiration (in presence of oligomycin) (S_{Omy}) is noted to be unchanged in weaning and adult female ODM. When the uncoupler FCCP was added to the chamber A, the complex II-dependent maximal respiration (S_{FCCP}), was noted to be increasing, eventhough not significant in weaning female ODM,but in the adult female ODM, it was significantly decreased (Figure 133 and 134).

Figure 133: Mitochondria of weaning female ODM showed unaltered fatty acid + carbohydrate substrate utilization

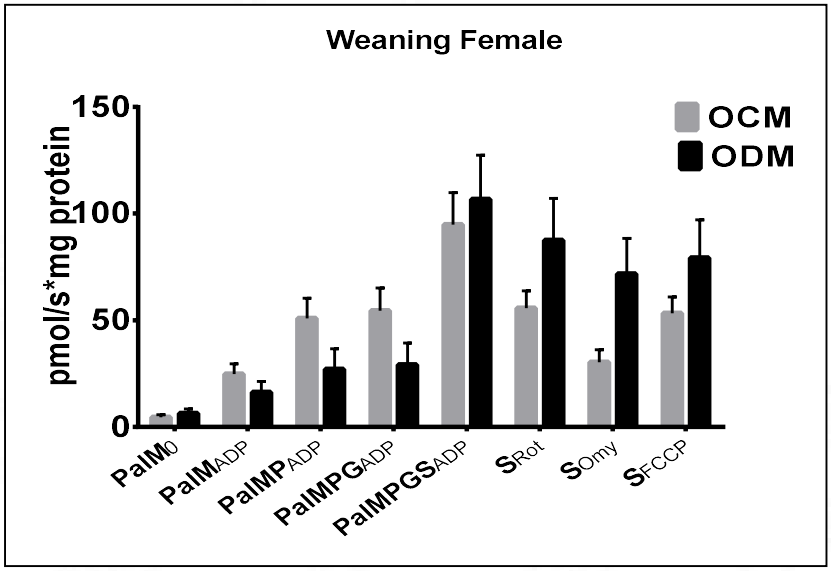

Mitochondrial states of respiration of weaning female offsprings with substrates palmitoyl L-carnitine and malate followed by pyruvate, glutamate and succinate, inhibitors rotenone and oligomycin and the uncoupler FCCP. $PalM_0$ - State 2 respiration, $PalM_{ADP}$ - State 3 respiration of palmitoyl L- carnitine and malate, $PalMP_{ADP}$ - State 3 respiration of both palmitoyl L-carnitine, malate and pyruvate, $PalMPG_{ADP}$- State 3 respiration of palmitoyl L-carnitine, malate with pyruvate and glutamate, $PalMPGS_{ADP}$- State 3 respiration of palmitoyl L-carnitine, malate with pyruvate, glutamate and succinate, S_{Rot} - State 3 respiration of succinate after inhibition of complex I activity by rotenone, S_{Omy} - State 4 respiration by oligomycin, where complex V activity is blocked and S_{FCCP} – complex II-dependent maximal respiratory capacity by FCCP. Values are represented as mean ± SD. (n=8 in each group).

Figure 134: Mitochondria of adult female ODM showed altered succinate mediated complex II respiration

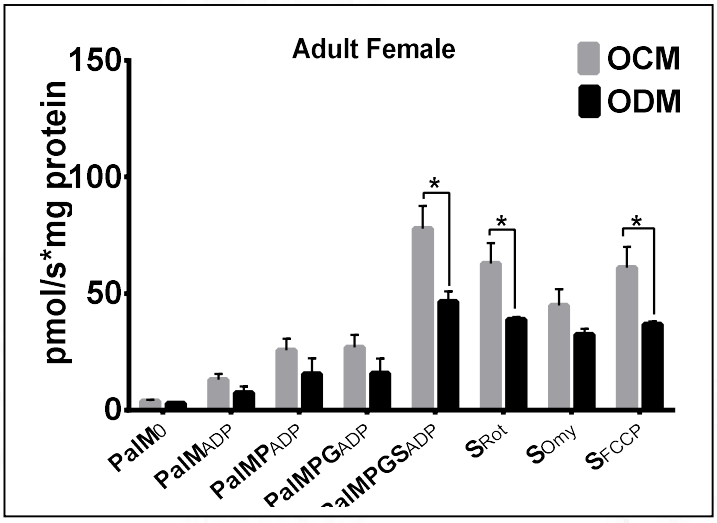

*Mitochondrial states of respiration of adult female offsprings with substrates palmitoyl L-carnitine and malate followed by pyruvate, glutamate and succinate, inhibitors rotenone and oligomycin and the uncoupler FCCP. $PalM_0$- State 2 respiration, $PalM_{ADP}$- State 3 respiration of palmitoyl L- carnitine and malate, $PalMP_{ADP}$- State 3 respiration of both palmitoyl L-carnitine/malate and pyruvate, $PalMPG_{ADP}$- State 3 respiration of palmitoyl L-carnitine/malate with pyruvate and glutamate, $PalMPGS_{ADP}$- State 3 respiration of palmitoyl L-carnitine/malate with pyruvate, glutamate and succinate, S_{Rot} - State 3 respiration of succinate after inhibition of complex I activity by rotenone, S_{Omy}- State 4 respiration byoligomycin, where complex V activity is blocked and S_{FCCP} – complex II dependent maximal respiratory capacity by FCCP. Values are represented as mean ± SD. (p-value *<0.05**<0.01***<0.001)(n=8 in each group).*

Findings:

- **The fatty acid-mediated state 2 complex I and palmitoyl L- carnitine/malate, pyruvate and glutamate-mediated and state 3 complex I respiration was unchanged in weaning female ODM corresponding to their female OCM**
- **Succinate-mediated complex I + II, complex II, complex II-dependent state 4 respiration and maximal respiratory capacity showed an increasing tendency, but it was not significant in weaning female ODM.**
- **No change was observed in fatty acid-mediated state 2 complex I, palmitoyl L- carnitine/malate, pyruvate and glutamate-mediated state 3 complex I and state 4 respiration was observed in adult female ODM**

- **Succinate-mediated state 3 complex I + II respiration, complex II respiration, and maximal respiratory capacity were significantly reduced in adult female ODM**

Carbohydrate SUIT protocol

When the substrates glutamate and malate were added to chamber B, the mitochondrial state 2 (GM_0) and state 3 (GM_{ADP}) complex I respiration in the weaning and adult female ODM were found to be unchanged. Mitochondria of weaning and adult female ODM showed no significant change in pyruvate-mediated state 3 complex I respiration(GMP_{ADP}). The succinate-mediated state 3 complex I + II ($GMPS_{ADP}$), complex II respiration (S_{Rot}), complex II dependent state 4 (S_{Omy}) and maximal respiratory capacity (S_{FCCP}) showed an increasing propensity in mitochondrial respiration, but not significant in weaning female ODM while adult female ODM showed a decreasing tendency, but not significant when compared with their corresponding female OCM (Figure 135 and 136).

Figure 135: Mitochondria of weaning female ODM showed unaltered

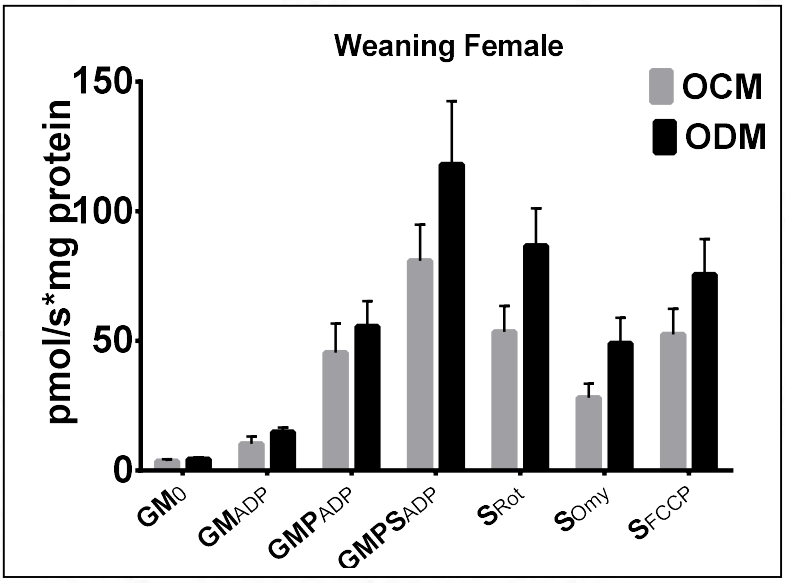

States of respiration in mitochondria of weaning female ODM with substrates glutamate/malate, pyruvate and succinate, inhibitors rotenone and oligomycin and the uncoupler FCCP.GM_0 - State 2 respiration, GM_{ADP} – glutamate/malate- mediated state 3 complex I respiration, GMP_{ADP}– glutamate/malate and pyruvate-mediated state 3 complex I

respiration, $GMPS_{ADP}$– glutamate/malate, pyruvate and succinate-mediated state 3 complex I + II respiration, S_{Rot} – succinate-mediated state 3 complex II respiration after inhibition of complex I by rotenone, S_{Omy}- State 4 respiration byoligomycin, where complex V activity is blocked and S_{FCCP} - complex II dependent maximal respiratory capacity by FCCP. Values are represented as mean ± SD. (n=8 in each group).

Figure 136: Mitochondria of adult female ODM showed unaltered carbohydrate substrate utilization

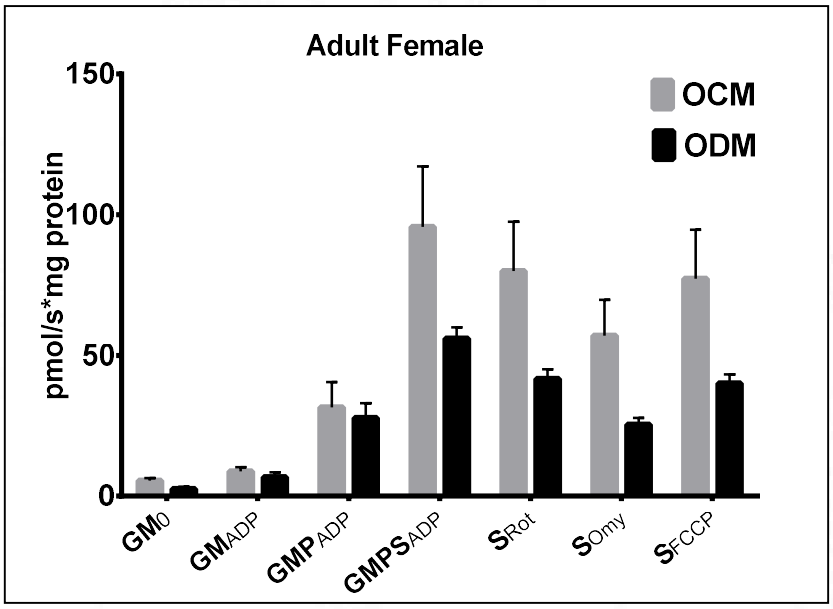

*States of respiration in mitochondria of adultfemale ODM with substrates glutamate/malate, pyruvate and succinate, inhibitors rotenone and oligomycin and the uncoupler FCCP.GM_0 - State 2 respiration, GM_{ADP} – glutamate/malate-mediated state 3 complex I respiration, GMP_{ADP}– glutamate/malate and pyruvate-mediated state 3 complex I respiration, $GMPS_{ADP}$– glutamate/malate, pyruvate and succinate mediated state 3 complex I + II respiration, S_{Rot} – succinate mediated state 3 complex II respiration after inhibition of complex I by rotenone, S_{Omy}- State 4 respiration byoligomycin, where complex V activity is blocked and S_{FCCP} - complex II dependent maximal respiratory capacity by FCCP. Values are represented as mean ± SD. (p-value *<0.05**<0.01)(n=8 in each group).*

Findings:

- **The glutamate/malate-mediated state 2 complex I respiration and the glutamate/malate and pyruvate-mediated state 3 complex I respiration was unchanged in weaning and adult female ODM**
- **Succinate-mediated complex I + II, complex II respiration, complex II-dependent state 4 respiration and maximal respiratory capacity shown an**

increasing tendency, but it was not significant in weaning female ODM.

- **Succinate-mediated complex I + II, complex II respiration, complex II-dependent state 4 respiration and maximal respiratory capacity shown a decreasing tendency, but it was not significant in adult female ODM.**

V.B. DISCUSSION
(GDM)

V.B.1. Gestational diabetic rat model

The present study was done to evaluate the effect of untreated gestational diabetes of mother on offspring's cardiac autophagy and mitochondrial respiration at two stages of their life, weaning and adult time period. For the study, pregnant wistar rats were used and GDM was induced by streptozotocin. On every 7^{th} day till the delivery of rat, body weight and random glucose of the mother were noted and it revealed that the animals were maintaining the hyperglycemic condition throughout the pregnancy period. HbA1c values checked at the time of euthanasia of diabetic mother (when the offsprings are weaned from the mother at the 22^{nd} day) was >7%. This indicated that till the weaning period, diabetic mother maintained hyperglycemia, so that the offsprings could drink the milk containing high glucose(Holemans et al., 1999).The number of offsprings in diabetic mothers was less than control mothers. Still birth was high in GDM mothers. Also the lactation was not properly maintained and the mortality rate of offsprings (immediately after delivery) was high in diabetic mothers. Body weight (taken at the time of euthanasia) of the weaning group (male and female) ODM didn't change when compared to their OCM, but the adult group (male and female) ODM showed a significant weight gain than the corresponding OCM. In human beings, usually macrosomic babies are born to GDM mothers (Ragnarsdottir and Conroy, 2010). Unchanged heart weight: body weight ratio was observed in weaning and adult group of male and female ODM when compared with their corresponding OCM indicated that no structural changes like hypertrophy/cardiomyopathy occurred in the heart tissue. Even though offsprings are born to a diabetic mother, both male and female offsprings were normoglycemic at weaning and adult period and their HbA1c level at the time of euthanasia was normal in range.

V.B.1.1 Autophagic profile of offsprings of gestational diabetic mothers

The aim of present study was to evaluate the status of cardiac autophagy in offsprings of untreated diabetic mothers at two stages of their life, weaning and adult time period. Both the male and female ODM are included in the study. This is the first report regarding cardiac autophagy at two stages of life of male and female offsprings of gestational diabetic mothers. Following the evaluation of various proteins involved in cardiac autophagy, no change in expression was observed in ULK1, Beclin 1, Rubicon, Atgs - 5, 7 and 12, mitophagic proteins (PINK 1 and Parkin), lysosomal proteins (Cathepsin D) and regulators of autophagy (pAMPKα, mTOR, pmTOR) of weaning and adult group of male and female ODM.

In adult female ODM, reduced expression of pULK1 (Atg 1) was noted indicates the initial complex formation with Atg 11, 13 and 17 may get altered and will affect the initiation process of autophagy (Mariño and López-Otín, 2004). A reduced expression of Atg 14 was noted in adult male ODM indicates the complex formation of Atg 14 with beclin 1 may get reduced, resulting in the reduced formation of autophagosome(Kang et al., 2011: 1). Atg 16 was found unchanged in weaning and adult male ODM, while a significant increase was noted in weaning female ODM and a reduction was noted in adult female ODM, indicates the multimeric complex formation of Atg 16 with Atg 5-Atg12 complex may get altered resulting in reduced formation of autophagosome in adult female ODM, while Atg 16 favours autophagosome formation in weaning female ODM. Atg 3 which helps in the incorporation of LC3 into PE was significantly reduced in adult male and weaning and adult female ODM, while no change was observed in weaning male ODM(Mariño and López-Otín, 2004). It indicates the reduced formation of autophagosome in adult male and weaning and adult female ODM. The increased expression of p62 in adult male and female ODM shows that the degradation of autophagosomes is blocked/reduced, while no change was observed in weaning male and female ODM. No change was observed in the steady state level of LC3 II and its LC3 II/I ratio in weaning female ODM, while a significant increase was noted in

weaning male ODM indicated autophagosome formation was increased. But in adult male and female ODM, there showed a significant reduction in steady state level of LC3 II and LC3 II/I ratio indicated reduced formation of autophagosome or reduced autophagy(Kabeya et al., 2000). In a study done in stillborn human fetal pancreas of GDM mothers, showed significant increase in the LC3 II levels. They also found increased LC3 II and P62 in the human diabetic placenta, while beclin -1 was significantly reduced and the data represents altered autophagy in diabetic pregnancy (Avagliano et al., 2017). Another study done in GDM patients showed autophagic activity was increased in placenta and extravillous trophoblast. In this study they observed increased LC3 II and decreased p62 expression in the diabetic placenta. Atg 5 expression, necessary for autophagosome formation and also in embryonic cavitation development was found to be significantly increased in placenta of GDM subjects than normal pregnant ones (Ji et al., 2017).Hyperglycemia-induced cardiovascular malformation in early chick embryos was attenuated by the treatment ofbaicalin, a polyphenolic flavanoid by suppressing the production of ROS and inhibiting autophagy. Bicalin administration reduced the expression of LC3 II, p62 and Beclin1 (Wang, Liang, et al., 2018).In our study, the lysosomal proteins LAMP-2 was seen unchanged in weaning male and female ODM, while it is significantly reduced in adult male and female ODM, shows that the number of lysososmes may be reduced in the adult group and as result, it will affect the fusion between autophagosomes and lysosomes and the cargoes will not get properly degraded. The regulator of autophagy, AMPKα were found unchanged in adult male and weaning female ODM, while a increase in weaning male ODM and decrease in adult female ODM was observed. Even though the phosphorylated form of AMPKα was found unchanged in all groups. Most of the autophagic proteins evaluated in male and female ODM at their weaning period didn't show a significant change when compared with corresponding OCM. But they became adult, both male and female showed reduced or altered autophagy suggesting an impaired recycling mechanism in cardiac tissue of offsprings of GDM mothers. As a result of altered autophagy, the accumulation of dysfunctional organelles especially mitochondria occurs in a terminally differentiated cell like

cardiomyocytes. Unchanged expression of the antioxidant enzymes, MnSOD and GPx in weaning and adult male and female ODM indicated that the diabetic pregnancy didn't influence the antioxidant mechanism in offsprings.

V.B.1.2. Mitochondrial respiration in offsprings of diabetic mothers

The main objective of this study was to evaluate the mitochondrial function of offsprings (male and female) of untreated gestational diabetic mothers at two different time points of their life, weaning and adult time period. The same gestational rat model and their groups for the cardiac autophagy study were used for mitochondrial respiration experiments. We adopted high resolution respirometry for mitochondrial OCR analysis.

The fatty acid-mediated state 2 complex I respiration was unchanged in weaning male ODM. Even though state 3 complex I respiration mediated by the substrates, palmitoyl L-carnitine/malate, pyruvate and glutamate was significantly reduced in weaning group,succinate-mediated complex I + II and complex II respirationwere not altered in weaning male ODM. Complex II-dependent state 4 respiration by oligomycin and maximal respiratory capacity obtained by FCCP in the fatty acid + carbohydrate protocol were observed to be unchanged in male weaning group. When followed the carbohydrate SUIT protocol, no change was noticed in the glutamate/malate-mediated state 2 and state 3 complex I respiration, pyruvate-mediated state 3 complex I respiration, succinate-mediated complex I + II respiration and complex II respiration, complex II-dependent state 4 respiration and FCCP-mediated maximal respiration in the waening male ODM. Even though a slight increase in mitochondrial OCR was noted in succinate-mediated complex I + II respiration and complex II respiration, complex II dependent state 4 respiration and FCCP-mediated maximal respiration in the weaning male ODM, those were not significant.

In adult male ODM, the fatty acid-mediated state 2 respiration, their state 3 complex I respiration mediated by the substrates, palmitoyl L- carnitine, malate, pyruvate and glutamate, succinate-mediated complex I + II and complex II respiration, complex II

dependent state 4 respiration by oligomycin and maximal respiratory capacity obtained by FCCP in the fatty acid + carbohydrate protocol were observed to be significantly reduced. In carbohydrate protocol also, glutamate/malate-mediated state 2 respiration, state 3 respiration mediated by pyruvate, succinate-mediated complex I + II and complex II respiration, complex II dependent state 4 respiration by oligomycin and maximal respiratory capacity obtained by FCCP were significantly lowered in adult male ODM than their corresponding adult OCM. The glutamate/malate-mediated state 3 complex I respiration was found unchanged.

In both protocols done in weaning female ODM,state 2 respiration, state 3 complex I respiration mediated by the substrates, palmitoyl L- carnitine/malate, pyruvate, glutamate, scuccinate-mediated complex I + II and complex II respiration, complex II-dependent state 4 respiration by oligomycin and maximal respiratory capacity obtained by FCCP were unchanged when compared to their respective OCM. Even though a slight increase in mitochondrial OCR was noted in succinate-mediated complex I + II respiration, complex II respiration, complex II-dependent state 4 respiration and FCCP-mediated maximal respiration in the weaning female ODM, those were not significant in the two SUIT protocols.

In adult female ODM, the fatty acid-mediated state 2 complex I respiration, state 3 complex I respiration mediated by pyruvate and glutamate and state 4 respiration were not altered with respect to their controls. But the succinate-mediated complex I + II and complex II respiration and maximal respiratory capacity obtained by FCCP were significantly reduced in the adult female ODM. When followed the carbohydrate SUIT protocol, no change was noticed in the glutamate/malate-mediated state 2 and state 3 respiration,pyruvate-mediated state 2 and state 3 complex I respiration, succinate-mediated complex I + II respiration, complex II respiration, complex II-dependent state 4 respiration and FCCP-mediated maximal respiration in the weaning female ODM. Even though a slight increase in mitochondrial OCR was noted in succinate-mediated complex I + II respiration, complex II

respiration, complex II-dependent state 4 respiration and FCCP-mediated maximal respiration in the weaning female ODM, those were not significant.

The mitochondrial respiration of the weaning (male and female)ODMirrespective of substrate combination was found to be unchanged compared to their respective OCM(except the state 3 complex I respiration in the fatty acid + carbohydrate protocol of male). But when the male ODM became adult, a significant reduction in mitochondrial OCR was observed in the two protocols followed.In the case of female adult ODM, the mitochondrial OCR show a decreased tendency, but insignificant in both protocols (except reduced succinate-mediated complex I + II, complex II and maximal respiratory capacity in fatty acid-mediated protocol)compared to their corresponding OCM. In a study of STZ model of diabetic pregnancy reported cardiovascular dysfunction like increased blood pressure, decreased heart rate, increased sensitivity to nor adrenaline and abnormal endothelium dependent relaxation to acetyl choline and bradykinin in the adult female offsprings (Holemans et al., 1999).In a study done to evaluate the effect of maternal diabetes on prostacyclin synthesis in aorta and heart tissue, they didn't observe any difference at birth, but during the weaning period, a significant rise in synthesis of prostacyclin in aorta and a decrease in the heart tissue were observed. Their study had shown that the consequence of maternal hyperglycemia on the offsprings may be evident/expressed during the later time period of life (Bydlowski, Yunker and Subbiah, 1985). Likewise in our study, effect of maternal diabetes on the cardiac mitochondrial respiration of offsprings was prominently expressed at their adult age in males, while no such significant changes were observed in the weaning period. Thus our study showed that the changes in offsprings due to diabetic pregnancy were evident in their future life. A study of maternal obesity where the skeletal muscle mitochondria of 3-month-old male offspring showed decreased complex II and III activity, while no change was observed in female offsprings (Shelley et al., 2009). Similar to this study, our results also denoted that the cardiac mitochondrial respiration was highly affected in adult male offsprings while the females were less affected by maternal hyperglycemia. When we compared the mitochondrial respiration of adult male and female

ODM, there seemed to be a protective mechanism in female offsprings of diabetic mothers in maintaining their cardiac mitochondrial respiration compared to male rats. The presence of estrogen may be a reason for the protective effect in females. The role of estrogen in maintaining cardiac mitochondrial functions were shown in a study done in ovariectomized rats. Those animals had reduced complex I mediated ATP synthesis, altered structural assembly of mitochondria, high ROS production etc, in the absence of estrogen (Rattanasopa et al., 2015). A reduced ETC enzyme complex activity in the liver tissue of offsprings was observed in a rat model of high fat diet pregnancy (Bruce et al., 2009). In another study of high fat-fed model of pregnancy, rat aortas showed reduced expression of mitochondrial complexes I, II and III in 6-month-old offsprings (Taylor et al., 2005). A work done in high fat fed pregnancy in rat showed reduced expression of complex I in soleus muscle of male offspring(Pileggi et al., 2016). Only a single work has been published recently, which showed showed impaired cardiac function due to mitochondrial dysfunction and metabolic stress in offsprings of high fat-fed STZ model of pregnancy. They had analyzed the cardiac and mitochondrial function in newborn pups and they showed altered contractile and diastolic function in them. Reduced basal, maximal mitochondrial respiration, reduced ATP levels, altered spare respiratory capacity and proton leak were observed in mitochondria of neonatal isolated cardiomyocytes of ODM (Mdaki et al., 2016).

VI.B. CONCLUSION (GDM)

The aim of present study was to evaluate the status of cardiac autophagy and mitochondrial respiration in male and female offsprings of untreated gestational diabetic mothers at two stages of their life, weaning and adult time period. Our results showed that cardiac autophagy is reduced or altered in the adult group of male and female ODM. But cardiac autophagy was less affected in the weaning group of male and female ODM. Most of the mitophagic and autophagic proteins were unchanged in male and female weaning group ODM. This is the first report on cardiac autophagy in male and female offsprings of gestational diabetic mothers. The study implies the impact of diabetic pregnancy or the hyperglycemic condition in the uterine environment in regulating a metabolic process, autophagy in the offsprings during their life time. It shows that the impairment or defects is more evident in their adult life. The another objective of this study was to evaluate the mitochondrial function of offsprings (male and female) of untreated gestational diabetic mothers at two different time points of their life, weaning and adult time period. The available single work published by Mdaki et al, showed significant reduction in cardiac mitochondrial respiration in new born pups of diabetic mothers. Our study didn't include new born pups, but included the weaning and adult stage of both male and female offsprings of diabetic mothers. The mitochondrial respiration of the weaning (male and female) ODM irrespective of substrate combination was found to be less affected or unchanged compared to their respective OCM. But in the adult group of male ODM, a significant reduction in mitochondrial oxygen consumption was observed. The mitochondrial respiration in female adult ODM are found unchanged or less affected by diabetic pregnancy, even though they exhibited significant reduction in succinate-mediated complex I and II respiration in one of the protocol. There seems to be a protective mechanism in female offsprings in maintaining their cardiac mitochondrial respiration, may be the specific role of estrogen in female heart.

Our results suggest that gestational diabetes can cause impaired cardiac autophagy and mitochondrial respiration in the offsprings which might become more evident in their future life. As a result of impairment in these cellular processes, the total generation of ATP may be reduced, affecting the normal function of heart in the offsprings of diabetic mothers.

VII. LIMITATION OF THE STUDY (T2DM & GDM)

- Both diabetic and non-diabetic patients were ischemic in the human study. A healthy heart tissue sample is needed in order to get a perfect control for the study.
- It is better to maintain hyperglycemia for a period of 20 weeks or more in order to study a later time point of diabetes in the mice study.
- Only hyperglycaemic model was generated for the mice and rat study. If a high fat model along with streptozotocin treatment is introduced, a hyperlipidemic and hyperglycaemic condition can be availed as in human patients.
- Transmission electron microscopic analysis needed for autophagic evaluation of autophagosomes and mitochondria were not analyzed.
- Cardiac functional analysis like ECG, Echo was not done in mice and rat models.
- Generalized autophagic activation and inhibition using pharmacological compounds.

VIII. BIBLIOGRAPHY

AMERICAN DIABETES ASSOCIATION, 2013. Diagnosis and Classification of Diabetes Mellitus. *Diabetes Care*. 36 (Supplement_1), pp. S67–S74.

ANDERSON, E.J., KYPSON, A.P., RODRIGUEZ, E., ANDERSON, C.A., LEHR, E.J., and NEUFER, P.D., 2009. Substrate-specific derangements in mitochondrial metabolism and redox balance in the atrium of the type 2 diabetic human heart. *Journal of the American College of Cardiology*. 54 (20), pp. 1891–1898.

ANDRIENKO, T., KUZNETSOV, A.V., KAAMBRE, T., USSON, Y., OROSCO, A., APPAIX, F., TIIVEL, T., SIKK, P., VENDELIN, M., MARGREITER, R., and SAKS, V.A., 2003. Metabolic consequences of functional complexes of mitochondria, myofibrils and sarcoplasmic reticulum in muscle cells. *Journal of Experimental Biology*. 206 (12), pp. 2059–2072.

AQBI, H.F., TYUTYUNYK-MASSEY, L., KEIM, R.C., BUTLER, S.E., THEKKUDAN, T., JOSHI, S., SMITH, T.M., BANDYOPADHYAY, D., IDOWU, M.O., BEAR, H.D., PAYNE, K.K., GEWIRTZ, D.A., and MANJILI, M.H., 2018. Autophagy-deficient breast cancer shows early tumor recurrence and escape from dormancy. *Oncotarget*. 9 (31), pp. 22113–22122.

ASHRAFI, G. and SCHWARZ, T.L., 2013. The pathways of mitophagy for quality control and clearance of mitochondria. *Cell Death and Differentiation*. 20 (1), pp. 31–42.

ATKINSON, M.A., 2012. The Pathogenesis and Natural History of Type 1 Diabetes. *Cold Spring Harbor Perspectives in Medicine* [online]. 2

(11). Available from: https://www.ncbi.nlm.nih.gov/pmc/articles/PMC3543105/.

AVAGLIANO, L., MASSA, V., TERRANEO, L., SAMAJA, M., DOI, P., BULFAMANTE, G.P., and MARCONI, A.M., 2017. Gestational diabetes affects fetal autophagy. *Placenta*. 55, pp. 90–93.

BAI, T., WANG, F., ZHENG, Y., LIANG, Q., WANG, Y., KONG, J., and CAI, L., 2016. Myocardial redox status, mitophagy and cardioprotection: a potential way to amend diabetic heart? *Clinical Science (London, England: 1979)*. 130 (17), pp. 1511–1521.

BARBOUR, L.A., MCCURDY, C.E., HERNANDEZ, T.L., KIRWAN, J.P., CATALANO, P.M., and FRIEDMAN, J.E., 2007. Cellular Mechanisms for Insulin Resistance in Normal Pregnancy and Gestational Diabetes. *Diabetes Care*. 30 (Supplement 2), pp. S112–S119.

BAZ, B., RIVELINE, J.-P., and GAUTIER, J.-F., 2016. ENDOCRINOLOGY OF PREGNANCY: Gestational diabetes mellitus: definition, aetiological and clinical aspects. *European Journal of Endocrinology*. 174 (2), pp. R43-51.

BECERRA, J.E., KHOURY, M.J., CORDERO, J.F., and ERICKSON, J.D., 1990. Diabetes mellitus during pregnancy and the risks for specific birth defects: a population-based case-control study. *Pediatrics*. 85 (1), pp. 1–9.

BERG, T.J., SNORGAARD, O., FABER, J., TORJESEN, P.A., HILDEBRANDT, P., MEHLSEN, J., and HANSSEN, K.F., 1999. Serum levels of advanced glycation end products are associated with

left ventricular diastolic function in patients with type 1 diabetes. *Diabetes Care*. 22 (7), pp. 1186–1190.

BERNARD, A. and KLIONSKY, D.J., 2013. Autophagosome Formation: Tracing the Source. *Developmental cell*. 25 (2), pp. 116–117.

BERTRAND, L., HORMAN, S., BEAULOYE, C., and VANOVERSCHELDE, J.-L., 2008. Insulin signalling in the heart. *Cardiovascular Research*. 79 (2), pp. 238–248.

BHANSALI, S., BHANSALI, A., WALIA, R., SAIKIA, U.N., and DHAWAN, V., 2017. Alterations in Mitochondrial Oxidative Stress and Mitophagy in Subjects with Prediabetes and Type 2 Diabetes Mellitus. *Frontiers in Endocrinology* [online]. 8. Available from: https://www.ncbi.nlm.nih.gov/pmc/articles/PMC5737033/ [Accessed 12 Jun 2018].

BI, Y., WANG, G., LIU, X., WEI, M., and ZHANG, Q., 2017. Low-after-high glucose down-regulated Cx43 in H9c2 cells by autophagy activation via cross-regulation by the PI3K/Akt/mTOR and MEK/ERK1/2 signal pathways. *Endocrine*. 56 (2), pp. 336–345.

BORENGASSER, S.J., LAU, F., KANG, P., BLACKBURN, M.L., RONIS, M.J.J., BADGER, T.M., and SHANKAR, K., 2011. Maternal Obesity during Gestation Impairs Fatty Acid Oxidation and Mitochondrial SIRT3 Expression in Rat Offspring at Weaning. *PLOS ONE*. 6 (8), p. e24068.

BOUDINA, S., SENA, S., O'NEILL, B.T., TATHIREDDY, P., YOUNG, M.E., and ABEL, E.D., 2005. Reduced mitochondrial oxidative capacity and

increased mitochondrial uncoupling impair myocardial energetics in obesity. *Circulation*. 112 (17), pp. 2686–2695.

BRAND, M.D., AFFOURTIT, C., ESTEVES, T.C., GREEN, K., LAMBERT, A.J., MIWA, S., PAKAY, J.L., and PARKER, N., 2004. Mitochondrial superoxide: production, biological effects, and activation of uncoupling proteins. *Free Radical Biology & Medicine*. 37 (6), pp. 755–767.

BRAND, M.D. and NICHOLLS, D.G., 2011. Assessing mitochondrial dysfunction in cells. *Biochemical Journal*. 435 (Pt 2), pp. 297–312.

BRUCE, K.D., CAGAMPANG, F.R., ARGENTON, M., ZHANG, J., ETHIRAJAN, P.L., BURDGE, G.C., BATEMAN, A.C., CLOUGH, G.F., POSTON, L., HANSON, M.A., MCCONNELL, J.M., and BYRNE, C.D., 2009. Maternal high-fat feeding primes steatohepatitis in adult mice offspring, involving mitochondrial dysfunction and altered lipogenesis gene expression. *Hepatology (Baltimore, Md.)*. 50 (6), pp. 1796–1808.

BUGGER, H. and ABEL, E.D., 2010. Mitochondria in the diabetic heart. *Cardiovascular Research*. 88 (2), pp. 229–240.

BURGEIRO, A., FONSECA, A.C., ESPINOZA, D., CARVALHO, L., LOURENÇO, N., ANTUNES, M., and CARVALHO, E., 2018. Proteostasis in epicardial versus subcutaneous adipose tissue in heart failure subjects with and without diabetes. *Biochimica et Biophysica Acta (BBA) - Molecular Basis of Disease*. 1864 (6, Part A), pp. 2183–2198.

BYDLOWSKI, S.P., YUNKER, R.L., and SUBBIAH, M.T., 1985. Delayed effects of experimental maternal diabetes on plasma cholesterol level and vascular prostacyclin synthesis in the offspring. *Proceedings of the Society for Experimental Biology and Medicine. Society for Experimental Biology and Medicine (New York, N.Y.)*. 179 (4), pp. 553–557.

CATALANO, P.M., KIRWAN, J.P., HAUGEL-DE MOUZON, S., and KING, J., 2003. Gestational diabetes and insulin resistance: role in short- and long-term implications for mother and fetus. *The Journal of Nutrition*. 133 (5 Suppl 2), pp. 1674S-1683S.

CHAANINE, A.H., GORDON, R.E., NONNENMACHER, M., KOHLBRENNER, E., BENARD, L., and HAJJAR, R.J., 2015. High-dose chloroquine is metabolically cardiotoxic by inducing lysosomes and mitochondria dysfunction in a rat model of pressure overload hypertrophy. *Physiological Reports* [online]. 3 (7). Available from: https://www.ncbi.nlm.nih.gov/pmc/articles/PMC4552516/ [Accessed 26 May 2018].

CHEN, Y. and KLIONSKY, D.J., 2011. The regulation of autophagy – unanswered questions. *J Cell Sci*. 124 (2), pp. 161–170.

CHENG, Y., REN, X., HAIT, W.N., and YANG, J.-M., 2013. Therapeutic Targeting of Autophagy in Disease: Biology and Pharmacology. *Pharmacological Reviews*. 65 (4), pp. 1162–1197.

CHI, R.-F., WANG, J.-P., WANG, K., ZHANG, X.-L., ZHANG, Y.-A., KANG, Y.-M., HAN, X.-B., LI, B., QIN, F.-Z., and FAN, B.-A., 2017.

Progressive Reduction in Myocyte Autophagy After Myocardial Infarction in Rabbits: Association with Oxidative Stress and Left Ventricular Remodeling. *Cellular Physiology and Biochemistry: International Journal of Experimental Cellular Physiology, Biochemistry, and Pharmacology*. 44 (6), pp. 2439–2454.

CHONG, C.-R., CLARKE, K., and LEVELT, E., 2017. Metabolic remodelling in diabetic cardiomyopathy. *Cardiovascular Research*. 113 (4), pp. 422–430.

CHOURASIA, A.H., TRACY, K., FRANKENBERGER, C., BOLAND, M.L., SHARIFI, M.N., DRAKE, L.E., SACHLEBEN, J.R., ASARA, J.M., LOCASALE, J.W., KARCZMAR, G.S., and MACLEOD, K.F., 2015. Mitophagy defects arising from BNip3 loss promote mammary tumor progression to metastasis. *EMBO reports*. 16 (9), pp. 1145–1163.

CROSTON, T.L., SHEPHERD, D.L., THAPA, D., NICHOLS, C.E., LEWIS, S.E., DABKOWSKI, E.R., JAGANNATHAN, R., BASELER, W.A., and HOLLANDER, J.M., 2013. Evaluation of the cardiolipin biosynthetic pathway and its interactions in the diabetic heart. *Life Sciences*. 93 (8), pp. 313–322.

DABKOWSKI, E.R., WILLIAMSON, C.L., BUKOWSKI, V.C., CHAPMAN, R.S., LEONARD, S.S., PEER, C.J., CALLERY, P.S., and HOLLANDER, J.M., 2009. Diabetic cardiomyopathy-associated dysfunction in spatially distinct mitochondrial subpopulations. *American Journal of Physiology. Heart and Circulatory Physiology*. 296 (2), pp. H359-369.

DAMASCENO, D.C., VOLPATO, G.T., DE MATTOS PARANHOS CALDERON, I., and CUNHA RUDGE, M.V., 2002. Oxidative stress and diabetes in pregnant rats. *Animal Reproduction Science*. 72 (3–4), pp. 235–244.

DAY, R.E. and INSLEY, J., 1976. Maternal diabetes mellitus and congenital malformation. Survey of 205 cases. *Archives of Disease in Childhood*. 51 (12), pp. 935–938.

DESISTO, C.L., 2014. Prevalence Estimates of Gestational Diabetes Mellitus in the United States, Pregnancy Risk Assessment Monitoring System (PRAMS), 2007–2010. *Preventing Chronic Disease* [online]. 11. Available from: https://www.cdc.gov/pcd/issues/2014/13_0415.htm [Accessed 25 Mar 2018].

DESOYE, G. and MOUZON, S.H., 2007. The Human Placenta in Gestational Diabetes Mellitus The insulin and cytokine network. *Diabetes Care*. 30 (Supplement 2), pp. S120–S126.

DOLIBA, N.M., QIN, W., NAJAFI, H., LIU, C., BUETTGER, C.W., SOTIRIS, J., COLLINS, H.W., LI, C., STANLEY, C.A., WILSON, D.F., GRIMSBY, J., SARABU, R., NAJI, A., and MATSCHINSKY, F.M., 2012. Glucokinase activation repairs defective bioenergetics of islets of Langerhans isolated from type 2 diabetics. *American Journal of Physiology. Endocrinology and Metabolism*. 302 (1), pp. E87–E102.

DOULAVERIS, G., ORFANELLI, T., BENN, K., ZERVOUDAKIS, I., SKUPSKI, D., and WITKIN, S.S., 2013. A polymorphism in an

autophagy-related gene, ATG16L1, influences time to delivery in women with an unfavorable cervix who require labor induction. *Journal of Perinatal Medicine*. 41 (4), pp. 411–414.

EGAWA, Y., SAIGO, C., KITO, Y., MORIKI, T., and TAKEUCHI, T., 2018. Therapeutic potential of CPI-613 for targeting tumorous mitochondrial energy metabolism and inhibiting autophagy in clear cell sarcoma. *PLOS ONE*. 13 (6), p. e0198940.

ESKELINEN, E.-L., ILLERT, A.L., TANAKA, Y., SCHWARZMANN, G., BLANZ, J., VON FIGURA, K., and SAFTIG, P., 2002. Role of LAMP-2 in Lysosome Biogenesis and Autophagy. *Molecular Biology of the Cell*. 13 (9), pp. 3355–3368.

ESKELINEN, E.-L. and SAFTIG, P., 2009. Autophagy: A lysosomal degradation pathway with a central role in health and disease. *Biochimica et Biophysica Acta (BBA) - Molecular Cell Research*. 1793 (4), pp. 664–673.

ESTAMPADOR, A.C. and FRANKS, P.W., 2014. Genetic and epigenetic catalysts in early-life programming of adult cardiometabolic disorders. *Diabetes, Metabolic Syndrome and Obesity: Targets and Therapy* [online]. Available from: https://www.dovepress.com/genetic-and-epigenetic-catalysts-in-early-life-programming-of-adult-ca-peer-reviewed-fulltext-article-DMSO [Accessed 8 Jun 2018].

FENG, Y., HE, D., YAO, Z., and KLIONSKY, D.J., 2014. The machinery of macroautophagy. *Cell Research*. 24 (1), pp. 24–41.

FERENCZ, C., RUBIN, J.D., MCCARTER, R.J., and CLARK, E.B., 1990. Maternal diabetes and cardiovascular malformations: predominance of double outlet right ventricle and truncus arteriosus. *Teratology*. 41 (3), pp. 319–326.

FERRETTA, A., GABALLO, A., TANZARELLA, P., PICCOLI, C., CAPITANIO, N., NICO, B., ANNESE, T., DI PAOLA, M., DELL'AQUILA, C., DE MARI, M., FERRANINI, E., BONIFATI, V., PACELLI, C., and COCCO, T., 2014. Effect of resveratrol on mitochondrial function: Implications in parkin-associated familiar Parkinson's disease. *Biochimica et Biophysica Acta (BBA) - Molecular Basis of Disease*. 1842 (7), pp. 902–915.

FILLMORE, N., MORI, J., and LOPASCHUK, G.D., 2014. Mitochondrial fatty acid oxidation alterations in heart failure, ischaemic heart disease and diabetic cardiomyopathy. *British Journal of Pharmacology*. 171 (8), pp. 2080–2090.

FORBES, J.M. and COOPER, M.E., 2013. Mechanisms of diabetic complications. *Physiological Reviews*. 93 (1), pp. 137–188.

FOWLER, M.J., 2008. Microvascular and Macrovascular Complications of Diabetes. *Clinical Diabetes*. 26 (2), pp. 77–82.

FUJITANI, Y., UENO, T., and WATADA, H., 2010. Autophagy in health and disease. 4. The role of pancreatic β-cell autophagy in health and diabetes. *American Journal of Physiology-Cell Physiology*. 299 (1), pp. C1–C6.

GALLUZZI, L., BAEHRECKE, E.H., BALLABIO, A., BOYA, P., PEDRO, J.M.B.-S., CECCONI, F., CHOI, A.M., CHU, C.T., CODOGNO, P., COLOMBO, M.I., CUERVO, A.M., DEBNATH, J., DERETIC, V., DIKIC, I., ESKELINEN, E.-L., FIMIA, G.M., FULDA, S., GEWIRTZ, D.A., GREEN, D.R., HANSEN, M., HARPER, J.W., JÄÄTTELÄ, M., JOHANSEN, T., JUHASZ, G., KIMMELMAN, A.C., KRAFT, C., KTISTAKIS, N.T., KUMAR, S., LEVINE, B., LOPEZ-OTIN, C., MADEO, F., MARTENS, S., MARTINEZ, J., MELENDEZ, A., MIZUSHIMA, N., MÜNZ, C., MURPHY, L.O., PENNINGER, J.M., PIACENTINI, M., REGGIORI, F., RUBINSZTEIN, D.C., RYAN, K.M., SANTAMBROGIO, L., SCORRANO, L., SIMON, A.K., SIMON, H.-U., SIMONSEN, A., TAVERNARAKIS, N., TOOZE, S.A., YOSHIMORI, T., YUAN, J., YUE, Z., ZHONG, Q., and KROEMER, G., 2017. Molecular definitions of autophagy and related processes. *The EMBO Journal*. 36 (13), pp. 1811–1836.

GAO, H., HOU, F., DONG, R., WANG, Z., ZHAO, C., TANG, W., and WU, Y., n.d. Rho-Kinase inhibitor fasudil suppresses high glucose-induced H9c2 cell apoptosis through activation of autophagy. *Cardiovascular Therapeutics*. 34 (5), pp. 352–359.

GLICK, D., BARTH, S., and MACLEOD, K.F., 2010. Autophagy: cellular and molecular mechanisms. *The Journal of pathology*. 221 (1), pp. 3–12.

GOYAL, B.R. and MEHTA, A.A., 2013. Diabetic cardiomyopathy: Pathophysiological mechanisms and cardiac dysfuntion. *Human & Experimental Toxicology*. 32 (6), pp. 571–590.

GREENE, A.W., GRENIER, K., AGUILETA, M.A., MUISE, S., FARAZIFARD, R., HAQUE, M.E., MCBRIDE, H.M., PARK, D.S., and FON, E.A., 2012. Mitochondrial processing peptidase regulates PINK1 processing, import and Parkin recruitment. *EMBO reports*. 13 (4), pp. 378–385.

GROS, F. and MULLER, S., 2014. Pharmacological regulators of autophagy and their link with modulators of lupus disease. *British Journal of Pharmacology*. 171 (19), pp. 4337–4359.

GULICK, T., CRESCI, S., CAIRA, T., MOORE, D.D., and KELLY, D.P., 1994. The peroxisome proliferator-activated receptor regulates mitochondrial fatty acid oxidative enzyme gene expression. *Proceedings of the National Academy of Sciences of the United States of America*. 91 (23), pp. 11012–11016.

GUSTAFSSON, A.B. and GOTTLIEB, R.A., 2003. Mechanisms of apoptosis in the heart. *Journal of Clinical Immunology*. 23 (6), pp. 447–459.

GUSTAFSSON, Å.B. and GOTTLIEB, R.A., 2008. Heart mitochondria: gates of life and death. *Cardiovascular Research*. 77 (2), pp. 334–343.

HAMACHER-BRADY, A., BRADY, N.R., and GOTTLIEB, R.A., 2006. Enhancing macroautophagy protects against ischemia/reperfusion injury in cardiac myocytes. *The Journal of Biological Chemistry*. 281 (40), pp. 29776–29787.

HARDIE, D.G., 2011. AMPK and autophagy get connected. *The EMBO Journal*. 30 (4), pp. 634–635.

HASUI, K., WANG, J., JIA, X., TANAKA, M., NAGAI, T., MATSUYAMA, T., and EIZURU, Y., 2011. Enhanced Autophagy and Reduced Expression of Cathepsin D Are Related to Autophagic Cell Death in Epstein-Barr Virus-Associated Nasal Natural Killer/T-Cell Lymphomas: An Immunohistochemical Analysis of Beclin-1, LC3, Mitochondria (AE-1), and Cathepsin D in Nasopharyngeal Lymphomas. *Acta Histochemica et Cytochemica*. 44 (3), pp. 119–131.

HE, C., ZHU, H., LI, H., ZOU, M.-H., and XIE, Z., 2013. Dissociation of Bcl-2-Beclin1 complex by activated AMPK enhances cardiac autophagy and protects against cardiomyocyte apoptosis in diabetes. *Diabetes*. 62 (4), pp. 1270–1281.

HEATHER, L.C. and CLARKE, K., 2011. Metabolism, hypoxia and the diabetic heart. *Journal of Molecular and Cellular Cardiology*. 50 (4), pp. 598–605.

HEINONEN M. T., MOULDER R., and LAHESMAA R., 2015. New Insights and Biomarkers for Type 1 Diabetes: Review for Scandinavian Journal of Immunology. *Scandinavian Journal of Immunology*. 82 (3), pp. 244–253.

HOLEMANS, K., GERBER, R.T., MEURRENS, K., DE CLERCK, F., POSTON, L., and VAN ASSCHE, F.A., 1999. Streptozotocin diabetes in the pregnant rat induces cardiovascular dysfunction in adult offspring. *Diabetologia*. 42 (1), pp. 81–89.

HOU, X., ZENG, H., TUO, Q.-H., LIAO, D.-F., and CHEN, J.-X., 2015. Apelin Gene Therapy Increases Autophagy via Activation of Sirtuin 3 in Diabetic Heart. *Diabetes Research (Fairfax, Va.)*. 1 (4), pp. 84–91.

HSU, H.-C., CHEN, C.-Y., LEE, B.-C., and CHEN, M.-F., 2016. High-fat diet induces cardiomyocyte apoptosis via the inhibition of autophagy. *European Journal of Nutrition*. 55 (7), pp. 2245–2254.

IKEDA, Y., SCIARRETTA, S., NAGARAJAN, N., RUBATTU, S., VOLPE, M., FRATI, G., and SADOSHIMA, J., 2014. New Insights into the Role of Mitochondrial Dynamics and Autophagy during Oxidative Stress and Aging in the Heart. *Oxidative Medicine and Cellular Longevity* [online]. Available from: https://www.hindawi.com/journals/omcl/2014/210934/ [Accessed 7 Apr 2018].

JI, L., CHEN, Z., XU, Y., XIONG, G., LIU, R., WU, C., HU, H., and WANG, L., 2017. Systematic Characterization of Autophagy in Gestational Diabetes Mellitus. *Endocrinology*. 158 (8), pp. 2522–2532.

JOSHI, M.S., WILLIAMS, D., HORLOCK, D., SAMARASINGHE, T., ANDREWS, K.L., JEFFERIS, A.-M., BERGER, P.J., CHIN-DUSTING, J.P., and KAYE, D.M., 2015. Role of mitochondrial dysfunction in hyperglycaemia-induced coronary microvascular dysfunction: Protective role of resveratrol. *Diabetes and Vascular Disease Research*. 12 (3), pp. 208–216.

JUNG, C.H., RO, S.-H., CAO, J., OTTO, N.M., and KIM, D.-H., 2010. mTOR regulation of autophagy. *FEBS letters*. 584 (7), pp. 1287–1295.

KABEYA, Y., MIZUSHIMA, N., UENO, T., YAMAMOTO, A., KIRISAKO, T., NODA, T., KOMINAMI, E., OHSUMI, Y., and YOSHIMORI, T., 2000. LC3, a mammalian homologue of yeast Apg8p, is localized in autophagosome membranes after processing. *The EMBO Journal*. 19 (21), pp. 5720–5728.

KAMPMANN, U., MADSEN, L.R., SKAJAA, G.O., IVERSEN, D.S., MOELLER, N., and OVESEN, P., 2015. Gestational diabetes: A clinical update. *World Journal of Diabetes*. 6 (8), pp. 1065–1072.

KANAMORI, H., TAKEMURA, G., GOTO, K., TSUJIMOTO, A., MIKAMI, A., OGINO, A., WATANABE, T., MORISHITA, K., OKADA, H., KAWASAKI, M., SEISHIMA, M., and MINATOGUCHI, S., 2015. Autophagic adaptations in diabetic cardiomyopathy differ between type 1 and type 2 diabetes. *Autophagy*. 11 (7), pp. 1146–1160.

KANG, R., ZEH, H.J., LOTZE, M.T., and TANG, D., 2011. The Beclin 1 network regulates autophagy and apoptosis. *Cell Death and Differentiation*. 18 (4), pp. 571–580.

KAUFMAN, B.A., LI, C., and SOLEIMANPOUR, S.A., 2015. Mitochondrial regulation of β-cell function: maintaining the momentum for insulin release. *Molecular aspects of medicine*. 42, pp. 91–104.

KAUSHIK, S., BANDYOPADHYAY, U., SRIDHAR, S., KIFFIN, R., MARTINEZ-VICENTE, M., KON, M., ORENSTEIN, S.J., WONG, E., and CUERVO, A.M., 2011. Chaperone-mediated autophagy at a glance. *J Cell Sci*. 124 (4), pp. 495–499.

KEATING, S.T., PLUTZKY, J., and EL-OSTA, A., 2016. Epigenetic Changes in Diabetes and Cardiovascular Risk. *Circulation research*. 118 (11), pp. 1706–1722.

KIM, I., RODRIGUEZ-ENRIQUEZ, S., and LEMASTERS, J.J., 2007. Selective degradation of mitochondria by mitophagy. *Archives of Biochemistry and Biophysics*. 462 (2), pp. 245–253.

KING, J.S., 2012. Mechanical stress meets autophagy: potential implications for physiology and pathology. *Trends in Molecular Medicine*. 18 (10), pp. 583–588.

KOBAYASHI, S. and LIANG, Q., 2015. Autophagy and mitophagy in diabetic cardiomyopathy. *Biochimica et Biophysica Acta (BBA) - Molecular Basis of Disease*. 1852 (2), pp. 252–261.

KOMATSU, M. and ICHIMURA, Y., 2010. Physiological significance of selective degradation of p62 by autophagy. *FEBS letters*. 584 (7), pp. 1374–1378.

KOYANO, F., OKATSU, K., KOSAKO, H., TAMURA, Y., GO, E., KIMURA, M., KIMURA, Y., TSUCHIYA, H., YOSHIHARA, H., HIROKAWA, T., ENDO, T., FON, E.A., TREMPE, J.-F., SAEKI, Y., TANAKA, K., and MATSUDA, N., 2014. Ubiquitin is phosphorylated by PINK1 to activate parkin. *Nature*. 510 (7503), pp. 162–166.

KRULJAC, I., ĆAĆIĆ, M., ĆAĆIĆ, P., OSTOJIĆ, V., ŠTEFANOVIĆ, M., ŠIKIĆ, A., and VRKLJAN, M., 2017. Diabetic ketosis during hyperglycemic crisis is associated with decreased all-cause mortality

in patients with type 2 diabetes mellitus. *Endocrine*. 55 (1), pp. 139–143.

KUBLI, D.A., CORTEZ, M.Q., MOYZIS, A.G., NAJOR, R.H., LEE, Y., and GUSTAFSSON, Å.B., 2015. PINK1 Is Dispensable for Mitochondrial Recruitment of Parkin and Activation of Mitophagy in Cardiac Myocytes. *PloS One*. 10 (6), p. e0130707.

KUBLI, D.A. and GUSTAFSSON, Å.B., 2012. Mitochondria and mitophagy: the yin and yang of cell death control. *Circulation Research*. 111 (9), pp. 1208–1221.

KÜHL, C. and HORNNES, P.J., 1986. Endocrine pancreatic function in women with gestational diabetes. *Acta Endocrinologica. Supplementum*. 277, pp. 19–23.

KUMA, A., HATANO, M., MATSUI, M., YAMAMOTO, A., NAKAYA, H., YOSHIMORI, T., OHSUMI, Y., TOKUHISA, T., and MIZUSHIMA, N., 2004. The role of autophagy during the early neonatal starvation period. *Nature*. 432 (7020), pp. 1032–1036.

KUNDU, M., LINDSTEN, T., YANG, C.-Y., WU, J., ZHAO, F., ZHANG, J., SELAK, M.A., NEY, P.A., and THOMPSON, C.B., 2008. Ulk1 plays a critical role in the autophagic clearance of mitochondria and ribosomes during reticulocyte maturation. *Blood*. 112 (4), pp. 1493–1502.

KUO, T.H., GIACOMELLI, F., and WIENER, J., 1985. Oxidative metabolism of Polytron versus Nagarse mitochondria in hearts of genetically diabetic mice. *Biochimica Et Biophysica Acta*. 806 (1), pp. 9–15.

KUO, T.H., MOORE, K.H., GIACOMELLI, F., and WIENER, J., 1983. Defective Oxidative Metabolism of Heart Mitochondria from Genetically Diabetic Mice. *Diabetes*. 32 (9), pp. 781–787.

LATOUCHE, C., HEYWOOD, S.E., HENRY, S.L., ZIEMANN, M., LAZARUS, R., EL-OSTA, A., ARMITAGE, J.A., and KINGWELL, B.A., 2014. Maternal overnutrition programs changes in the expression of skeletal muscle genes that are associated with insulin resistance and defects of oxidative phosphorylation in adult male rat offspring. *The Journal of Nutrition*. 144 (3), pp. 237–244.

LEE, Y., HONG, Y., LEE, S.-R., CHANG, K.-T., and HONG, Y., 2012. Autophagy contributes to retardation of cardiac growth in diabetic rats. *Laboratory Animal Research*. 28 (2), pp. 99–107.

LEMIEUX, H., SEMSROTH, S., ANTRETTER, H., HÖFER, D., and GNAIGER, E., 2011. Mitochondrial respiratory control and early defects of oxidative phosphorylation in the failing human heart. *The International Journal of Biochemistry & Cell Biology*. 43 (12), pp. 1729–1738.

LEVELT, E., MAHMOD, M., PIECHNIK, S.K., ARIGA, R., FRANCIS, J.M., RODGERS, C.T., CLARKE, W.T., SABHARWAL, N., SCHNEIDER, J.E., KARAMITSOS, T.D., CLARKE, K., RIDER, O.J., and NEUBAUER, S., 2016. Relationship Between Left Ventricular Structural and Metabolic Remodeling in Type 2 Diabetes. *Diabetes*. 65 (1), pp. 44–52.

LEVINE, B. and KROEMER, G., 2008. Autophagy in the pathogenesis of disease. *Cell*. 132 (1), pp. 27–42.

LI, P., HAO, L., GUO, Y.-Y., YANG, G.-L., MEI, H., LI, X.-H., and ZHAI, Q.-X., 2018. Chloroquine inhibits autophagy and deteriorates the mitochondrial dysfunction and apoptosis in hypoxic rat neurons. *Life Sciences*. 202, pp. 70–77.

LI, W., LI, J., and BAO, J., 2012. Microautophagy: lesser-known self-eating. *Cellular and molecular life sciences: CMLS*. 69 (7), pp. 1125–1136.

LI, X., ZHU, G., GOU, X., HE, W., YIN, H., YANG, X., and LI, J., 2018. Negative feedback loop of autophagy and endoplasmic reticulum stress in rapamycin protection against renal ischemia-reperfusion injury during initial reperfusion phase. *FASEB journal: official publication of the Federation of American Societies for Experimental Biology*. p. fj201800299R.

LIEDTKE, A.J., DEMAISON, L., EGGLESTON, A.M., COHEN, L.M., and NELLIS, S.H., 1988. Changes in substrate metabolism and effects of excess fatty acids in reperfused myocardium. *Circulation Research*. 62 (3), pp. 535–542.

LIN, C., ZHANG, M., ZHANG, Y., YANG, K., HU, J., SI, R., ZHANG, G., GAO, B., LI, X., XU, C., LI, C., HAO, Q., and GUO, W., 2017. Helix B surface peptide attenuates diabetic cardiomyopathy via AMPK-dependent autophagy. *Biochemical and Biophysical Research Communications*. 482 (4), pp. 665–671.

LIU, J., TANG, Y., FENG, Z., HOU, C., WANG, H., YAN, J., LIU, J., SHEN, W., ZANG, W., LIU, J., and LONG, J., 2014. Acetylated FoxO1 mediates high-glucose induced autophagy in H9c2 cardiomyoblasts: regulation by a polyphenol -(-)-epigallocatechin-3-gallate. *Metabolism: Clinical and Experimental*. 63 (10), pp. 1314–1323.

LIU, L., FENG, D., CHEN, G., CHEN, M., ZHENG, Q., SONG, P., MA, Q., ZHU, C., WANG, R., QI, W., HUANG, L., XUE, P., LI, B., WANG, X., JIN, H., WANG, J., YANG, F., LIU, P., ZHU, Y., SUI, S., and CHEN, Q., 2012. Mitochondrial outer-membrane protein FUNDC1 mediates hypoxia-induced mitophagy in mammalian cells. *Nature Cell Biology*. 14 (2), pp. 177–185.

LIU, M., LU, S., HE, W., ZHANG, L., MA, Y., LV, P., MA, M., YU, W., WANG, J., ZHANG, M., ZHANG, Y., and LI, Y., 2018. ULK1-regulated autophagy: A mechanism in cellular protection for ALDH2 against hyperglycemia. *Toxicology Letters*. 283, pp. 106–115.

LOPASCHUK, G.D., USSHER, J.R., FOLMES, C.D.L., JASWAL, J.S., and STANLEY, W.C., 2010. Myocardial fatty acid metabolism in health and disease. *Physiological Reviews*. 90 (1), pp. 207–258.

MAKINO, N., OYAMA, J., MAEDA, T., KOYANAGI, M., HIGUCHI, Y., and TSUCHIDA, K., 2015. Calorie restriction increases telomerase activity, enhances autophagy, and improves diastolic dysfunction in diabetic rat hearts. *Molecular and Cellular Biochemistry*. 403 (1–2), pp. 1–11.

MARCINIAK, C., MARECHAL, X., MONTAIGNE, D., NEVIERE, R., and LANCEL, S., 2014. Cardiac contractile function and mitochondrial respiration in diabetes-related mouse models. *Cardiovascular Diabetology*. 13, p. 118.

MARIÑO, G. and LÓPEZ-OTÍN, C., 2004. Autophagy: molecular mechanisms, physiological functions and relevance in human pathology. *Cellular and molecular life sciences: CMLS*. 61 (12), pp. 1439–1454.

MARSH, S.A., POWELL, P.C., DELL'ITALIA, L.J., and CHATHAM, J.C., 2013. Cardiac O-GlcNAcylation blunts autophagic signaling in the diabetic heart. *Life Sciences*. 92 (11), pp. 648–656.

MATHEUS, A.S. de M., TANNUS, L.R.M., COBAS, R.A., PALMA, C.C.S., NEGRATO, C.A., and GOMES, M. de B., 2013. Impact of Diabetes on Cardiovascular Disease: An Update. *International Journal of Hypertension* [online]. Available from: https://www.hindawi.com/journals/ijhy/2013/653789/ [Accessed 1 Apr 2018].

MCCURDY, C.E., SCHENK, S., HETRICK, B., HOUCK, J., DREW, B.G., KAYE, S., LASHBROOK, M., BERGMAN, B.C., TAKAHASHI, D.L., DEAN, T.A., NEMKOV, T., GERTSMAN, I., HANSEN, K.C., PHILP, A., HEVENER, A.L., CHICCO, A.J., AAGAARD, K.M., GROVE, K.L., and FRIEDMAN, J.E., 2016. Maternal obesity reduces oxidative capacity in fetal skeletal muscle of Japanese macaques. *JCI*

Insight[online]. 1 (16). Available from: https://insight.jci.org/articles/view/86612 [Accessed 10 Jun 2018].

MCGAVOCK, J.M., LINGVAY, I., ZIB, I., TILLERY, T., SALAS, N., UNGER, R., LEVINE, B.D., RASKIN, P., VICTOR, R.G., and SZCZEPANIAK, L.S., 2007. Cardiac steatosis in diabetes mellitus: a 1H-magnetic resonance spectroscopy study. *Circulation*. 116 (10), pp. 1170–1175.

MDAKI, K.S., LARSEN, T.D., WACHAL, A.L., SCHIMELPFENIG, M.D., WEAVER, L.J., DOOYEMA, S.D.R., LOUWAGIE, E.J., and BAACK, M.L., 2016. Maternal high-fat diet impairs cardiac function in offspring of diabetic pregnancy through metabolic stress and mitochondrial dysfunction. *American Journal of Physiology-Heart and Circulatory Physiology*. 310 (6), pp. H681–H692.

MIZUSHIMA, N., KUMA, A., KOBAYASHI, Y., YAMAMOTO, A., MATSUBAE, M., TAKAO, T., NATSUME, T., OHSUMI, Y., and YOSHIMORI, T., 2003. Mouse Apg16L, a novel WD-repeat protein, targets to the autophagic isolation membrane with the Apg12-Apg5 conjugate. *Journal of Cell Science*. 116 (Pt 9), pp. 1679–1688.

MIZUSHIMA, N., LEVINE, B., CUERVO, A.M., and KLIONSKY, D.J., 2008. Autophagy fights disease through cellular self-digestion. *Nature*. 451 (7182), pp. 1069–1075.

MORSELLI, E., MAIURI, M.C., MARKAKI, M., MEGALOU, E., PASPARAKI, A., PALIKARAS, K., CRIOLLO, A., GALLUZZI, L., MALIK, S.A., VITALE, I., MICHAUD, M., MADEO, F., TAVERNARAKIS, N., and

KROEMER, G., 2010. The life span-prolonging effect of sirtuin-1 is mediated by autophagy. *Autophagy*. 6 (1), pp. 186–188.

MPONDO, B.C.T., ERNEST, A., and DEE, H.E., 2015. Gestational diabetes mellitus: challenges in diagnosis and management. *Journal of Diabetes and Metabolic Disorders* [online]. 14. Available from: https://www.ncbi.nlm.nih.gov/pmc/articles/PMC4430906/ [Accessed 28 Mar 2018].

MUNASINGHE, P.E., RIU, F., DIXIT, P., EDAMATSU, M., SAXENA, P., HAMER, N.S.J., GALVIN, I.F., BUNTON, R.W., LEQUEUX, S., JONES, G., LAMBERTS, R.R., EMANUELI, C., MADEDDU, P., and KATARE, R., 2016. Type-2 diabetes increases autophagy in the human heart through promotion of Beclin-1 mediated pathway. *International Journal of Cardiology*. 202, pp. 13–20.

MURASE, H., KUNO, A., MIKI, T., TANNO, M., YANO, T., KOUZU, H., ISHIKAWA, S., TOBISAWA, T., OGASAWARA, M., NISHIZAWA, K., and MIURA, T., 2015. Inhibition of DPP-4 reduces acute mortality after myocardial infarction with restoration of autophagic response in type 2 diabetic rats. *Cardiovascular Diabetology* [online]. 14. Available from: https://www.ncbi.nlm.nih.gov/pmc/articles/PMC4531441/ [Accessed 11 Jun 2018].

NAKAMURA, T., TERAJIMA, T., OGATA, T., UENO, K., HASHIMOTO, N., ONO, K., and YANO, S., 2006. Establishment and pathophysiological characterization of type 2 diabetic mouse model produced by

streptozotocin and nicotinamide. *Biological & Pharmaceutical Bulletin*. 29 (6), pp. 1167–1174.

NAKASHIMA, A., AOKI, A., and SAITO, S., 2016. The Role of Autophagy in Maintaining Pregnancy. *Autophagy in Current Trends in Cellular Physiology and Pathology* [online]. Available from: http://www.intechopen.com/books/autophagy-in-current-trends-in-cellular-physiology-and-pathology/the-role-of-autophagy-in-maintaining-pregnancy [Accessed 7 Apr 2018].

NANDI, S.S., DURYEE, M.J., SHAHSHAHAN, H.R., THIELE, G.M., ANDERSON, D.R., and MISHRA, P.K., 2015. Induction of autophagy markers is associated with attenuation of miR-133a in diabetic heart failure patients undergoing mechanical unloading. *American Journal of Translational Research*. 7 (4), pp. 683–696.

NASU-KAWAHARADA, R., NAKAMURA, A., KAKARLA, S.K., BLOUGH, E.R., KOHAMA, K., and KOHAMA, T., 2013. A maternal diet rich in fish oil may improve cardiac Akt-related signaling in the offspring of diabetic mother rats. *Nutrition*. 29 (4), pp. 688–692.

NISHIDA, K., KYOI, S., YAMAGUCHI, O., SADOSHIMA, J., and OTSU, K., 2009. The role of autophagy in the heart. *Cell Death and Differentiation*. 16 (1), pp. 31–38.

NISHINO, I., FU, J., TANJI, K., YAMADA, T., SHIMOJO, S., KOORI, T., MORA, M., RIGGS, J.E., OH, S.J., KOGA, Y., SUE, C.M., YAMAMOTO, A., MURAKAMI, N., SHANSKE, S., BYRNE, E., BONILLA, E., NONAKA, I., DIMAURO, S., and HIRANO, M., 2000.

Primary LAMP-2 deficiency causes X-linked vacuolar cardiomyopathy and myopathy (Danon disease). *Nature*. 406 (6798), pp. 906–910.

NODA, T., SUZUKI, K., and OHSUMI, Y., 2002. Yeast autophagosomes: de novo formation of a membrane structure. *Trends in Cell Biology*. 12 (5), pp. 231–235.

OLOWE, Y. and SCHULZ, H., 1980. Regulation of thiolases from pig heart. Control of fatty acid oxidation in heart. *European Journal of Biochemistry*. 109 (2), pp. 425–429.

PAPATHEODOROU, K., PAPANAS, N., BANACH, M., PAPAZOGLOU, D., and EDMONDS, M., 2016. Complications of Diabetes 2016. *Journal of Diabetes Research* [online]. Available from: https://www.hindawi.com/journals/jdr/2016/6989453/ [Accessed 17 Mar 2018].

PARK, D., JEONG, H., LEE, M.N., KOH, A., KWON, O., YANG, Y.R., NOH, J., SUH, P.-G., PARK, H., and RYU, S.H., 2016. Resveratrol induces autophagy by directly inhibiting mTOR through ATP competition. *Scientific Reports*. 6, p. 21772.

PAULSON, D.J., WARD, K.M., and SHUG, A.L., 1984. Malonyl CoA inhibition of carnitine palmityltransferase in rat heart mitochondria. *FEBS letters*. 176 (2), pp. 381–384.

PEI, Z., DENG, Q., BABCOCK, S.A., HE, E.Y., REN, J., and ZHANG, Y., 2018. Inhibition of advanced glycation endproduct (AGE) rescues against streptozotocin-induced diabetic cardiomyopathy: Role of autophagy and ER stress. *Toxicology Letters*. 284, pp. 10–20.

PILEGGI, C.A., HEDGES, C.P., SEGOVIA, S.A., MARKWORTH, J.F., DURAINAYAGAM, B.R., GRAY, C., ZHANG, X.D., BARNETT, M.P.G., VICKERS, M.H., HICKEY, A.J.R., REYNOLDS, C.M., and CAMERON-SMITH, D., 2016. Maternal High Fat Diet Alters Skeletal Muscle Mitochondrial Catalytic Activity in Adult Male Rat Offspring. *Frontiers in Physiology* [online]. 7. Available from: https://www.ncbi.nlm.nih.gov/pmc/articles/PMC5114294/ [Accessed 30 May 2018].

PIRES, K.M., BUFFOLO, M., SCHAAF, C., DAVID SYMONS, J., COX, J., ABEL, E.D., SELZMAN, C.H., and BOUDINA, S., 2017. Activation of IGF-1 receptors and Akt signaling by systemic hyperinsulinemia contributes to cardiac hypertrophy but does not regulate cardiac autophagy in obese diabetic mice. *Journal of Molecular and Cellular Cardiology*. 113, pp. 39–50.

QIAN, L.-B., JIANG, S.-Z., TANG, X.-Q., ZHANG, J., LIANG, Y.-Q., YU, H.-T., CHEN, J., XU, Z., LIU, R.-M., KELLER, B.B., JI, H.-L., and CAI, L., 2017. Exacerbation of diabetic cardiac hypertrophy in OVE26 mice by angiotensin II is associated with JNK/c-Jun/miR-221-mediated autophagy inhibition. *Oncotarget*. 8 (63), pp. 106661–106671.

RAGNARSDOTTIR, L.H. and CONROY, S., 2010. Development of macrosomia resulting from gestational diabetes mellitus: physiology and social determinants of health. *Advances in Neonatal Care: Official Journal of the National Association of Neonatal Nurses*. 10 (1), pp. 7–12.

RANDLE, P.J., ENGLAND, P.J., and DENTON, R.M., 1970. Control of the tricarboxylate cycle and its interactions with glycolysis during acetate utilization in rat heart. *Biochemical Journal*. 117 (4), pp. 677–695.

RATTANASOPA, C., PHUNGPHONG, S., WATTANAPERMPOOL, J., and BUPHA-INTR, T., 2015. Significant role of estrogen in maintaining cardiac mitochondrial functions. *The Journal of Steroid Biochemistry and Molecular Biology*. 147, pp. 1–9.

REDMANN, M., BENAVIDES, G.A., BERRYHILL, T.F., WANI, W.Y., OUYANG, X., JOHNSON, M.S., RAVI, S., BARNES, S., DARLEY-USMAR, V.M., and ZHANG, J., 2016. Inhibition of autophagy with bafilomycin and chloroquine decreases mitochondrial quality and bioenergetic function in primary neurons. *Redox Biology*. 11, pp. 73–81.

RELLER, M.D. and KAPLAN, S., 1988. Hypertrophic cardiomyopathy in infants of diabetic mothers: an update. *American Journal of Perinatology*. 5 (4), pp. 353–358.

RIJZEWIJK, L.J., VAN DER MEER, R.W., SMIT, J.W.A., DIAMANT, M., BAX, J.J., HAMMER, S., ROMIJN, J.A., DE ROOS, A., and LAMB, H.J., 2008. Myocardial steatosis is an independent predictor of diastolic dysfunction in type 2 diabetes mellitus. *Journal of the American College of Cardiology*. 52 (22), pp. 1793–1799.

ROACH, P.J., 2011. AMPK → ULK1 → Autophagy. *Molecular and Cellular Biology*. 31 (15), pp. 3082–3084.

RODRIGUES, B., CAM, M.C., and MCNEILL, J.H., 1998. Metabolic disturbances in diabetic cardiomyopathy. *Molecular and Cellular Biochemistry*. 180 (1–2), pp. 53–57.

ROVITO, D., GIORDANO, C., PLASTINA, P., BARONE, I., DE AMICIS, F., MAURO, L., RIZZA, P., LANZINO, M., CATALANO, S., BONOFIGLIO, D., and ANDÒ, S., 2015. Omega-3 DHA- and EPA-dopamine conjugates induce PPARγ-dependent breast cancer cell death through autophagy and apoptosis. *Biochimica Et Biophysica Acta*. 1850 (11), pp. 2185–2195.

RUBLER, S., DLUGASH, J., YUCEOGLU, Y.Z., KUMRAL, T., BRANWOOD, A.W., and GRISHMAN, A., 1972. New type of cardiomyopathy associated with diabetic glomerulosclerosis. *The American Journal of Cardiology*. 30 (6), pp. 595–602.

RUSSELL, R.R., YIN, R., CAPLAN, M.J., HU, X., REN, J., SHULMAN, G.I., SINUSAS, A.J., and YOUNG, L.H., 1998. Additive Effects of Hyperinsulinemia and Ischemia on Myocardial GLUT1 and GLUT4 Translocation In Vivo. *Circulation*. 98 (20), pp. 2180–2186.

SABEN, J.L., BOUDOURES, A.L., ASGHAR, Z., THOMPSON, A., DRURY, A., ZHANG, W., CHI, M., CUSUMANO, A., SCHEAFFER, S., and MOLEY, K., 2016. Maternal metabolic syndrome programs mitochondrial dysfunction via germline changes across three generations. *Cell reports*. 16 (1), pp. 1–8.

SATO, K., KASHIWAYA, Y., KEON, C.A., TSUCHIYA, N., KING, M.T., RADDA, G.K., CHANCE, B., CLARKE, K., and VEECH, R.L., 1995.

Insulin, ketone bodies, and mitochondrial energy transduction. *FASEB journal: official publication of the Federation of American Societies for Experimental Biology*. 9 (8), pp. 651–658.

SCHEUERMANN-FREESTONE, M., MADSEN, P.L., MANNERS, D., BLAMIRE, A.M., BUCKINGHAM, R.E., STYLES, P., RADDA, G.K., NEUBAUER, S., and CLARKE, K., 2003. Abnormal cardiac and skeletal muscle energy metabolism in patients with type 2 diabetes. *Circulation*. 107 (24), pp. 3040–3046.

SCIARRETTA, S., YEE, D., SHENOY, V., NAGARAJAN, N., and SADOSHIMA, J., 2014. The importance of autophagy in cardioprotection. *High Blood Pressure & Cardiovascular Prevention: The Official Journal of the Italian Society of Hypertension*. 21 (1), pp. 21–28.

SCIARRETTA, S., ZHAI, P., SHAO, D., MAEJIMA, Y., ROBBINS, J., VOLPE, M., CONDORELLI, G., and SADOSHIMA, J., 2012. Rheb is a critical regulator of autophagy during myocardial ischemia: pathophysiological implications in obesity and metabolic syndrome. *Circulation*. 125 (9), pp. 1134–1146.

SHELLEY, P., MARTIN-GRONERT, M.S., ROWLERSON, A., POSTON, L., HEALES, S.J.R., HARGREAVES, I.P., MCCONNELL, J.M., OZANNE, S.E., and FERNANDEZ-TWINN, D.S., 2009. Altered skeletal muscle insulin signaling and mitochondrial complex II-III linked activity in adult offspring of obese mice. *American Journal of*

Physiology-Regulatory, Integrative and Comparative Physiology. 297 (3), pp. R675–R681.

SHINTANI, T., HUANG, W.-P., STROMHAUG, P.E., and KLIONSKY, D.J., 2002. Mechanism of cargo selection in the cytoplasm to vacuole targeting pathway. *Developmental Cell*. 3 (6), pp. 825–837.

SOHAL, D.S., NGHIEM, M., CRACKOWER, M.A., WITT, S.A., KIMBALL, T.R., TYMITZ, K.M., PENNINGER, J.M., and MOLKENTIN, J.D., 2001. Temporally regulated and tissue-specific gene manipulations in the adult and embryonic heart using a tamoxifen-inducible Cre protein. *Circulation Research*. 89 (1), pp. 20–25.

SYMINGTON, B., MAPANGA, R.F., NORTON, G.R., and ESSOP, M.F., 2017. Resveratrol Co-Treatment Attenuates the Effects of HIV Protease Inhibitors on Rat Body Weight and Enhances Cardiac Mitochondrial Respiration. *PLOS ONE*. 12 (1), p. e0170344.

TASSA, A., ROUX, M.P., ATTAIX, D., and BECHET, D.M., 2003. Class III phosphoinositide 3-kinase--Beclin1 complex mediates the amino acid-dependent regulation of autophagy in C2C12 myotubes. *Biochemical Journal*. 376 (Pt 3), pp. 577–586.

TAYLOR, P.D., MCCONNELL, J., KHAN, I.Y., HOLEMANS, K., LAWRENCE, K.M., ASARE-ANANE, H., PERSAUD, S.J., JONES, P.M., PETRIE, L., HANSON, M.A., and POSTON, L., 2005. Impaired glucose homeostasis and mitochondrial abnormalities in offspring of rats fed a fat-rich diet in pregnancy. *American Journal of Physiology.*

Regulatory, Integrative and Comparative Physiology. 288 (1), pp. R134-139.

TODD, J.A., 2010. Etiology of Type 1 Diabetes. *Immunity*. 32 (4), pp. 457–467.

TROST, S.U., BELKE, D.D., BLUHM, W.F., MEYER, M., SWANSON, E., and DILLMANN, W.H., 2002. Overexpression of the sarcoplasmic reticulum Ca(2+)-ATPase improves myocardial contractility in diabetic cardiomyopathy. *Diabetes*. 51 (4), pp. 1166–1171.

TSUKADA, M. and OHSUMI, Y., 1993. Isolation and characterization of autophagy-defective mutants of Saccharomyces cerevisiae. *FEBS letters*. 333 (1–2), pp. 169–174.

UM, J.-H., PARK, S.-J., KANG, H., YANG, S., FORETZ, M., MCBURNEY, M.W., KIM, M.K., VIOLLET, B., and CHUNG, J.H., 2010. AMP-activated protein kinase-deficient mice are resistant to the metabolic effects of resveratrol. *Diabetes*. 59 (3), pp. 554–563.

VEERANKI, S., GIVVIMANI, S., KUNDU, S., METREVELI, N., PUSHPAKUMAR, S., and TYAGI, S.C., 2016. Moderate intensity exercise prevents diabetic cardiomyopathy associated contractile dysfunction through restoration of mitochondrial function and connexin 43 levels in db/db mice. *Journal of Molecular and Cellular Cardiology*. 92, pp. 163–173.

WANG, B., YANG, Q., SUN, Y., XING, Y., WANG, Y., LU, X., BAI, W., LIU, X., and ZHAO, Y., n.d. Resveratrol-enhanced autophagic flux

ameliorates myocardial oxidative stress injury in diabetic mice. *Journal of Cellular and Molecular Medicine*. 18 (8), pp. 1599–1611.

WANG, G., DAI, G., SONG, J., ZHU, M., LIU, Y., HOU, X., KE, Z., ZHOU, Y., QIU, H., WANG, F., JIANG, N., JIA, X., and FENG, L., 2018. Lactone Component From Ligusticum chuanxiong Alleviates Myocardial Ischemia Injury Through Inhibiting Autophagy. *Frontiers in Pharmacology* [online]. 9. Available from: https://www.ncbi.nlm.nih.gov/pmc/articles/PMC5884868/ [Accessed 10 Jun 2018].

WANG, G., HUANG, W., CUI, S., LI, S., WANG, X., LI, Y., CHUAI, M., CAO, L., LI, J., LU, D., and YANG, X., 2015. Autophagy is involved in high glucose-induced heart tube malformation. *Cell Cycle (Georgetown, Tex.)*. 14 (5), pp. 772–783.

WANG, G., LIANG, J., GAO, L.-R., SI, Z.-P., ZHANG, X.-T., LIANG, G., YAN, Y., LI, K., CHENG, X., BAO, Y., CHUAI, M., CHEN, L.-G., LU, D.-X., and YANG, X., 2018. Baicalin administration attenuates hyperglycemia-induced malformation of cardiovascular system. *Cell Death & Disease*. 9 (2), p. 234.

WANG, G.-Y., BI, Y.-G., LIU, X.-D., HAN, J.-F., WEI, M., and ZHANG, Q.-Y., 2017. Upregulation of connexin 43 and apoptosis-associated protein expression by high glucose in H9c2 cells was improved by resveratrol via the autophagy signaling pathway. *Molecular Medicine Reports*. 16 (3), pp. 3262–3268.

WANG, G.-Y., BI, Y.-G., LIU, X.-D., ZHAO, Y., HAN, J.-F., WEI, M., and ZHANG, Q.-Y., 2017. Autophagy was involved in the protective effect of metformin on hyperglycemia-induced cardiomyocyte apoptosis and Connexin43 downregulation in H9c2 cells. *International Journal of Medical Sciences*. 14 (7), pp. 698–704.

WANG, S., WANG, C., YAN, F., WANG, T., HE, Y., LI, H., XIA, Z., and ZHANG, Z., 2017. N-Acetylcysteine Attenuates Diabetic Myocardial Ischemia Reperfusion Injury through Inhibiting Excessive Autophagy. *Mediators of Inflammation* [online]. Available from: https://www.hindawi.com/journals/mi/2017/9257291/ [Accessed 11 Jun 2018].

WANG, X., TAO, Y., HUANG, Y., ZHAN, K., XUE, M., WANG, Y., RUAN, D., LIANG, Y., HUANG, X., LIN, J., CHEN, Z., LV, L., LI, S., CHEN, G., WANG, Y., CHEN, R., CONG, W., and JIN, L., 2017. Catalase ameliorates diabetes-induced cardiac injury through reduced p65/RelA- mediated transcription of BECN1. *Journal of Cellular and Molecular Medicine*. 21 (12), pp. 3420–3434.

WEI, Y., CHIANG, W.-C., SUMPTER, R., MISHRA, P., and LEVINE, B., 2017. Prohibitin 2 Is an Inner Mitochondrial Membrane Mitophagy Receptor. *Cell*. 168 (1–2), pp. 224-238.e10.

WILCOX, G., 2005. Insulin and Insulin Resistance. *Clinical Biochemist Reviews*. 26 (2), pp. 19–39.

WILD, S., ROGLIC, G., GREEN, A., SICREE, R., and KING, H., 2004. Global prevalence of diabetes: estimates for the year 2000 and projections for 2030. *Diabetes Care*. 27 (5), pp. 1047–1053.

WU, B., LIN, J., LUO, J., HAN, D., FAN, M., GUO, T., TAO, L., YUAN, M., and YI, F., 2017. Dihydromyricetin Protects against Diabetic Cardiomyopathy in Streptozotocin-Induced Diabetic Mice. *BioMed Research International* [online]. Available from: https://www.hindawi.com/journals/bmri/2017/3764370/ [Accessed 10 Jun 2018].

WU, J.J., QUIJANO, C., CHEN, E., LIU, H., CAO, L., FERGUSSON, M.M., ROVIRA, I.I., GUTKIND, S., DANIELS, M.P., KOMATSU, M., and FINKEL, T., 2009. Mitochondrial dysfunction and oxidative stress mediate the physiological impairment induced by the disruption of autophagy. *Aging*. 1 (4), pp. 425–437.

WU, L.L., 1999. Review of risk factors for cardiovascular diseases. *Annals of Clinical and Laboratory Science*. 29 (2), pp. 127–133.

XIAO, T., LUO, J., WU, Z., LI, F., ZENG, O., and YANG, J., 2016. Effects of hydrogen sulfide on myocardial fibrosis and PI3K/AKT1-regulated autophagy in diabetic rats. *Molecular Medicine Reports*. 13 (2), pp. 1765–1773.

XIAO, Y., WU, Q.Q., DUAN, M.X., LIU, C., YUAN, Y., YANG, Z., LIAO, H.H., FAN, D., and TANG, Q.Z., 2018. TAX1BP1 overexpression attenuates cardiac dysfunction and remodeling in STZ-induced

diabetic cardiomyopathy in mice by regulating autophagy. *Biochimica Et Biophysica Acta*. 1864 (5 Pt A), pp. 1728–1743.

XIE, Z., LAU, K., EBY, B., LOZANO, P., HE, C., PENNINGTON, B., LI, H., RATHI, S., DONG, Y., TIAN, R., KEM, D., and ZOU, M.-H., 2011. Improvement of cardiac functions by chronic metformin treatment is associated with enhanced cardiac autophagy in diabetic OVE26 mice. *Diabetes*. 60 (6), pp. 1770–1778.

YANG, Z. and KLIONSKY, D.J., 2010. Eaten alive: a history of macroautophagy. *Nature Cell Biology*. 12 (9), pp. 814–822.

YESSOUFOU, A. and MOUTAIROU, K., 2011. Maternal Diabetes in Pregnancy: Early and Long-Term Outcomes on the Offspring and the Concept of “Metabolic Memory” *Journal of Diabetes Research*. 2011, p. e218598.

YU, L., CHEN, Y., and TOOZE, S.A., 2017. Autophagy pathway: Cellular and molecular mechanisms. *Autophagy*. 0 (0), pp. 1–9.

YU, W., GAO, B., LI, N., WANG, J., QIU, C., ZHANG, G., LIU, M., ZHANG, R., LI, C., JI, G., and ZHANG, Y., 2017. Sirt3 deficiency exacerbates diabetic cardiac dysfunction: Role of Foxo3A-Parkin-mediated mitophagy. *Biochimica Et Biophysica Acta*. 1863 (8), pp. 1973–1983.

YU, Y., WANG, L., DELGUSTE, F., DURAND, A., GUILBAUD, A., ROUSSELIN, C., SCHMIDT, A.M., TESSIER, F., BOULANGER, E., and NEVIERE, R., 2017. Advanced glycation end products receptor RAGE controls myocardial dysfunction and oxidative stress in high-fat fed mice by sustaining mitochondrial dynamics and autophagy-

lysosome pathway. *Free Radical Biology & Medicine*. 112, pp. 397–410.

YUAN, X., XIAO, Y.-C., ZHANG, G.-P., HOU, N., WU, X.-Q., CHEN, W.-L., LUO, J.-D., and ZHANG, G.-S., 2016. Chloroquine improves left ventricle diastolic function in streptozotocin-induced diabetic mice. *Drug Design, Development and Therapy*. 10, pp. 2729–2737.

ZHANG, B., XU, L., ZHUO, N., and SHEN, J., 2017. Resveratrol protects against mitochondrial dysfunction through autophagy activation in human nucleus pulposus cells. *Biochemical and Biophysical Research Communications*. 493 (1), pp. 373–381.

ZHANG, M., WANG, S., CHENG, Z., XIONG, Z., LV, J., YANG, Z., LI, T., JIANG, S., GU, J., SUN, D., and FAN, Y., 2017. Polydatin ameliorates diabetic cardiomyopathy via Sirt3 activation. *Biochemical and Biophysical Research Communications*. 493 (3), pp. 1280–1287.

ZHANG, Y., LING, Y., YANG, L., CHENG, Y., YANG, P., SONG, X., TANG, H., ZHONG, Y., TANG, L., HE, S., YANG, S., CHEN, A., and WANG, X., 2017. Liraglutide relieves myocardial damage by promoting autophagy via AMPK-mTOR signaling pathway in zucker diabetic fatty rat. *Molecular and Cellular Endocrinology*. 448, pp. 98–107.

IX. List of Publications and Abstracts

1) **Raji S R**, Nandini R J, Ashok S, Anand C R, Vivek V Pillai, Jayakumar K, Harikrishnan V S, S Manjunatha, Srinivas G. Diminished substrate-mediated cardiac mitochondrial respiration and elevated autophagy in adult male offspring of gestational diabetic rats**. IUBMB life, 2020**.

2) Nandini R J, **Raji S R**, Ashok S, Sulfath T P, Anand C R, Harikrishnan V S, Srinivas G. Honokiol regulates mitochondrial substrate utilization and cellular fatty acid metabolism in diabetic mice heart. **European Journal of Pharmacology, 2021.**

3) Nandini.R J, **Raji S R**, Ashok S, Surabhi S V, Saurabh Nanda, S Manjunatha, Vivek V Pillai, Jayakumar K, Srinivas Gopala. Impaired substrate-mediated cardiac mitochondrial complex I respiration with unaltered regulation of fatty acid metabolism and oxidative stress status in type 2 diabetic Asian Indians. **Journal of Diabetes, 2020.**

4) Nandini R J, Anand C R**, Raji S R**, Vivek Velayudhan Pillai, Jayakumar Karunakaran, Harikrishnan Vijayakumar Sreelatha, Srinivas Gopala, Are nitric oxide-mediated protein modifications of functional significance in diabetic heart? ye'S, -NO', wh'Y-NO't? **Nitric Oxide, 2014**.

Poster presentations

1) Impairment of cardiac mitochondrial respiration and autophagy in the offsprings of gestational diabetic rats', **Raji S.R**, Nandini R.J, Anand C. R, Ashok.S, Harikrishnan V.S, Jayakumar K, Vivek V. Pillai, Srinivas G, at 76th Scientific Sessions of American Diabetes Association, 2016

2) Unaltered fatty acid uptake, utilization and mitochondrial respiration in right atrial appendage of type 2 diabetic human heart, Nandini. R J, **Raji S R**, Vivek V Pillai, Jayakumar K, Srinivas G, at 78th Scientific Sessions of American Diabetes Association, 2018

3) Augmented Mitochondrial Complex II Activity and Low Expression of Long Chain Acyl CoA Dehydrogenase_in Prolonged_Untreated Type 2 Diabetes, Nandini R.J, **Raji S.R**, Anand C. R, Sulfath T.P, Jayakumar K, Harikrishnan V.S, Srinivas G, at 76th Scientific Sessions of American Diabetes Association, 2016

Oral Presentations

1) Altered cardiac autophagy and mitochondrial respiration in the offspring of gestational diabetic rats, **Raji S.R**, Nandini R.J, Harikrishnan V.S, Srinivas G, at international seminar on Recent Biochemical Approaches in Therapeutics (RBAT - 2018), organized by Department of Biochemistry,University of Kerala.